

**Climatological study on local wind and
temperature around Kobe, Japan**

Ieyasu TAKIMOTO

**Department of Geography,
Graduate School of Urban Environmental Science,
Tokyo Metropolitan University**

March 2023

東京都立大学 博士（理学） 学位論文（論文博士）

論文名

神戸周辺地域における局地風と気温に関する気候学的
研究（英文）

著者

瀧本 家康

審査担当者

主査

委員

委員

委員

上記の論文を合格と判定する

年 月 日

東京都立大学院都市環境科学研究科教授会

研究科長

DISSERTATION FOR A DEGREE OF
DOCTOR OF PHILOSOPHY (SCIENCE)
TOKYO METROPOLITAN UNIVERSITY

TITLE: Climatological study on local wind and temperature around Kobe, Japan

AUTHOR: Ieyasu TAKIMOTO

EXAMINED BY

Chief examiner:

Examiner:

Examiner:

Examiner:

QUALIFIED BY THE GRADUATE SCHOOL OF
URBAN ENVIRONMENT SCIENCES
TOKYO METROPOLITAN UNIVERSITY

Dean:

Date:

**Climatological study on local wind and
temperature around Kobe, Japan**

Ieyasu TAKIMOTO

**Department of Geography,
Graduate School of Urban Environmental Science,
Tokyo Metropolitan University**

March 2023

Contents

| | |
|--|-----|
| Acknowledgment | ix |
| Abstract..... | x |
| 1. Introduction | 1 |
| 1.1 Local winds in Japan | 1 |
| 1.2 Sea and land breezes..... | 2 |
| 1.3 Mountain and valley breeze, cold air drainage..... | 15 |
| 1.4 Downslope winds | 23 |
| 1.5 Objectives | 27 |
| 1.6 Composition of this thesis..... | 31 |
| 2. Study area and data..... | 32 |
| 2.1 Study area and its characteristics..... | 32 |
| 2.2 Data and analysis period..... | 32 |
| 3. Thermally induced local circulation in Kobe and its effect on air temperature | 37 |
| 3.1 Statistical analysis of sea and land breeze in Kobe City | 37 |
| 3.2 Case study on the days with different diurnal variation of the local wind system | 53 |
| 3.3 Effects of local wind systems on temperature distribution..... | 61 |
| 3.4 Cooling effect of cold air drainage on the lower-slope of Mt. Rokko..... | 77 |
| 4. Rokko-oroshi and its effect on temperature | 86 |
| 4.1 Objective..... | 86 |
| 4.2 Data used | 87 |
| 4.3 Selection of dates for analysis | 88 |
| 4.4 Statistical analysis of Rokko-oroshi | 89 |
| 4.5 Case study on Rokko-oroshi (November,4 2017) | 90 |
| 5. Summary..... | 96 |
| References..... | 104 |
| Figures and Tables | 124 |

List of figures

- Fig. 1-1 Local winds in Japan (Yoshino, 1975). 125
- Fig. 1-2 Composite diagrams of D2 and D3 wind systems. Of the 37 days selected as summer pressure type days in 1982-1984, D2 type winds appeared mostly at 12:00, 15:00, and 18:00 JST, in that order, and were generally strong, especially with a southerly component. D3 type winds mostly appear at 15:00 JST, and are characterized by high wind speeds, sea breezes, and valley breezes that develop significantly in various locations. The starting point of the arrow corresponds to the AMeDAS station. Each wind system type was obtained by cluster analysis for 296 wind distribution maps per 3-hourly a day for the 37 days selected. Areas above 400 m elevation are shaded. (Suzuki and Kawamura, 1987) 126
- Fig. 1-3 Diurnal variations of sea surface temperature (\times and broken line) and ground surface temperature (\bigcirc and solid line) obtained by the special observation in the Sagami Bay area which was carried out in the periods from 00:00JST 12 August to 00:00JST 14 August in 1980, and from 12:00JST 9 August to 12:00 JST 11 August in 1981. The latter is the average value for all the observation points except Oshima, and both are four days averages at each time of the day. Squares indicate the results of aircraft observation. The sea surface temperature was measured by bucket sampling at the Tansei-maru. The ground surface temperature was measured by bent stem earth thermometers at six points in 1980 and at three points in 1981 (Fujibe and Asai, 1984). 127
- Fig. 1-4 Extended sea breeze. A: sea breeze, B: extended sea breeze, C: valley breeze, D: large-scale wind blowing into a thermal low (Kurita *et al.*, 1988). 128
- Fig. 1-5 Typical wind fields at 15:00 JST for (a) type NN (July 10, 1979), (b) type ND (June 1, 1979). The thick solid line represents a convergence line between the winds from the Pacific Ocean and the Japan Sea, and the cross represents a thermal low center. High concentrations of Ox appeared after 8:00 a.m. were considered "Night smog" and those before 8:00 a.m. were considered "Day smog". During the 35 days when high concentrations of Ox appeared in Ueda, we classified them into the following three types according to the appearance of "night smog". Type NN: "Night smog" appeared in Ueda and Nagano (6 days). Type ND: "Night smog" appeared in Ueda only and did not appear in Nagano (19 days). See the next figure for the location of Ueda and Nagano. The thick solid line represents a convergence line between the winds from the Pacific Ocean and the Japan Sea, and the cross represents a thermal low center. (Kurita and Ueda, 1985). 129
- Fig. 1-6 Route of long-distance transport of contaminants from the Kanto Plain to the Chubu mountainous region on 29 July, 1983 when typical long-range transport of air pollutants occurred. Black circle: Meteorological observation sites, white circle: Meteorological stations, and solid line: polluted air mass transport route (Stream trace line) (Kurita *et al.* 1988). 130
- Fig. 1-7 Time-height sections of southerly wind components at (a) Machida (1980) and Sagamihara (1981), (b) Chigasaki and (c) Tansei-maru obtained by the special observation in the Sagami Bay area which was carried out in the periods from 00:00JST 12 August to 00:00JST 14 August in 1980, and from 12:00JST 9 August to 12:00 JST 11 August in 1981. Contour interval is 1 m/s, and the dotted contour lines represent negative values (northerly wind) (Fujibe and Asai, 1984). 131

- Fig. 1-8 Composite distribution map of temperature anomalies and winds on sea breeze front days (8 days) when sea breeze fronts were observed in the Tokyo metropolitan area in August 2006 and 2007. (a) 12:00 JST (b) 14:00 JST. Sea breeze front days were defined as days when sea breeze fronts were clearly visible among the days selected using the criteria at all AMeDAS stations of mean sunshine duration (7 hours more), precipitation amount (less than 0.5 mm from 6:00 to 18:00 JST), wind direction (average wind direction from 16 to 20 JST is 150 to 225°), and the geostrophic wind speed calculated by data of four stations (less than 6 m/s). Temperature anomalies are obtained by subtracting spatially averaged values (upper right number) from the data at each point. The green curves represent sea breeze front. Wind arrows indicating less than 3 m/s are shown based on the length of the thin arrow, and wind arrows indicating more than 3 m/s are shown based on the length of the thick arrow (Yamato *et al.*, 2011). 132
- Fig. 1-9 Vector mean wind and daily elliptical distributions in July, 1967-1977. The ellipse indicates the endpoint of the diurnal variation vector, and the black circle on the ellipse indicates the position at 00:00 JST. The solid line indicates clockwise rotation and the dotted line indicates counterclockwise rotation. (Mori, 1983). 133
- Fig. 1-10 Frequency of occurrence of sea and land breeze by average of the maximum wind speed. The maximum wind speeds were averaged over about 60 observation points along the Seto Inland Sea coastline for sea and land winds in summer and winter, respectively, and then divided into six wind speed classes (Neyama, 1982). 134
- Fig. 1-11 Spatial distribution of sea level pressure, wind direction and speed from 13:00 to 19:00 JST composited of 13 days obtained as summer calm days in July and August from 1996 to 2007. The isopleths indicate sea level pressure at intervals of 0.25 hPa. Vectors indicate wind speed and direction. White circles indicate wind speed of 0 m/s. Black squares indicate meteorological offices. Shading indicates elevation (Kasuya and Kawamura, 2011). 135
- Fig. 1-12 Vector-mean winds at 15:00 and 03:00 JST for Type I-SE. The wind velocity data from the 1st of January, 1989 to the 31st of December, 1990 are utilized. The daily wind maps are drawn for each day of the study period by using seven AMeDAS stations data in Osaka Prefecture. Visual inspection of the daily wind maps leads to the type classification of the diurnal variation of winds. The type I is the observed temporal change in the wind direction of the sea breeze; the northwesterly breeze in the morning gradually backs to a southwesterly breeze in the late afternoon. This southwesterly breeze is considered to be the sea breeze from the Kii Channel. The “SE” in Type I-SE means that the southeasterly sea breeze at Okayama occurs. Type I-SE having the greatest frequency appears during April to September compared to the other four types. Constancy is the vector mean wind speed divided by the scalar mean wind speed. (Mizuma, 1995). 136
- Fig. 1-13 Horizontal structure of the wind at 16:00 JST at $z^* = 100$ m by numerical experiment. Contours are at 500 m and 800 m altitude, and are shaded above 500 m. This numerical experiment was computed using realistic terrain conditions in a basic numerical experiment. The horizontal grid of the model is a staggered grid with a grid spacing of 5 km. The vertical grid consists of 20 layers, starting from the bottom at 0, 10, 50, and 100 m. From there, the grid is spaced at 200 m intervals up to 1700 m, then at 300 m intervals up to 3200 m, and finally at 400 m intervals up to 4400 m. The time step is 20 seconds. Integration began at 6:00 a.m. local time and continued until 24:00 on the second day. Results were stored every 30 minutes (Itoh, 1995). 137

| | |
|--|-----|
| Fig. 1-14 Windrose at night for weak extended sea and land breeze (July 25-26, 1999 at 18:00 and 16:00 JST) The largest scale on the windrose is the 50% frequency (Takebayashi <i>et al.</i> , 2001). | 138 |
| Fig. 1-15 Horizontal wind by statics analysis of 2-dimensional over-mountain airflow. $N \sim 0.01$ /s, $U = 12$ m/s. Left: Solution with nonlinear boundary conditions for bell-shaped mountains. Right: Solution with nonlinear boundary conditions for Shikoku topography. The horizontal axis indicates distance (km), the vertical axis indicates altitude (km), and the numbers in the figure indicate horizontal wind speed (m/s) (Saito and Ikawa, 1991). | 139 |
| Fig. 1-16 Vertical cross section of potential temperature during downslope wind near Boulder, Colorado in USA obtained by special observation on January 11, 1972. Analysis of the potential temperature field (solid lines) from aircraft flight data and sondes taken on 11 January 1972. The dashed lines show aircraft track. The heavy dashed line separates data taken by the Queen Air at lower levels before 22:00 GMT from that taken by the Sabreliner in the middle and upper troposphere after 00:00 GMT (12 January). The aircraft flight tracks were made along an approximate 130° - 310° azimuth, but the distances shown are along the east-west projection of those tracks. From Lilly and Zipser (1972). (Saito, 1994). | 140 |
| Fig. 1-17 Surface weather chart at the time of <i>Yamaji-kaze</i> (09JST, April 21, 1987, arrow indicates depression storm track) (Saito and Ikawa, 1991). | 141 |
| Fig. 1-18 Schematic diagram of <i>Yamaji-kaze</i> (Saito, 1994; adapted from Ogura, 1994) (Kii <i>et al.</i> , 2019). | 142 |
| Fig. 1-19 Typical example of surface wind system at the appearance of daily maximum wind speed on the day when the <i>Rokko-oroshi</i> occurred. (Left) Case of strong winds blowing from the mountainous direction, (Right) Case of wind direction to the west during strong winds (Ino <i>et al.</i> , 2009). | 143 |
| Fig. 1-20 Typical examples of surface weather chart when the <i>Rokko-oroshi</i> occurred for type B (Ino <i>et al.</i> , 2009). Type B: A case in which an extratropical low cyclone or front passed through the area 6 to 12 hours before the downslope winds blew, followed by an overhang of anticyclone from the Yangtze River area on the continent, resulting in a close to winter pressure pattern or a condition before a winter pressure pattern. | 144 |
| Fig. 1-21 Frequency distribution (based on Kobe University observation data) on 528 days of analysis during the cold season from November to March 2001-2005. Left: daily maximum wind speed. Upper right: wind direction at daily maximum wind speed. Lower right: time of appearance of daily maximum wind speed (Ino <i>et al.</i> , 2009). | 145 |
| Fig. 2-1 Location of the study area. Red square is the target area. Matsue and Shionomisaki are the upper-level sonde observatories. | 146 |
| Fig. 2-2 Topography and geographical names of study area. Red square is the JR Sannomiya Station at the center of the Kobe City. Contour lines every 100 m. | 147 |
| Fig. 2-3 The distribution of the AEROS (blue), AMeDAS (orange) and KS (green). Black square is the SST measurement point. Red square is the JR Sannomiya Station at the center of the Kobe City. Contour lines are shown only at elevation 0 and 100 m. | 148 |
| Fig. 2-4 The distribution of the AEROS (blue and green) and AMeDAS (orange) in the Kyoto-Osaka-Kobe area. Blue and green squares indicate wind and temperature observation points, respectively. The red squares indicate the area in Figs. 2-2, 2-3, and 2-6. Contour lines every 200 m. | 149 |

| | |
|--|-----|
| Fig. 2-5 Details of KS station (158 m above sea level; 15 m above ground level). (a) Photograph of the temperature and wind measurement instruments. (b) topography around the KS. Red circle is the point where the device is installed. From Google map (https://www.google.co.jp/maps). | 150 |
| Fig. 2-6 The distribution of the original measurement sites (blue). Red, orange, green and black squares are as described above. Contour lines are shown only at elevation 0 and 100 m. | 151 |
| Fig. 2-7 Photographs and schematic diagram of the temperature measurement site. | 152 |
| Fig. 2-8 Details of temperature measuring instruments. | 153 |
| Fig. 3-1 Windrose at Na. (a) 15:00 JST (b) 03:00 JST. Averaged over 53days. Total of all wind directions is 100%. | 154 |
| Fig. 3-2 Monthly number of days for analysis on selected 31days. | 155 |
| Fig. 3-3 Windrose on selected sunny calm 31 days. (a) 15:00 JST (b) 03:00 JST Contour lines are shown only at elevation 0 and 100 m. Total of all wind directions is 100%. | 156 |
| Fig. 3-4 Vector mean wind distributions on selected sunny calm 31 days. (a) 15:00 JST (b) 03:00 JST Contour lines are shown only at elevation 0, 100, 300 and 500 m. | 158 |
| Fig. 3-5 Hourly vector mean wind distribution on selected 31days. Contour lines are shown only at elevation 0 and 100 m. | 159 |
| Fig. 3-6 Diurnal change in vector mean wind direction on selected sunny calm 31 days. (a) At artificial island (Ri, Mi, AKw and AKA), (b) at En, Na and Hu. Dashed lines in the figure indicate criterion values for wind system classification (15°, 105°, 195°, 270°) | 163 |
| Fig. 3-7 Dendrogram of vector mean wind direction of each station..... | 164 |
| Fig. 3-8 Classification of target area by cluster analysis. Contour lines are shown only at elevation 0 and 100 m..... | 165 |
| Fig. 3-9 Diurnal changes in vector mean wind direction (WD: blue) and speed (WS: orange) averaged over the target 31 days in AKw. | 166 |
| Fig. 3-10 Diurnal changes in temperature and sea surface temperature of AKt (red) and Kobe Port (SST, blue) averaged over the analysis days..... | 167 |
| Fig. 3-11 (a) Weather and sea conditions before and after the start of sea breeze on June 12, 1984. The black arrows indicate wind direction, and the white arrows indicate wind direction at the start of sea breeze. Numbers (e.g., 0837) in the figure are observation times. (b) Horizontal temperature gradients over land and sea before and after the onset of sea breeze, June 12, 1984, K: Hiroshima meteorological observatory temperature, A: Hiroshima airport temperature, C: temperature over the sea. (Nakata, 1985)..... | 168 |
| Fig. 3-12 Surface weather chart at 09:00 JST on October 9 and 10, 2017..... | 169 |
| Fig. 3-13 Diurnal change in wind at Nh on October 9-10, 2017..... | 170 |
| Fig. 3-14 Surface wind distribution on October 9 and 10, 2017. (a) 03:00, (b) 08:00 and (c) 20:00 JST. Contour lines are shown only at elevation 0, 100, 300 and 500 m. | 171 |
| Fig. 3-15 Diurnal change in wind in the plains on October 9-10, 2017. (a) En, (b) Na... .. | 172 |
| Fig. 3-16 Diurnal change in wind on artificial islands on October 9-10, 2017. (a) AKA, (b) AKw, (c) Ri. | 173 |
| Fig. 3-17 Diurnal change in wind and temperature in the lower-slope of the Rokko Mountains (KS) on October 9-10, 2017. | 175 |

| | |
|---|-----|
| Fig. 3-18 Diurnal change in wind at the top of Mt. Rokko (Ro) on October 9-10, 2017. | 176 |
| Fig. 3-19 Diurnal change in temperature at AKt on October 9-10, 2017..... | 177 |
| Fig. 3-20 Surface wind and temperature anomaly distributions at 03:00, 08:00 and 20:00 JST, October 9 and 10, 2017. Contour lines are shown only at elevation 0, 100, 300 and 500 m. | 178 |
| Fig. 3-21 Diurnal change in the pressure difference between AKY and AK on October 9-10, 2017. | 179 |
| Fig. 3-22 Topography and distribution of air temperature observation points in Kobe City. Contour lines are shown only at elevation 0, 100, 300 and 500 m. The red dotted line in the figure indicates the regional classification based on diurnal changes in air temperature. West, Central, Island, East and Mountain are the names of regional divisions. Numbers indicate surface air temperature stations, and alphabets indicate AEROS and AMeDAS stations. | 180 |
| Fig. 3-23 Surface weather chart at 09:00 JST on October 8 (left), 18 (middle), 24 (right), 2014. | 181 |
| Fig. 3-24 Diurnal change of temperature averaged over all locations (October 18, 2014). | 182 |
| Fig. 3-25 Diurnal change in averaged temperature for five regions (October 18, 2014). | 183 |
| Fig. 3-26 Diurnal change in air temperature at sites 2, 4, and 5 (October 18, 2014). | 184 |
| Fig. 3-27 Approximate influence range (red broken line) of cold air drainage on October 18, 2014. The values in the figure indicate the amount of temperature drop from 16:00 to 18:00 JST. Contour lines are shown only at elevation 0, 100, 300 and 500 m. | 185 |
| Fig. 3-28 Surface wind and temperature anomaly distribution on October 18, 2014 (19:00-24:00 JST). Contour lines are shown only at elevation 0, 100, 300 and 500 m. | 186 |
| Fig. 3-29 Diurnal change in averaged temperature at the artificial island on October 8 (black), 18 (red) and 24 (blue), 2014..... | 187 |
| Fig. 3-30 Surface wind and temperature anomaly distribution at 23:00 JST. (a) October 8, 2014, (b) October 18, 2014 and (c) October 24, 2014. Contour lines are shown only at elevation 0, 100, 300 and 500 m..... | 188 |
| Fig. 3-31 Diurnal change in wind direction and speed at AKA. (a) October 8, 2014, (b) October 18, 2014 and (c) October 24, 2014. | 189 |
| Fig. 3-32 Diurnal change in the temperature difference between AKA and AO. (a) October 8, 2014, (b) October 18, 2014 and (c) October 24, 2014..... | 190 |
| Fig. 3-33 Change in temperature difference in 10 min (5-term moving average) for five regions (October 18, 2014). | 191 |
| Fig. 3-34 Observed surface wind field at 07:00-10:00 JST (October 18, 2014). Contour lines are shown only at elevation 0 and 100 m..... | 192 |
| Fig. 3-35 Distribution of wind and air temperature anomaly at 10:00 JST on October 18, 2014. Contour lines are shown only at elevation 0 and 100 meters. | 193 |
| Fig. 3-36 Distribution of wind and air temperature anomaly at 10:00 JST on October 18, 2014. Contour lines are shown only at elevation 0, 100, 300 and 500 m..... | 194 |
| Fig. 3-37 Distribution of wind and air temperature anomaly at 03:00 JST averaged on October 8, 18, 24, 2014. Contour lines are shown only at elevation 0, 100, 300 and 500 m. | 195 |

| | |
|---|-----|
| Fig. 3-38 Distribution of wind and air temperature anomaly at 09:00 JST averaged on October 8, 18, 24, 2014. Contour lines are shown only at elevation 0, 100, 300 and 500 m. | 196 |
| Fig. 3-39 Distribution of wind and air temperature anomaly at 14:00 JST averaged on October 8, 18, 24, 2014. Contour lines are shown only at elevation 0, 100, 300 and 500 m. | 197 |
| Fig. 3-40 Distribution of wind and air temperature anomaly at 16:00 JST averaged on October 8, 18, 24, 2014. Contour lines are shown only at elevation 0, 100, 300 and 500 m. | 198 |
| Fig. 3-41 Distribution of 2-hours air temperature change averaged on October 8, 18, 24, 2014. (a) 15:00-17:00 JST, (b) 06:00-08:00 JST. Contour lines are shown only at elevation 0, 100, 300 and 500 m. | 199 |
| Fig. 3-42 Wind direction frequency for 11 sunny days in KS (Total of all wind directions is 100%). | 200 |
| Fig. 3-43 Diurnal change of wind and temperature at KS and AKt averaged on 11 sunny days. (a) Mean wind direction and air temperature, (b) mean wind speed. | 201 |
| Fig. 3-44 Wind direction frequency from 07:00 to 15:00 JST for 11 sunny days in KS (Total of all wind directions is 100%). | 202 |
| Fig. 3-45 Wind direction frequency for 4 cloudy days in KS (Total of all wind directions is 100%). | 203 |
| Fig. 3-46 Diurnal change of wind and temperature at KS and AKt on 4 cloudy days. (a) Mean wind direction and air temperature, (b) mean wind speed. | 204 |
| Fig. 3-47 Surface weather chart at 09:00 JST on November 4, 2016. | 205 |
| Fig. 3-48 Diurnal change of wind and temperature at KS and AKt on a clear day (November 4, 2016). (a) Mean wind direction and air temperature, (b) mean wind speed. | 206 |
| Fig. 3-49 Diurnal change of wind and temperature at AKA averaged on 11 sunny days. (a) Mean wind direction and air temperature, (b) mean wind speed. | 207 |
| Fig. 4-1 Distribution of wind direction in minute and speed at KS during the research period. | 208 |
| Fig. 4-2 Wind speed frequency distribution at KS during the research period. | 209 |
| Fig. 4-3 Wind direction and speed frequency distribution during the occurrence of <i>Rokko-oroshi</i> at KS during the research period. | 210 |
| Fig. 4-4 Wind speed frequency distribution during the occurrence of <i>Rokko-oroshi</i> at KS during the research period. | 211 |
| Fig. 4-5 Distribution of <i>Rokko-oroshi</i> occurrence time during the research period. | 212 |
| Fig. 4-6 Surface weather chart at 09:00 JST on November 4, 2017. | 213 |
| Fig. 4-7 Diurnal change of temperature on November 4, 2017. (a) KS (black), Ro (green) and SA (blue), (b) AKt (red) and AKA (blue) | 214 |
| Fig. 4-8 Diurnal change of wind speed on November 4, 2017. (a) KS, Ro and SA, (b) AKw and AKA | 215 |
| Fig. 4-9 Diurnal change of wind direction on November 4, 2017. (a) KS, Ro and SA, (b) AKw and AKA | 216 |
| Fig. 4-10 Observed surface wind field at 12:00-17:00 JST on November 4, 2017. Contour lines are shown only at elevation 0 and 100 m. | 217 |

List of tables

| | |
|---|-----|
| Table 1-1 Name and synoptic conditions associated with local winds in Japan. The numbers refer to their location on the map in Fig. 1-14 (b) (Kusaka and Fudeyasu, 2017)..... | 218 |
| Table 2-1 Summary of original meteorological sites. | 219 |
| Table 2-2 Summary of AMeDAS and radiosonde sites. | 220 |
| Table 2-3 Summary of AEROS sites..... | 221 |
| Table 3-1 List of dates for the analysis days (31 days when the sea and land breeze alternation occurred, April to November 2011) | 222 |
| Table 3-2 Direction of prevailing wind at 15:00 and 03:00 JST at each location and wind direction..... | 223 |
| Table 3-3 Classification of wind systems and wind direction range in this study. | 224 |
| Table 3-4 Classification of observation points by cluster analysis. | 225 |
| Table 3-5 Hourly changes in vector mean wind direction and speed. (a) Wind direction, (b) wind speed | 226 |
| Table 3-6 Hourly wind direction at each station (October 18, 2014)..... | 228 |

Acknowledgment

I would like to express my gratitude to my chief examiner, Professor Jun Matsumoto of Department of Geography, Tokyo Metropolitan University (Dept. Geogr., TMU) for giving me insightful comments and suggestions that make my research of great achievement.

I am deeply grateful to Professors Hideo Takahashi, Hiroshi Matsuyama and Fumiaki Fujibe (Dept. Geogr., TMU) for their constructive comments and considerable encouragement.

I also owe my deepest gratitude to Doctor Yoshinori Shigeta of Tottori University of Environment for his assistance during the observation. Without his guidance and persistent help the observation would not have been possible.

The observation was supported by the Kobe City Office.

Finally, I greatly appreciate all members of the Laboratory of Climatology and Department of Geography, Tokyo Metropolitan University, as well as deeply gratefulness to my wife, colleagues and pupils for their understanding, support, and warm encouragement.

Abstract

It has been known that thermally induced local circulation such as sea and land breeze and mountain and valley breeze develop on sunny calm days in the Seto Inland Sea area in Japan. In this study, we investigated the relationship between temperature and local wind systems focused on the diurnal variation around Kobe, western Japan, where the mountains and the bay are close to each other and the urban area is located in a narrow zone area between the mountains and the bay. By using data from existing meteorological observation stations as well as data from our own wind and temperature observation stations, we obtained the following findings on the diurnal variation of the local wind system and its effect on temperatures.

Based on previous studies, it is known that sea and land breeze circulation prevails as the diurnal variation of wind on sunny calm days around the target area. However, in previous studies, sea and land breeze around Kobe was often considered as a part of sea and land breeze around Osaka Bay or the Seto Inland Sea from the viewpoint of meso-scale climatology. Therefore, for example, the winds in Kobe were represented by a single AMeDAS station in Kobe, and the time of analysis was every three hours. This level of temporal and spatial resolution is sufficient to obtain the characteristics of the wind system over a broad area. However, the temporal and spatial data were not sufficient to capture the diurnal variation of wind and temperature around Kobe from the small climatological scale of sea and land breeze and mountain and valley breeze. Under these circumstances, the knowledge of diurnal variations in the Kobe area on a small scale is not sufficient, and we do not necessarily have clear understanding of the alternation times of sea and land breezes, extended sea breezes and mountain breezes, and the magnitude and range of their effects on temperatures.

We first clarified the climatological characteristics of sea and land breezes around Kobe. In this study, we analyzed the average diurnal variation of wind by

selecting days when the sea and land breeze alternated among sunny calm days during the warm season and the autumn season. The results show that the region can be divided into three groups based on the characteristics of diurnal variations in wind direction, and that there are five stages in the transition of the local wind system. Specifically, the target area was divided into eastern area, western area, and coastal areas to artificial islands according to the different influence of thermally induced local circulation at different scales. The wind system consists of four types of circulation: sea breeze, southwesterly extended sea breeze, mountain breeze from the Rokko Mountains, and easterly land breeze, which shift in five phases. In previous studies, the southwesterly winds prevailing around Kobe and the northeasterly to easterly winds have sometimes been referred to as "extended sea and land breezes. However, there are few cases that have confirmed the correspondence with the broad-scale wind system when such winds actually occur. In this study, using AEROS observation data, we were able to grasp the relationship with the broad-scale wind system in the Kyoto-Osaka-Kobe area and to confirm, although qualitatively, that sea and land breezes of different scales are observed in the target area.

Among the four wind systems, sea breeze tended to have a relatively short duration of blowing compared to the other wind systems. However, same as extended sea breeze, the effect on temperature in the target area was observed, suggesting that the onset of sea breeze suppressed the temperature increase in the morning and that the rate of temperature decrease was enhanced by extended sea breeze in the afternoon.

Next, we conducted a case study of two consecutive sunny calm days with different diurnal variations of wind on the plains and examined the differences. The results suggest that the diurnal variation of winds over the two days mainly reflects the diurnal variation of extended sea breeze and land breeze, and that the wind systems around Kobe show different diurnal variation of winds even on the same sunny calm day due to their influence. We found the possibility that the diurnal variation of these broad-scale wind systems is determined by the pressure system differences between

the Kyoto-Osaka-Kobe area.

Next, we examined the relationship between local wind systems and temperature. As a result of examining the diurnal variation of temperature on sunny calm days at individual stations using temperature data from 33 originally developed stations, it became clear that the target area can be divided into five regions (east, west, central, mountain, and artificial islands) based on the characteristics of their characteristics. Among the five regions, the rapid drop in temperature after 16:00 JST at the foot of the mountains and the re-rise in temperature around 22:00 JST on the artificial islands were the most distinctive features. It is possible that the cool mountain breeze is responsible for the temperature decrease at the foot of the mountain, while the relatively warm land breeze is related to the temperature increase on the artificial island. Previous studies have shown that the range of the effect of mountain breeze on temperature reduction is about 1 km. The study showed that the range of influence varied from station to station, with the eastern part of the target area extending up to the coastal stations and the central part of the city tending to have a smaller range. The mountain breeze begins to blow around 15:00 to 16:00 JST when extended sea breeze prevails over the plains and artificial islands in the target area, and that the temperature drops by 4 to 5°C rapidly. This mountain breeze is generally stable at wind speeds of 1-2 m/s from evening to dawn in the lower-slope of the mountain and at stations near the foot of the mountain.

Finally, we attempted to understand the general characteristic of *Rokko-oroshi*, which is a downslope wind caused by the dynamic effect of mountain, contrasting with sea and land breezes and mountain and valley breezes, which are thermally induced local circulation. We conducted a case study of *Rokko-oroshi* by installing original observation point for temperature and wind in the lower-slope of the Rokko Mountains. The maximum wind speed of *Rokko-oroshi* during the observation period was 13 m/s, and 7.5 to 8.5 m/s accounted for almost 45% of the observed wind speeds. With the start of the *Rokko-oroshi*, there was a sharp drop in temperature of about 8°C

in the lower-slope of the mountains, which is twice the amount of the temperature reduction caused by mountain breeze. The effect was not limited to the foot of the mountains but was also observed at a station about 10 km from the foot of the mountains, where a temperature reduction of about 5°C was also observed.

As described above, this study clarified the relationship between the local wind system around Kobe and temperature from the viewpoint of diurnal change in local circulation, using data from existing stations and original observations. As a result, we found that there are regional differences in the local wind system and diurnal variation of temperature as a characteristic of the local climate in the Kobe area, which has not been clarified so far. Specifically, the Kobe area can be divided into three regions according to the diurnal change in local wind system and five regions according to that in temperature. In the Kobe area, where the Rokko Mountains are located behind the city, mountain breeze (cold air drainage) from the Rokko Mountains have a significant influence. Therefore, it is suggested that mountain breeze may be more dominant than extended land breeze from the evening to early morning in the foot area, indicating that mountain breeze characterize the unique climate of the target area. The effect of mountain breeze and *Rokko-oroshi* on temperature reduction and its range could also be quantitatively evaluated to a certain extent.

However, numerical simulations are required to verify the mechanism of each circulation. In addition, since the case study in this research was limited to a certain number of days, it is necessary to verify the generality of the results of this research by increasing the number of cases to be analyzed, as well as by further theoretical verification.

1. Introduction

1.1 Local winds in Japan

The distribution of surface winds is generally highly localized (e.g., Kitabayashi, 1976) because it is greatly affected by regional characteristics such as sea, land, and mountain distributions. Such region-specific winds that blow over a limited area of a few kilometers to 100 kilometers are called local winds (Arakawa, 2011).

Local winds can be divided into two main types according to their causes: kinetic winds and thermally induced winds caused by topographical factors and thermal inhomogeneity, respectively. Japan has a complex topography, which makes it susceptible to local winds, and in fact, there are various types of local winds in Japan (Yoshino, 1975; Fig. 1-1). Kusaka and Nishi (2012) provide an overview of the local winds in Japan, and discuss the relationship between topography and winds, focusing on the famous *Yamaji-kaze* and *Kiyokawa-dashi*, which are strong winds driven by topography and are closely related to human life. *Yamaji-kaze* is a strong southerly wind that occurs in the northern part of the Shikoku Mountains and the plains facing Hiuchi-nada on the Seto Inland Sea, western Japan. *Kiyokawa-dashi* is a strong easterly wind that blows from the Kiyokawa area to the Shonai Plain, which is the outlet of the Mogami Gorge in Yamagata Prefecture, northeastern Japan. Additionally, they introduce *Karak-kaze*, which is influenced not only by topography but also by thermal causes. Thermally induced wind is a local circulation that develops over rough terrain due to thermal causes (Kimura, 1994); sea and land breezes and mountain and valley breezes are well known examples. Most Japanese cities are located on coastal plains and are therefore strongly influenced by sea and land breezes.

Local winds are also known as local circulation, and the kinetic and thermal winds shown by Kusaka and Nishi (2012) are sometimes described as dynamic and thermal local circulations, respectively (Kimura, 1994). They are known to have a close

relationship with synoptic scale pressure patterns and pressure gradients (e.g., Yoshikado, 1978; Suzuki and Kawamura, 1987; Fig. 1-2), though they are highly localized. Therefore, many studies have discussed the differences in the appearance patterns of surface wind systems depending on the wind direction and speed of geostrophic or general winds (e.g., Kawamura, 1963, 1966).

1.2 Sea and land breezes

1.2.1 Outline of sea and land breezes

Sea and land breezes are thermal local winds caused by the difference in surface temperature between the sea and land. The energy source is sensible heat from the ground and sea surface (Kimura, 1992). Specifically, this is a convection phenomenon caused by the difference in surface temperatures due to the distribution and topography of the sea and land (Atkinson, 1981; Local Wind Research Division of the Agricultural Meteorological Society of Japan, 1995).

Defant (1951) is a general text on local winds including sea and land breezes, and Yoshino (1975) covers local climate widely. The Meteorological Society of Japan (1975, 1988) is comprehensive Japanese reference that summarizes sea and land breezes. A relatively newer review has been provided by the Local Wind Research Division of the Agricultural Meteorological Society of Japan (1995a, b).

The basic cause of sea and land breezes is horizontal convection caused by the difference in temperature between the sea and land. The sea breeze is a phenomenon in which cold and dense sea air flows under warm, less dense land air during the daytime at the limited to the surface level (Local Wind Research Division of the Agricultural Meteorological Society of Japan, 1995b). Generally, the horizontal scale of sea and land breezes circulation is several 10 to 100 km, and the vertical scale is about 1000 m (Fujibe and Asai, 1979; Asai, 1996). The sea and land breezes has a range of 20 to 40 km from the coastline in the Kanto region (Fujibe and Asai, 1979) and that of 30 to 40

km in the Tohoku region (Takimoto and Sakaida, 2012).

As the thermal local circulation, including sea and land breezes, develops on sunny calm days, statistical analysis of sea and land breezes often are conducted using weather (solar radiation and sunshine duration) and general wind strength (pressure gradient) as criteria to determine days when the sea and land breezes occur. In this regard, Kawamura (1977a) pointed out that when the geostrophic wind speed is 7 m/s or stronger, a local wind system is formed due to the deflection of the geostrophic wind by the topography, and when the geostrophic wind speed is 7 m/s or lower, thermal circulation, such as sea and land breezes, becomes prominent. On the other hand, Suzuki (1994) shows that in the case of sea and land breezes in Japan, they generally do not appear when the synoptic pressure gradient exceeds 1.8 hPa/100 km.

Sea and land breezes are caused by the difference in temperature between the sea and land, but there is insufficient data to quantitatively support this. This is because air temperatures on land and water temperatures are generally measured along the coast, and offshore sea surface temperatures are often not observed.

Fujibe and Asai (1984) measured temperatures at sea and on land in summer around Sagami Bay and showed diurnal variations (Fig. 1-3). The reason for the large difference in daily temperature variation between the land and sea, i.e., the solar radiation reaches the ocean water and the incident heat is distributed much deeper than on land, resulting in smaller diurnal variations in water temperature (Oke, 1978). The mixing of seawater also serves to disperse the heat, such that there is almost no difference in sea surface temperature between day and night, and diurnal variations in air temperature over the sea are also very small. Therefore, the air temperature on land is higher than that on sea during the daytime, and this difference in air temperature leads to the occurrence of sea breeze blowing from the sea to the land. At night, the land cools and the air temperature distribution between land and sea is reversed, and the land breeze blows from land to sea (Fujibe, 2012).

Mori (1994) investigated the seasonal variation of monthly maximum and minimum temperatures on land and sea surface temperature in Matsuyama, Ehime prefecture in Shikoku district and found that the difference between daily maximum temperature and sea surface temperature increases from spring to summer, which facilitates the development of sea breeze, whereas the difference between daily minimum temperature and sea surface temperature decreases, which makes it difficult for land breeze to develop at night. This relationship is reversed from autumn to winter. Neyama (1982) confirmed this relationship by showing the difference in mean wind speeds between sea and land breezes in different seasons.

Previous studies on sea and land breezes have been conducted from various perspectives, including clarification of its formation mechanism, understanding of its three-dimensional structure, and verification by modeling. So far, many studies on sea and land breeze have been widely conducted both nationally and internationally. Particularly, in the case of Japan each region has different characteristics not only because it is surrounded by the sea, but also because the topography of each region varies greatly. For this reason, studies on sea and land breezes were actively conducted in various regions of Japan, including the case of Sahashi (1978) in Okayama and Mori (1996) along the Seto Inland Sea coast, as described below. There are also reports on the occurrence of sea breeze in winter in Tokyo Bay (Tsuchida and Yoshikado, 1995), statistical analysis of the frequency of sea and land breezes in Ise Bay (Mori *et al.*, 1994), and the differences in properties between sea and land breezes in Osaka Bay (Eguchi, 1977).

1.2.2 Extended sea breeze

In Japan, sea and land breeze has been studied in many areas because most of the population is concentrated in the plains facing the sea. Among them, sea and land breeze around Sagami Bay has been studied in many cases due to the interest in air

pollution in the Kanto plain, as well as many studies that deal with mountain and valley breezes in combination due to the effect of undulating land (Okouchi and Wakata, 1984).

In the Kanto plain, it is known that sea breeze and valley breeze combine due to the thermal effect of the mountains to form extended sea breeze that cover the entire plain in the afternoon. Particularly, a wind system is known to cover the entire Kanto plain (Fujibe and Asai, 1979), and the combined sea and valley breezes is called "extended sea breeze" (Kondo, 1990a). According to Kawamura (1977b; 1977c), the synoptic pressure gradient is weak, and the entire Kanto region is covered by southerly winds at approximately 15:00 JST on clear days in warm season. Fujibe and Asai (1979) found that such large-scale wind systems have two scales of diurnal variation, with the horizontal extent of the larger wind system being 200 km and its thickness being 1–1.5 km, and they named this large-scale wind system "extended sea breeze". It was also clarified that this extended sea breeze is caused by the combination of four different wind systems (Kurita *et al.*, 1988, Figs. 1-4,1-5,1-6) and was revealed the relationship between its penetration limit and synoptic field (Kurita and Ueda, 1985). Low and high pressure areas were shown to appear locally during the daytime and night, respectively, over the inland areas of central Japan, and many studies related to such thermal low and high were conducted on surface wind systems (e.g., Shimizu, 1964; Kuwagata and Sumioka, 1991). Kurita *et al.* (1988) and other studies pointed out that these thermal lows are involved in the formation of extended sea breeze over the Kanto Plain.

1.2.3 Sea and land breezes in the Kanto Plain

There are many plains in Japan, including the Kanto Plain which has the largest area. In addition to studies on sea and land breeze in the Kanto Plain, the Nobi Plain, the Osaka Plain, and the area around the Seto Inland Sea, where the population is

concentrated, there have been also many studies in the other plains. For example, Sumi (2013) in the Ishikari Plain in Hokkaido, Akita (1993) in the Tsugaru Peninsula in Aomori Prefecture in the Tohoku region, Sakaida *et al.* (2011) in Sendai City, Miyagi Prefecture, Chiba *et al.* (1993) in Kochi Prefecture in Shikoku, and Kusuda and Abe (1982) in Oita City, Oita Prefecture in Kyushu. These studies are just a few examples among many. The Kanto Plain is the largest plain in Japan. It is bordered on the east and south by Tokyo Bay, Sagami Bay, and the Kashima Sea, and on the west and north by the Kanto Mountains and other mountainous areas. This topography contributes to the formation of local winds, such as sea and land breezes and mountain and valley breezes, which are generated by thermal effects during sunny summer days. The wind system in the Kanto Plain is complex due to the complicated distribution of sea and lands in the region and the mountains surrounding the Kanto Plain. However, when the pressure gradient of the synoptic field is weak, the diurnal variation of the wind system is mostly caused by sea and land breezes (Fujibe, 1985), and the local wind system in the Kanto region in summer is dominated by the sea and land breezes.

Regarding the wind system in the Kanto Plain on clear summer days, Kawamura (1970; 1974) pointed out that sea breeze orthogonal to the coastline occurs in the morning, whereas the inland wind system becomes obscured in the afternoon and the whole area of the Kanto Plain is covered by southerly winds. Fujibe and Asai (1984) conducted a detailed observational study in the coastal area of Sagami Bay to investigate the vertical structure and diurnal variation of sea and land breeze in Sagami Bay. Their results showed that sea breezes begin to blow from the lower coastal layer and increase in thickness. In the afternoon, sea breezes spread both horizontally and vertically. In the late afternoon, the air pressure gradient near the coast decreases, and the sea breeze from the lower coastal layer weakens (Fig. 1-7).

Fujibe and Asai (1979) showed that in addition to typical sea and land breezes, large-scale winds play an important role in the diurnal variation of the wind system

over the Kanto Plain. This large-scale wind system is extended sea breeze, as mentioned earlier and its existence has been pointed out in the Nobi Plain and the Kinki region (Mori *et al.*, 1994; Itoh, 1995; Kitada *et al.*, 1998). The formation of extended sea breeze in the Kanto Plain was studied using vertical observations (Fujibe and Asai, 1979; Kurita *et al.*, 1988; 1990) and numerical model calculations (Kondo, 1990b). According to these studies, a complex wind system, consisting of local wind systems such as sea and land breezes and mountain and valley breezes, is observed in the morning, but these local wind systems are integrated in the afternoon. Therefore, large-scale winds blow toward the thermal low that occurs in the central mountainous region. It has also been noted that the valley-like inland topography and distance to the coastline act to combine sea and valley breezes (Kondo, 1990c).

The local wind system in the Kanto region is known to be affected by the synoptic scale pressure gradient (Suzuki and Kawamura, 1987), and the wind system changes depending on the direction and magnitude of the pressure gradient. For example, when the direction of the geostrophic wind corresponding to the pressure gradient coincides with that of the sea breeze, the sea breeze is stronger. However, when the geostrophic winds blow in the opposite direction, the sea breeze is rarely generated (Yoshikado, 1978; 1981). The relationship between geostrophic and surface winds is affected by topography and other factors. Therefore, the wind direction of surface winds varies with the geostrophic winds (Mori, 1985), and geostrophic winds alone cannot explain the changes in the wind system.

1.2.4 Effect of sea and land breezes on air temperature

On sunny summer days when the general winds are weak, sea and land breezes blow near the coast due to thermal factors, and sea breezes with cold air advection blowing toward the land during the daytime. Many Japanese cities are located near the sea, and the sea breeze is expected to suppress the rise in air temperature in the cities

during the daytime in the summer. Many studies have discussed the relationship between sea breeze and air temperature distribution, especially in the Tokyo metropolitan area (Mikami, 2006).

On calm, sunny days when sea and land breezes develop, the heat island phenomenon, in which the difference in air temperature between the inside and outside of an urban area becomes apparent, is also likely to occur. This phenomenon was found to occur not only in large cities but also in small villages (e.g., Tamiya and Oyama, 1981). Therefore, these two atmospheric phenomena, i.e., sea and land breezes and heat island phenomenon, are highly likely to occur simultaneously under a similar synoptic field in urban areas located in a coastal plain. Many studies have been conducted on the relationship between the two phenomena.

In a study of local wind systems and air temperature distributions in southern Kanto, Yamato *et al.* (2011) investigated the impact of sea breeze on the metropolitan heat island phenomenon during summer days using data from the Meteorological Observation System for High-Density Observations (Metropolitan Environmental Temperature and Rainfall Observation System; METROS), which was installed to determine detailed temperature distributions in Tokyo. The study revealed that the movement of the center of the high-temperature region is closely related to the inland movement of sea breeze fronts. Takahashi and Takahashi (2014) also showed that land breezes blowing from inland at night are related to the air pressure drop associated with urban heat islands, and that land breeze fronts may be stationary near the city center or may pass through the city center and reach the sea. Furthermore, the slow intrusion of sea breeze with cold air advection on the leeward side of the urban area was shown to be a factor contributing to the high temperatures in the inland plains in summer afternoons (Yamato *et al.*, 2017; Fig. 1-8).

Additionally, Sakaida *et al.* (2011) conducted detailed meteorological observations in Sendai city and its surrounding suburbs, northeastern Japan to clarify

the effect of sea breezes on the urban heat island. They confirmed that air temperature at the central Sendai city increases is capped by the entry of sea breezes during spring and summer days, and that the cooling effect is almost the same in the city center and the suburbs, which are located at about the same distance from the coast. Furthermore, Junimura and Watanabe (2008) showed that in Sendai city in August, the suppression effect of sea breeze on the increase in air temperature is stronger with higher wind speed, and that the temperature suppression effect ranges from 4 to 11 °C, with the effect extending inland by approximately 13 km. Regarding the effect of sea breeze on the distribution of air temperatures near the ground surface during the daytime, Takebayashi *et al.* (2005), based on observations by Osaka Prefecture, stated that the effect is generally explained by the distance from the coast. As a case study of a coastal urban city similar to Osaka, Sato and Kimura (2014) reported the relationship between sea and land breeze circulation and air mass movements in an urban area in Hiratsuka City, Kanagawa Prefecture and showed that the high temperature area in the Hiratsuka city area which occurs during the nighttime on calm days in the warm season moves inland to the north with the onset of sea breeze after sunrise. The sea breeze intrusion along the Sagami River is also clear and suppresses the daytime temperature increase.

1.2.5 Sea and land breeze around Kobe

Sea and land breezes often develop in the Kobe area due to its proximity to the Seto Inland Sea and Osaka Bay. Sea and land breezes have been focused not only around Kobe but also along the Seto Inland Sea coast since ancient times, and many studies have been conducted mainly in the 1970s (e.g., Osaka District Meteorological Observatory, 1971; 1972; Mizuma, 1995; Miyata and Okamoto, 1972; Ino and Neyama, 1972; 1973; Yamamoto, 1974; Kishida, 1974; Neyama, 1974; Kuniyasu and Neyama, 1975). The term "*Seto no Yu-nagi*" (evening calm) is also well known in this regard. Mori (1983) investigated the climatological characteristics of diurnal variation in wind

at 16 sites along the coast of the Seto Inland Sea, and showed that the direction of rotation of the vector mean wind is clockwise throughout the year in Osaka, Kobe, Fukuyama, Takamatsu, Tokushima, and Hiroshima (Fig. 1-9).

The sea and land breeze over the Seto Inland Sea was reviewed by Neyama (1982), who found that the development of sea and land breezes and the duration of calm periods (“*Nagi*”) varied considerably from region to region, reflecting the complex topography of the Seto Inland Sea, and that Himeji and Hiroshima Cities experience land breeze of a certain strength, whereas land breeze in Okayama are considerably weaker. The study points out that Kobe has a typical sea and land breeze system where the wind direction at 15:00 and 03:00 JST is almost orthogonal to the coastline and reverses 180° during the day and night. As for sea and land breeze speeds, based on the mean maximum wind speeds at 60 observation sites, 70% of sea breezes had a speed of 2.5–4.4 m/s, and 82% of land breezes had a speed of 0.6–3.4 m/s indicating that the average maximum sea breeze speed is 4 to 5 m/s and land breeze speed is approximately 1 to 3 m/s (Fig. 1-10). Moreover, they pointed out that the sea and land breezes along the coast of the Seto Inland Sea are not likely to appear alone due to the geographical features and are more likely to appear in combination with mountain and valley breeze in the mountainous areas behind the coast.

In the Harima Plain of Hyogo Prefecture, the wind direction is mostly north-south. From spring to autumn (March to September), sea breezes blow from the Seto Inland Sea in the south toward the land in the north during the daytime, and land breezes blow from the land in the north toward the sea during the night all year round. Sea breezes blow only from spring to summer, and not during autumn or winter (October to February). Land breezes have wind speeds of approximately 2 m/s and include mountain breezes from the Chugoku Mountains, which bring cool air to the urban area on summer nights. Sea breeze wind speeds are the strongest in summer, at around 3–4 m/s (Kusaka and Fujibe, 2018).

Kasuya and Kawamura (2011) investigated wind system variations during calm summer days over the entire Chugoku and Shikoku regions in order to clarify the relationship between diurnal variations in Global Positioning System (GPS) precipitable water amounts and thermally induced local circulation. The composite distribution of sea level pressure and surface winds shows that thermal low occurs in the Chugoku region in the afternoon during the summer season, and that the peak period is from 16:00 to 17:00 JST, and that sea breeze continues until around 18:00 JST in coastal areas, but changes to land breeze after 19:00 JST, while inland areas also change from valley breeze to mountain breeze or calm conditions during the same time period (Fig. 1-11).

Sahashi (1978) pointed out that there are two types of sea breeze with different directions around Okayama, and that their directions are determined by the location of synoptic scale anticyclones. Mori (1996), focusing on the relationship with air pressure field, pointed out that there are two prevailing wind directions in sea breeze, which are determined by geostrophic wind, not only in Okayama but also in Tadotsu and Takamatsu on the opposite shore of the Seto Inland Sea. Kono and Nishizuka (2006) examined the relationship between sea and land breeze and sea surface temperature in Himeji, and found that in the Harima Plain, northerly winds are very frequent at night and blow regardless of the season, and sea breeze is frequent from spring to summer and very rare from autumn to winter, based on the difference in sea and land temperatures and the wind direction in Himeji City.

Fukushima and Nonaka (2020) investigated the relationship between the number of heat stroke cases in Kobe and the occurrence of sea breeze, and showed that southwest and south-southwest sea breezes are frequently observed for a long period of time from around 11:00 JST to after midnight based on statistical analysis of wind direction. The number of heat stroke victims on sea breeze days and not sea breeze days in July was compared, and the number of heat stroke victims on sea breeze days

was found to be smaller than that on not sea breeze days.

Meanwhile, many studies have examined sea and land breezes in the Osaka Plain, among which Eguchi (1977), who conducted a statistical analysis regarding summer (June-September) to evaluate the general characteristics of sea and land breeze in Osaka, evaluated the sea breeze penetration velocity and found that a sea breeze front passes through Osaka City in approximately two hours and that the maximum wind speed reaches in approximately four hours after the sea breeze begins to blow. Takebayashi and Moriyama (2009) found that sea breezes penetrate inland to the Osaka Plain on clear summer days, but that the air temperature moderation effect of this intrusion is smaller than that near the coast. Mizuma (1995), who analyzed the general characteristics of sea and land breeze over western Japan, including the Osaka Plain, found that there are five types of sea breeze behavior, with the most frequent type characterized by sea and valley breezes or upslope winds occurring almost simultaneously and southerly sea breeze continuing until late afternoon in the Osaka Bay coastal area (Fig. 1-12).

In the Kinki district, extended sea breeze is known to blow from offshore Kii Channel to inland areas of the Kinki district via Osaka Bay and the Harima Nada Sea (e.g. Sato, 1982; Ito and Kawazoe, 1983; Mizuma, 1985). Mizuma (1995) analyzed Automated Meteorological Data Acquisition System (hereinafter referred to as AMeDAS) data for the Kinki region and found that extended sea breezes prevailed around Osaka Bay from 15:00 to 16:00 and 22:00 to 23:00, with wind speeds similar to or higher than those of the local sea breezes. Ito (1995) conducted detailed numerical model experiments to reproduce extended sea breeze (Fig. 1-13), and discussed the important topography for its occurrence. The results of these studies indicate that extended sea breeze around Kobe generally has a southwesterly wind direction, and similar results are shown in Ishii *et al.* (2000) and Tamai and Arimitsu (2008).

Mizomoto and Ishihara (2009) showed that the diurnal variation of wind

direction in Kobe, located at the northern end of Osaka Bay, prevails throughout the year with a clockwise rotating component, especially in June, August, and September, as a result of the combination of normal-scale sea and land breezes with diurnal variation of extended sea breezes.

On the other hand, the Architectural Institute of Japan (2000) investigated the diurnal variation of wind in the Osaka Bay area on sunny summer days from 1990 to 1992, and pointed out that the wind direction in Kobe changes from north to northeast due to the influence of large scale land breeze blowing from the Osaka Plain toward Osaka Bay during the night.

Thus, knowledge of sea and land breezes has been accumulated in the Seto Inland Sea area including Kobe. As a result, it is clear that in the diurnal variation of wind on sunny calm days in Kobe, the diurnal variation of sea and land breezes prevails, and that two types of sea and land breezes with different scales shift.

However, in many previous studies, the diurnal variation of wind in Kobe has been represented by AMeDAS Kobe, which does not necessarily provide a sufficient understanding of the characteristics of the diurnal variation of the local wind system at the urban scale in the area surrounding Kobe. Even though Kobe is one of the cities where the sea and land breezes prevail around the Seto Inland Sea and Osaka Bay, the Rokko Mountains are located behind the urban area. Therefore, Kobe has different geographical characteristic from other cities where urban areas are located between the mountains and the bay. Therefore, it is important to consider the influence of the Rokko Mountains when considering the diurnal variation of wind around Kobe. For this purpose, an analysis using data of AMeDAS Kobe alone is not sufficient, and an analysis using wind data located at a higher density is required..

The extended sea breeze of southwesterly prevailing winds from afternoon to night has also been analyzed using AMeDAS data over a wide area and reproduced by numerical experiments. Although the extended sea breeze develops from 15:00 to

17:00 JST, the detailed conditions in the area around Kobe are not captured due to the small density of observation stations. The Architectural Institute of Japan (2000), on the other hand, used the data from the Atmospheric Environmental Regional Observation System under the control of the Ministry of the Environment (AEROS), which is deployed in the Kobe area, to show the distribution of wind rose during the daytime (06:00-18:00 JST) and nighttime (19:00-05:00 JST). However, data over artificial islands, which is considered to be important stations for capturing the alternation of sea and land breezes, are not used. Therefore, in order to capture the characteristics of diurnal variations of wind including sea and land breezes shift of different scales, the stations on the artificial islands should be included. Additionally, it is necessary to analyze the wind system on an hourly scale.

On the other hand, the Architectural Institute of Japan (2000) suggests that "extended land breeze" blowing on the scale of between the Osaka plain and Osaka bay occurs at night, but no detailed study has yet been conducted on this point. In the following, the term "extended land breeze" is used for the sake of convenience to refer to the broad land breeze described by the Architectural Institute of Japan (2000). Mizuma (1995) shows a broad-scale wind system at 03:00 JST, but the density of observation points is small due to the use of AMeDAS, so it does not capture the "extended land breeze" as suggested by the Architectural Institute of Japan (2000). Ito (1995) shows the results of numerical experiments at 08:00 and 20:00 JST, but in both cases the wind system is unclear, and it is not possible to determine whether a wind system exists from the Osaka Plain to Osaka Bay.

From the above, it can be inferred that the diurnal variation of the wind system in the vicinity of Kobe may differ from that of other cities in the Osaka Bay area because of its unique topographical features, including the presence of mountains in the background. It is especially important to clarify the influence of the Rokko Mountains on the wind system and how the nighttime "extended land breeze" is observed in the

area around Kobe in order to better understand the diurnal variation of the local wind system.

1.3 Mountain and valley breeze, cold air drainage

1.3.1 Outline of mountain and valley breeze

Slope winds and mountain and valley breezes are wind systems caused by the heating and cooling of slopes. Under calm, clear nighttime weather with a weak synoptic pressure gradient, a ground inversion layer is formed in conjunction with the progression of radiative cooling. If the ground surface is sloping, the ground layer atmosphere, which has become gravitationally heavier due to the cooling, moves to lower elevations. When this phenomenon occurs on mountain slopes, it is called "cold air drainage" or "downslope wind." Furthermore, the flow of air blowing down from higher elevations at night in mountain valleys is called "mountain breeze" (Sato, 2014). Mountain breezes have small inter-diurnal or temporal variations in wind direction because they are less affected by general winds when cold, heavy air covers the surface winds (Fujibe, 2012).

Both the mountain and valley breezes and the sea and land breezes described in the previous section are local winds in which the horizontal temperature gradient (pressure gradient) is reversed during the daytime and at night, and the wind direction changes in a daily cycle due to the shift in the location of heat sources receiving solar radiation between sea and land, or between flat land and mountain slopes. Sea and land breezes prevail in coastal areas, while mountain and valley breezes appear in valleys and mountainous areas.

However, Neyama (1974) noted that in places such as the Seto Inland Sea, where coastal areas and mountainous areas coexist within a distance of only a few tens of kilometers, sea and land breeze and mountain and valley breezes should mutually

influence each other in some manner at some time and place, and analyzed data from Kure, Hiroshima Prefecture. Sea breeze and upslope wind (during the daytime) were found to always have the same wind direction (same circulation system), and land breeze (at night), upslope and downslope winds were found to occur sometimes depending on the difference in the east and west components of the wind at 1000 m altitude.

Two major models were proposed for such mountain and valley breezes. Wagner (1932) classified mountain and valley breezes into two categories based on the results of pilot balloon observations in the valley. The first is the slope wind (upwind and downwind), which is the circulation in the plane perpendicular to the axis of the valley, and the second is the mountain and valley breeze, which is the circulation along the axis of the valley in a narrower sense. The former is the ascending and descending airflow caused by the temperature difference between the temperatures on the slope and at the same altitude above the center of the valley, while the latter is the airflow blowing from low to high elevations and vice versa along the axis of a large valley in mountainous regions. In both cases, the wind direction is reversed during the daytime and at night.

Contrarily, Defant (1951) showed a typical schematic diagram of the combined state of mountain and valley breezes and stated that the strongest upslope winds occur at approximately 09:00 JST (mountain breeze to valley breeze) and the strongest downslope winds occur in the evening (valley breeze to mountain breeze), with a phase shift of about 6 hours between the two.

Many agricultural meteorology studies were conducted on such mountain and valley breezes in relation to land use in mountainous slopes (Tateishi, 1961; Imaoka, 1964a; Nakamura, 1976, etc.). However, few studies focus on mountain and valley breezes in Japan. Among these are the studies by Yoshino and Fusuki (1953), who pointed out differences in air temperature on north-south slopes in mountain river

valleys, and by Sato *et al.* (1987), who compared valley sites with different valley orientations and contrasted diurnal variations in the air temperature.

1.3.2 Outline of cold air drainage

Cold air drainage is a phenomenon in which cold air generated on a slope by radiative cooling flows down by gravity during nighttime on sunny calm days (Yoshino, 1986; Mori *et al.*, 1999), and is closely related to cold air lakes (Hamada, 2001) or slope thermal belts (Ueda *et al.*, 2003). This cold air drainage not only has a significant impact on the distribution of vegetation and crop-growing areas, but is also closely related to the occurrence of frost damage. Therefore, the actual status of cold air drainage should be elucidated in Japan, where 70% of the land area is mountainous, and many studies have been conducted (Local Wind Research Division of the Agricultural Meteorological Society of Japan, 2000).

Research on cold air drainage has been conducted in Japan since around the 1930s (Yoshino, 1960), and subsequent studies in the 1960s revealed the following characteristics of cold air drainage (Koresawa, 1960; Kimura, 1961; Sahashi, 1962; Imaoka, 1964a; 1964b; 1965).

1. When the general wind is weak, the cold air drainage blows almost steadily. However, when the general wind becomes stronger, the inversion layer is destroyed and the air temperature rises sharply, weakening the cold air drainage. The wind speed of the cold air drainage varies with the direction and speed of the general wind.
2. The cold air drainage most develops in the center of the slope.
3. Wind speed increases with the intensity of radiative cooling.
4. Wind speed on the slope has a vertical profile, with maxima appearing at altitudes of 1.5–5.0 m. The thickness of the cold air layer is 20–30 m.

5. Wind speed has a periodicity.

This characteristic of cold air drainage is part of a local circulation system created by the slope and surrounding topography (Local Wind Research Division of the Agricultural Meteorological Society of Japan, 2000). Contrarily, some studies consider cold air drainage as "cold air runoff associated with a decrease in air temperature," and Yoshino (1960; 1961) and others (Yoshino and Nishizawa, 1960; Tateishi, 1961) have been very influential. Among these, Tateishi (1961) conducted observations in Sugadaira, Nagano Prefecture, which has a relatively simple topography, because the results of previous studies of cold air drainage were specific to individual regions, making it difficult to generalize them and apply the conclusions to other regions. Their findings were obtained on the intermittency of cold air drainage, air temperature drop patterns, and cold air source locations. Regarding the intermittency of cold air drainage, Yoshino (1960; 1961), based on observations of air temperatures in Inawashiro and at the foot of Bandai, Fukushima Prefecture (Mano, 1953; 1956), showed that cold air drainage occurs intermittently three to four times during the night. This intermittent nature of cold air drainage on mountain slopes is explained by the time required for the cold air mass to grow to the point where it can overcome friction with the ground surface and flow down the slope. Kurose *et al.* (2002), which defined "*Aso-oroshi*" as winds that blow when cold air accumulated in the Aso Basin flows down a break in the outer rim of the mountain, showed that the wind speed of *Aso-oroshi* is determined by the amount of cold air accumulated in the basin, and revealed that the maximum wind speed reaches 6 m/s.

Mountain breezes are generally observed from night to dawn because they are caused by the runoff of cold air produced by radiative cooling (e.g. Yoshino, 1986). Nakamura (1976) showed that cold air drainage occurs three to four times during the night, with the highest frequency at dawn (approximately 04:00 to 06:00 JST), based on summer observations in Suga-daira. Contrarily, a case was reported in Kyoto

Prefecture, where downslope winds that were 7 to 9 °C colder than air temperatures in the city occurred during the daytime, and their range of influence was about 200 m from the valley mouth (Yamada and Toba, 2010).

Thus, in mountainous Japan, where plains and mountains tend to be relatively close to each other, mountain and valley breeze and cold air drainage, which are closely related to agriculture, have been studied in individual regions in the same way as sea and land breeze. As a result, common characteristics of them have been clarified to some extent, but it is difficult to generalize them to all regions, and analysis for each region is required. The reason is that mountain and valley breeze and cold air drainage are considered to be possibly more affected by the surrounding microtopography than sea and land breeze. In addition, mountain breezes and cold air drainage from mountain also bring cool air to urban areas, so the perspective of urban climate, studies in individual areas are important for clarifying local climate.

1.3.3 Effect of mountain and valley breeze, cold air drainage on air temperature

Many studies on the effects of mountain and valley breeze on air temperature considered the effects on urban air temperature as well as sea and land breezes. In this section, we will first discuss some examples of studies on mountain breezes mainly in the Nagano area, and the effects of cold air drainage in the Kobe area, which is the target area of this study, will be discussed in the next section.

Hamada and Ichinose (2011) installed temperature and wind observation equipment in the urban area of Nagano City, Nagano Prefecture, and discussed the effect of cool mountain breezes that flow at night along river from the northwest of the Nagano Basin on lowering the temperature in the urban area. Takasaki *et al.* (2017) then confirmed using Doppler lidar observations and numerical simulations that mountain breezes To quantitatively evaluate the effect of mountain breezes on air temperatures in urban areas, they compared the data from urban areas with that from suburbs, and demonstrated that air temperatures decrease more significantly from night

to early morning due to mountain breezes in urban area than in the suburbs. In Nagano City, the mountain breeze is reported to have a peak wind speed (6 m/s) at approximately 22:00 JST from summer to autumn, followed by a gradual decrease in wind speed toward dawn (Hamada, 2001).

Yamato *et al.* (2019) similarly analyzed the relationship between the heat island phenomenon and cold air lake and mountain breezes over the entire city of Nagano for 100 calm sunny nights during the fall and winter seasons, and showed that the central part of Nagano City was affected by mountain breezes and that the amount of air temperature decrease just before sunset was larger at the observation points located at the valley mouth. At other times, a near-neutral stratification corresponding to the urban boundary layer was formed by mechanical mixing by mountain breezes, suggesting that mountain breezes may have contributed to the maintenance of high temperatures in the city except just before sunset.

There are some case reports on the shift in air temperature distribution caused by mountain breezes focusing on the interaction between mountain and valley breezes and the heat island phenomenon, with observations made in Ome City, Tokyo (Sato and Kanou, 2011) and Imaichi City, Tochigi Prefecture (Sato *et al.*, 2004), which are located at the mouths of valleys. Specifically, Sato and Kanou (2011) showed that westerly winds, which correspond to mountain breezes, cause the warm area in the urban area to move eastward, and Sato *et al.* (2004) showed that mountain breezes make the warm area in the urban area dissipate and spread to the suburbs on the leeward side.

The effect of mountain breezes on air temperature reduction was observed in Nagano City by Nishikawa and Takagi (2007) to be about 0.5–1.0 °C in summer. Moreover they indicate that the cool air from mountain breezes is more humid and that the amount of air temperature reduction due to mountain breezes varies seasonally.

1.3.4 Mountain and valley breeze, cold air drainage around Kobe

Around Kobe, mountain breezes and cold air drainage from the Rokko Mountains located to the north of the urban area occur. Observational studies of these winds were conducted mainly by Takebayashi's group of Kobe University. Takebayashi *et al.* (1998) stated that the frequency of winds outbreaking from the valley into the city area is high during the night in summer. Takebayashi *et al.* (2001) conducted a study during the summer of 1999, and defined the north, north-northeast, and north-northwest components of wind direction in the Soma Valley, in Kobe city as cold air drainage that accumulates and outflows in the mountain valleys. The occurrence is more frequent when extended sea breeze speeds are low, and the cold air drainage can be expected to lower air temperatures in the urban area up to approximately 1 km from the mountain edge (Fig. 1-14). However, this is limited to conditions where the extended sea breeze is weak; when the extended sea breeze is strong, the cold air drainage is blown away before it can affect air temperatures in the city. Takebayashi and Moriyama (2002) validated the results of Takebayashi *et al.* (2001) by performing calculations and observations using a shallow water equation model, and showed that cold air drainage is at most 2 °C cooler. Contrarily, Takebayashi *et al.* (2005) showed that the area along the river always tends to be cooler than the surrounding urban areas due to the large wind speed of the northerly winds and the large effect of the cold air drainage on air temperature. Furthermore, Itokawa *et al.* (1998) conducted observations in September and October 1997, and showed that cold air drainage from the mountains affects the distribution of air temperatures.

Thus, mountain breeze around Kobe was intensively studied by Takebayashi's group of Kobe University around the year 2000. In particular, observational studies have quantitatively captured the characteristics of cold air drainage with a temperature reduction effect. On the other hand, however, their study targets the case of runoff of cold air accumulated in a specific valley in the Rokko Mountains. As mentioned above, the phenomenon in which cold air formed on a slope flows down due to gravity is also

a cold air drainage, and therefore, it is necessary to observe the winds flowing down on the slope to understand the actual condition of the cold air drainage in the Rokko Mountains in order to grasp its characteristics. In a series of studies by Takebayashi's group, the analysis period was limited to the nighttime from 18:00 to 06:00 JST. However, there are cases such as the observation results on an island in the Seto Inland Sea by Imaoka (1964a) and in Nagano City by Yamato et al. (2019), which show that cold air drainage occurs before and immediately after sunset. Therefore, it is important to observe diurnal variations in wind throughout the day in order to capture the actual conditions of cold air drainage.

Takebayashi *et al.* (2001) reported wind speeds of approximately 2 m/s for cold air drainage, but Hamada and Ichinose (2011) observed mean wind speeds of approximately 5 m/s for mountain breeze in Nagano. Therefore, it is possible that the wind speed of the cold air drainage flowing down the slope is higher than that of the outflow of cold air accumulated in the valley. In such a case, the impact on the area around Kobe may be even greater. Takebayashi *et al.* (2001) stated that the range of influence of cold air drainage is approximately 1 km from the edge of the mountains, but they did not provide sufficient data to support this statement. Therefore, it is still unclear how far the cold air drainage actually affects the area.

The details of the onset time as well as the wind speed and its range of influence of cold air drainage are very important knowledge when considering its effect on temperatures in the area surrounding Kobe. In particular, as Hamada and Ichinose (2011) reported that relatively cold mountain breezes enter the central part of the Nagano urban area and reduce the temperature of the urban area, it is important to understand the basic characteristics of cold air drainage when evaluating its effect on mitigating urban climate.

1.4 Downslope winds

1.4.1 Outline of downslope winds

Downslope winds are strong winds that occur on the leeward side of mountains as air flows over the tops of mountains (Kusaka and Nishi, 2012). Downslope winds are one of the typical phenomena associated with airflows over mountain ranges, in which the airflow over the mountains blows downslope to the leeward side and foot of the mountains, sometimes producing strong winds with damaging effects (Saito, 1994).

Downslope winds have long been one of the most interesting research subjects of local meteorological phenomena. Because downslope winds are strongly influenced on topography, the locations of their occurrences and their strengths are often determined to some extent, and they are often named as local winds that are unique to a particular region. Famous local downslope winds in Japan include the *Yamaji-kaze* in Ehime Prefecture (e.g., Furukawa, 1966), the *Hiroto-kaze* in Okayama Prefecture (Osaka District Meteorological Observatory, 1956), the *Rokko-oroshi* in Hyogo Prefecture (Yokota and Nakajima, 1992), the *Rausu-oroshi* in Hokkaido (Arakawa, 1969) and the *Matsubori-kaze* in Kumamoto Prefecture (Onodera, 1975; Kurose *et al.*, 2002; Inamura *et al.*, 2009). Globally, "*Foehn*" at the foot of the Alps (Brinkmann, 1971; Seibert, 1990; Jaubert and Stein, 2003), "*Bora*" in the Adriatic Sea (Smith, 1987; Yoshino, 1971; Grisogono and Belušić, 2009; Lepri *et al.*, 2014), and "*Chinook*" in the Rocky Mountain foothills (Cook and Topil, 1952; Oard, 1993) are well known.

Japan is a mountainous country with complex topography, and local winds such as downslope winds, which are influenced by the topography, occur in many parts of the country. Kusaka and Fudeyasu (2017) reviewed the local winds in Japan, focusing on downslope winds, based mainly on recent research results in meteorology and geography. Yoshino (1975) provides detailed information on the relationship between local winds, natural geography, and human life.

Table 1-1 show 28 types of local winds in Japan (Kusaka and Fudeyasu, 2017). Comparing Fig. 1-1, most of these local winds occur at the foot of mountainous regions. Winds are often given region-specific names with the suffixes "wind," "downslope wind," and "*dashi*". Generally, the "*dashi*" type winds are gap winds that blow from a channel between two mountain ranges or a gap between mountains (e.g., Reed, 1931; Overland and Walter, 1981; Colle and Mass, 2000). The names of local winds are often derived from the names of local places or mountains, and these storms can cause serious damage to buildings and trees, with the most famous in Japan being the *Yamaji-kaze*, *Hiroto-kaze*, and *Kiyokawa-dashi*.

Common characteristics of topography in areas where downslope winds occur are mountain ranges behind those areas, with good two-dimensionality to some extent, and slopes that are gentle on the windward side and steep on the leeward side (Saito and Ikawa, 1991; Fig. 1-15). In many cases, bays and lakes are located on the leeward side (Yoshino, 1986). Generally, strong winds are experienced in relatively limited areas up to 10 km from the leeward slope, and winds are particularly strong on the leeward side of a mountain range where there is a saddle or other open area (Saito, 1994).

The mechanism by which downslope winds become strong is largely related to the hydraulic jump. The three-dimensional structure of downslope winds is well known from airplane observations on the eastern slopes of the Rocky Mountains (Liily and Zipser, 1972; Fig. 1-16). As the isentrope shows, the flow over the mountains is displaced significantly downward at the back of the mountains, causing strong winds on the surface, which rise rapidly downstream. This rise is called a hydraulic jump, a phenomenon that is seen in many significant downslope winds (Saito, 1994).

Yamaji-kaze, regarded as one of the three most harmful winds in Japan, is a strong southerly wind that occurs on the northern side of the Shikoku Mountains and on the plains facing Hiuchi-nada on the Seto Inland Sea. Strong *Yamaji-kaze* occurs

when a well-developed extratropical cyclone passes over the Sea of Japan or when a typhoon passes over the west to northwest side of the Shikoku region (Yoshino, 1986; Fig. 1-17). According to Kii *et al.* (2019), who investigated the meteorological conditions when this *Yamaji-kaze* is generated, when a stable stratification airflow crosses the saddle of the Shikoku Mountains from the Pacific Ocean side, it undergoes convergence due to topographical effects, and when it further descends the northern slope of the Hoho Mountains, it becomes stronger, descends to the foot, then changes direction to blow skyward again (hydraulic jump) (Fig. 1-18).

The existence of an inversion layer above is important for the generation of local winds such as downslope winds, and this inversion layer acts like a lid against air masses (e.g., Arakawa, 1969). Based on previous studies on downslope wind, Saito (1994) showed the relationship between the height of the mountain, non-dimensionalized by the depth of the flow on the inflow side, and the velocity on the inflow side (Froude number: F), non-dimensionalized by the phase velocity of the external gravity wave. Then, it is shown that the flow state varies depending on the height of the non-dimensionalized mountain and the Froude number. When the height of the mountain exceeds the range where the flow can maintain a steady state, the flow becomes unsteady. When $F = 1$, the flow becomes unsteady, energy is dissipated, and the velocity changes discontinuously (hydraulic jump). This tendency is more pronounced when the stable layer is low or the valley width is narrow (Sasaki *et al.*, 2004).

Nishi and Kusaka (2019a, b, c) proposed a new theory that the "*Karak-kaze*" blowing in the Kanto region is a type of downslope wind, but that it comes down from the mountains more easily than usual downslope winds due to the bending of the mountain range.

As described above, local strong winds, such as downslope winds, have been the subject of many studies on local meteorology because of their impact on human life. As

a result, the characteristics and generation mechanisms of them, especially those with strong wind speeds, have been studied. On the other hand, the local winds are considered to be strongly influenced by the topography of the area where they occur, and the conditions of the synoptic field at the occurrence and the influence on the surrounding area are also assumed to be unique to each local wind. Data from existing stations such as AMeDAS alone are often insufficient for the analysis of these local winds. Therefore, original meteorological observation is needed, but in many cases, such observational studies have not been conducted for local winds in individual regions.

1.4.2 Downslope wind around Kobe

In the area surrounding Kobe City, winds blowing in an east-west direction prevail because the Rokko Mountains run east to west near the coast. In winter, westerly winds are particularly strong, but downslope winds called "*Rokko-oroshi*" are known to occur when northerly winds blow down from the Rokko Mountains (Yokota and Nakashima, 1992; Yoshida *et al.*, 1998; 1999). *Rokko-oroshi* often occur during typhoon season and in March, and the Nada region in the eastern part of Kobe City is famous for its *sake* (Japanese rice wine) production using the cold *Rokko-oroshi* in winter (Kusaka and Fujibe, 2018).

Ino *et al.* (2009) analyzed data for the cold season from November to March during 2001–2005, and investigated pressure patterns and changes in air temperature at the occurrence of the *Rokko-oroshi* (Fig. 1-19). Based on their results, they pointed out that the most common pressure pattern is a depression or a front passing before the *Rokko-oroshi*, followed by a transition to a winter type pressure pattern (Fig. 1-20), and the temperature difference between the leeward and windward sides is large before and after the *Rokko-oroshi* blows. The diurnal variation of *Rokko-oroshi* showed that maximum wind speeds were more frequent in the late night and during the daytime,

and less frequent in the early morning (06:00 and 07:00 JST) (Fig. 1-21). Kiyohara *et al.* (2001), based on their analysis of AMeDAS Kobe data from 1976 to 1994, noted that *Rokko-oroshi* were more frequent from October to March and appeared during the winter type pressure patterns after the passage of a cold front. Contrarily, Kusaka *et al.* (2007) analyzed data for the winter months of December through March from 2001 to 2006, and noted that the occurrence rate of *Rokko-oroshi* was about the same for both day and night.

As mentioned above, many studies have been conducted on individual cases of local winds in Japan, because each region has its own unique characteristics and local strong winds sometimes causes damage. Although *Rokko-oroshi* has not caused frequent damage due to strong winds, its name is widely known, and it has had a close relationship with local residents, as it has been used to produce local specialties since ancient times.

Previous studies have clarified to some extent the general knowledge on the wind direction or speed and the pressure patterns in which *Rokko-oroshi* tends to occur. However, the empirical and objective nature of these studies is not necessarily sufficient, and even the general characteristics of *Rokko-oroshi* have not been fully clarified. Furthermore, little is known about the effects of *Rokko-oroshi* on temperature reduction, the general characteristics of the wind system in the Kobe urban area when *Rokko-oroshi* blows, and the characteristics of the meteorological conditions when *Rokko-oroshi* occurs, which are essential for understanding *Rokko-oroshi*.

1.5 Objectives

As described above, local winds occur in many parts of Japan due to the rugged topography of the country surrounded by the sea, and knowledge of these winds is accumulating. Studies on local winds and air temperatures around Kobe, the target region of this study, were conducted as described in the previous section. Analytical

and observational studies were also conducted especially for the Seto Inland Sea and the Kinki regions, and the characteristics of the average local mesoscale wind system were obtained.

Kobe is a city developed on a slope between Osaka Bay and the Rokko Mountains. Therefore, the climate around Kobe is strongly influenced by Osaka Bay, the Osaka Plain, and the Rokko Mountains, and is considered to form a local climate unique to the region. The Rokko Mountains located behind the city are expected to have particularly large influences on the wind systems and temperatures that characterize the local climate. The wind system is expected to develop a local circulation due to the unique topography between the bay and the mountains, and a wind system with distinct diurnal variations is expected to occur.

However, the knowledge of the general characteristics of individual phenomena in the Kobe area, where sea and land breezes, and mountain and valley breezes occur together, and interact with the extended sea breeze on the scale of Osaka Bay and the Osaka Plain, is still insufficient. In particular there is currently no evidence that the westerly and easterly winds that generally follow the direction of the coastline in the Kobe area are equivalent to “extended land and sea breezes”.

In order to verify this fact, first, it is necessary to select appropriate days when local wind systems are likely to develop, and then carefully analyze the diurnal variations of these days. Then, it is also needed to examine how the wind system in the Kobe area is characterized from a broad area scale viewpoint. However, there are few examples of analysis of diurnal variations of local wind systems in the area from this perspective, and it cannot be said that the local wind system and the broad scale wind system are sufficiently distinguished and understood.

The Kobe area is located between Osaka Bay to the south and the Rokko Mountains to the north, and is one of the rare areas in Japan where a city has developed in a very narrow area between mountains and the sea. As mentioned above, thermal

induced local circulation such as sea and land breeze has been well developed in the coastal areas of the Seto Inland Sea and Osaka Bay, and the knowledge of such circulation has accumulated. However, local climatological studies on wind and temperature with a focus on the Kobe area have not been sufficiently conducted, so the general characteristics of diurnal variations in local wind system and temperature are not necessarily clear. In addition to thermally induced local circulation, *Rokko-oroshi*, which is caused by the dynamic effect of the Rokko Mountains, has not been well characterized in terms of wind and temperature changes at its occurrence.

Generally, winds blowing from the mountains and the sea bring cooler air, so local winds have an impact on the lives of local residents. Specifically, sea breeze and mountain breeze have a mitigating effect on heat, while downslope winds bring strong winds, making the physical experience of cold more severe. Therefore, understanding the characteristics of diurnal variations of these local winds, their effect on temperature reduction, and the range of their influence is important for the lives of local residents.

Additionally, quantitative evaluation of the impact of such local winds on air temperatures in the Kobe area has not been sufficiently carried out. One of the reasons for this is that existing observation stations are not sufficient to capture temperature distributions, and it is necessary to establish original observation stations with higher densities. For this reason, few observational studies have been conducted in the region by setting up original own stations at many locations.

Furthermore, since the Kobe area is adjacent to the western side of the larger Osaka urban area, it is known to be affected not only by local winds but also by extended sea breeze, although the actual situation of diurnal variations in thermally induced local circulation, considering the relationship between the two wind systems is not sufficiently understood yet. This means that we still do not have sufficient knowledge to understand the local climate in the Kobe area. Therefore, in addition to the previous findings, a further investigation of the relationship between the local wind

system and temperature in the Kobe area will allow us to grasp some common aspects of the local climate unique to a climate in other cities located between a mountainous region and a bay. This study will also contribute to the understanding of the local climate in other Japanese cities with similar geographical environments. In particular, clarification of diurnal variations in wind and temperature is necessary from the perspective of assessing the urban living environment. In addition, local wind systems and temperatures are expected to be affected by smaller-scale landforms and surrounding conditions, and there may be regional differences in wind systems and temperatures even within the same region.

Therefore, in order to advance our understanding of regional climate in Kobe, it is necessary to conduct observations at higher spatial and temporal densities and to analyze the results. In the Kobe area, where local circulation is well developed, sea and land breeze and mountain and valley breeze as thermally induced local circulation in the warm season, and downslope wind as dynamically induced local circulation in the cold season are important factors in defining the local climate, and it is most important to capture their typical diurnal variations.

Based on the above, this study aims to elucidate the general characteristics of the local climate peculiar to the Kobe area from the perspective of diurnal change of local wind and air temperature by clarifying the following six points.

1. Characteristics of the diurnal variation of the local wind system around Kobe on averaged sea and land breeze occurrence days
2. Relationship between sea and land breeze around Kobe and the broad-scale wind system in the Kyoto-Osaka-Kobe area
3. Characteristics of temperature diurnal variations and the relationship with local wind system
4. Changes in wind and temperature during the occurrence of cold air drainage

from the Rokko Mountains

5. Changes in wind and temperature during the occurrence of the *Rokko-oroshi*
6. Magnitude and influence range of the effect of cold air drainage and the *Rokko-oroshi* on temperature decrease

1.6 Composition of this thesis

The outline of the present study is as follows.

In Chapter 2, we describe the study area, an overview of meteorological observations, and the method for extracting the days for analysis.

In Chapter 3, we first clarified the climatological characteristics of the local wind system represented by sea and land breeze around Kobe were analyzed by selecting alternating days of sea and land breeze with sunny calm days from the one-year period. Next, Case studies were conducted for two days with different patterns of diurnal variation in the local wind system even on the same sunny calm day, and the differences in the diurnal variation and its relationship to the broad-scale wind system were examined. Next, we examined the relationship between local wind systems and temperature using temperature data from 33 original stations. Finally, we investigated the cooling effect of mountain breeze and its influence range.

In Chapter 4, we attempted to understand the characteristics and temperature reduction effect of "*Rokko-oroshi*," which is a downslope wind caused by the dynamic effect of mountain, contrasting with sea and land breeze and mountain and valley breeze, which are thermally induced local circulation.

Finally chapter 5 summarizes the findings of this paper and discusses future issues and prospects.

2. Study area and data

2.1 Study area and its characteristics

Kobe City, the target area of this study, has a population of over 1.5 million people as of April 1, 2022, and continues to develop as a hub city in the Kinki region. Kobe has an area of approximately 553 km² and is divided into two parts by the Rokko Mountains, the main peak of which is 931 m high (Figs. 2-1; 2-2). The southern side facing Osaka Bay is a series of fans, coastal lowlands, and reclaimed land formed by small- and medium-sized rivers along the foothills of the Rokko Mountains. The urban area of the city is located in a narrow area extending in an east-west direction between the Rokko Mountains and Osaka Bay to the south. New towns are expanding on the northern side of the Rokko Mountains, and maritime cities, such as Port Island and Rokko Island, are being constructed in Osaka Bay.

2.2 Data and analysis period

The following is a detailed description of the data used in this study. The analysis was performed on data from April 2011 to February 2018. Details of the analysis period are described in each chapter.

2.2.1 AEROS (Atmospheric Environmental Regional Observation System) and

AMeDAS

To investigate the local wind system, around Kobe area, wind direction and speed data were obtained from 11 sites (Higashinada, Rokko Island, Nadahama, Nada, Hukiai, Minatojima, Southern Hyogo, Nagata, Suma, Port Tower, Mt. Rokko; hereinafter called En, Ri, Nh, Na, Hu, Mi, Hs, Ng, Su, Pt and Ro respectively) from the Atmospheric Environmental Regional Observation System under the control of the Ministry of the Environment (AEROS), and 4 AMeDAS stations (Kobe, Kobe Airport,

Sanda and Kyoto; hereinafter called AK, AKA, SA, and AKY respectively) were used (Figs. 2-3; 2-4). For AMeDAS Kobe (AK), the temperature and wind measurement locations are different, so the temperature and wind measurement stations are denoted as AKt and AKw, respectively, for the distinguishing purpose. AKA is a station adjacent to Kobe Airport on a man-made island, and there are no buildings around it. Moreover, to investigate the relationship between the local wind system around Kobe and the broad-scale wind system between Kyoto, Osaka, and Hyogo area, AEROS wind and temperature data for Kyoto, Osaka, and Hyogo prefectures were used (Fig. 2-4).

Wind direction and wind speed at the AEROS were measured by sonic anemometers, which recorded wind speeds in the 0.1 m/s to 0.1 m/s increments. The wind direction was recorded in CALM when the wind speed was 0.2 m/s or less and in 16 directions when the wind speed was 0.3 m/s or more.

On the other hand, wind direction and speed are measured at AMeDAS by windmill anemometer, which recorded wind speeds in the 0.1 m/s to 0.1 m/s increments. The wind direction was recorded in CALM when the wind speed was 0.2 m/s or less and in 16 directions when the wind speed was 0.3 m/s or more.

For the 11 stations in the Kobe area, except for a building 50 to 100 m to the southwest of En, there was no environment around the AEROS or AMeDAS stations that would affect wind observations.

Tables 2-1; 2-2; 2-3 lists the meteorological stations used in this study.

2.2.2 The lower-slope observation in the Rokko Mountains

To investigate the effect of the *Rokko-oroshi* and mountain breeze from the Rokko Mountains on air temperature, an original meteorological observation station, i.e., a wind and temperature measurement station was installed on the roof (158 m above sea level; 15 m above ground level) of Kobe University Secondary School

(135.254 E 34.732 N, 158 m above sea level; hereinafter KS), located on the lower-slope of the Rokko Mountains. The observation instruments were not located on the ground, which is easily affected by buildings, but on the roof of the school building, from which the slopes of the Rokko Mountains can be observed (Figs.2-3; 2-5). The installation period was from June to November, 2016 and from September, 2017 to February, 2018. In the former period, a windmill anemometer (Mistral, WDL-01) and an ondotori (T&D) were used to measure wind and temperature, respectively. Air temperature was measured at a naturally ventilated shelter (Shigeta, 2012) equipped with a temperature sensor. In the latter period, wind was measured with a wind cup anemometer (Onset, S-WCF-M003) and temperature was monitored with an air temperature sensor (Onset, S-TMB-M002). Air temperature was measured at a naturally ventilated shelter (Onset, RS3-B) equipped with a temperature sensor. The measurement interval was 1 min. A wind cup anemometer (S-WCF-M003) failed on October 24, 2017, and a windmill anemometer (WDL-01) was installed from November 3, 2017, until November 21, when repairs to the device were completed.

2.2.3 Air temperature observation

To understand the relationship between the local wind system and air temperature changes, the surface air temperature was observed at 33 locations in a city park in Kobe City. The locations are shown in Fig. 2-6 and Table 2-1.

Observation equipment was installed at a height of 2.5 to 3.0 m above the ground using streetlights in the parks to avoid being affected by exhaust heat from automobiles and local heat from the ground surface (Fig. 2-7). The air temperature was measured using a naturally ventilated shelter (Shigeta, 2012) with a temperature sensor (T&D, Ondo-tori) (Fig. 2-8). The observation was conducted from August to October 2014. The measurement interval was 10 minutes, and the resolution was 0.1 °C.

To confirm the instrument error of each temperature and humidity sensor, an

indoor test was conducted using an artificial weather instrument (LH-300-r; Nippon Ikakikai Seisakusho Co., Ltd.). The results showed that the instrument error was within 0.5°C. The obtained instrument error values were used for instrument error correction. In addition, to understand the effects of solar radiation and wind speed on naturally ventilated shelters, we examined the temperature difference between forced ventilation shelters and naturally ventilated shelters. As a result, no significant relationship was found between the two shelters.

2.2.4 Selection of dates for analysis

The thermally induced local circulations such as sea and land breezes generally develop during the season from spring to autumn (e.g., Yoshino *et al.*, 1973). Since synoptic scale conditions that cause local circulation to emerge generally occur during the warm season, in this study March to November were selected as the analysis period excluding the period when the winter type patterns often occur around Japan.

Because thermally induced local circulations develop better when the synoptic scale pressure gradient is weak and the temperature difference between sea and land is large, days were selected for analysis as sunny calm days based on sunshine duration, cloud amount from AMeDAS Kobe, and 850hPa wind speed on 09:00 JST from the nearest aerological observation stations (Matsue or/and Shionomisaki), based on previous studies by Tsuchida and Yoshikado (1995), Kawamura (1977a), Fujibe (1981) and others, excluding days with synoptic scale disturbances such as extratropical cyclones around the target area on the weather charts by visual inspection.

Specifically, with reference to Tsuchida and Yoshikado (1995), days with a daily total sunshine duration of 6 h or more at AMeDAS Kobe were selected, of which days with a daily mean cloud amount of less than 5 were selected as sunny days with reference to Fujibe (1981). Days with 850 hPa wind speeds of less than 7 m/s at both Matsue and Shionomisaki, which are located near the target area, were selected as

sunny and calm days. The 7 m/s criterion was used here because, when the general wind speed is 7 m/s or higher, local wind systems are formed as a deflection of the general wind because of the topography, and when the wind speed is less than 7 m/s, thermally induced local circulations such as sea and land breezes become prominent (Kawamura, 1977a).

Conversely, unlike thermally induced local circulation, *Rokko-oroshi* does not necessarily occur under a specific air pressure pattern. But previous studies have indicated that *Rokko-oroshi* tend to occur during the transition to winter type pressure patterns after the passage of cold front during the cold season. Therefore, the target dates for analysis were selected based on the wind direction and speed of downslope winds and their duration in the cold season.

The selection of days for analysis in each analysis is described in detail in the respective chapters.

3. Thermally induced local circulation in Kobe and its effect on air temperature

3.1 Statistical analysis of sea and land breeze in Kobe City

3.1.1 Objective

Many of Japanese large cities face the sea. In these cities, the influence of sea breezes on the urban environment should be considered. The heat island phenomenon has recently become increasingly prominent in urban areas owing to the increased heat generation by humans and other processes. Actively driving sea breezes to urban areas is one of the measures to control this phenomenon (Masuda *et al.*, 2005). Many researchers have examined the cooling effect of region-specific winds such as sea breezes on the urban atmosphere and the interaction between the heat island phenomenon and sea breezes (e.g., Kiyota and Kiyota, 2005; Sakaida *et al.*, 2011). Takebayashi and Moriyama (2005) conducted long-term observations of air temperatures in Osaka Prefecture during the warm season. They found that the influence of sea breezes on the distribution of air temperatures near the ground surface during daytime is a function of the distance from the coast.

Using thermometers placed in instrument shelters at 31 elementary schools in Kobe during the summer of 2004, Miyazaki (2006) found that the total number of hours in which temperatures exceeded 30 °C was particularly high in the coastal urban area east of Chuo Ward, suggesting that high-temperature areas tend to be moved to eastern regions in response to a prevailing wind direction being to the west during daytime.

Many studies have been conducted on sea and land breezes over the Seto Inland Sea, including Kobe (e.g., Osaka District Meteorological Observatory, 1971; 1972; Mizuma, 1995). Kitabayashi (1976) investigated the entry time of sea and land breezes in the Harima Plain using data from AEROS. Kono and Nishizuka (2006) conducted a

statistical analysis of data covering one year. They emphasized that sea breeze is more frequent in spring and summer because the daily maximum temperature on land exceeds the sea surface temperature from spring to early autumn. Furthermore, the temporal variations in the air temperature difference between land and sea and the wind direction in Himeji City were analyzed, revealing that they were well correlated.

However, few statistical analyses have been performed that focused on sea and land breezes and mountain and valley breezes on an urban scale in the vicinity of Kobe. Neyama (1982) analyzed the mean wind speed and prevailing wind direction at 15:00 and 03:00 JST in August, and found that SW and ENE winds prevailed at 15:00 and 03:00 JST, respectively. He also revealed that the most typical sea and land breezes were recorded in May and August, with the sea breeze being the strongest from 12:00 to 15:00 JST. This is generally consistent with the results, as numerous studies have indicated that sea breeze most develops around 15:00 (Mori *et al.*, 1994; Mizuma, 1995; Ohashi and Kawamura, 2006; Sawada and Kawamura, 2010; Takimoto and Sakaida, 2012, etc.). However, with regard to the peak period of land breeze, an analysis for the warm season (June - September) in Osaka, near Kobe, showed that wind speeds during the night were generally constant (Eguchi, 1977), and no consistent trend has been obtained for the strength of land breeze (Yoshino, 1975).

The Architectural Institute of Japan (2000) investigated the average diurnal variations in wind on clear summer days in 1990–1992 using wind data from AEROS in Kobe and other cities. The report included windroses for daytime and nighttime. However, in the report, daytime was defined as the period from 06:00 to 18:00 JST and nighttime from 19:00 to 05:00 JST. Consequently, information on diurnal variations in sea and land breezes could not be obtained at hourly scale.

The Architectural Institute of Japan (2000) noted that the Kobe urban area is strongly influenced by the Rokko Mountains, especially in the distribution of airflows. Specifically, based on wind rose during the daytime (06:00-18:00 JST) and nighttime (19:00-05:00 JST) on sunny summer days, the paper suggests that sea breeze

dominates during the daytime, while cold air drainage and mountain breeze from the Rokko Mountains are dominant during the nighttime. Also, in the area at the foot of the Rokko Mountains, easterly land breeze ("extended land breeze") at night is weaker than sea breeze during the daytime, suggesting that prevailing winds from the Rokko Mountains are dominant.

However, the "extended land breeze" pointed out by the Architectural Institute of Japan (2000) has not been captured in other studies (e.g., Ito, 1995) that show the wider-area wind system. The airflow from the Rokko Mountains has also not been well captured in existing studies, because the density of observation stations is small and the wind system in Kobe is often represented by only a single AMeDAS station. Although it is clear that sea and land breezes prevail in this area, the diurnal variations and the range of influence of these circulation, i.e., the broad-scale wind system and the local circulation in the Rokko Mountains and plains, have not been clarified.

In this section, the characteristics of the diurnal variation of the wind system in the Kobe area are investigated using AEROS data for sunny calm days during the warm season, which has a higher station density than that of AMeDAS.

3.1.2 Data used

Ten of AEROS stations (En, Ri, Nh, Na, Hu, Mi, Hs, Ng, Su, Pt), two of AMeDAS (AK and AKA), and sea surface temperature data (1 m below the water surface) at Kobe Port from the 5th Regional Coast Guard Headquarters, Japan Coast Guard, were used for the analysis. The observation period of the data used in the study was from April to November 2011 and March 2012.

3.1.3 Selection of dates for analysis

According to the method described in Section 2.2.4, the number of sunny calm days when sea and land breezes, and thermal circulation are to be developed during the

study period was selected, resulting in 53 days available for analysis. Furthermore, in this paper, in order to analyze only the days when the sea and land breezes actually shifted between daytime and night, the days when the wind direction at 15:00 and 03:00 JST at Na was shifted were selected with reference to the results of Miyazaki *et al.* (1995). They showed using windroses and diurnal variations of vector mean wind speed at each station on clear summer days, the wind direction at Na shifted almost in the opposite direction during the daytime and night, and the frequency of each wind direction was generally similar. So it was considered to be suitable station for determining the alternation of the sea and land breezes direction.

On the other hand, the alternation of sea and land breezes was determined based on the wind directions at 15:00 and 03:00 JST was because the sea breeze is a thermally induced circulation that is most developed around 15:00 JST (e.g., Mori *et al.*, 1994; Mizuma, 1995; Ohashi and Kawamura, 2006; Sawada and Kawamura, 2010; Takimoto and Sakaida, 2012). With regard to land breezes, certain knowledge on the time of the peak period has not necessarily been obtained. Among them, Neyama (1982) pointed out 03:00 JST as the time when land breezes are most pronounced in the Seto Inland Sea coastal area from the viewpoint of wind direction frequency, Kono and Nishizuka (2006) indicated 03:00 JST as the time of maximum land breeze frequency from the analysis results in Himeji, near Kobe in August, and Eguchi (1977) showed that the wind speed of land breeze during the nighttime is almost constant in the warm season in Osaka. So, in this chapter, 03:00 JST is taken as a representative time when land breeze is blowing. Therefore, we analyzed the prevailing wind direction and vector mean wind at 15:00 and 03:00 JST at each location.

Figure 3-1 shows the windroses at 15:00 and 03:00 JST on 53 sunny calm days at Na. It can be seen that three prevailing wind directions (S, SSW, and SW) are dominant at 15:00 JST, while five wind directions (NW to NE) are more frequent at 03:00 JST. Therefore, in this paper, the days when the wind directions at 15:00 and 03:00 JST showed the above range were extracted from the 53 days. As a result, as

shown in Fig. 3-2, 31 days out of the 53 days were selected for analysis as sea and land breezes days (Table 3-1).

3.1.4 Wind direction distribution during the peak period of sea breeze and land breeze (15:00 and 03:00 JST)

The windrose at each point at 15:00 JST shown in Fig. 3-3a, indicates that the wind blew primarily from the southwest. In fact, the prevailing wind direction was southwest at 7 of the 12 sites. If stations with second prevailing wind direction south-southwest are included, the number of stations is 11 out of 12 (Table 3-2). At Hu and Na, two prevailing wind directions could be identified: south and west-southwest or south and south-southwest.

The windrose at each point at 03:00 JST shown in Fig. 3-3b, differs significantly from that at 15:00 JST, with some locations showing a prevailing north-northwest wind direction and others showing a prevailing northeast. The relationship between the prevailing wind direction and topography highlights that wind tends to blow from north-northwest at sites near the Rokko Mountains, and from northeast at sites along the coast and on artificial islands. Among them, northerly wind direction and northeast to easterly wind direction prevailing in En, Nh and Hs.

As described above, a significant change in wind direction occurred at each point between 15:00 and 03:00 JST. The Kobe area faces Osaka Bay. Therefore, on sunny calm days, thermally induced local circulations (including sea and land breezes, mountain and valley breezes, and local winds resulting from the interaction of both) develop. Using a hodograph of Kobe, the Architectural Institute of Japan (2000) revealed that northeasterly winds prevail during nighttime and southwesterly winds prevail during daytime, indicating a clockwise rotation in wind direction throughout the day. The reason for this rotation is that sea breezes initially blow perpendicularly to the coastline but become westerly under the influence of extended sea breezes

blowing from Osaka Bay to the Osaka Plain. These cause the winds in Kobe to shift from southerly in the morning to southwesterly in the afternoon. The distribution of windroses in the Kobe area during daytime (06:00–18:00 JST) and nighttime (19:00–05:00 JST) show that sea breezes dominate almost the entire area during daytime. However, during nighttime, not only easterly land breezes blow but also mountain breezes from the valley of Mt. Rokko are prominent at some locations. These results are consistent with those of the Architectural Institute of Japan (2000). The southwesterly wind observed at 15:00 JST is considered part of the extended sea breeze blowing from Osaka Bay to the Osaka Plain. The north-northwesterly wind at 03:00 JST, which was observed near the Rokko Mountains, is considered to be a mountain breeze from the Rokko Mountains.

The data used by the Architectural Institute of Japan (2000) and this paper are both from AEROS, but the former analysis is based on the classification of daytime and nighttime on clear days. On the other hand, the analysis in this paper is based on the time of day when both sea and land breezes are most likely to develop during the daytime and nighttime. Therefore, the prevailing wind directions of sea breeze and mountain breeze were captured more clearly in this paper than in the Architectural Institute of Japan (2000). Specifically, while the maximum frequency of prevailing wind direction in the Architectural Institute of Japan (2000) is about 20-30%, the results of this paper show that sea breeze is blowing at a maximum frequency of 80% of Mi and mountain breeze at a frequency of about 60% of Hu (Fig. 3-3).

The frequency of easterly winds is significantly higher at stations away from the Rokko Mountains and on artificial islands during the nighttime. Also, at Nh and Hs, two prevailing wind directions, northerly and easterly, are observed. The Architectural Institute of Japan (2000) suggested that these easterly winds are "extended land breeze," but there is no information on where it is actually blowing from.

Next, we will capture the broad-scale wind system at the same time (15:00 and 03:00 JST), and confirm the origin of the wind system seen around Kobe. Here,

vector-mean wind distribution maps at both times are drawn using AEROS data for Osaka and Kyoto prefectures in addition to Hyogo prefecture.

According to the broad-scale wind system at 15:00 JST, the prevailing wind system is from the sea to the inland area over the entire Osaka Plain (Fig. 3-4a). The wind speed tends to be relatively strong along the coast. The southwesterly winds in the Kobe area can be regarded as part of the wind system blowing from the northwestern Osaka Plain to Kyoto, and these southwesterly winds can be regarded as extended sea breeze.

On the other hand, the wind speed in the Kyoto-Osaka-Kobe area at 03:00 JST was lower than that at 15:00 JST, but prevailing winds were generally from inland to the sea (Fig. 3-4b). Unlike at 15:00 JST, the wind direction in the area around Kobe was highly variable. Northerly wind direction prevails at stations near the Rokko Mountains and in the western part of Kobe City, while easterly winds prevail over the artificial islands. On the other hand, although wind speeds are low as a general trend, strong northerly winds are blowing in the eastern part of the Rokko Mountains. Then, it appears that the northerly winds turned northeasterly in the coastal areas, and as an extension, easterly winds are blowing on the artificial islands in the area around Kobe. Though it is not possible to make a definite determination due to the lack of data over the sea, the easterly wind at 03:00 JST was not considered to be extended land breeze blowing from the Osaka Plain to Osaka Bay, as described in previous studies.

3.1.5 Diurnal variation of surface wind field

Based on the result of the previous section, as we selected the days when the alternation of wind direction was clearly observed during the daytime and night in Na, and the switch of sea and land breezes was clearly observed at each station in the Kobe area as well. On the other hand, two prevailing wind directions were observed at Hu at 15:00 JST and En, Nh, and Hs at 03:00 JST, showing different characteristics from other stations. This may be due to the fact that, as mentioned earlier, the local wind

system around Kobe is affected by the extended sea breeze that occurs due to the difference in pressure between the inland Kinki region and off the Kii Channel (Itoh and Kawazoe, 1983; Itoh, 1995), and the diurnal changes in the local wind system are caused by the shifting of the sea and land breezes at multiple scales, but the diurnal variations are somewhat different from day to day. Therefore, in order to understand the characteristics of sea and land breezes direction in this area unlike other regions, it is important to capture the diurnal variation of wind direction at least on an hourly time scale, and not only on a specific time scale. Therefore, in this section, we analyze the diurnal variation of the local wind system in the area based on the distribution of the hourly vector mean wind.

Figure 3-5 shows the hourly surface wind field. The wind system at 03:00 JST shown in Section 3.1.4 (Fig. 3-3) is characterized by northerly wind direction over the plains and easterly wind direction over the artificial island, and the similar wind system continues until around 06:00 JST. Thereafter, around 07:00-08:00 JST, prevailing winds are generally easterly over the entire target area, and their wind speeds are also enhanced. On the other hand, after 08:00-09:00 JST, the wind direction over the entire area begins to rotate to the clockwise, and at around 12:00 JST, southerly winds that are generally orthogonal to the direction of the coastline of the area prevailing over the entire area. The wind direction continues to change to the clockwise direction. At 15:00 JST, the southwesterly wind is prevailing seen in the previous section and the wind speeds reach its peak. At around 18:00 JST, wind direction from the Rokko Mountains begins to prevail at the eastern station. Westerly wind prevails in the western area and on the artificial islands until around 21:00 JST, but easterly winds begin to blow again in the western area and on the artificial island at 22:00-23:00 JST. This suggests that the diurnal variation of the wind system in the target area is caused by the interaction of sea and land breezes circulations of different scales, but that there are regional differences in the way they interact, which may result in stepwise transitions of the wind system.

Itoh and Kawazoe (1983) pointed out that when sea breezes begin to blow in the Osaka Bay coastal area, the local pressure difference between sea and land takes effect and winds prevailing from a direction near perpendicular to the coastline, but as time passes, winds on a much larger scale prevail. Itoh (1995) indicates that the wind direction at AMeDAS Kobe is southwest and that its constancy is more than 0.8 on the extended sea breeze blowing days at 17:00 JST. Mizuma (1995) shows that the wind direction of the vector mean wind at AMeDAS Kobe at 11:00 on an extended sea breeze blowing days is generally orthogonal to the coastline, and its constancy is 0.6 to 0.8.

Therefore, in this paper, we attempted to classify the wind system by wind direction with reference to these findings. Figure 3-6a shows the diurnal variation of the vector mean wind direction at the stations on the artificial islands (Ri, Mi, AKw, and AKA) on the selected 31 days. Here, we used the stations on the artificial islands because they are surrounded by the sea, and the wind is less affected by land cover than in the plains, so that the transitions of the sea breeze with time can be captured more clearly.

As shown by Itoh (1995) and Mizuma (1995), the wind direction on the artificial island is 150 to 180 degrees, which is orthogonal to the coastline around Kobe at 11:00 JST, and around 240 degrees, which is southwest wind at 17:00 JST. Diurnal variations in wind direction indicate that easterly winds (45 to 105 degrees) blow continuously from 01:00 to 09:00 JST, while westerly winds (195 to 270 degrees) blow continuously from 12:00 to 19:00 JST. On the other hand, the diurnal variation of vector mean wind direction at stations near the Rokko Mountains (En, Na, and Hu) on the plain (Fig. 3-6b) shows that northerly winds of 270 to 15 degrees blow continuously from 17:00 to 06:00 JST, which is not observed on the artificial islands. Based on the above, the local wind system in the target area was classified into the following four categories, using 15, 105, 195 and 270 degree as the criteria for wind system classification (Table 3-3). Itoh (1995) and others define an extended sea

breeze as a wind blowing from the Kii Channel to the interior of the Kinki region, but since the constancy of the wind direction of both sea breeze and extended sea breeze at AMeDAS Kobe is high on days when the extended sea breeze blows, as described above, it is judged in this paper that the sea breeze and extended sea breeze can be classified according to wind direction. The easterly wind indicated as "extended land breeze" by the Architectural Institute of Japan (2000) are referred to as a land breeze in this paper, based on the results of the previous section.

1. Sea breeze: prevailing winds with predominant southerly component, which is perpendicular to the coastline around Kobe (wind direction: 105-195 degrees)
2. Mountain breeze: prevailing winds with a predominant northerly component blowing down from the Rokko Mountains (wind direction: 270-360 degrees; 0-15 degrees)
3. Extended sea breeze: prevailing winds with a predominant westerly component from the eastern part of the Seto Inland Sea or Osaka Bay to the Osaka Plain (wind direction: 195-270 degrees)
4. Land breeze: prevailing winds with a predominant easterly component (wind direction: 15-105 degrees).

In order to determine whether winds that meet the above wind direction criteria are thermally induced local circulation driven by thermal contrast with the surrounding environment, it is necessary to verify the formation mechanism using numerical models and simulations. In this paper, however, we leave this point as a future issue and refer to winds that satisfy the above wind direction criteria as sea or land breeze, mountain breeze and extended sea breeze.

3.1.6 Classification of region and wind system stage by diurnal change in wind direction

The results of the previous sections suggest that there are regional differences in the diurnal variation of the local wind system in the target area, and that there are

differences in the transition between on the plain and on the artificial islands. Therefore, this section aims to clarify the regional classification of the target area and the stage of transition of the wind system based on the diurnal variation of wind direction at each station. First, the regions were objectively classified based on a cluster analysis of the direction of the hourly vector mean wind at each location. In the cluster analysis, the dissimilarity was defined as Euclidean distance, referring to Ikegai *et al.* (2013) and Hirano and Shibasaki (2001). For clustering, we used the Ward method, which is said to produce the clearest clusters with high classification sensitivity. The number of clusters was determined by comprehensively considering the location of the stations, instead of dividing the clusters uniformly by the distance of the tree diagram (Fig. 3-7). In the analysis the wind direction values were used as they are, for example, 355° and 05° for the same northerly wind, the values would differ greatly. Therefore, in this paper, the east-west and north-south components are calculated using the hourly vector mean wind direction as the unit vector, and a cluster analysis is performed on these values. We define the Euclidean distance between the stations as follows where U and V are the x and y components of the unit vector, U and V at time t at station a are U_{at} and V_{bt} , respectively, and D_{ab} is the Euclidean distance between the stations.

$$D_{ab} = \sum_{t=1}^{24} \sqrt{(U_{at} - U_{bt})^2 + (V_{at} - V_{bt})^2}$$

As a result, the observation sites were divided into the following three groups (Table 3-4).

Group 1: En, Na, Hu

Group 2: Hs, Ng, Su

Group 3: Ri, Mi, AKw, Nh, Pt, AKA

The three regional groups obtained from the cluster analysis generally correspond to the eastern area (Group 1), western area (Group 2), and coastal area or on artificial islands (Group 3) of the target area (Fig. 3-8).

Next, the hourly wind direction at each station was classified into the four wind systems defined in the previous section, and their transition was captured (Table 3-5). Based on this result and the hourly surface wind system characteristics described in the previous section, the local wind system in the target area has five major stages, which can be summarized as follows. The classification of time by wind system is somewhat subjective, but was done on the basis of the trend of the distribution of the vector mean wind system by visual inspection.

1. 22:00–06:00 JST: Mountain breeze from the Rokko Mountains and land breeze prevail.
2. 07:00–09:00 JST: Land breeze prevails.
3. 10:00–12:00 JST: Sea breeze prevails.
4. 13:00–17:00 JST: Extended sea breeze prevails.
5. 18:00–21:00 JST: Mountain breeze and extended sea breeze prevail.

The results of this section suggest that the target area can be divided into three regions according to the transition of the local wind system, and that there are five stages in it. In summary, the eastern part of the target area (Group 1) is characterized by a relatively short duration of sea breeze and extended sea breeze compared to the other two groups, and a longer duration of mountain breeze from the Rokko Mountains. On the other hand, both the western part (Group 2) and on the artificial island (Group 3) have a longer duration of sea breeze and extended sea breeze, but the western part is characterized by the predominance of mountain breeze at night, and the artificial island is characterized by the predominance of land breeze continuously after the extended sea breeze has finished. In terms of the different scales of sea and land breezes, the eastern plain area is dominated by small-scale sea and land breezes (including mountain breeze), while the area on the artificial island is dominated by large-scale extended sea breezes.

Table 3-5b shows the diurnal variation of wind speed corrected for height by the logarithmic rule indicated by Takenaka *et al.* (2006). Comparing sea breeze and

extended sea breeze, extended sea breeze wind speeds are generally larger, especially around 15:00 JST at AKw and AKA, where wind speeds exceed 3 m/s. There is also a tendency for wind speeds to be higher in AKA compared to AKw. The strength of sea breeze during the daytime varies among the stations, and wind speeds tend to be higher at Na, Ng, and Nh than at other station on the plain. On the other hand, for nighttime mountain breeze and land breeze, wind speed differences between stations tend to be smaller than those for sea breeze.

3.1.7 Diurnal variation in sea and land breezes at AK with 10min. data

Since the wind data used in the previous analyses were hourly values, using 10-min resolution data for AK (AKw), daily variations were analyzed for temperature, vector mean wind direction and speed averaged over the days under analysis to comprehensively investigate sea and land breeze behaviors. Diurnal variations in the direction and speed of the vector mean wind are shown in Fig. 3-7.

Figure 3-9 shows that the northeasterly wind was blowing steadily until around 07:00 JST, after which the wind direction gradually rotated clockwise. The change in wind direction during the morning hours, especially from 07:00 to 12:00 JST, is more rapid than at other times of the day. The vector mean wind speed peaks around 08:00-09:00 JST and 15:00, JST while it weakens most around 11:00 JST and 20:00-21:00 JST. The first wind speed peak at 08:00-09:00 JST corresponds to the time when the land breeze is changing to sea breeze. The land breeze speed continues to increase from the start to the end of the duration, reaching their peak around the time of the end of the period. The wind speed is approximately 2.5 m/s. On the other hand, the wind speed around 11:00-12:00 JST when the southerly sea breeze is blowing is about 2.5 m/s, similar to the peak speed of the land breeze, but then the extended sea breeze reaches its peak and the wind speed increases to about 3.5 m/s around 15:00 JST when the second peak period occurs. This is in agreement with Neyama (1982), who

considered 15:00 JST to be the peak for sea breeze. Then the extended sea breeze continues to blow, but the wind speed rapidly decreases, and by 20:00-21:00 JST, there is almost no wind. Since then, the easterly land breeze speed continues to increase. Neyama (1982) shows the average diurnal variation of winds in May and August, and indicates that easterly winds increase at 09:00 JST. His analysis does not define this easterly wind as land breeze, but it is consistent with the diurnal variation of wind speed.

Neyama (1982) analyzed the diurnal variations in winds in Kobe and found that in May and August, the wind direction significantly shifts from east to south between 09:00 and 12:00 JST and from southwest to northwest between 18:00 and 21:00 JST. The results of this study show a similar trend, and these significant changes in wind direction correspond to a switch from land breeze to sea breeze and from extended sea breeze to mountain breeze, respectively.

Neyama (1982) captured an overview of the diurnal variation of winds during the warm season at Kobe, showing wind shifts every three hours. However, he simply defines sea and land breeze direction as bounded by east to west direction without distinguishing between sea and land breeze and extended sea breeze. On the other hand, in this paper, the two types of breezes were analyzed by subdividing by wind direction each other, so, compared to Neyama (1982), this study was able to capture more details on the diurnal variations in the local wind system around Kobe.

These results indicate that the wind direction in Kobe on sunny calm days rotates clockwise over time. This is consistent with the findings of Sakazaki and Fujiwara (2008) and Mizomoto and Ishihara (2009). However, previous studies did not necessarily use wind data with high temporal resolution, and thus did not capture the detailed characteristics of the clockwise wind direction change. In contrast, the analysis of 10-minute data in this paper reveals that wind direction does not change clockwise at a constant rate throughout the diurnal variation, but rather that there is slow and sudden change in wind direction.

The diurnal variation of the vector mean wind speed clearly shows two peaks twice a day, with the wind speed being at its lowest around 11:00 and 20:00 JST. These periods of decreased wind speed are considered to correspond to "*Nagi*," and the results generally correspond to those of Ino and Neyama (1973) and Neyama (1982). Considering this result together with Table 3-5, this decrease in wind speed roughly corresponds to an extended sea breeze alternation. The vector mean wind speeds indicate the peak strength of the extended sea breeze and land breeze to be about 3.5 m/s and 2.5 m/s, respectively. This result is generally consistent with the analysis by Neyama (1982). In addition, the use of wind data with high temporal resolution in this paper enables us to capture differences in wind speeds between sea breezes of different scales, and it is suggested that extended sea breeze may be stronger about 1 m/s at its peak compared to sea breeze.

3.1.8 Diurnal variations in temperature at sea and on land

The results of the previous section suggest that the diurnal variation of wind direction at AKw, which is located on an artificial island, is generally smooth and clockwise, indicating a continuous transition of sea and land breezes of different scales. However, as mentioned earlier, numerical models and simulations are needed to verify whether the thermally induced local circulation defined by wind direction is really caused by thermal contrast. On the other hand, Kono and Nishizuka (2006) investigated the relationship between the diurnal variation of wind direction and the sea and land temperature difference in Himeji, Hyogo Prefecture, in August, and found a good correspondence between them. Thus, the occurrence of sea and land breezes can be determined to some extent from the sea and land temperature difference. To examine the diurnal variation in wind direction in relation to the temperature differences between sea and land at AKw, we analyzed the temperatures of the air and the sea surface using temperature data from AKt, as well as hourly sea surface temperature data (1 m below the surface) from the Kobe Port provided by the 5th

Regional Coast Guard Headquarters of the Japan Coast Guard. The results are shown in Fig. 3-10, which indicate that the diurnal variations in SST at Kobe Port is smaller than that in air temperature at AKt, which ranges between 21 °C and 22 °C throughout the day. A higher temperature at AKt than at SST was observed from after 10:00 to after 18:00 JST.

Nakata (1985) investigated the meteorological conditions near the sea surface in the western part of the Seto Inland Sea and found that the air temperature difference between land and sea before and after the onset of the sea breeze is approximately 0.5 °C (Fig. 3-11). Assuming that sea breeze changes are consistent with the air temperature difference between land and sea around Kobe, the sea breeze at AKw starts at around 10:00 (Table 3-5), and the change in wind direction is consistent with the change in the sea-land temperature difference. On the other hand, the sea breeze at stations closer to the Rokko Mountains, such as Na and Hu, tends to start about 2 hours earlier than that at AKw. At these stations, the sea breeze may begin blowing earlier than at other locations owing to the presence of local valley breeze after sunrise before the start of sea breeze. Neyama (1974) investigated the relationship between sea and land breeze and slope winds on the mountainside in Kure City, Hiroshima Prefecture. He found that even when the land breeze was blowing at Kure on the coast, slope winds began to blow on the mountainside in some cases. In Kobe City, the distance between the sea and the mountains is smaller than that in Kure, so the interaction between sea and land breeze and mountain and valley breeze can be even larger.

On the other hand, the sea-land temperature difference inverses again around 19:00 JST, but sea breezes continue to blow at AKw. However, around 19:00 JST, the sea breeze has shifted to an extended sea breeze with a large scale. Therefore, it is considered that the driving source of the sea breeze is the temperature difference between sea and land on a larger scale, as pointed out by the Architectural Institute of Japan (2000), and it does not coincide with the inversion of the temperature difference

between land and sea around Kobe Port.

The reversal of the sea-land temperature difference around 19:00 JST generally corresponds to the end of sea breeze at En, Na, and Hu, which are located in the eastern part of the target area (Table 3-5). In the eastern part of the region, the extended sea breeze and land breeze have relatively short duration compared to other regions, while mountain breeze from the Rokko Mountains prevails for a long time. Therefore, it is possible that the changes in sea and land temperatures around Kobe Bay may correspond better to the changes in wind direction in areas where the influence of extended sea breeze and land breeze are relatively small. We would like to verify this point in the future.

3.2 Case study on the days with different diurnal variation of the local wind system

3.2.1 Objective

The analysis in the previous section has enabled us to capture the diurnal variation of the wind system averaged over the sea and land breeze blowing days in the Kobe area. The hourly windrose showed that prevailing wind directions were observed in several directions, especially at nighttime at the stations near the Rokko Mountains. In the previous section, the distribution of the vector mean wind was used to capture the averaged wind system. The results of the previous section suggest that the diurnal variation may differ from day to day even on the same sea and land breeze blowing day.

Therefore, in this section, we focus on the eastern part of Kobe City, in which Nh is located, where two prevailing wind directions were observed at 03:00 JST at night in the previous section. The diurnal variation of the wind system is examined by extracting the days that show different diurnal variations in Nh and conducting a case study. In this section, in addition to the stations in the previous section, we use data

from a station on the top of Mt. Rokko (Ro) and our original station on the lower Mt. Rokko to capture the wind pattern from the mountain area to the sea.

3.2.2 Data used

To capture changes in the local wind system from the Rokko Mountains to Kobe urban area and over Osaka Bay, AEROS wind direction and speed data (En, Ri, Na, Nh, Ro) were used (Fig. 2-3). Wind and air temperature data from AKw, AKt and AKA also were used. In addition, KS data is also used to capture changes in wind and air temperature in the lower-slope of the Rokko Mountains (Fig. 2-3).

3.2.3 Selection of dates for analysis

In this section, to capture diurnal variations in local circulation, including mountain breeze and the cold air drainage from the Rokko Mountains, the three-month autumn period (September–November 2017) was set as the study period. Then a case study was conducted on sunny calm days. As mentioned in section 2.2.2, the period from October 24 to November 3, 2017 was excluded from the analysis because the wind direction and speed sensor at KS failed.

According to the method described in Section 2.2.4, the 13 days were extracted as sunny calm days during the study period. Excluding instrument failure days, 8 days (September 25 and 26, October 8 to 10, and November 5, 12, and 27) were selected. The Kinki District was influenced by a migratory high, on the surface weather map analyzed by Japan Meteorological Agency (JMA) during all of these 8 days.

The purpose of this section is to identify cases in which the diurnal variation of the nighttime local wind system in the eastern part of Kobe City differs even on the same sunny calm day, and to capture the characteristics of the diurnal variation. For the above eight days, we focused on the period from 00:00 to 06:00 JST, centering on

03:00 JST, when the nighttime local wind system is considered to develop, and selected two consecutive sunny calm days, October 9 and 10, when the nighttime wind direction variation at Nh was different, as the days for case study. The surface weather charts for the subject day are shown in Fig. 3-12. Figure 3-13 shows the wind direction of Nh during these two days. The wind direction between 00:00 and 06:00 JST shows that on October 9, the wind direction was northeasterly, while on October 10, it was prevailing wind direction was almost northerly. For example, comparing the wind system at 03:00 JST (Fig. 3-14a), on October 9, the winds are blowing northeastward at Nh and Na located to the northwest of Nh, while on October 10, the wind direction at the two stations is generally northward. However, there is no significant difference between the wind systems of the two days in the entire area.

The diurnal variation of wind direction also differs between the two days. On October 9, the wind direction shifted generally to the clockwise direction, while on October 10, after the northerly winds ended around 06:00 JST, the wind direction suddenly shifted to the southerly direction from around 07:00 JST (Fig. 3-13). For example, comparing the wind system at 08:00 JST (Fig. 3-14b), the wind system on October 9 was generally easterly over the entire area, while on October 10 it was southerly at Nh and Na and easterly over the artificial islands, while the wind direction at other stations varied from station to station.

On the other hand, a peculiarity observed at Nh was that the westerly wind was stable from 18:00 to 00:00 JST on the October 9, whereas it was more variable on the October 10 (Fig. 3-13). For example, a comparison of the wind system at 20:00 JST shows that on October 9 (Fig. 3-14c), winds were generally westerly at all stations except En and Na, while on October 10, winds were generally easterly in the eastern part of the target area, but there were large differences in wind direction between stations in the western part.

In the followings, the diurnal variation of the wind system is captured for three regions: the plains, the artificial island, and the mountainous area.

3.2.4 Diurnal variation of wind in three areas (artificial island, plain, and mountain) around Kobe City

(1) The plain area

Figure 3-15 shows the diurnal variation of winds at En, and Na in the plain area.

The diurnal variation of wind direction on both days was similar at the three sites (Fig. 3-15). However, as well as Nh, a difference was observed in the diurnal variation of wind direction between October 9 and 10. On October 9, the wind direction changed in a clockwise direction; on October 10, the wind direction was relatively stable from north-northwest from 00:00 to 06:00 JST, then rapidly shifted to the south from 07:00 to 08:00 JST. On October 9, a northerly wind blowing from 00:00 to 06:00 JST was also observed, but it had peculiar characteristics in that it was mixed with easterly winds.

The trend of diurnal variation in wind direction is similar for En and Na, but there is a difference in the way the wind direction varies. In particular, a comparison of the diurnal variations on October 9 shows that the wind direction in En is more discontinuous than that in Na, with two major wind direction changes, one from north to south around 12:00 pm and the other from south to north around 18:00 pm.

(2) The artificial islands

Figures 3-16 shows the diurnal variations in wind at AKA (Fig. 3-16a), AKw (Fig. 3-16b) and Ri (Fig. 3-16c), the stations on the artificial island. Although simple comparisons cannot be made between AKw or AKA and Ri because of the different time intervals of the measurements, the diurnal variations in the wind at these three stations were almost similar. The wind direction changed clockwise from northeast to east, south, and southwest in the morning on both days, and the southwesterly wind in the afternoon was more stable than the other wind directions for a longer period. Compared to the stations on the plain described in the previous section, these stations are characterized by continuous southwesterly winds, and their wind direction

indicates that the extended sea breeze is stable. However, the wind direction at AKw was different from that at the other two sites in that the wind direction remained northerly from 00:00 to 06:00 JST on October 10. In addition, the wind direction between 18:00 and 00:00 JST at AKw and Ri exhibited significant fluctuations on October 10 as opposed to the stable westerly winds at AKw and Ri on October 9.

(3) The lower-slope and summit of the Rokko Mountains

Figure 3-17 shows the diurnal variation of wind and air temperature in the lower-slope of Mt. Rokko (KS). Figure 3-18 shows the diurnal variation of wind at the top of the Rokko Mountains (Ro) at AEROS. Northerly mountain breezes blew steadily in the lower-slope of the Rokko Mountains, particularly during nighttime.

Diurnal variations in air temperature generally showed a rapid drop in temperature after 16:00 JST. On the other hand, the rapid rise in air temperature that began around 07:00 JST in the morning on both days tended to be stagnation around 08:00–09:00 JST and then rose again, showing a characteristic diurnal change.

Also, the diurnal variation of wind speed remained in the order of 1 m/s throughout the day. However, KS was characterized by a so-called “*Nagi*” (Yoshino, 1986), a phenomenon in which wind speeds weaken for a certain period in response to a sudden change in wind direction around 07:00 JST. Although not seen on October 9, a “*Nagi*” corresponding to a northerly wind direction diurnal variation was also observed around 16:00 JST on October 10.

Ro is located at an elevation of 881 m. During on October 9 and 10, wind speeds at Ro were generally lower than 4 m/s (Fig. 3-18). Comparing the diurnal variation of wind direction on the two days, there is a difference in wind direction during the daytime (06-18:00), with a large wind direction variation on October 9, while the wind is generally blowing from the west on October 10. the north to easterly (0–90°) winds observed at other sites did not occur during the two days.

The local circulation pattern at lower-slope on the Rokko Mountains is different

from that in the urban plain. Even on October 9, when stable land breeze was observed over the plain, mountain breezes were stable at lower-slope on the Rokko Mountains.

Yoshino (1986) showed that the land breeze at Kobe has a thickness of approximately 200 to 300 m. However, no detailed data is presented on the thickness of it. Therefore, as a simple comparison cannot be made, KS lies at approximately 160 m above sea level, it is considered to be affected by the land breeze. However, as the ridge to the east of KS extends to the south, it is believed that mountain breeze blows steadily during the night because the ridge prevents the intrusion of easterly land breeze.

The diurnal variation of temperature is characterized by a temporary interruption of the temperature increase around 08:00 JST. This interruption lasts for approximately 2 to 3 hours, after which the temperature rises again. This interruption is also observed at AKt on the plain (Fig. 3-19). The time of cessation of temperature increase in KS generally corresponds to the end of northerly mountain breeze and shift to the southerly wind direction as the overall trend in the target area (Table 3-5). The time around 08:00 JST also corresponds to the time of transition from land breeze to sea breeze at AKw. Consequently, the temporary cessation of temperature at that time may have been caused by the intrusion of cool sea breeze that suppressed the temperature rise.

3.2.5 Relationship between wind systems and temperature anomaly distribution

The results of the previous section indicate that even during two consecutive sunny calm days, diurnal variations in the wind system can be different. In particular, there are large differences in the degree of easterly land breeze prevailing between 08:00 and 09:00 JST and that of extended sea breeze prevailing after sunset between October 9 and 10. On the other hand, the difference in Nh wind direction observed at 03:00 JST was relatively localized, and the wind system over the entire area was

generally similar on both days. Therefore, it is considered that the differences in the wind system in the target area on both days were greatly influenced by the diurnal variations in the wind system over a broader region. Therefore, in this section, we capture the differences between the wind systems on the two days in terms of the distributions of wind and temperature anomaly over the area between Kyoto, Osaka, and Kobe using AEROS wind data at these three prefectures. Temperatures were altitude-corrected using the general lower troposphere temperature lapse rate ($6.5^{\circ}\text{C}/\text{km}$), referring to Kasuya and Kawamura (2011).

Figure 3-20 shows the distribution of broad-scale winds and elevation-corrected temperature anomalies at 03:00, 08:00, and 20:00 JST on October 9 and 10. At 03:00 JST, the wind systems were generally the same over the entire area between Kyoto, Osaka, and Kobe, as shown in the previous section, showing no significant differences in the overall wind system in the Kobe area. The wind speed tends to be slightly stronger on October 10, but prevailing winds are outbreaks from inland. The distribution of temperature anomaly was not significantly different between the two days.

At 08:00 JST, a large difference was observed between the two days, with easterly land breezes prevailing on October 9, and their wind speeds were higher. In particular, strong winds appear from breaks in the mountainous terrain, and easterly winds are prevailing over the entire area around Kobe. On the other hand, winds from inland to the sea were observed along the eastern coast of Osaka Bay on 10 October, but wind direction differences between stations were large and wind speeds were small compared to those on 9 October in the Kyoto-Osaka-Kobe area as a whole. The wind direction in the area surrounding Kobe also varied significantly from station to station. However, the differences in the distribution of temperature anomalies were smaller than those of the wind systems, and were generally similar for both days.

At 20:00 JST, extended sea breeze was dominant on 9 October, extending 20-25 km inland from the Osaka Plain. The prevailing winds in the Kobe area are also

generally westerly. On the other hand, on October 10, there were few stations with wind direction from the sea to inland, and there was a large difference in wind direction among the stations. The prevailing winds were generally easterly over the Kobe area, but northerly winds were observed over the western part of the Kobe area. There is no significant difference in temperature anomaly distribution between the two days.

As described above, even on the same sunny calm day, there was a difference in the diurnal variation of the broad-scale wind system between October 9 and 10, and this difference caused the difference in the diurnal variation of the local wind system in the Kobe area. Although four types of wind systems of different scales are generated in the Kobe area, it can be inferred that the diurnal variations are greatly influenced by extended sea breezes and land breezes of larger scale.

Circulations such as sea and land breeze are driven by pressure differences caused by thermal contrasts. Therefore, the extended sea breeze and land breeze that are the subject of this study may correspond to the pressure differences between the Kyoto-Osaka-Kobe area.

Therefore, although qualitative, here we examined diurnal variations in the difference in corrected sea-level pressure between AK and AKY, which corresponds to the inland area of the Osaka Plain (Figs. 2-4; 3-21). Comparing the pressure differences around 08:00 and 20:00 JST, when differences were observed in the appearance of extended sea breeze and land breeze on the target days, pressure differences corresponding to the wind systems were observed at both 08:00 and 20:00 JST on the 9th, when extended sea breeze and land breeze were prominent. In other words, AK has higher pressure when sea breeze occurs, and AKY has higher pressure when land breeze occurs. On 10 October, the pressure gradient was almost zero at 08:00 JST, and at 20:00 JST, it was higher at AKY, indicating a pressure gradient that makes it difficult for sea breezes to blow. Although the pressure gradient between AK and AKY alone does not necessarily determine the regional wind system, and a more

detailed study is needed, it is suggested that the broad-scale wind system in the Kyoto-Osaka-Kobe region may correspond to the pressure gradient in the same region.

3.3 Effects of local wind systems on temperature distribution

3.3.1 Objective

The results up to the previous section indicate that local wind systems such as sea and land breezes and mountain breezes prevail on sunny calm days in the Kobe area. Sea breeze and extended sea breeze prevail over the entire area during the daytime, while mountain breeze prevails near the Rokko Mountains, and easterly land breeze prevails in other areas at night. As mentioned earlier, many studies have shown that such local wind systems influence the formation of temperature distributions, and it is considered that there is a relationship between wind systems and temperatures in this region.

Miyazaki *et al.* (2006) studied the distribution of temperatures around Kobe City on a clear day in August 1990. They investigated the relationship between thermally induced local circulation and diurnal variations in temperature and pointed out that temperature tends to decrease (increase) when the sea and land breezes strengthen (weaken). Ueki (2005) also pointed out that in Kobe City, temperature at Kobe Marine Observatory increased at a rate of 0.028 °C per year since 1961 owing to urbanization. Along with this long-term trend of urban warming in the Kobe urban area, a warm region is formed over the entire urban area at night in summer. However, its center appears to have shifted to the east during daytime, suggesting a shift of the warm area to the leeward side of the sea breeze (Miyazaki *et al.*, 2006). Many such studies on local wind systems and temperature distributions in urban areas have been conducted outside of Kobe City (e.g., Ishii *et al.*, 2000; Kanou and Mikami, 2003; Kiyota and Kiyota, 2005; Sakaida *et al.*, 2011; Yamato *et al.*, 2011; Takahashi and Takahashi, 2013). However, Miyazaki *et al.* (2006), who measured the temperature distribution in

the urban area of Kobe using a large number of thermometers and analyzed its relationship with the wind system, only suggested a relationship based on observation data from a single location for wind.

As described in section 1.3.4, the Takebayashi's group has obtained certain findings on the interaction between mountain breezes from the Rokko Mountains and temperature. Specifically, the following findings were obtained: (1) the outflow of cold air accumulated in mountain valley can be expected to reduce the temperature of urban areas in a range up to about 1 km from the mountain edge; (2) the occurrence of cold air drainage is limited to conditions with weak extended sea breeze; and (3) the temperature of cold air drainage is at most 2°C cooler. Cold air drainage is an important factor affecting the distribution of urban temperatures because it brings cool air to urban areas. Therefore, it is important to understand the diurnal variation of cold air drainage, especially its onset time and the range of its influence. However, observational studies of cold air drainage as down slope wind have not yet been conducted, and the range of influence of cold air drainage is not necessarily clear.

The Kobe urban area lies between the mountains and the sea on the north and south sides, respectively. Clarifying the actual conditions of temperature distribution and local wind systems in the target region will provide important information for clarifying local climate in urban areas, where plains and mountains are typically located near each other in Japan.

This section reports high-density temperature observations conducted in Kobe City and analyzed together with AEROS data to understand the relationship between the diurnal variation of the local wind system and the temperatures. The purpose of this section is to clarify the characteristics of the diurnal variation of the local wind system and temperature distribution in the city of Kobe on a typical sunny calm day in the autumn season.

3.3.2 Data used

Wind data from 10 of the AEROS stations (En, Ri, Nh, Na, Hu, Mi, Hs, Ng, Su, and Pt) and 2 AMeDAS stations (AK and AKA) were used to investigate the local wind system (Figs. 2-3, 3-22).

To capture the relationship between local wind systems and temperature changes, the total of 33 fixed point original observation data of surface air temperature were used.

3.3.3 Selection of dates for analysis

In this section, the period from August to October 2014 was set as the study period. According to the method described in Section 2.2.4, sunny days were selected for analysis, for a total of 15 days (September: 6 days; 9, 13, 14, 23, 28 and 29, October: 9 days; 7, 8, 16, 17, 18, 19, 23, 24 and 28).

Next, to investigate the relationship between the local wind system and temperature diurnal variations in the Kobe urban area, the days in which a local wind system typical of sunny calm days was considered to have occurred were further selected from the target days. Among the 15 target days, three sunny calm days (October 8, 18, and 24) were selected using 850 hPa wind speeds on 09:00 JST at Matsue and Shionomisaki, located near the target area. On the selected three days, migratory high was widely covering the target area (Fig. 3-23).

The diurnal variation of wind direction on each day was investigated, and the results were almost the same in each day. In this section, we focus on the case study of October 18, 2014, when the diurnal variation in wind direction was most pronounced and thermally induced local circulation was most likely to have developed.

Table 3-6 shows the hourly wind direction at each location. (Fig. 3-15)The overall trend of diurnal variation in wind direction is similar to that of the direction of the vector mean wind in Section 3.1.5. However, the differences between

En and Na, Hu, which were not clearly observed in the vector mean wind direction, became evident on the subject day. In the previous section, we reported that a mountain breeze was prevailing during nighttime in En. Conversely, during the subject day, relatively easterly winds were steadily prevailing, and land breeze was prevailing throughout 01:00–09:00 JST. In addition, a comparison of the wind direction during the day in En shows that the sea breeze observed in Na and Hu was not as clear in En, while the land breeze turned into an extended sea breeze around 10:00–11:00 JST. In the previous sections, we showed that En tended to have a different wind system from that of Na and Hu located in the same plain area (Fig. 3-15). This section similarly shows diurnal variations in the winds that are peculiar to En. In addition, at Nh, located relatively far from the Rokko Mountains, and at sites on artificial islands, the vector mean mountain breeze was relatively short-lived, while at some sites (Nh, Mi, AKw, and AKA), it was continuous for approximately 5 to 6 hours on the day.

3.3.4 Regional classification by diurnal variation of temperature and estimation of cold air drainage range

3.3.4.1 Diurnal variation of temperature averaged for all locations

To investigate the relationship between the local wind system and the diurnal variation of temperature, the diurnal variation of temperature averaged for all original 33 stations in target area was investigated (Fig. 3-24), except for point 18, which was failed on the target day. The rapid drop in temperature that occurred between 16:00 and 18:00 JST is characteristic.

Next, the target area was divided into the following five regions based on the similarity of the characteristics of diurnal variations in temperature at individual stations by visual inspection. For convenience, each region is referred to as the mountain, west, central, east, and island regions, respectively.

1. Mountain (5, 6, 7, 8, 9, 11, 19, 25)

2. West (1, 2, 3, 4, 12, 13)
3. Central (10, 14, 15, 16, 17, 26, 28, 33)
4. East (20, 21, 22, 23, 27, 29, 30)
5. Island (24, 31, 32)

The averaged diurnal variations of temperature for each region were then compared (Fig. 3-25).

3.3.4.2 Characteristics of temperature diurnal variations in each region

(1) The mountain area

At the foot of the mountain, temperatures began to drop rapidly from around 16:00 JST and continued to do so until around 17:30 JST. However, the rate of temperature change in the other four regions during the same period was almost same but smaller than that at the mountain. Therefore, the temperature decrease occurring at the mountain was captured in Fig. 3-24. The magnitude of the temperature drop at the foot of the mountain area (Mount) was approximately 4 °C over 90 min. The wind direction at Hu, the AEROS station closest to the Rokko Mountains, changed significantly from south-southeast to northwest around 16:00 JST (Table 3-6). This suggests that the cool mountain breeze from the Rokko Mountains is responsible for the temperature drop at the foot of the mountains during this period. Takebayashi and Moriyama (2002) pointed out that the cold air drainage is at most 2 °C cooler. This study reports a value approximately twice as large as their result. This suggests that the effect of cold air drainage in lowering temperature may vary from place to place, even at the foot of the same mountain.

Takebayashi *et al.* (2001) pointed out that mountain breezes can be expected to cause lower temperatures in a range of up to 1 km from the mountain edge. However, Takebayashi *et al.* (2001) only presented the results for one valley (river) in the Kobe City area and did not conduct sufficient research for the entire Kobe City area. In Fig. 3-24, the rapid drop in temperature between 16:00 and 18:00 JST, which appears in

the diurnal variation of the average temperature at all stations, is approximately 2°C. We attempted to examine the range of influence of cold air drainage by examining the amount of temperature drop during the same period at each station using this value as a reference. For example, Fig. 3-26 shows the diurnal variations in temperature at locations 2, 4, and 5 at western Kobe area. The temperature at the foot of the mountain at Station 5 dropped sharply by 4.2 °C from 15:40 to 17:20 JST. After that, the temperature remained almost constant until around 23:00 JST. On the other hand, at stations 2 and 4, the temperature decrease during the same time period is generally less than 2°C, which is smaller than that at station 5. Therefore, in this case, applying the aforementioned thresholds, the effect of cold air drainage was limited to the area between (5) and (4).

Hamada and Ichinose (2011) investigated the effect of mountain breezes on urban temperatures in Nagano City. They observed that mountain breezes cause a decrease in temperature of approximately 4 °C in 40 min from approximately 19:30 and that temperatures remain at a lower level until the end of the mountain breeze. The results of this study are consistent with the findings of Hamada and Ichinose (2011).

Figure 3-27 shows the range of influence of cold air drainage from the Rokko Mountains, estimated from the amount of temperature decrease from 16:00 to 18:00 JST at each station. This suggests that the range of influence of cold air drainage varies among the stations. Therefore, the results of Takebayashi *et al.* (2001), which indicated that the influence extends up to about 1 km from the foot of the mountain, may be a limited trend for a particular station. Based on the definition in this paper, the largest horizontal range of influence of cold air drainage is found at station 23, where the temperature drop over a 2-hour period reaches 3.1°C even at the coastal station. The contour line at 100 m elevation in the figure is considered to be the boundary between the Rokko Mountains and the plain, and the straight line distance from there to station 23 is estimated to be about 2.5 km. On the other hand, the distance influenced by cold air drainage is relatively short in the central area near stations 15

and 16. Although it is not possible to make a precise analysis based on this study alone, it can be inferred that the influence range of cold air drainage is narrower than in other areas due to the influence of high-rise buildings and dense buildings in the center of the urban area. In the western part of the area, the influence of cold air drainage extends to a range of about 2 km parallel to the foot of the Rokko Mountains. Furthermore, a comparison of the degree of influence of cold air drainage shows that station 7 has the largest temperature drop of -5.0°C . Stations 5 and 25, which are at the same elevation as station 7, also have temperature drops of -4°C or more. On the other hand, stations about 1 km away from the foot of the mountain generally show a temperature decrease of about -3°C , but the magnitude of the decrease varies from station to station.

Although it is not possible to determine the cause of the difference, it may be related to local topographic features such as the presence or absence of rivers and valleys, or to differences in ground surface coverage such as the degree of building density.

(2) The west, central, and east area

A comparison of diurnal variations of temperatures in the west, central, and east regions shows that the central region tends to be warmer than the east and west regions during nighttime (Fig. 3-25). On the other hand, during daytime, temperatures were higher in the west, followed by those in the center and in the east.

In particular, the rate of temperature increase in the west decreases around 09:00 JST, and the subsequent temperature rise is suppressed, resulting in relatively low temperatures compared to other regions. The wind direction at Su and Ng located in the west shows that the wind direction changes from northerly to easterly or southerly around 09:00 JST (Table 3-6). This suggests that the change in the rate of temperature increase in the west is caused by the suppression of temperature increase by the cool sea breeze. However, it is unclear why the temperature increase rate changes only in

the west since 09:00 JST is roughly the time when the wind direction starts to change from the sea over most of the Kobe urban area.

(3) The artificial islands

The diurnal variations of temperatures on Port Island and Rokko Island, artificial islands in Osaka Bay, tend to be smaller because they are surrounded by the sea (Fig. 3-25). Briefly, temperature tends to be lower during daytime and higher during nighttime. On the artificial island, temperature dropped at a constant rate from 16:00 to 21:00 JST and then rose again from 21:00 to 22:00 JST. In addition, a temporary stabilization of temperature decrease was observed around 18:00 JST during the 16:00-21:00 JST. Notably, the period from 16:00 to 19:00 JST coincides with the end of the sea breeze (Table 3-6). On the other hand, the period from 21:00 to 22:00 JST corresponds to the time in which the wind direction begins to change significantly to an easterly land breeze. It can be speculated that the temperature increases from 21:00 to 22:00 JST may be due to the passage of relatively warm land breeze.

Therefore, in this section, wind system and temperature anomaly distributions over a wider area in the Kyoto, Osaka and Kobe region are considered for the period from 19:00 to 24:00 JST, which includes the period from 21:00 to 22:00 JST when temperature increases were observed over the artificial islands (Fig. 3-28). According to this figure, land breeze toward Osaka Bay began to blow in the coastal area around 19:00 JST, and the strength and scale of it increased with the passage of time. At 21:00 JST, land breeze is generally observed over the entire region, and then wind speed increases in the inland area. The wind system at 22:00 JST suggests that the easterly winds in the area around Kobe are the result of the extension of two major wind directions: land breezes bypassing the Rokko Mountains and land breezes outbreaking from the Osaka Plain. The relationship between the distribution of temperature anomaly and the land breeze shows that the coastal areas of the Osaka Plain generally

tend to be relatively warm, and it is possible that the land breeze that has passed through there has the same characteristics. Therefore, it is suggested that the inflow of winds from Osaka plain where is the relatively higher temperature onto the artificial islands may have caused the temperature increase.

Such nighttime temperature increases over the artificial island occurred also on October 24 within the three days selected in Section 3.3.3 (Fig. 3-29), in addition to October 18 when the case study was conducted in this section. Comparing the wind system and temperature anomaly distributions for these three days at 23:00 JST before and after the temperature increase (Fig. 3-30), no significant differences were found in both of them. However, wind speeds on October 8, when no temperature increase occurred, tended to be stronger than those on the other two days.

Therefore, we compared the diurnal variation of the winds over the three days using 10-minute data for AKA on the artificial island (Fig. 3-31). The results show that on October 8, when no temperature increase occurred, the easterly land breeze started about 3 hours earlier than on the other two days, around 18:00 JST. In contrast, on the 18th and 24th, the transition from northerly to easterly land breezes occurred around 21:00 JST, which roughly corresponds to the time of the onset of the temperature increase. On the other hand, on the 8th, the land breeze changed to land breeze around 18:00 JST, but no warming occurred around that time.

This suggests that the temperature on the artificial islands does not necessarily increase when land breezes blow, but only when the land breeze is relatively warmer than the temperature on the artificial islands. Although it is difficult to make a detailed study, we compared the diurnal variation of the temperature difference between AKA and AO as a simplified evaluation of the temperature difference between the land breeze and the artificial island (Fig. 3-32). The results show that the amplitude of the diurnal variation of the temperature difference is small on the 8th when no temperature increase occurs, and that the temperature tends to be higher on the artificial island at around 18:00 JST and after the time of the conversion to the land breeze. In contrast,

on the 18th and 24th, the amplitude of the diurnal variation of the temperature difference is large, and the temperature on the artificial island tends to be relatively lower during the period after the shift to land breeze. This suggests that the reason for the absence of temperature increase on the artificial island on the 8th may be that the land breeze was blowing, but its temperature was relatively lower than that of the other two days.

These results suggest that the nighttime temperature increase over the artificial island may have occurred when the wind system shifted to easterly land breezes, which were relatively hot compared to the temperature over the artificial island. Furthermore, considering the fact that the warming occurred on an artificial island, it is possible that easterly winds blowing over a relatively warm ocean may have been the cause of the warming. However, the density of AEROS data is currently too small to capture the temperature distribution over land, and there are no data available over the ocean. Therefore, numerical models should be used to analyze the mechanism of the temperature increase.

(4) Suppression of temperature rise by sea breeze

The results up to the previous section suggest that the onset of the sea breeze halts the temperature rise in some regions. Therefore, to capture the effect of sea breeze on the diurnal variation of temperature, we calculated the amount of the temperature change for each region. Fig. 3-33 shows the diurnal variation of temperature changes. The temperature increase was calculated as the difference of 10-min data at each station, and a five-term moving average was used to remove minute variations and understand the trend of the temperature change.

Excluding the temperature rise on the artificial island around 22:00 JST, differences were observed in the amount of temperature change between the five regions from 06:00 to 10:00 JST and 15:00 to 20:00 JST.

After sunrise, the amount of temperature increase rose rapidly with time from

06:00 to 07:00 JST in the west, central, east, and mountain regions, whereas the degree of change is small on the artificial islands. This is considered to be characteristics of artificial islands surrounded by the sea, which has a large heat capacity.

As to the four regions other than those on the artificial island, the trend of the temperature increase generally turned to decrease between 07:20 and 07:40 JST, which may correspond to a change in the wind system. Looking at Table 3-6, which shows the wind direction at each station on the target day, and the hourly wind distribution from 07:00 to 10:00 JST (Fig. 3-34), the period from 07:00 to 08:00 JST coincides with the time when the sea breeze began to blow from a situation in which the mountain breeze and land breeze are blowing. In particular, from 07:00 to 09:00 JST, the wind direction at each station rotated clockwise significantly, and the wind speed increased. By 10:00 JST, the entire target area was generally under the influence of the sea breeze.

In the previous section, we showed that temperatures in the west tend to be relatively lower than those in other regions during the daytime because the rate of temperature rise decreases around 09:00 JST and the subsequent rise in temperature becomes slower. Figure 3-33 shows a large decrease in the rate of temperature rise from 08:30 to 10:00 JST, especially in the west. This is thought to be responsible for the relatively low temperatures during the daytime in this area. In fact, the distribution of wind systems and temperature anomalies at 10:00 JST (Fig. 3-35) shows prevailing winds from the ocean at many stations in the target area, and temperature anomalies are negative at stations on artificial islands and in coastal areas. Table 3-6 shows that sea breeze and easterly land breeze are mixed at 10:00 JST. The broad area wind system at 10:00 JST (Fig. 3-36) shows that it is shifting to southerly sea breeze at the stations on the plains in the target area, but easterly land breeze is generally dominant in the Kyoto-Osaka-Kobe area. Sea breezes are almost non-existent along the Osaka Plain.

From the above, it can be inferred that the cessation of the temperature increase

seen between around 07:00 and 08:00 JST was due to the influence of cool air brought by sea breeze beginning to blow during the same period, as we saw a similar trend in Section 3.2.4. Then, as the sea breeze developed and its area expanded, the temperature change rates at all stations were generally similar.

After the suppression of the temperature increase by sea breeze, the rate of change of temperature generally decreases at almost constant rate from 10:00 to 15:00 JST. However, the rate of change rapidly decreases from 15:00 to 17:00 JST, and after that, the rate of change tends to remain constant at approximately -0.1°C per ten minutes. Compared to the diurnal variation of wind direction on the subject day, the wind direction in the area generally changes from sea breeze to extended sea breeze around 15:00 JST (Table 3-6). Therefore, it is possible that the sudden change in the rate of temperature change during this time period, as well as the suppression of the temperature increase associated with the onset of sea breeze in the morning, is due to the intrusion of extended sea breeze, which strengthens the decrease in the temperature.

The role of the sea breeze in temporarily halting the temperature rise has been investigated by Hisada *et al.* (2005), who focused on the urban area of Fukuoka. They showed that the rate of temperature rises at the station closest to the coast decreases rapidly as soon as sea breezes entered the area. Yamato *et al.* (2011), who investigated the effect of sea breezes on the heat island phenomenon in the Tokyo metropolitan area, also showed that on sea breeze blowing days, the magnitude of temperature rise at the coastal stations was small from the early time of the day. Therefore, it can be inferred that the rapid decrease in the temperature rise rate and the subsequent suppression of the temperature rise observed in this study may be the effect of the sea breeze blowing.

3.3.5 Relationship between local wind systems and temperature anomaly distribution

In this section, using the hourly mean temperature values for the three days

(October 8, 18, and 24, 2014), the anomaly of each station from the mean of all stations was calculated, and a temperature anomaly distribution was drawn. The hourly average values were calculated from the six 10-min temperature data from 00 to 50 min. Station 18 was missing on all three days of the analysis owing to instrument malfunction. Vector mean wind data were calculated from the hourly data of the AEROS stations, and a distribution map of the wind system was prepared.

The hourly temperature anomaly distributions revealed four time periods in which the distributions were similar. Specifically, the following four time periods were identified: 17:00–06:00, 07:00–09:00, 10:00–15:00, and 16:00 JST. This section describes the characteristics of each temperature anomaly distribution for the above four periods.

(1) 17:00 to 06:00 JST

Figure 3-37 shows the distribution of temperature anomaly and wind at 03:00 JST, which is representative of the period from 17:00 to 06:00 JST.

The spatial pattern of the temperature anomaly distribution during this period is characterized by a zonal band of negative temperature anomaly at the foot of the Rokko Mountains and high-temperature areas spanning from the center of the urban area to the artificial island. Relatively low temperatures are also observed in the eastern and western parts of the city, which are slightly distant from the foot of the Rokko Mountains. The maximum temperature anomaly was +1.8 °C at station 31, and the minimum was -1.7 °C at station 25, resulting in a temperature difference of 3.5 °C.

The surface wind system at 03:00 JST is that at the foot of the Rokko Mountains, northerly mountain breezes prevail during nighttime which is confirmed in the previous section. Also, easterly land breeze prevail along the coast and on the artificial islands.

From the above, the low temperatures observed from 17:00 to 06:00 JST at the foot of the Rokko Mountains in this study are expected to be related by mountain

breezes from the Rokko Mountains.

Miyazaki *et al.* (2006) pointed out the formation of a warm region over the entire area in their summer nighttime observations covering the period from July to September 2004. However, during sunny calm days, cool air from the Rokko Mountains is expected to have a significant impact on temperatures in the urban area.

The results of the previous section showed that the central part of the city and the artificial island tend to have higher temperatures during nighttime. The results of this section also show the same tendency. Moreover, the wind direction in the high-temperature area from the artificial island to the coastal area of the Kobe City center is generally easterly. From the above, it can be inferred that coastal areas and artificial islands not affected by mountain breeze from the Rokko Mountains are affected by land breeze, resulting in relatively high temperatures.

(2) 07:00 to 09:00 JST

Figure 3-38 shows the distribution of temperature anomaly and wind at 09:00 JST, which is representative of the period from 07:00 to 09:00 JST.

The temperature anomaly distribution during this period is characterized by a positive temperature anomaly at the stations near the foot of the Rokko Mountains, which showed low temperatures in the previous section, and a negative temperature anomaly from the center of the urban area to the artificial island. Therefore, the temperature anomaly pattern was almost opposite to that occurring in the time period described in the previous subsection. The maximum temperature anomaly was +0.9 °C at station 8, and the minimum was -1.2 °C at Station 31, resulting in a temperature difference of 2.1 °C.

The wind system was characterized by winds blowing toward the Rokko Mountains and winds generally blowing from the east. Considering the results in Section 3.1, the winds blowing toward the Rokko Mountains are considered to be local valley breezes that occur before sea breeze blow predominantly over the whole area.

The results of Section 3.1 show that the sea breeze prevails over the entire urban area, including on the artificial islands, after 10:00–11:00 JST.

The temperature anomaly distribution between 07:00 and 09:00 JST is consistent with a shift in the wind system from mountain breeze and land breeze to sea breeze. Temperatures at stations located on artificial islands (surrounded by the ocean, which has a large heat capacity) and city centers (featuring high-rise buildings, which has also a large heat capacity) rise relatively slowly when they are warmed by solar radiation after sunrise, which is expected to result in lower temperatures.

(3) 10:00 to 15:00 JST

Figure 3-39 shows the distribution of temperature anomaly and wind at 14:00 JST, which is representative of the temperature anomaly distribution from 10:00 to 15:00 JST.

The temperature anomaly distribution during this period was characterized by a low-temperature in the western part of the city, including the artificial island, while the eastern part showed a generally high-temperature. The maximum temperature anomaly was +1.3 °C at station 19, and the minimum was -1.4 °C at station 33, resulting in a temperature difference of 2.7 °C. The prevailing winds are generally southerly, indicating that the entire urban area is under the influence of sea breeze.

A study of temperature distribution in summer shows that the entire urban area features relatively high temperatures at night (Miyazaki *et al.*, 2006). However, during the daytime, the high-temperature area shifts to the east owing to westerly winds. The results of this study show a similar tendency toward higher temperatures in the eastern part of the city. However, the prevailing winds are southerly sea breeze, not westerly wind, so it is unlikely that the high-temperature area is shifted to the east by the wind.

The observations in this study alone cannot explain the relationship between the characteristics of these temperature anomaly distributions and the wind system; therefore, additional work is warranted in the future to investigate the role of land use

and the amount of anthropogenic heat emissions during daytime.

(4) 16:00 JST

Figure 3-40 shows the distribution of temperature anomaly and wind at 16:00 JST. The temperature anomaly distribution during this period is characterized by the fact that only the stations at the foot of the Rokko Mountains show significantly lower temperatures, while the relatively high temperature trend in the eastern part of the city area as shown in the previous section continues to some extent. In addition, the relative low temperature trend at 14:00 on the artificial island is weakening. The maximum temperature anomaly was +1.5 °C at station 22, whereas the minimum was -2.4 °C at station 5, resulting in a temperature difference of 3.9 °C.

The 16:00 JST temperature anomaly distribution indicates a transition between the 10:00–15:00 JST and 17:00–06:00 JST, which were described in the previous subsection. The wind system featured westerly winds over the entire city area, which was under the influence of extended sea breeze.

From the above, it can be inferred that 16:00 JST is the stage at which the positive anomaly in the urban area remains unevenly distributed in the east after switching the local wind system from sea breeze to extended sea breeze, while the foot of the Rokko Mountains begins to be influenced by the mountain breeze.

(5) 06:00 to 08:00 JST and 15:00 to 17:00 JST

The analysis of the diurnal variation of the average temperature in the target area in Section 3.3.4.1 shows that the 2-h periods from 06:00 to 08:00 JST and from 15:00 to 17:00 JST were those in which temperatures changed most rapidly (Fig. 3-24). Figures. 3-41 shows the distribution of temperature changes during these time periods.

Evidently, from 15:00 to 17:00 JST, the temperature decrease was larger at stations closer to the Rokko Mountains (Fig. 3-41a). The largest temperature decrease was observed at station 25, with a magnitude of -4.8 °C. The temperature increase

between 06:00 and 08:00 JST was also large at the stations near the Rokko Mountains (Fig. 3-41b). The largest temperature increase during this period was also observed at station 25, with a magnitude of 6.3 °C.

These results indicate that in the urban area of Kobe, the change in temperature after sunrise and before and after sunset tends to be larger at stations near the Rokko Mountains.

The period from 15:00 to 17:00 JST corresponds to the time when mountain breezes from the Rokko Mountains begin to blow. It is known from the previous sections that there is a sharp drop in temperature of approximately 4 to 5 °C. Therefore, the large drop in temperature at the stations near the Rokko Mountains during this period is considered to be related by mountain breezes. On the other hand, the period from 06:00 to 08:00 JST corresponds to the time around sunrise. The temperature increase due to solar radiation after sunrise is larger at stations farther from the ocean, which has a larger heat capacity, suggesting that the temperature increase is larger at stations closer to the Rokko Mountains.

3.4 Cooling effect of cold air drainage on the lower-slope of Mt.

Rokko

3.4.1 Objective

The analysis reported in the previous section revealed that mountain breezes start blowing around 15:00–17:00 JST, causing a rapid drop in temperature in the area surrounding the Rokko Mountains. Takebayashi's research group considers these cool mountain breezes from the Rokko Mountains as “cold air drainage” and conducted observational studies of it described below. Mountain breeze and cold air drainage are the names given to winds that descend down mountain slopes. They do not distinguish between mountain breeze and cold air drainage in their analysis. Sato (2014)

describes the phenomenon which the ground layer atmosphere cooled by progressive radiative cooling moves to lower elevations under calm, clear nighttime weather with weak pressure gradient, as "cold air drainage" when it occurs on mountain slope and as "mountain breeze" when it blows downstream from the upper stream in mountain valley. Therefore, mountain breeze and cold air drainage are different expressions for the essentially same phenomenon, with the distinction being based on the location of the occurrence. In this section, we use "cold air drainage" to refer to mountain breezes from the Rokko Mountains consistently with Takebayashi's group because we aim to clarify the effect of mountain breezes from the Rokko Mountains on temperature reduction.

The results of this paper and the studies by Takebayashi's group have provided some information on cold air drainage from the Rokko Mountains. However, as mentioned earlier, the analysis by Takebayashi's group is limited to the nighttime (18:00-06:00 JST), and the analyses in the previous sections also used hourly data or were based on the change in temperature. Therefore, the diurnal variation of cold air drainage in the Rokko Mountains is not necessarily clear.

Since cold air drainage brings cool air to urban areas, there are many case studies that focus on this point and analyze its effect on urban climate (e.g., Sato and Kano, 2011). Since the effect of cold air drainage in dropping temperatures is caused by its arrival time (e.g., Yamato et al., 2019), it is important to know the onset time of cold air drainage in order to consider its relationship with the urban climate.

In this section, we set up an observation station on the lower- slope of the Rokko Mountains to capture the diurnal variation of wind on a typical cold air drainage blowing days with high temporal resolution, and also to clarify its effect on reducing temperature by comparing with cloudy days when cold air drainage is less likely to occur.

3.4.2 Data used

To investigate the effect of cold air drainage from the Rokko Mountains on air temperature reduction, KS data was used. In addition, air temperature and wind data from AKt, AKw and AKA were also used.

3.4.3 Selection of dates for analysis

In this section, the period from June to November 2016 was set as the study period. According to the method described in Section 2.2.4, a number of sunny calm days during the study period, in which cold air drainage was likely to occur, was selected, resulting in 11 days available for analysis (July: 1 day; 19, August: 6 days; 4, 8, 13, 14, 20, and 21, October: 1 day; 10, November: 3 days; 3, 4, and 5).

(12, 13, 25 and 26 July). In order to quantitatively evaluate the effect of cold air drainage on air temperature, cloudy days were also selected for comparison. Cloudy days defined as days with a daily total sunshine duration of less than 1 hour, a daily mean cloud amount of 10 and average daily wind speed of generally 3m/s or less in AKt and AKw were used for the analysis. To assess precipitation conditions, the weather conditions in the morning and afternoon at AK were also used as references in selecting the target days. As a result, 4 days in July were included in the analysis (12, 13, 25 and 26 July).

3.4.4 Frequency distribution of wind direction on the day of analysis

Figure 3-42 shows the windrose for 11 clear days in KS in 24 h. Wind from north-northwest to north-northeast was most frequent, accounting for approximately 51% of the total wind direction frequency. These northerly winds are considered to be mountain breezes from the Rokko Mountains, including cold air drainage.

The results in Sections 3.1 and 3.3, as well as the study by Takebayashi *et al.* (2001), show that several prevailing wind directions exist, which correspond to

changes in sea and land breeze direction at points in the plain area. The results for KS are significantly different from them, as they only exhibit one prevailing wind direction.

3.4.5 Average diurnal variations in air temperature and wind for the analyzed days

(1) On sunny days

Figure 3-43a shows the diurnal variation of vector mean wind direction and speed at KS and that of temperature at KS and AKt. The figure shows that northerly winds, which were frequent in Fig. 3-42, were steadily blowing from 15:00 to 07:00 JST. On the other hand, the wind direction is not stable from 07:00 to 15:00 JST than during the night; however, the frequency of easterly winds was higher.

In general, sea breezes, which are thermally induced local circulations that develop on clear days, are most pronounced around 15:00 JST (e.g., Mori *et al.*, 1994; Mizuma, 1995; Ohashi and Kawamura, 2006; Sawada and Kawamura, 2010; Takimoto and Sakaida, 2012). Southwesterly winds are extended sea breezes that most develops around 15:00 JST in the urban Kobe area. In contrast, at KS, a sharp shift to northerly winds occurred around 15:00 JST, indicating that the diurnal variation of winds differs greatly between locations at lower-slope and on the plains.

As for air temperatures, both KS and AKt began to rise around 06:00 JST; however, AKt exhibited a slower rate of temperature increase, thus the maximum temperature recorded between 14:00 and 15:00 JST was higher at KS than at AKt (Fig. 3-43a).

On the other hand, after 15:00 JST, air temperatures began to decrease at both locations. However, air temperature dropped more rapidly at KS than at AKt by approximately 4 to 5 °C from 15:00 to 18:00 JST. This result is consistent with that reported in Section 3.3, where the rapid drop in air temperature at KS occurred at the same time as the onset and strengthening of northerly winds. This suggests that the

beginning of cold air drainage and the increase in wind speed are responsible for the sudden drop in air temperature (Fig. 3-43b).

This difference in the rate of air temperature decrease between 15:00 and 18:00 JST results in a difference in nighttime air temperature between AKt and KS, with AKt remaining approximately 1 °C warmer from dusk to dawn. The rate of air temperature decrease changes after 18:00 JST at KS and around 20:00 JST at AKt. This change in the rate of air temperature decrease is roughly consistent with the cold air drainage halting its increase at 18:00 JST, and the wind speed of the cold air drainage decreasing in stages after 20:00 JST.

Around 06:00 JST, air temperatures at KS and AKt began to increase. The air temperature increase at KS was greater than that at Akt. The temperature increase at KS is consistent with an abrupt change in the steady northerly winds that had been prevailing until that time.

Figure 3-43b shows that the mean wind speed of the cold air drainage during the night was in the order of 1–2 m/s. Takebayashi *et al.* (2001) observed an average wind speed of 2.3 m/s for the cold air drainage in Soma valley in Kobe City, and Hamada and Ichinose (2011) observed an average wind speed of 3–4 m/s in Nagano. Compared to these studies, our results highlight smaller wind speeds. On the other hand, in addition to the gradual decrease as described above, there is an intermittent nature to the wind speed change, which temporarily intensifies around 18-20, 00, and 05 JST. These characteristics in wind speed change are consistent to the dynamics of slope cold air drainage in Hiroshima described by Nakamura *et al.* (2014).

Based on these results, cold air drainage at KS can be considered to prevail from 15:00 to 07:00 JST, which is the period between successive rapid changes in wind direction and speed.

Therefore, the wind direction frequency was analyzed by dividing the day into a period from 15:00 to 07:00 JST and that from 07:00 to 15:00 JST. Owing to this subdivision, we found that the wind direction tends to be between easterly and

southerly from 07:00 to 15:00 JST, when cold air drainage is not occurring (Fig. 3-44).

Thus, during the daytime before the cold air drainage blows, easterly to southerly winds often blow, which is thought to be due to the fact that the station is influenced by easterly land breeze and southerly sea breeze. Yoshino (1986) indicates that the thickness of land breeze at Kobe is about 200 to 300 m. Since sea breezes are generally thicker than land breeze, it can be inferred that KS, which is located at an elevation of about 160 m, is also affected by these winds.

(2) On cloudy days

Figure 3-45 shows the windrose for four cloudy days in KS. As with sunny days, northerly winds are frequent, but some southwesterly winds also prevail.

The analysis of the direction of the vector mean wind shows no significant variation in wind direction as on a clear day. However, northerly wind from 17:00 to 08:00 JST, and southwesterly wind from 08:00 to 17:00 JST are prevailing (Fig. 3-46a). Wind speeds did not vary significantly as on a clear day and remained at around 0.5 m/s throughout the day (Fig. 3-46b).

The difference in air temperature between KS and AKt was smaller than that on a clear day (Fig. 3-46a). Moreover, although a drop in air temperature was observed at KS from 17:00 to 20:00 JST, the magnitude of such drop was only approximately 2 °C, half of that recorded on a clear day.

3.4.6 Air temperature and wind diurnal variations on a typical cold air drainage occurrence day

In the previous section, the average air temperature and wind conditions on clear days were identified. In this section, we present air temperature and wind diurnal variations on November 4, 2016, the most typical cold air drainage occurred among the studied days, in order to confirm whether the results in the previous section can be generalized. On November 4, a migratory high widely covered except but northern

Japan, so a synoptic field is favorable for the occurrence of cold air drainage (Fig. 3-47).

Figure 3-48 shows the diurnal variation of air temperature and wind on November 4, 2016. The diurnal variations of air temperatures at KS and AKt exhibit similar patterns to those shown for averaged target days. The rapid drop in air temperature after 15:00 JST, which was observed in Fig. 3-43a, is also clearly shown.

The diurnal variation of the wind is also consistent with that shown by the daily average analysis, although a difference of approximately 1 hour is observed. In fact, cold air drainage occurred steadily from 16:00 to 08:00 JST. The wind speeds were generally 1.5 to 2.0 m/s, with a gradual decrease during the night.

From the above, it can be inferred that the diurnal variations in air temperature and wind on the average of the target days in the previous section can be considered to represent the average characteristic of cold air drainage at KS.

Comparing the results of this study with those of Takebayashi *et al.* (2001), the time of significant air temperature decrease due to cold air drainage in Takebayashi *et al.* (2001) is that from 19:00 to 20:00 JST, that is approximately 4 to 5 hours later than that evaluated in this study. In addition, the wind speeds of the cold air drainage in this study are generally the same as those evaluated by Takebayashi *et al.* (2001).

Because the observation points and elevations are different from those of the wind speeds in this study, a simple comparison cannot be made. The observation points used by Takebayashi *et al.* (2001) were located within a valley at a lower elevation than that of the mountain lower-slope. Thus, it is assumed that it takes longer for the cold air drainage to arrive, resulting in the observed difference in the time of air temperature decrease.

3.4.7 The relationship between cold air drainage and extended sea breeze

As shown in Section 3.1, extended sea breeze with a southwesterly component

prevails during the daytime in the Kobe area, while easterly land breeze prevails from nighttime to morning. Regarding the relationship between “extended sea and land breeze” and cold air drainage, Takebayashi *et al.* (2001) investigated cold air drainage in the Rokko Mountains during summer and found that cold air drainage develops only under conditions of weak “extended sea and land breeze”, and that cold air drainage is blown away when the “extended sea and land breeze” is strong. They consider the wind at 100 m above the ground at the Pt to be “extended sea and land breeze”, and indicate that cold air drainage is less likely to appear when the wind speed exceeds 4 m/s at Pt. However, their analysis uses the wind speed at Pt as it is, so the wind speed near the ground is not used as a criterion. In fact, if the wind speed of 4 m/s at 100 m above the ground is converted to 10 m above the ground based on the logarithmic law, the wind speed is about 56% of that at 100 m above the ground. Therefore, a wind speed of 4 m/s at Pt is about 2.3 m/s near the ground, which is not necessarily a large wind speed.

In Section 3.1 of this paper, the diurnal variation of the local wind system was clearly captured for AKw on the artificial island (Fig. 3-9). Similarly, it was also obtained that AKA, which is located on an artificial island, has similar diurnal variations of wind as AKw (Table 3-5a). A comparison of wind speeds between AKw and AKA shows that extended sea breeze wind speeds tend to be stronger in AKA (Table 3-5b). Therefore, in this section, we analyzed the diurnal variation of AKA wind on cold air drainage blowing days and verified the results of Takebayashi *et al.* (2001).

Figure 3-49 shows the diurnal variation of air temperature and wind at AKA. The plot shows that discontinuous changes in wind direction occurred around 10:00-11:00, 18:00, and 21:00 JST. All of the wind direction changes occurred within approximately 1 hour. This result is generally consistent with the results of Section 3.1 (Table 3-5a), which is analyzed on AKw, but the fact that northerly wind blows continuously for about 2 hours from 19:00 to 21:00 JST is a characteristic of the day

analyzed.

Based on the wind system defined in Section 3.1.6 (Table 3-3), the three wind direction changes at AKA are considered to correspond to the change from extended sea breeze to mountain breeze (18:00 JST), from mountain breeze to land breeze (21:00 JST), from land breeze to sea breeze (11:00 JST), respectively. From 10:00 to 11:00 JST, the wind direction gradually shifted from southerly to southwesterly, quickly shifting from sea breeze to extended sea breeze.

Here, to capture the relationship between cold air drainage and extended sea breeze or land breeze, looking at the diurnal variation of wind speed in AKA, it is about 3-4 m/s at the peak of extended sea breeze around 15:00-16:00 JST, and it stays around 2 m/s around 16:00-18:00 JST. Wind speeds during the night also generally remained at 2 m/s, although the wind direction varied. Since the wind measurement height of AKA is 10 m above the ground, if the wind speed is 2.0 m/s, the wind speed is 3.6 m/s when converted to the measurement height of Pt of 100 m, which is close to the "extended sea and land breeze" threshold of Takebayashi *et al.* (2001). Since the results in this section are vector mean wind speeds for the 11 days of cold air drainage, they tend to be smaller than wind speeds on individual target days, so it can be said that cold air drainage is actually generated even if the wind speeds are the same as their threshold value.

4. *Rokko-oroshi* and its effect on temperature

4.1 Objective

Downslope windstorms have been observed in many places worldwide. They are given variable local names. In Japan, several local strong winds that are highly unique to a particular region are known as “*oroshi*,” “*dashi*,” and “*kaze*,” including *Akagi-oroshi* (Gunma Prefecture) and *Kiyokawa-dashi* (Yamagata Prefecture; Arakawa, 2011). Kusaka and Fudeyasu (2017) prepared a review of the downslope windstorms of Japan and introduced 28 local winds, including *Rokko-oroshi*, a downslope wind from Mt. Rokko. Downslope windstorms require a mountain range of ~1 km high (or more) and a steep leeside slope (American Meteorological Society, 2016). Japan is a mountainous country with complex topography and has a variety of downslope windstorms. An *oroshi* is a type of local wind forcibly generated when a mountain acts as an obstacle.

Especially strong winds commonly occur within ~10 km from the foot of the mountain (Yamagishi, 2002). This is the case for the northern part of coastal area of Kobe City, where the impact of *Rokko-oroshi* is more easily felt (Yokota and Nakajima, 1992; Yoshida *et al.*, 1998; Yoshida *et al.*, 1999; Kusaka and Fudeyasu, 2017). Ultimately, understanding the general characteristics of strong local winds like *Rokko-oroshi* are important for disaster prevention and effective usage of wind resources as shown in examples of the *Kiyokawa-dashi* of Yamagata or the *Suttsu-dashi* of Hokkaido, which is used for wind power generation (Rikiishi and Yomogita, 2006).

Our existing understanding of *Rokko-oroshi* can be attributed to the many studies that have been undergone over 20 years. For instance, based on Yoshida *et al.* (1998) analysis of data provided by the AMeDAS between 1976 and 1994, *Rokko-oroshi* was found to frequently occur between the months of October and March. Ino *et al.* (2009) investigated the characteristics of the synoptic field at the occurrence of

the Rokko-oroshi and showed that the Rokko-oroshi during the cold season (November to March) occurs most frequently when the pressure air pressure pattern becomes a winter type pressure pattern after the passage of a cold front, which is also consistent with the findings of Yoshida *et al.* (1998).

As mentioned above, local winds such as the *Rokko-oroshi* often bring strong winds and lower temperatures, and thus have a significant impact on the daily lives of local residents. However, since local winds have characteristics unique to the region where they occur, it is necessary to conduct research in each region where local winds occur. As mentioned above, studies on *Rokko-oroshi* winds have been conducted in the target area, but the diurnal variations of meteorological elements and the distribution of wind systems during the occurrence of *Rokko-oroshi* winds have not been fully clarified. In particular, the magnitude and range of the temperature reduction effect caused by *Rokko-oroshi* have not been quantitatively investigated. In addition, when the time of onset varies with the synoptic field conditions, as is the case with *Rokko-oroshi*, a careful case study on a typical day of its occurrence is necessary to understand its characteristics.

In this chapter, we examine the diurnal variation of temperature and wind, and the effect of *Rokko-oroshi* on lowering temperature and its range of influence through a case study of a day when *Rokko-oroshi* occurs, using existing AMeDAS and AEROS data together with our own observation data.

4.2 Data used

To capture the detailed behavior of *Rokko-oroshi*, KS data was used. Other data used in this study include temperature, wind speed and direction from the AKA, AKw/AKt and SA of AMeDAS. SA is used to capture wind behaviors on the north side and south side of Mt. Rokko. Note that SA is located ~19 km north–northwest of KS. The AEROS data at Ro and around Kobe area is also used.

Garratt (1992) indicates that the altitude of the atmospheric boundary layer during the day is about 1 to 2 km. Because the elevation of Ro is 881 m, we judged to capture the winds in the free atmosphere above the atmospheric boundary layer to some extent.

4.3 Selection of dates for analysis

In general, downslope winds refer to the strong west to north winds that occur during the northwest monsoon in winter (Takahashi and Koizumi, 2008). Moreover, it has been clarified that *Rokko-oroshi* tends to occur in the winter type pressure pattern after the passage of a cold front (Kiyohara, 2002). Therefore, the period between November 3, 2017 and February 28, 2018 was selected as the research period, which is during the cold season.

The following process was used to extract the days when *Rokko-oroshi* could have blown during the research period:

1. Wind directions between 290° and 30° (only the north side) and a speed of 7.5 m/s or more were termed *Rokko-oroshi* by referring to the study by Kiyohara (2002). Other studies used thresholds of 8.5 m/s (e.g., Ino *et al.*, 2009), referring to the daily wind gust. In this study, the high temporal resolution of wind data permitted to use the Kiyohara (2002)'s threshold.
2. The dates when *Rokko-oroshi* was observed during the research period were extracted as “the days *Rokko-oroshi* blew”.
3. The case study days were selected as the days when *Rokko-oroshi* blew continuously more than 60 minutes among the date extracted in “the days *Rokko-oroshi* blew” selected in (2).

Consequently, November 4, 2017 and November 18, 2017 were selected as the analysis subject days. The total blowing durations of *Rokko-oroshi* on these days were 109 and 278 min, respectively.

Preliminary analysis of diurnal changes in wind and temperature for the two extracted days showed that on November 4 the temperature dropped conspicuously owing to cold northerly winds blowing from the Rokko Mountains. On November 18, however, no significant reduction in temperatures was recorded. Therefore, in this study, a case analysis is conducted with November 4 as a typical day for this specific type of wind.

First, before understanding the characteristics of the *Rokko-oroshi*, the characteristics of winter winds in Mt. Rokko are clarified using data from an original observation station established in the lower-slope of Mt. Rokko. The characteristics of the synoptic field on the day when the *Rokko-oroshi* blew are also captured. Next, changes in wind speed and direction of the *Rokko-oroshi* in the lower-slope and associated changes in air temperature are captured. Finally, the changes in meteorological variables at windward and leeward stations across Mt. Rokko and the surface wind system in the Kobe urban area when the *Rokko-oroshi* is blowing are investigated.

4.4 Statistical analysis of Rokko-oroshi

4.4.1 Wind characteristics in the lower-slope of Mt. Rokko during the cold season

Figure 4-1 shows the distribution of wind direction and wind speed in the lower-slope of Mt. Rokko (KS) during the research period. From this figure, at KS during the cold season, western to northern winds were prominent. The wind direction frequency of western to northern winds from 270° to 360° was 56.4%. Especially, the wind direction frequency of north–northwestern wind (350°) was the highest at 16.8%. While the speed of north–northeastern to western winds (30°–270°) was mostly 2 m/s or less, higher wind speeds were recorded for western to northern winds. The northwestern wind was particularly strong, with up to 14 m/s wind speed recorded.

Figure 4-2 shows the frequency of wind with different speeds binned at 1 m/s

interval. From this figure, winds with a speed of 4 m/s or less frequently occurred, and those of 2 m/s or less accounted for 78.2% of the total number of recorded wind speed measurements, as is the case in Fig. 4-1. Moreover, the frequency of wind speeds of 7.5 m/s or faster, which is the threshold of *Rokko-oroshi* in this study, was small throughout the cold season, i.e., less than 1% of the total duration.

4.4.2 Characteristics of *Rokko-oroshi* in the lower-slope of Mt. Rokko

Figure 4-3 shows the distribution of the wind direction and speed during the blowing of *Rokko-oroshi* at KS. While 290° to 30° was used as the threshold for the wind direction of *Rokko-oroshi* in this study, Fig. 4-3 indicates that the wind direction was primarily from the north-northwest (340° – 360°) with wind speeds up to 12-13 m/s. The frequency distribution of wind speed (Figure 4-4) shows that 7.5-8.5 m/s accounts for about half (45.1%), and wind speeds of 10 m/s or higher account for a little more than 10%. (Fig. 4-4).

Figure 4-5 shows the frequency of *Rokko-oroshi* at KS at each hour. From this figure, winds frequently blew during the daytime between 13:00 and 14:00 JST, during the night between 18:00 and 23:00 JST, and at ~01:00 JST. Ino *et al.* (2009) demonstrated that *Rokko-oroshi* winds tend to frequently occur during late night and daytime and less frequently in the early morning (06:00–07:00 JST). Their results are obtained from the threshold of daily maximum wind speed of 8.5 m/s or more during the cold season between November 2001 and March 2005.

4.5 Case study on *Rokko-oroshi* (November, 4 2017)

4.5.1 Atmospheric pressure distribution on November 4, 2017 in the synoptic-scale

Figure 4-6 shows the surface weather charts at 09:00 JST on November 4, 2017. From this figure, a cold front passed above Japan, including Kobe City, and the weather experienced a gradual transition to a winter type pressure pattern, with high

barometric pressure in the west and low barometric pressure in the east. This result matches the findings of the previous studies, and it corresponds to the type of atmospheric pressure distribution in which *Rokko-oroshi* can occur in the study by Ino *et al.* (2009).

4.5.2 Changes in temperature, wind speed and direction on November 4, 2017 with Rokko-oroshi blowing

(1) Lower-slope of the mountain (KS)

Figures 4-7a, 4-8a and 4-9a Figures 4-7a, 4-8a and 4-9a (KS: black) shows the changes in temperature, wind speed and direction on November 4 at KS. In terms of wind direction and speed, *Rokko-oroshi* continuously blew from just after 13:00 to 16:00 JST. The wind speed during this time varied in the range of 7–12 m/s. Moreover, the wind direction of *Rokko-oroshi* was consistently ranged from 300° to 360°, and the temperature momentarily decreased from 21 to 13°C during the time when the wind speed of *Rokko-oroshi* increased from around 12:45 to 14:00 JST. From 14:00 to 16:00 JST, when *Rokko-oroshi* blew steadily, the temperature drop was small and remained around 13–14°C.

(2) Mountain summit: Mt. Rokko (Ro)

Figures 4-7a, 4-8a and 4-9a Figures 4-7a, 4-8a and 4-9a (Ro: green) shows the changes in temperature, wind speed and direction on November 4 at Ro. From this figure, the wind blew from the north almost throughout the day, its speed increased rapidly between 12:00 and 15:00 JST from 4 m/s to 14 m/s, and the temperature rapidly decreased by ~6°C after 12:00 JST.

Comparing KS and Ro, the rapid drop in temperature before and after the start of the *Rokko-oroshi* is common to both locations. However, the change in wind speed is different among the two sites, with Ro showing an enhanced wind speed followed by a continuation of that wind speed. At KS, on the other hand, the wind speed

continues to be strong for about 2 hours, but then it decreases to about 2 m/s.

(3) Windward: Sanda (SA)

Figures 4-7a, 4-8a and 4-9a (SA: blue) shows the changes in temperature, wind speed and direction on November 4 at SA. This figure shows steady northerly winds and an increase in wind speed after 12:00 JST that correspond well with changes in wind direction and speed at KS and Ro.

However, unlike KS and Ro, the increase in wind speed was temporary and only lasted for approximately 30 min. Nevertheless, the wind speeds are on average greater than what they were prior to the blowing of *Rokko-oroshi*, which is also observed at Ro. For KS, this phenomenon is less obvious.

Furthermore, the changes in temperature mostly corresponded to the changes in the wind direction and speed, and a rapid decrease in the temperature by $\sim 4^{\circ}\text{C}$ was observed between 12:00 and after 13:00 JST.

(4) Leeward: Plain and artificial island (AKt/w and AKA)

Figures 4-7b, 4-8b and 4-9b (AKw/t: red; AKA: blue) shows the changes in temperature, wind speed and direction on November 4 at AKt/w and AKA. From this figure, a rapid decrease in temperature by approximately 5°C was observed on both station between 12:00 and 14:00 JST, which correlates well with temperature reductions at the other measurement locations. The drop in temperature corresponds well with the change in wind direction from westerly to northerly winds in AKA, but the correspondence is unclear in AKw, and the stability of the northerly winds and the increase in wind speeds are generally not persistent. On the other hand, at AKA, after the westerly winds shifted to northerly winds around 13:00 JST, the wind direction generally remained stable to the north-northwest. This is very different from AKw. The maximum wind speeds after 13:00 JST were almost the same at the two sites, but the wind speeds after that were on average 2-3 m/s higher at AKA. These results

indicate that the temperature drop caused by the *Rokko-oroshi* occurs at AKA, which is approximately 10 km away from the foot of the Rokko Mountains, and that the magnitude of the drop is the same as that at AKt, which is about half the distance from the foot of the Mountains. Considering the stability of wind direction and the magnitude of wind speed, the *Rokko-oroshi* is also considered to reach the AKA on the artificial island. Therefore, the effect of *Rokko-oroshi* on temperatures is assumed to extend over almost the entire plains of the Kobe area.

(5) Surface wind field

The results so far show that the *Rokko-oroshi* on the day of the case study generally began to blow around 12:00 JST, and that there was a good correspondence between the different sites in terms of the decreasing trend of the temperature. However, there are differences in changes of wind direction and speed among the sites, indicating that the enhancement of wind speed after the *Rokko-oroshi* is blown is less sustained at the sites other than Ro. Therefore, this section aims to capture changes in the wind system around the target area during the *Rokko-oroshi* is blown.

The wind system distribution within the urban area of Kobe between 12:00 and 17:00 JST, where the wind speed increased rapidly and then decreased again at KS, was analyzed using the data from the survey stations of AEROS (Fig. 4-10). From this data, we observe that at 12:00, westerly winds were dominant in roughly the entire urban area, including Ro. At 13:00 JST, the wind at Ro changed to northerly wind and the wind speed increased. Moreover, the wind direction changed to the almost northerly wind in the entire urban area. At 14:00 JST, when the wind speed became the strongest at KS, the northerly wind in the urban area was also the strongest. Similar to KS, the maximum wind speed was observed across all observation points at 14:00 JST with little-to-no changes in direction and speed until 16:00 JST. At 16:00 JST, the wind speed rapidly decreased, and the wind direction varied over the entire urban area. From these facts, on the date of analysis of this case, it can be said that during the

blowing of *Rokko-oroshi* at KS, strong northerly winds blow in roughly the entire urban area of Kobe, suggesting the generation of *Rokko-oroshi* in the entire Mt. Rokko.

4.5.3 Temperature reduction effect of *Rokko-oroshi*

Rokko-oroshi is considered to be similar to the Bora-type air flows that form over the mountains of Eastern Europe (Yoshino, 1992, Takahashi and Koizumi, 2008). When Bora-type winds flow downslope of a mountain range, a temperature reduction of the ambient air is often observed (Yoshino, 1992). Similarly, in this study, a tendency for the temperature to decrease was found to accompany the blowing of *Rokko-oroshi*. In particular, a temperature reduction of about 8°C was observed at the KS station located in the lower-slope of Mt. Rokko, while the AKt or AKA located within the urban area of Kobe exhibited a temperature reduction of about 5°C. These results agree well with the findings of Yoshino (1992) and further verify *Rokko-oroshi* as a Bora-type local wind.

In this chapter, the observations of wind and temperature at lower-slope of Mt. Rokko were conducted to elucidate the characteristics of *Rokko-oroshi*, which blows down from Mt. Rokko in Kobe. By conducting case analysis, the changes in meteorological variables and the wind system in the urban area of Kobe during the blowing of *Rokko-oroshi* were understood.

From these facts, on the target date, the characteristics of *Rokko-oroshi* during its occurrence can be summarized in the following four points:

- (1) The synoptic situation must be the type where a cold front passes above Japan, and the weather experiences a gradual transition to a winter type pressure pattern.
- (2) During the blowing of *Rokko-oroshi*, wind up to 12 m/s can be observed at the leeward side while experiencing a rapid temperature drop by 5–8°C.
- (3) The temperature reduction effect of the *Rokko-oroshi* extends more than

10 km from the foot of the mountains.

- (4) During the blowing of *Rokko-oroshi*, the wind direction of the entire area changes to northerly wind, and the wind speed also increases.

5. Summary

In the Seto Inland Sea region in Japan, it has long been known that thermally induced local circulation such as sea and land breezes and mountain and valley breezes develop on sunny calm days. In this study, we investigated the relationship between local wind systems and temperatures, focusing on their diurnal variations, especially in the Kobe area, where mountain and bay are close to each other and urban area is located in a narrow zonal area between the mountain and bay. In this research, by using meteorological data from AMeDAS and AEROS, which are under the control of the Japan Meteorological Agency and the Ministry of the Environment, respectively, as well as data from our own original wind and temperature observation stations, we obtained the following findings regarding the diurnal variation of the local wind system specific to the Kobe area and its effect on temperature.

Based on previous studies, it is known that sea and land breeze circulation prevails as the diurnal variation of wind on sunny calm days around the target area. In addition to the sea and land breezes driven by the thermal contrast between land and sea around Kobe, extended sea breeze is generated by the thermal contrast between Osaka Bay and the Osaka Plain on a larger scale, and it is known that the wind direction changes to the clockwise direction throughout the day. On the other hand, in the vicinity of Kobe, where the Rokko Mountains are located behind the city, land breeze occurring at nighttime can be regarded as mountain breeze or cold air drainage due to their topographical characteristics.

Thus, in the area surrounding Kobe, thermally induced local circulation of sea breeze, extended sea breeze during the daytime and mountain breeze during the nighttime interrelate to form the local climate of a large city with a population of more than 1.5 million people. These local wind systems also have an impact on temperature, which is related to the daily life of many local residents and the heat island phenomenon, which has become more serious in recent years. Therefore, it is very

important to understand the local wind systems when considering the local climate in the Kobe area. Sea and land breezes and mountain and valley breezes, which are caused by thermal contrasts, may change in a short period of time, and sea and mountain breezes may bring cooler air. Therefore, it is important to accurately capture the diurnal variations in wind and temperature.

However, in previous studies, sea and land breeze around Kobe was often considered as a part of sea and land breeze around Osaka Bay or the Seto Inland Sea from the viewpoint of meso-scale climatology. Therefore, for example, the winds in Kobe were represented by a single AMeDAS station in Kobe, and the time of analysis was every three hours. This level of temporal and spatial resolution is sufficient to obtain the characteristics of the wind system over a broad area. However, the temporal and spatial data were not sufficient to capture the diurnal variation of wind and temperature around Kobe from the small climatological scale of sea and land breeze and mountain and valley breeze. Under these circumstances, the knowledge of diurnal variations in the Kobe area on a small scale is not sufficient, and we do not necessarily have clear understanding of the alternation times of sea and land breezes, extended sea breezes and mountain breezes, and the magnitude and range of their effects on temperatures.

In this study, we analyzed the average diurnal variation of wind by selecting days when the sea and land breeze alternated among sunny calm days during the warm season and the autumn season. The results show that the region can be divided into three groups based on the characteristics of diurnal variations in wind direction, and that there are five stages in the transition of the local wind system.

Specifically, the target area was divided into eastern area, western area, and coastal areas to artificial islands according to the different influence of thermally induced local circulation at different scales. The wind system consists of four types of circulation: sea breeze, southwesterly extended sea breeze, mountain breeze from the Rokko Mountains, and easterly land breeze, which shift in five phases.

In previous studies, the southwesterly winds prevailing around Kobe and the northeasterly to easterly winds have sometimes been referred to as "extended sea and land breezes. However, there are few cases that have confirmed the correspondence with the broad-scale wind system when such winds actually occur. In this study, using AEROS observation data, we were able to suggest the relationship with the broad-scale wind system in the Kyoto-Osaka-Kobe area and to confirm, although qualitatively, that sea and land breezes of different scales are observed in the target area.

Among the four wind systems, sea breeze tended to have a relatively short duration of blowing compared to the other wind systems. However, along with extended sea breeze, the effect on temperature in the target area was observed, suggesting that the onset of sea breeze suppressed the temperature increase in the morning and that the rate of temperature decrease was enhanced by extended sea breeze in the afternoon.

In this study, sunny calm days were selected objectively based on conditions such as sunshine duration, cloud amount, and wind speed of the general wind. However, even on sunny calm days with similar meteorological conditions, there were some stations in the study area where multiple prevailing wind directions occurred during the peak period of thermally induced local circulation. This suggests that there are diurnal variations in the local wind system from day to day. Therefore, we conducted a case study of two consecutive sunny calm days with different diurnal variations of wind on the plains and examined the differences.

The results suggest that the diurnal variation of winds over the two days mainly reflects the diurnal variation of extended sea breeze and land breeze, and that the wind systems around Kobe show different diurnal variation of winds even on the same sunny calm day due to their influence. We found the possibility that the diurnal variation of these broad-scale wind systems is determined by the pressure system differences between the Kyoto-Osaka-Kobe area.

As a result of examining the diurnal variation of temperature on sunny calm days at individual stations using temperature data from 33 originally developed stations, it became clear that the target area can be divided into five regions (east, west, central, mountain, and artificial islands) based on the characteristics of their characteristics. Comparison of diurnal variations of temperatures in each region revealed that the regions with relatively higher temperatures during the daytime and nighttime differed, with the former in the eastern part and the latter in the central part of the region. Previous studies have pointed out the possibility that the warmer air is brought to the east by westerly sea breezes during the daytime, but in fact, the warmer region is unevenly distributed even when southerly sea breeze prevails. The high temperatures in the central part at the nighttime suggest the influence of the heat island effect in the urban center of the area. Among the five regions, the rapid drop in temperature after 16:00 JST at the foot of the mountains and the re-rise in temperature around 22:00 JST on the artificial islands were the most distinctive features. It is possible that the cool mountain breeze is responsible for the temperature decrease at the foot of the mountain, while the relatively warm land breeze is related to the temperature increase on the artificial island. Previous studies have shown that the range of the effect of mountain breeze on temperature reduction is about 1 km. The study showed that the range of influence varied from station to station, with the eastern part of the target area extending up to the coastal stations and the central part of the city tending to have a smaller range.

The wind and temperature data from the original observation station located on the lower-slope of the Rokko Mountains show that the mountain breeze begins to blow around 15:00 to 16:00 JST when extended sea breeze prevails over the plains and artificial islands in the target area, and that the temperature drops by 4 to 5°C rapidly. This mountain breeze is generally stable at wind speeds of 1-2 m/s from evening to dawn in the lower-slope of the mountain and at stations near the foot of the mountain. Compared to the case in Nagano, for example, the temperature reduction effect is

almost the same, but the wind speed is smaller. Also, the onset time was about 4 hours earlier, suggesting the possibility of a original characteristic of mountain breezes in the Rokko Mountains.

As described above, mountain breezes are very important in considering the local climate of the study area because of the close distance of the mountainous terrain to the urban area.

The winds blowing down from the mountains are not only thermally induced local circulation such as mountain breezes, but also downslope winds, which are dynamically induced circulation. *Rokko-oroshi* has been well-known as a downslope wind in the target area, but there have not been many studies on its actual conditions and effects on temperatures. In particular, few observational studies have been conducted. In this study, an original observation station for temperature and wind was set up in the lower-slope of the mountain, and the general characteristic of *Rokko-oroshi* was captured by a case study.

The maximum wind speed of *Rokko-oroshi* during the observation period was 13 m/s, and 7.5 to 8.5 m/s accounted for almost 45% of the observed wind speeds. Wind speeds of 10 m/s or higher accounted for a little more than 10%. The day of the case study was when a cold front passed through the area, and the weather conditions shifted to a winter type pressure pattern, which had been pointed out in previous studies to be a likely to cause *Rokko-oroshi*. With the start of the *Rokko-oroshi*, there was a sharp drop in temperature of about 8°C in the lower-slope of the mountains, which is twice the amount of the temperature reduction caused by mountain breeze. The effect was not limited to the foot of the mountains but was also observed at a station about 10 km from the foot of the mountains, where a temperature reduction of about 5°C was also observed.

This study clarified the relationship between the local wind system around Kobe and temperature from the viewpoint of diurnal change in local circulation, using data from existing stations and original observations. As a result, it was found that there are

regional differences in the local wind system and diurnal variation of temperature as a characteristic of the local climate in the Kobe area, which has not been clarified so far.

In this study, the following five new findings were obtained.

1. The target area can be divided into three groups according to the diurnal variation of four types of wind systems (sea breeze and extended sea breeze, mountain breeze, and land breeze)
2. There are five phases in the transition of the local wind system on average, and they change under the influence of diurnal variation of the large-scale wind system in the Kyoto-Osaka-Kobe area.
3. Five regions can be classified according to the characteristics of diurnal variation of temperature, and the temperature decrease caused by mountain breeze from the Rokko Mountains is distinctive.
4. Mountain breezes begin to blow around 15:00-16:00 JST, and the range of their temperature reduction effect varies from station to station.
5. The temperature drop associated with the *Rokko-oroshi* is about 5°C even at a station 10 km from the foot of the mountain.

In this paper, the characteristics of local wind systems and temperatures around Kobe are clarified, focusing on their diurnal variations. As mentioned above, sea and land breeze and mountain and valley breeze, which are thermally induced local circulation, are familiar phenomena in people's daily lives, and have been the subject of many studies.

In the 1960s, as industrialization progressed in Japan's coastal areas, sea and land breeze began to attract attention as a carrier of pollutants. In the 1970s and 1980s, several studies were conducted on sea and land breeze in the Seto Inland Sea coastal area, and from 1974 to 1976, the Japan Meteorological Agency conducted studies in the Kanto region to clarify the actual conditions of sea and land breeze, and obtained many findings. One of the results was the clarification of the existence of extended sea breeze over the entire Kanto region.

The situation of air pollution in Japan has been improving since then, but the health effects of fine particulate matter (PM_{2.5}), one of the pollutants, continue to be a concern (Ministry of the Environment, 2009a,b). In Japan as a whole, the achievement rate of environmental standards for PM_{2.5} is improving (Ministry of the Environment, 2020). However, the achievement rate is low in the area facing the Seto Inland Sea, which is caused not only by sources from the surrounding industrial areas, but also by pollution from ships navigating in Osaka Bay. The Akashi Strait, located west of Kobe, is one of the most congested sea areas in Japan, with an average of more than 800 vessels per day (Gao *et al.*, 2013). Nakatsubo *et al.* (2018) pointed out that ship-derived exhaust gases are an important source of the high PM_{2.5} concentration phenomenon in the area surrounding the Seto Inland Sea.

The effects of urbanization on climate around Kobe, including the occurrence and magnitude of the heat island phenomenon, have not yet been fully elucidated. However, as suggested by some previous studies and the results of this paper, the central part of Kobe tends to be hotter than the surrounding areas, and it is possible that the hotter areas are displaced by local winds. Furthermore, it has been shown that the number of people transported to the hospital for heat stroke decreases on days when sea breezes are blowing during the summer season.

Thus, it is very important to understand the details of the diurnal variation of the local wind system and temperature in the Kobe area from the viewpoints of air pollution, urban warming, and heat stroke, which continue to be of concern in the region. Although this paper is a single-year analysis, we were able to obtain an average view of the diurnal variation of the local wind system on sea and land breeze days and to clarify some of the effects of the wind from the Rokko Mountains on temperatures through case study. As described above, the purpose of this study is to understand the characteristics of the local climate around Kobe in terms of the diurnal variation of the local wind system and temperature on sunny calm days from the warm season to the autumn season. As a result, the daily variation of wind in the area is

indeed determined by sea and land breeze circulation, but the degree of prevailing wind differs between extended sea breeze and sea breeze at different scales, and on average, extended sea breeze tends to dominate for a longer period of time. However, the diurnal variation of the broad-scale wind system may affect the diurnal variation of the local wind system in the Kobe area, resulting in differences in the duration of the four types of wind systems in the area surrounding Kobe. In particular, differences in synoptic-scale pressure gradients may cause differences in the diurnal variation of the large-scale wind system, which in turn may cause differences in the duration of extended sea breeze and sea breeze in the area surrounding Kobe. This is an issue to be addressed in the future, and we would like to further investigate the relationship with synoptic scale pressure gradients and geostrophic winds.

The general characteristics of mountain breezes from the Rokko Mountains were clarified to some extent in terms of their onset time and temperature lowering effect. The general characteristics of mountain breezes from the Rokko Mountains were clarified to some extent in terms of their onset time and temperature lowering effect. However, since there were some differences in the onset time and wind speed compared to other regions, we would like to further investigate the characteristics of mountain breezes by conducting observations at different stations in the Rokko Mountains.

In this study, thermally induced local circulation was defined mainly by wind direction. However, numerical model simulations are needed to verify the actual mechanism of each circulation. In addition, since the case study in this research was limited to a few days, it is necessary to verify the generality of the results in this research by adding more cases to be analyzed in the future, as well as by further theoretical verification.

References

- Adrian E. Gill, 1982: *Atmosphere-Ocean Dynamics*, Academic Press, 649pp.
- Akita, M., 1993: Local Climatological Study on Sea and land breeze in the Tsugaru Peninsula. *Hirodai-chiri*, 29,1–6 (in Japanese).
- American Meteorological Society, 2016: Glossary of Meteorology. Available from <http://glossary.ametsoc.org/wiki>
- Arakawa, S., 1969: Climatological and dynamical studies on the local strong winds, mainly in Hokkaido. *The Geophysical Magazine*, **34**, 359–425.
- Arakawa, S., 2011: *Kyokuchi-fu No Iroiro*. Seizando-Shoten, 174pp (in Japanese).
- Asai, T., 1996: *Local Meteorology*. University of Tokyo Press, 233pp (in Japanese).
- Atkinson, B. W., 1981: *Meso-scale Atmospheric Circulations*. Academic Press, 495pp.
- Brinkmann, W. A. R., 1971: What is a foehn? *Weather*, **26**, 230–241.
- Chiba, O., Kondo, Y., and Kawamura, G., 1993: Characteristics of the sea breeze penetrated into Kochi Prefecture. *Tenki*, **40**, 109–117 (in Japanese).
- Colle, B. A., and Mass, C. F., 2000: High-resolution observations and numerical simulations of easterly gap flow through the strait of Juan de Fuca on 9-10 December 1995. *Monthly Weather Review*, **128**, 2398–2422.
- Cook, A. W., and Topil, A. G., 1952: Some examples of chinooks east of the mountains in Colorado. *Bulletin of the American Meteorological Society*, **33**, 42–47.
- Defant, F., 1951: Local Wind, *Compendium of Meteorology*, American Meteorological Society, 655–672.
- Durrant, D. R., and Klemp, J. B., 1987: Another look at downslope winds. Part II: nonlinear amplification beneath wave-overturning layers. *Journal of the Atmospheric Sciences*, **44**, 3402–3412.
- Eguchi, T., 1977: Properties of sea breezes at Osaka City. *Tenki*, **24**, 739–746 (in Japanese).

- Fujibe, F., and Asai, T., 1979: A study of local winds in Kanto District. Part I: Structures of wind systems with diurnal variation. *Tenki*, **26**, 595–604 (in Japanese).
- Fujibe, F., 1981: Seasonal characteristics of land and sea breezes. *Tenki*, **28**, 367–375 (in Japanese).
- Fujibe, F., and Asai, T., 1984: A detailed analysis of the land and sea breeze in the Sagami Bay area in summer. *Journal of the Meteorological Society of Japan*, **62**, 534–551.
- Fujibe, F., 1985: An effect of pressure gradient on the diurnal variation of wind in the atmospheric boundary layer. *Journal of the Meteorological Society of Japan*, **63**, 52–59.
- Fujibe, F., 2007: The urban heat island. *Tenki*, **54**, 9–12 (in Japanese).
- Fujibe, F., 2012: *Urban Climate Change and Extreme Weather - Extreme Heat and Heavy Rainfall*. Asakura Publishing, 161pp (in Japanese).
- Fukushima, A., and Nonaka, T., 2020: Relationship between the number of heat stroke patient and sea breeze circulation in Kobe City: A case study on 2018 summer. *Faculty Bulletin Humanities and Science*, **40**, 63–75 (in Japanese).
- Furukawa, T., 1966: On the "Yamaji Wind". *Tenki*, **13**, 261–268 (in Japanese).
- Gao, X., and Shiotani, S., 2013: A study on analysis of actual situation of vessel traffic in Osaka Bay using AIS. *Journal of Japan society of civil engineers, ser. B3 ocean engineering*, **69**, 616–621 (in Japanese with English abstract).
- Garratt, J. R., 1992: *The Atmospheric Boundary Layer*. Cambridge University Press, 316pp.
- Grisogono, B., and Belušić, D., 2009: A review of recent advances in understanding the meso-and micro-scale properties of the severe Bora wind. *Tellus*, **61**, 1–16.
- Hamada, T., 2001: Local climate in the Nagano basin - A case study of cold air lakes and mountain breezes. *Bulletin of Nagano Nature Conservation Research Institute*, **4**, 235–242 (in Japanese with English abstract).

- Hamada, T., and Ichinose, T., 2011: Effects of mountain winds on air temperature in an urban area during summer nights. *Journal of Geography (Chigaku Zasshi)*, **120**, 403–410 (in Japanese with English abstract).
- Hisada, Y., Matsunaga, N., and Ando, S., 2005: Effect of sea breeze on mitigation of urban temperature increase. *Proceedings of the Meteorological Society of Japan*, **88**, 338 (in Japanese).
- Hirano, Y., and Shibasaki, R., 2001: Classification of the wind systems in Kanto plain by using cluster analysis. *Annual journal of hydraulic engineering*, **45**, 235–240 (in Japanese).
- Ikegai, T., Hotta, K., Sato, A., Miura, S., and Suzuki, R., 2013: An examination about the optimum relocation of atmospheric monitoring stations, *Bulletin of Kanagawa Environmental Research Center*, **36**, 36–41 (in Japanese).
- Imaoka, E., 1964a: Observation and considerations on the structure of the down slope wind. *Journal of Agricultural Meteorology*, **20**, 17–24 (in Japanese with English abstract).
- Imaoka, E., 1964b: Relation between down slope wind and general wind. *Journal of Agricultural Meteorology*, **20**, 41–45 (in Japanese with English abstract).
- Imaoka, E., 1965: Cold layer on a small hill in clear night and relation to frost fall distribution. *Journal of Agricultural Meteorology*, **20**, 113–118 (in Japanese with English abstract).
- Inamura, T., Iwasaki, K., Saito, H., Nakayama, D., Izumi, T., and Matsuyama, H., 2009: Numerical simulation investigating how local wind “*Matsubori-kaze*” is affected by unique topography of Mt. Aso. *Tenki*, **56**, 123–138 (in Japanese).
- Ino, H., and Neyama, Y., 1972: A study of the land and sea breeze. *Tenki*, **19**, 299–310 (in Japanese).
- Ino, H., and Neyama, Y., 1973: On land and sea breeze in the vicinity of Hiroshima Bay (No. 1) Characteristics of land and sea breeze circulation. *Tenki*, **20**, 547–555 (in Japanese).

- Ino, T., Kiyohara, Y., Higashi, K., Nagano, Y., and Kato, H., 2009: The analysis of down-slope wind over the south side of Rokko Mountains during the cold season. *Proceedings of the Institute of Natural Sciences, Nihon University*, **44**, 219–226 (in Japanese with English abstract).
- Ishii, Y., Tamai, M., and Muraoka, K., 2000: An Interaction between Heat-island and Sea Breeze in the Osaka Plain. *Nagare: Journal of Japan Society of Fluid Mechanics*, **19**, 139–142 (in Japanese with English abstract).
- Itoh, H., and Kawazoe, T., 1983: Land and sea breezes in Wakayama prefecture. *Tenki*, **42**, 151–159 (in Japanese).
- Itoh, H., 1995: Numerical experiments on the extended sea breeze in the Kinki district. *Tenki*, **42**, 17–27 (in Japanese).
- Itokawa, F., Moriyama, M., and Takebayashi, H., 1998: Study on the effect of cold air drainage from the valley mouth on nocturnal cooling of urban areas in summer. *Technical Papers of Kinki-chapter Meeting the Society of Heating, Air-conditioning and Sanitary Engineers of Japan*, **1997**, 35–38 (in Japanese).
- Jaubert, G., and Stein, J., 2003: Multiscale and unsteady aspects of a deep föehn event during MAP. *Quarterly Journal of the Royal Meteorological Society*, **129**, 755–776.
- Junimura, Y., and Watanabe, H., 2008: Study on the effects of sea breeze for decreasing urban air temperatures in summer: analyses based on long-term multi-point measurements and observed wind conditions. *Transactions of AIJ. Journal of Environmental Engineering*, **73**, 9399 (in Japanese with English abstract).
- Kanou, M., and Mikami, T., 2003: Interaction between the heat island phenomena and the mountain breeze in an urban area located on a valley mouth. *Tenki*, **50**, 81–89 (in Japanese).
- Kasuya, T., and Kawamura, R., 2011: Diurnal variation of GPS precipitable water related to the thermally-induced local circulation over the Chugoku and Shikoku district and Setonaikai during clear summer days. *Tenki*, **58**, 291–303 (in Japanese).

- Kawamura, T., 1963: Distribution of surface winds in winter in Hokkaido. *Journal of Meteorological Research*, **15**, 533–537 (in Japanese).
- Kawamura, T., 1964: Analysis of the temperature distribution in the Kumagaya city — A typical example of the urban climate of a small city—. *Geographical Review of Japan*, **37**, 243–254 (in Japanese).
- Kawamura, T., 1966: Surface wind systems over central Japan in the winter season — with special reference to winter monsoons—. *Geographical Review of Japan*, **39**, 538–554 (in Japanese).
- Kawamura, T., 1970: Surface wind systems over central Japan in the warm season: with special reference to the southwesterly flow pattern. *Geographical Review of Japan*, **43**, 203–210 (in Japanese with English abstract).
- Kawamura, T., 1974: Recent trend of air pollution meteorology in Japan. *Journal of Geography (Chigaku Zasshi)*, **83**, 172–181 (in Japanese with English abstract).
- Kawamura, T., 1977a: Surface wind distribution map. *Technical Report of the Japan Meteorological Agency*, **91**, 76pp (in Japanese).
- Kawamura, T., 1977b: The climate of the land-sea breezes. *Report of the Atmospheric Environmental Experiment in the South Kanto Area I*. Japan Meteorological Agency, 46–52 (in Japanese).
- Kawamura, T., 1977c: Climate value of the diffusion field. *Report of the Atmospheric Environmental Experiment in the South Kanto Area III*. Japan Meteorological Agency, 175–186 (in Japanese).
- Kawamura, T., 1977d: Actual condition of the urban climate. *Meteorological Research Note*, **133**, 26–47 (in Japanese).
- Kii, N., Terao, T., and Mori, Y., 2019: Meteorological Conditions at the Occurrence of the Local Severe Wind “Yamaji-Kaze”: On the Case of April 29, 2003. *Tenki*, **66**, 799–807 (in Japanese).

- Kimura, H., 1961: A micrometeorological study on small islands. *Meteorological Notes, Kyoto University*, Ser. 2, **22**, 1–60 (in Japanese).
- Kimura, F., 1992: Local circulation. *Tenki*, **39**, 377–383 (in Japanese).
- Kimura, F., 1994: Thermally induced local circulation. *Tenki*, **41**, 5–12 (in Japanese).
- Kishida, K., 1974: Month-to-month characteristics of the land and sea breezes circulation in Hiroshima. *Tenki*, **21**, 579–586 (in Japanese).
- Kitabayashi, K., 1976: Statistical analysis of sea and land winds. *Pollution Control (Kougai)*, **11**, 288–306 (in Japanese with English abstract).
- Kitada, T., Okamura, K., and Tanaka, S., 1998: Effects of topography and urbanization on local winds and thermal environment in the Nohbi Plain, Coastal region of Central Japan: A numerical analysis by mesoscale meteorological model with a k - ϵ turbulence model. *Journal of Applied Meteorology*, **37**, 1026–1046.
- Kiyohara, Y., Ogino, S., and Yamanaka, D., 2001: Statistical analysis of wind at the southern foot of the Rokko Mountains. *Proceedings of the Kansai Branch Meeting of Meteorological Society of Japan*, 13–16 (in Japanese).
- Kiyohara, Y., 2002: Observational study on the strengthening of the air-flow over mountain in the area around Kobe (*Rokko-oroshi*). Masters thesis, Department of Planetology, Graduate School of Science, Kobe University (in Japanese with English abstract).
- Kiyota, T., and Kiyota, N., 2005: A study on influence of land and sea breeze on air temperature in Hiroshima wide area in summer season. *Transactions of AIJ. Journal of Environmental Engineering*, **587**, 45–51 (in Japanese with English abstract).
- Kondo, H., 1990a: Extended sea breeze. *Tenki*, **37**, 539–540 (in Japanese).
- Kondo, H., 1990b: A numerical experiment of the “extended sea breeze” over the Kanto plain. *Journal of the Meteorological Society of Japan*, **68**, 419–434.

- Kondo, H., 1990c: A numerical experiment on the interaction between sea breeze and valley wind to generate the so-called “extended sea breeze”. *Journal of the Meteorological Society of Japan*, **68**, 435–446.
- Kono, H., and Nishizuka, S., 2006: Statistical analysis of land and sea breeze in Harima Plain (Himeji City): Relation between sea surface temperature and wind. *Tenki*, **53**, 701–706 (in Japanese).
- Koresawa, S., 1960: A study on downslope wind and temperature distribution near the ground in clear and calm night. *Meteorological Notes, Kyoto University*, Ser. 2, **24**, 1–42 (in Japanese).
- Kuniyasu, S., and Neyama, Y., 1975: The effects of the geostrophic wind on land and sea breezes. *Tenki*, **22**, 565–567 (in Japanese).
- Kurita, H., and Ueda H., 1985: Relation between synoptic-scale meteorology, thermal low and long-range transport of air pollutant under light gradient winds. *Journal of Japan Society of Air Pollution*, **20**, 251–260 (in Japanese with English abstract).
- Kurita, H., Ueda, H., and Mitsumoto, S., 1988: Three-dimensional meteorological structure of long-range transport of air pollution under light gradient wind. *Tenki*, **35**, 23–35 (in Japanese).
- Kurita, H., Ueda, H., and Mitsumoto, S., 1990: Combination of local wind systems under light gradient wind conditions and its contribution to the long-range transport of air pollutants. *Journal of Applied Meteorology*, **29**, 331–348.
- Kurose, Y., Ohba, K., Maruyama, A., and Maki, T., 2002: Characteristics of local wind “Aso Oroshi”. *Journal of Agricultural Meteorology*, **58**, 93–101 (in Japanese with English abstract).
- Kurose, Y., Ohba, K., Maruyama, A., and Maki, T., 2002: Characteristics of local wind “Matsubori Kaze” and its wind damage. *Journal of Agricultural Meteorology*, **58**, 103–113. (in Japanese with English abstract) .

- Kusaka, H., Ohashi, Y., Kataoka, K., Miya, Y., and Tsukamoto, O., 2007: Classification of "Rokko-oroshi" and investigation of its generation mechanism. *Proceedings of the 2007 Autumn Meeting of the Meteorological Society of Japan*, **92**, 516 (in Japanese).
- Kusaka, H., and Nishi, A., 2012: Local winds in Japan. *Journal of Wind Engineering*, **37**, 164–171 (in Japanese).
- Kusaka, H., and Fudeyasu, H., 2017: Review of downslope windstorms in Japan. *Wind and Structures*, **24**, 637–656.
- Kusaka, H., and Fujibe, F. (Eds), 2018: *Japanese Climate Encyclopedia*, Maruzen-Shuppan, 516pp (in Japanese).
- Kusuda, M., and Abe, N., 1982: The land and sea breeze in Oita City in summer. *Tenki*, **29**, 81–86 (in Japanese).
- Kuwagata, T., and Sumioka, M., 1991: The daytime PBL heating process over complex terrain in Central Japan under fair and calm weather conditions Part III : Daytime thermal low and nocturnal thermal high, *Journal of the Meteorological Society of Japan*, **69**, 91–104.
- Lepri, P., Kozmar, H., Večenaj, Ž., and Grisogono, B., 2014: A summertime near-ground velocity profile of the bora wind. *Wind and Structures*, **19**, 505–522.
- Lilly, D. K., and E. J. Zipser, 1972: The front range windstorm of 11 January 1972 — a meteorological narrative. *Weatherwise*, **25**, 56–63.
- Lin, Y. L., and Wang, T. A., 1996: Flow regimes and transient dynamics of two-dimensional stratified flow over an isolated mountain ridge. *Journal of the Atmospheric Sciences*, **53**, 139–158.
- Local Wind Research Division of the Agricultural Meteorological Society of Japan, 1995: Local wind (1): Land and sea breeze circulation. *Journal of Agricultural Meteorology*, **51**, 279–284 (in Japanese with English abstract).

- Local Wind Research Division of the Agricultural Meteorological Society of Japan, 1995: The 10th local wind research division "Local wind (1): Land and sea breeze circulation". *Journal of Agricultural Meteorology*, **52**, 175–177 (in Japanese with English abstract).
- Local Wind Research Division of the Agricultural Meteorological Society of Japan, 2000: Local wind (2): Cold air drainage. *Journal of Agricultural Meteorology*, **56**, 311–316 (in Japanese with English abstract).
- Mano, H., 1953: Sudden increase of nocturnal temperature in the valley and the basin. *Journal of Meteorological Research*, **5**, 525–545 (in Japanese).
- Mano, H., 1956: A study on the sudden nocturnal temperature rises in the valley and on the basin. *The Geophysical Magazine*, **27**, 169–204.
- Masuda, Y., Ikeda, N., Seno, T., Takahashi, N., and Ojima, T., 2005: A basic study on utilization of the cooling effect of sea breeze in waterfront areas along Tokyo Bay. *Journal of Asian Architecture and Building Engineering*, **4**, 483–487.
- Mikami, T., 2006: Recent progress in urban heat island studies: Focusing on the case studies in Tokyo. *E-journal GEO*, **1**, 79–88 (in Japanese with English abstract).
- Ministry of the Environment, 2019a: Status of air pollution (excluding hazardous air pollutants, etc.) in fiscal year 2017. https://www.env.go.jp/air/ref_h29.pdf (accessed 2023.1.12).
- Ministry of the Environment, 2019b: Component analysis of fine particulate matter (PM2.5) in the atmosphere component measurement manual. <https://www.env.go.jp/air/osen/pm/ca/manual.html> (accessed 2023.1.12).
- Ministry of the Environment, 2020: Results of the continuous monitoring and measurements of air pollutants (excluding hazardous air pollutants, etc.) in fiscal year 2018. <https://www.env.go.jp/air/osen/matH30taikiosenjokyofull.pdf> (accessed 2023.1.12)

- Miyata, K., and Okamoto, M., 1972: Studies on sea and land breeze in the Seto Inland Sea (Report 1). *Bulletin of the Faculty of Home Economics, Hiroshima Women's University*, **7**, 71–88 (in Japanese).
- Miyazaki, H., Moriyama, M., and Tadokoro, A., 1995: Characteristics of wind environment in Kobe City. *Summaries of technical papers of Annual Meeting Architectural Institute of Japan*, 965–966 (in Japanese).
- Miyazaki, H., 2005: Survey of urban heat island in Kobe region: Investigations using thermometer screen shelter. *Summaries of Technical Papers of Annual Meeting Architectural Institute of Japan*. D-1, 711–712 (in Japanese).
- Miyazaki, H., Niimoto, M., Kyakuno, T., and Tahara, N., 2006: Urban heat island investigation in Kobe using natural ventilated screen shelter, The formation of mass of hot air in summer and the effect of current of air. *Humans and Nature*, **16**, 21–33 (in Japanese with English abstract).
- Mizomoto, S., and Ishihara, M., 2009: Distribution and seasonal change of anticlockwise rotated land-sea breeze around the Osaka Bay as seen by rotary spectral analysis. *Tenki*, **56**, 764–774 (in Japanese).
- Mizuma, M., 1985: An observational study of land and sea breezes in the southern part of the Osaka district. *Annual Reports of the Research Reactor Institute, Kyoto University*, **18**, 68–81.
- Mizuma, M., 1995: General aspects of land and sea breezes in Osaka Bay and Surrounding area. *Journal of the Meteorological Society of Japan*, **73**, 1029–1040.
- Mori, H., Ogawa, H., and Kitada, T., 1994: Characteristics of land and sea breezes in the Nobi plain, and the conditions of occurrence of the “extended sea breeze”. *Tenki*, **41**, 379–385 (in Japanese).
- Mori, M., 1994: Characteristics of sea and land breeze along the Seto Inland Sea coast from a statistical viewpoint. *Proceedings of the Society of Local Meteorology*, **10**, *Local winds (1) Sea and land breeze*, 12–20 (in Japanese).

- Mori, Y., 1983: On climatological aspects of daily variation of surface winds on the coast of Seto Inland Sea — Monthly variation —. *Tenki*, **30**, 19–23 (in Japanese).
- Mori, Y., 1985: On the relationships between surface geostrophic wind and surface wind at Tadotsu and Okayama. *Tenki*, **32**, 523–529 (in Japanese).
- Mori, Y., 1996: On the relationship between land-and sea-breezes and the pressure field in the Central Part of the Seto-Inland Sea District. *Tenki*, **43**, 33–41 (in Japanese).
- Mori, M., Komoda, H., Kobayashi, T., Noda, M., and Takemasa, T., 1999: Characteristics of down-slope wind (nocturnal drainage wind) observed on the south foot of Mt. Kuju. *Tenki*, **46**, 281–288 (in Japanese with English abstract).
- Nakamura, A., Matsuo, K., and Tanaka, T., 2014: A study on cooling effect to residential area by cold air drainage from the mountains in summer night: An analysis on the factors forming temperature distribution based on field measurement. *Proceedings of Annual Research Meeting, Chugoku Chapter, Architectural Institute of Japan*, **37**, 385–388 (in Japanese).
- Nakamura, K., 1976: The nocturnal cold air drainage and distribution of air temperature on the gentle slope. *Geographical Review of Japan*, **49**, 380–387 (in Japanese with English abstract).
- Nakamura, M., Joko, M., Tsukamoto, O., Kanamori, T., Azuma, K., Kawata, K., Kimura, H., Kamei, N., Kamata, T., and Fudeyasu, H., 2002: Experimental study of the downslope wind (“*Hiroto-Kaze*”) occurrence at Mt Nagi. *Tenki*, **49**, 129–139 (in Japanese).
- Nakata, R., 1985: Some observed features for the beginning of sea breeze circulations. *Tenki*, **32**, 167–173 (in Japanese).
- Nakatsubo, R., Horie, Y., Takimoto, M., Matsumura, C., and Hiraki, T., 2018: Analysis of hourly observation data of PM2.5 chemical components at a coastal area in Seto Inland Sea. *Eaorozoru Kenkyu*, **33**, 175–182 (in Japanese with English abstract).

- Neyama, Y., 1974: On interaction between the land and sea breezes and the mountain and valley breezes. *Tenki*, **21**, 587–589 (in Japanese).
- Neyama, Y., 1982: On sea and land breeze in the Seto Inland Sea (popular lecture). *Tenki*, **29**, 653–668 (in Japanese).
- Nishi, A., and Kusaka, H., 2019a: Effect of mountain convexity on the locally strong "Karak-kaze" wind. *Journal of the Meteorological Society of Japan*, **97**, 787–803.
- Nishi, A., and Kusaka, H., 2019b: Comparison of spatial pattern and mechanism between convexity and gap winds. *SOLA*, **15**, 12–16.
- Nishi, A., and Kusaka, H., 2019c: The "Karak-kaze" local wind as a convexity wind: A case study using dual-sonde observations and numerical simulations. *SOLA*, **15**, 160–165.
- Nishikawa, T., and Takagi, N., 2007: A study about change of the temperature and the humidity broken out by mountain wind in urban district of Nagano. *Proceedings of Annual Meeting of Hokuriku Chapter, Architectural Institute of Japan*, **50**, 153–156 (in Japanese).
- Nomura, M., 2015: Generation and development process of the strong wind around the mountain area Part I —Case study of the local downslope wind "Zao-oroshi" by passing the rapidly intensified low—. *Report of the Central Research Institute of Electric Power Industry*, **N15002** (in Japanese).
- Oard, M. J., 1993: A method for predicting Chinook winds east of the Montana Rockies. *Weather and Forecasting*, **8**, 166–180.
- Ogura, Y., 1994: *Science of Weather - To protect yourself from meteorological disasters*. Morikita Publishing, 188pp (in Japanese).
- Ohashi, Y., and Kawamura, R., 2006: Diurnal variation of GPS precipitable water over the Central Japan during clear summer days, *Tenki*, **53**, 277–291 (in Japanese).
- Oke, T. R., 1978: *Boundary Layer Climates*, Methuen, 372pp.

- Okouchi, Y., and Wakata, Y., 1984: Numerical simulation for the topographical effect on the sea-land breeze on the Kyushu Island. *Journal of the Meteorological Society of Japan*, **62**, 864–879.
- Onodera, S., 1975: On the local strong wind “*Matsubori kaze*”. *Tenki*, **22**, 139–143 (in Japanese) .
- Osaka District Meteorological Observatory, 1956: *Hiroto-Kaze General Survey Report*, 58pp (in Japanese).
- Osaka District Meteorological Observatory, 1971: *Wind of Kinki District*, 170pp (in Japanese).
- Osaka District Meteorological Observatory, 1972: *Sea and Land Breeze over the Seto Inland Sea*, 186pp (in Japanese).
- Overland, J. E., and Walter, B. A., 1981: Gap winds in the Strait of Juan de Fuca. *Monthly Weather Review*, **109**, 2221–2233.
- Reed, T. R., 1931: Gap winds of the Strait of Juan de Fuca. *Monthly Weather Review*, **59**, 373–376.
- Rikiishi, K., and Yomogita, Y., 2006: On the generation of the strong northwesterly winds in the Tokachi plain. *Tenki*, **53**, 773–784 (in Japanese with English abstract).
- Sahashi, K., 1962: A study of the down-slope wind (I). *Meteorological Notes, Kyoto University*, **26**, 1–72 (in Japanese).
- Sahashi, K., 1978: On the land and sea breeze around Okayama area. *Tenki*, **25**, 357–363 (in Japanese).
- Saito, K. and Ikawa, M., 1991: A numerical study of the local downslope wind "Yamaji-kaze" in Japan. *Journal of the Meteorological Society of Japan*, **69**, 31–56.
- Saito, K., 1992: Shallow water flow having a lee hydraulic jump over a mountain range in a channel of variable width. *Journal of the Meteorological Society of Japan*, **70**, 775–782.

- Saito, K., 1994: On the downslope wind. *Tenki*, **41**, 3–22 (in Japanese).
- Sakaida, K., Egoshi, A., and Kuramochi, M., 2011: Effects of sea breezes on mitigating urban heat island phenomenon: Vertical observation results in the urban center of Sendai. *Journal of Geography (Chigaku Zasshi)*, **120**, 382–391 (in Japanese with English abstract).
- Sakazaki, T., and Fujiwara, M., 2008: Diurnal variations in summertime surface wind upon Japanese plains: Hodograph rotation and its dynamics. *Journal of the Meteorological Society of Japan*, **86**, 787–803.
- Sasaki, K., Kanno, H., Yokoyama, K., Matsushima, D., Moriyama, M., Fukabori, K., and Wei-ming, S., 2004: Observational evidence of the spatial distribution of wind speed and the vertical structure of the local easterly strong wind "Kiyokawa-dashi" on the Shonai Plain, Yamagata. *Tenki*, **51**, 881–894 (in Japanese with English abstract).
- Sato, I., 1982: Sea and land breeze over southern Osaka Prefecture. *Proceedings of the Kansai Branch Meeting of the Meteorological Society of Japan*, **25**, 5–7 (in Japanese).
- Sato, N., Okada, K., Sugiyama, T., and Naito, J., 1987: Difference of grown direction of valleys and distribution of temperature, *Water Science*, **31**, 39–58 (in Japanese).
- Sato, N., Ohira, K., Sanpe, T., Watanabe, N., Kimura, N., Watanabe, R., and Osawa, K., 2004: Correspondence to heat island phenomenon and mountain breeze in Imaichi City, Tochigi Prefecture. *Journal of the Geographical Society of Hosei University*, **36**, 1–16 (in Japanese).
- Sato, N., and Kanou, M., 2011: Nighttime temperature distribution and its determinants in Ome, Tokyo. *Journal of the Geographical Society of Hosei University*, **43**, 13–26 (in Japanese).
- Sato, N., 2014: The interaction between nocturnal heat islands and mountain breezes in several cities located on a valley mouth in Japan. *Bulletin of the Faculty of Letters, Hosei University*, **68**, 71–98 (in Japanese with English abstract).

- Sato, N., and Kimura, N., 2014: Temperature distribution and sea and land breeze circulation in Hiratsuka City. *Journal of the Geographical Society of Hosei University*, **46**, 5–16 (in Japanese).
- Sawada, T., and Kawamura, R., 2010: Diurnal variation of GPS precipitable water over Hokkaido during clear summer days. *Tenki*, **57**, 305–314 (in Japanese).
- Seibert, P., 1990: South foehn studies since the ALPEX experiment. *Meteorology and Atmospheric Physics*, **43**, 91–103.
- Shigeta, Y., 2012: Development of natural ventilated shelter and compact glove thermometer – Applicability to thermal indicator index WBGT observation – . *Japanese Journal of Biometeorology*, **49**, S83 (in Japanese).
- Shimizu, S., 1964: On the Diurnal variation of the winds accompanied by thermal high or low in the central region of Japan. *Tenki*, **11**, 138–141 (in Japanese).
- Smith, R. B., 1985: On severe downslope winds. *Journal of the Atmospheric Sciences*, **42**, 2597–2603.
- Smith, R. B., 1987: Aerial observations of the Yugoslavian bora. *Journal of the Atmospheric Sciences*, **44**, 269–297.
- Stephens, T. E., 1952: Temperatures in the state of Washington influenced by the westward spread of polar air over the Rocky and Cascade Mountain barriers. M.S. thesis, Dept. of Atmospheric Sciences, University of Washington, Seattle, 38pp.
- Sumi, Y., 2013: Climatic consideration of sea breezes convergence in Ishikari Plain, Hokkaido. *Journal of the Geographical Society of Hosei University*, **45**, 11–24 (in Japanese).
- Suzuki, R., and Kawamura, T., 1987: Characteristics of the wind systems under typical summer conditions in the Central Japan. *Tenki*, **34**, 715–722 (in Japanese).
- Suzuki, R., 1994: Surface geostrophic and observed winds in the coastal zone of Japan. *Journal of the Meteorological Society of Japan*, **72**, 81–90.
- Takahashi, H., and Koizumi, T., 2008: *Basic Geography Series 2. Shizen Chirigaku Gairon*. Asakura Publishing, 180pp (in Japanese).

- Takahashi, K., and Takahashi, H., 2013: Influence of urban heat island phenomenon in the central Tokyo on nocturnal local wind system in summer: A case study using atmospheric pressure data of high density observation network. *Tenki*, **60**, 505–519 (in Japanese with English abstract).
- Takahashi, K., and Takahashi, H., 2014: Influence of urban heat island phenomenon in the central Tokyo on nocturnal local wind system in summer (Continued study): Relationship between stagnation or passage of local wind front and atmospheric pressure field in surroundings. *Tenki*, **61**, 525–540 (in Japanese with English abstract).
- Takasaki, Y., Yoshizaki, M., Suzuki-Parker, A., Watarai, Y., Takei, Y., Sakakibara, Y., and Hamada, T., 2017: Numerical experiment with WRF model and doppler lidar observation of mountain breezes in Nagano City. *Bulletin of Geo-environmental Science*, **19**, 63–71 (in Japanese with English abstract).
- Takebayashi, H., Moriyama, M., and Murakami, S., 1998: Study on wind distribution in Kobe area based on observed meteorological data. *Bulletin of Geo-environmental Science*, **D-1**, 677–678 (in Japanese).
- Takebayashi, H., Moriyama, M., and Itokawa, F., 2001: The appearance frequency of cold air drainage and its influence distance in a built-up area in summer night. *Transactions of AIJ. Journal of Architecture, Planning and Environmental Engineering*, **542**, 99–104 (in Japanese with English abstract).
- Takebayashi, H., and Moriyama, M., 2002: Filling progress in a valley and outflow process into in a built-up area of cold drainage on summer night. *Transactions of AIJ. Journal of Architecture, Planning and Environmental Engineering*, **558**, 57–61 (in Japanese with English abstract).
- Takebayashi, H., and Moriyama, M., 2005: Urban heat island phenomena influenced by sea breeze. *AIJ Journal of Technology and Design*, **21**, 199–202 (in Japanese with English abstract).

- Takebayashi, H., Moriyama, M., and Shibaike, H., 2005: Cooling effects on a built-up area caused by cold drainage on summer night. *Transactions of AIJ. Journal of Environmental Engineering*, **591**, 69–74 (in Japanese with English abstract).
- Takebayashi, H., and Moriyama, M., 2009: Study on air temperature reduction by sea breeze based on upper weather data analysis. *Transactions of AIJ. Journal of Environmental Engineering*, **643**, 1099–1105 (in Japanese with English abstract).
- Takenaka, S., Kasai, M., and Nanjyo, H., 2006: On the accuracy of the power law formula for the vertical profile of the wind speed. *Wind energy*, **30**, 86–91 (in Japanese).
- Takimoto, I., and Sakaida, K., 2012: Climatological study on the occurrence of land and sea breezes in Tohoku district on calm days during warm period. *Quarterly Journal of Geography*, **64**, 1–11 (in Japanese with English abstract).
- Tamai, M., and Arimitsu, T., 2008: Relationship between nocturnal temperature and sea- and land-breezes in the Osaka Bay area in a summer season. *Environmental Systems Research*, **36**, 397–405 (in Japanese with English abstract).
- Tamiya, H., and Oyama, H., 1981: Nocturnal heat island of small town, its manifestation and mechanism. *Geographical Review of Japan*, **54**, 1–21 (in Japanese with English abstract).
- Tateishi, Y., 1961: Cold air drainage in Sugadaira, Nagano. *Tenki*, **8**, 366–371 (in Japanese).
- The Architectural Institute of Japan, 2000: *Klimaatlas of Urban Environments — Urban Development Utilizing Climate Information*. Gyosei, 113pp (in Japanese).
- The Meteorological Society of Japan, 1975: Sea and land breeze and downslope wind. *Meteorological Research Note*, **125** (in Japanese).
- The Meteorological Society of Japan, 1988: Local circulation. *Meteorological Research Note*, **163** (in Japanese).
- Tsuchida, M., and Yoshikado, H., 1995: The winter sea breeze in the Tokyo Bay area. *Tenki*, **42**, 283–292 (in Japanese).

- Ueda, H., Hori, M., and Nohara, D., 2003: Observational study of the thermal belt over the slope of Mt. Tsukuba. *Journal of the Meteorological Society of Japan*, **81**, 1283–1288.
- Ueki, K., 2005: Temperature rise in Kobe —in relation to global warming and heat island phenomenon—. *Annual Report of Kobe Institute of Health*, **33**, 67–73 (in Japanese).
- Wagner, A., 1932: Hangwind-Ausgleichströmung-Berg und Tal Wind. *Met., Zeit.*, **49**, 209–217.
- Yamada, H., and Toba, K., 2010: Basic analysis of cool mountain and valley breeze observed around Mt. Otoko-yama, Kyoto Prefecture, Yawata City. *Environmental Systems Research*, **38**, 73–80 (in Japanese with English abstract).
- Yamagishi, Y. Y., 2002: *Basic Knowledge of Wind for Weather Forecast*. Ohmsha, 193pp (in Japanese).
- Yamamoto, K., 1974: Local characteristics of the land and sea breeze in the vicinity of Hiroshima. *Tenki*, **21**, 575–578 (in Japanese).
- Yamato, H., Mikami, T., and Takahashi, H., 2011: Influence of sea breeze on the daytime urban heat island in summer in the Tokyo Metropolitan area. *Journal of Geography (Chigaku Zasshi)*, **120**, 325–340 (in Japanese with English abstract).
- Yamato, H., Mikami, T., and Takahashi, H., 2017: Impact of sea breeze penetration over urban areas on midsummer temperature distributions in the Tokyo Metropolitan area. *International Journal of Climatology*, **37**, 5154–5169.
- Yamato, H., Hamada, T., Tanaka, H., and Kuribayashi, M., 2019: Relationships among the urban heat island phenomenon, cold air pool, and mountain breeze on clear, calm nights during autumn and winter in Nagano City. *E-journal GEO*, **14**, 197–212 (in Japanese with English abstract).
- Yokota, H., and Nakajima, H., 1992: A roll cloud accompanied by the local down-slope wind “ROKKO-OROSHI”. *Tenki*, **39**, 469–471 (in Japanese).

- Yoshida, K., Nishitani, M., and Furusawa, C., 1998: On the survey of *Rokko-oroshi*. *Journal of Osaka District Prefectural Meteorological Research Association 1998*, 145–146 (in Japanese).
- Yoshida, K., Saeki, R., Nishitani, M., and Nakanishi, N., 1999: On the survey of *Rokko-oroshi* (Part 2). *Journal of Osaka District Prefectural Meteorological Research Association 1999*, 130–131 (in Japanese).
- Yoshikado, H., 1978: The characteristics of the sea breeze in relation to the pressure field. *Pollution Control (Kougai)*, **13**, 292–301 (in Japanese with English abstract).
- Yoshikado, H., 1981: Statistical analyses of the sea breeze pattern in relation to general weather conditions. *Journal of the Meteorological Society of Japan*, **59**, 98–107.
- Yoshino, M., and Fusuki, K., 1953: Air temperature at southern and northern valley sides. *Journal of Agricultural Meteorology*, **8**, 33–36 (in Japanese with English abstract).
- Yoshino, M., 1960: Recent researches on cold air drainage and cold air lakes. *Journal of Agricultural Meteorology*, **15**, 161–165 (in Japanese with English abstract).
- Yoshino, M., and Nishizawa, N., 1960: Cold air drainage and local distribution of frost — Results of preliminary observation in Matsukawa-machi, Nagano Prefecture —. *Journal of Agricultural Meteorology*, **15**, 133–138 (in Japanese with English abstract).
- Yoshino, M., 1961: *Shokiko*. Chijin-shokan, 274pp (in Japanese).
- Yoshino, M., 1971: Die Bora in Jugosla wien: Eine synoptisch-klimatologische Betrachtung. *Annalen der Meteorologie N. F.*, **5**, 117–121.
- Yoshino, M., Kudo, T., and Hoshino, M., 1973: Land and sea breezes on the coast of Japan Sea. *Geographical Review of Japan*, **46**, 205–210 (in Japanese with English abstract).
- Yoshino, M., 1975: *Climate in a Small Area*, University of Tokyo Press, 549pp.
- Yoshino, M., 1986: *Shinpan Shokiko*. Chijin-shokan, 298pp (in Japanese).

Yoshino, M., 1992: Climatological, meteorological and geographical study of Föhn-type and bora-type local winds. *Geographical Review of Japan*, **65**, 1–6 (in Japanese with English abstract).

Figures and Tables

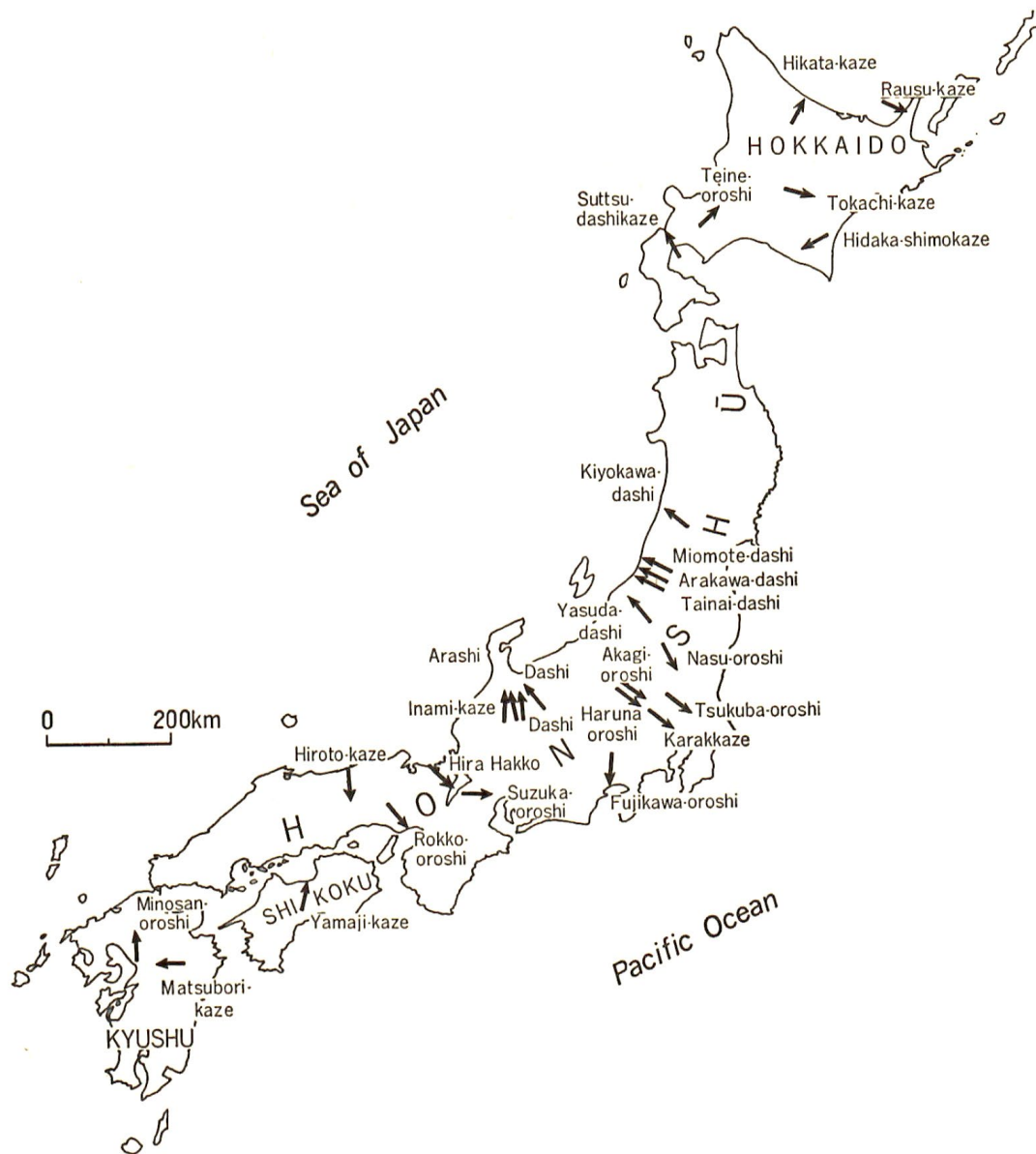


Fig. 1-1 Local winds in Japan (Yoshino, 1975).

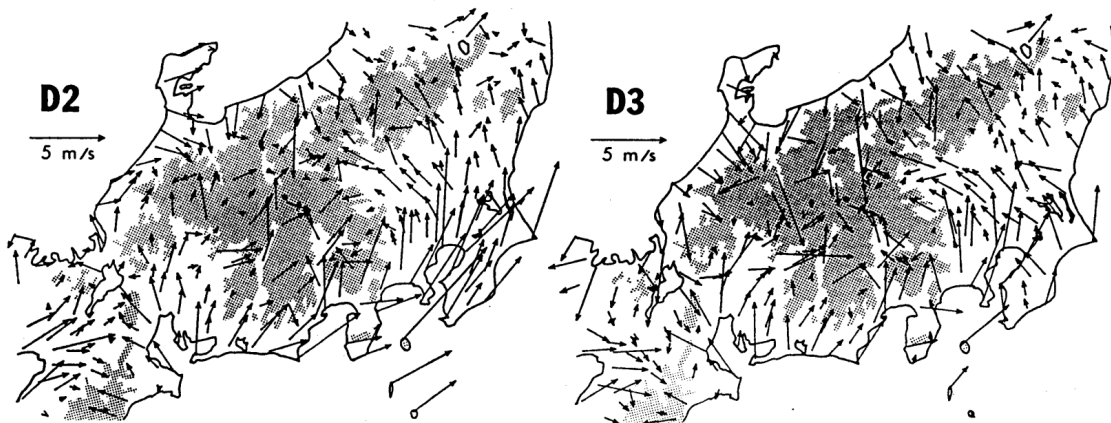


Fig. 1-2 Composite diagrams of D2 and D3 wind systems. Of the 37 days selected as summer pressure type days in 1982-1984, D2 type winds appeared mostly at 12:00, 15:00, and 18:00 JST, in that order, and were generally strong, especially with a southerly component. D3 type winds mostly appear at 15:00 JST, and are characterized by high wind speeds, sea breezes, and valley breezes that develop significantly in various locations. The starting point of the arrow corresponds to the AMeDAS station. Each wind system type was obtained by cluster analysis for 296 wind distribution maps per 3-hourly a day for the 37 days selected. Areas above 400 m elevation are shaded. (Suzuki and Kawamura, 1987)

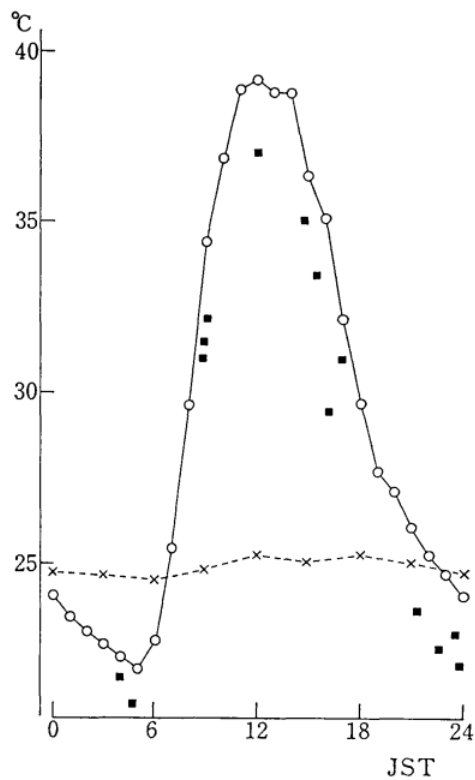


Fig. 1-3 Diurnal variations of sea surface temperature (\times and broken line) and ground surface temperature (\circ and solid line) obtained by the special observation in the Sagami Bay area which was carried out in the periods from 00:00JST 12 August to 00:00JST 14 August in 1980, and from 12:00JST 9 August to 12:00 JST 11 August in 1981. The latter is the average value for all the observation points except Oshima, and both are four days averages at each time of the day. Squares indicate the results of aircraft observation. The sea surface temperature was measured by bucket sampling at the Tansei-maru. The ground surface temperature was measured by bent stem earth thermometers at six points in 1980 and at three points in 1981 (Fujibe and Asai, 1984).

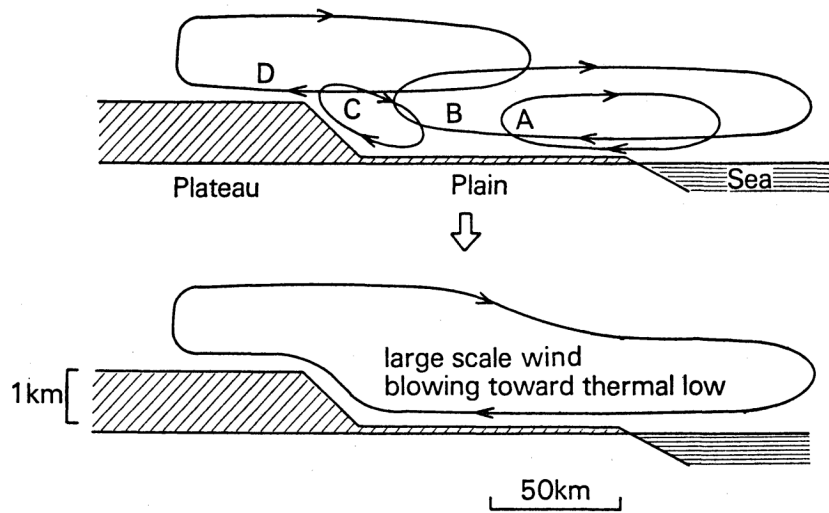


Fig. 1-4 Extended sea breeze. A: sea breeze, B: extended sea breeze, C: valley breeze, D: large-scale wind blowing into a thermal low (Kurita *et al.*, 1988).

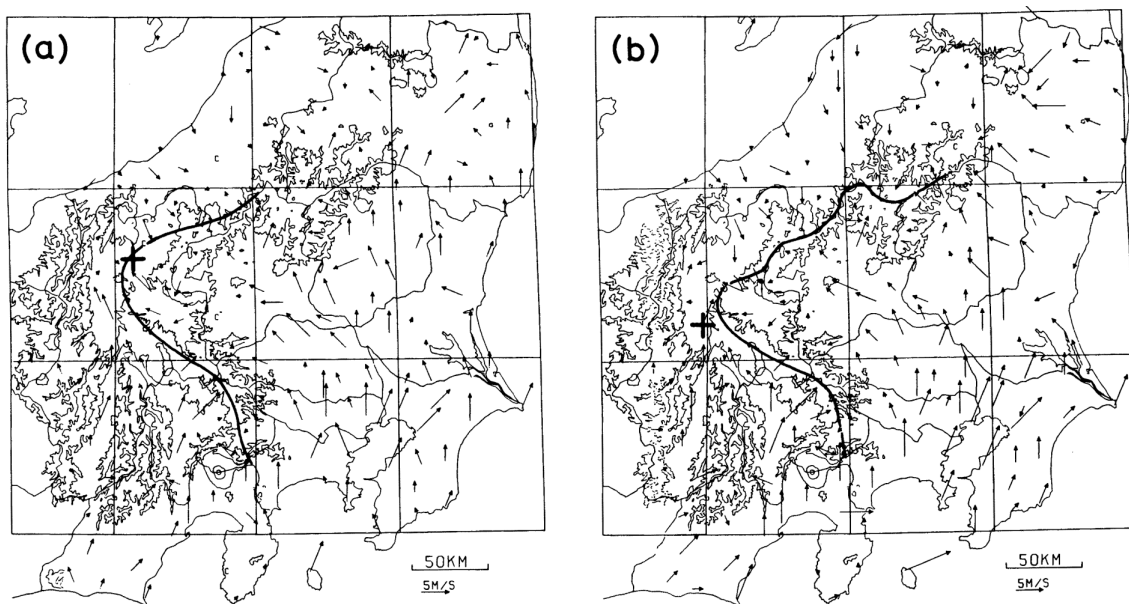


Fig. 1-5 Typical wind fields at 15:00 JST for (a) type NN (July 10, 1979), (b) type ND (June 1, 1979). The thick solid line represents a convergence line between the winds from the Pacific Ocean and the Japan Sea, and the cross represents a thermal low center. High concentrations of Ox appeared after 8:00 a.m. were considered "Night smog" and those before 8:00 a.m. were considered "Day smog". During the 35 days when high concentrations of Ox appeared in Ueda, we classified them into the following three types according to the appearance of "night smog". Type NN: "Night smog" appeared in Ueda and Nagano (6 days). Type ND: "Night smog" appeared in Ueda only and did not appear in Nagano (19 days). See the next figure for the location of Ueda and Nagano. The thick solid line represents a convergence line between the winds from the Pacific Ocean and the Japan Sea, and the cross represents a thermal low center. (Kurita and Ueda, 1985).

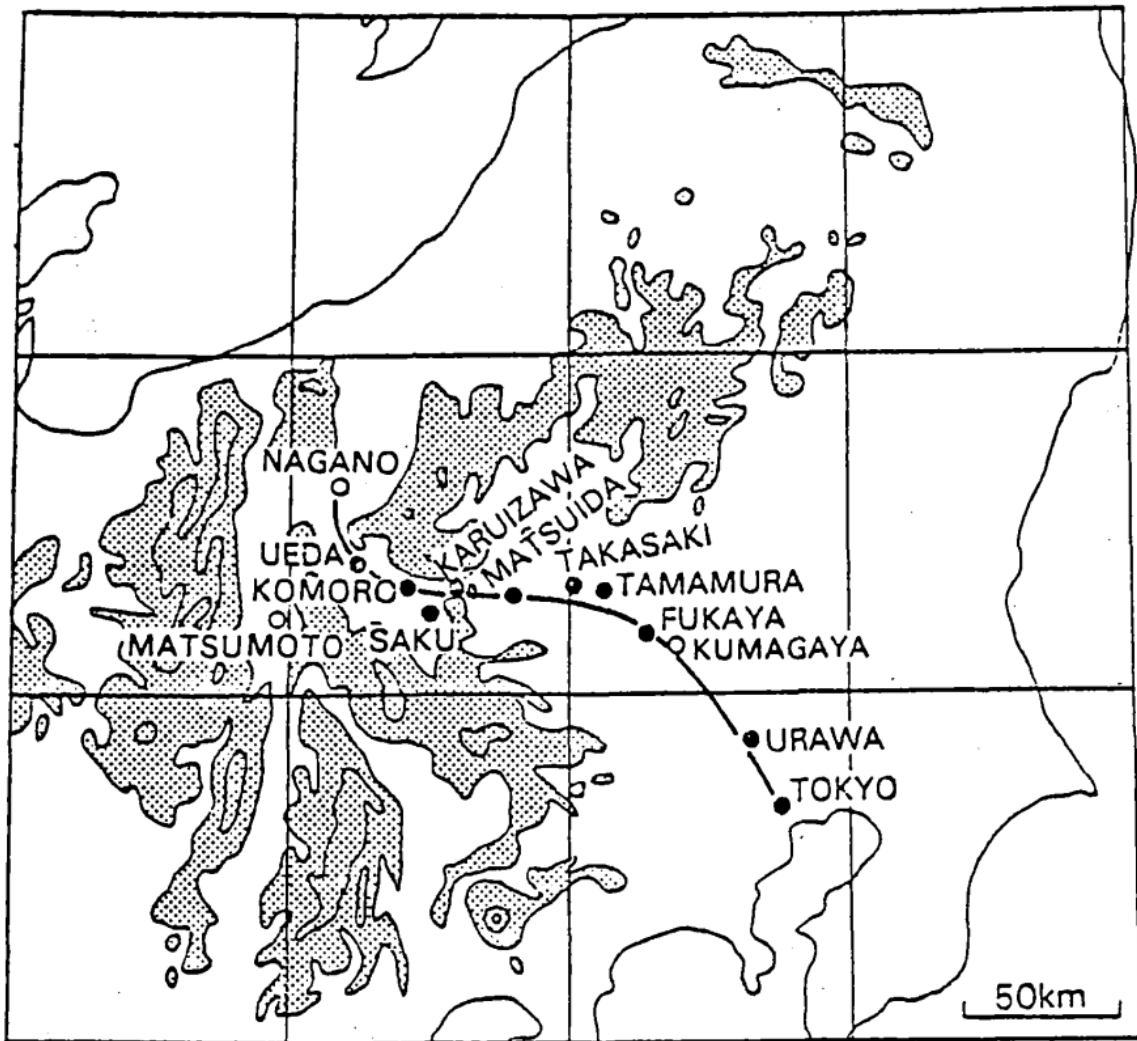


Fig. 1-6 Route of long-distance transport of contaminants from the Kanto Plain to the Chubu mountainous region on 29 July, 1983 when typical long-range transport of air pollutants occurred. Black circle: Meteorological observation sites, white circle: Meteorological stations, and solid line: polluted air mass transport route (Stream trace line) (Kurita *et al.* 1988).

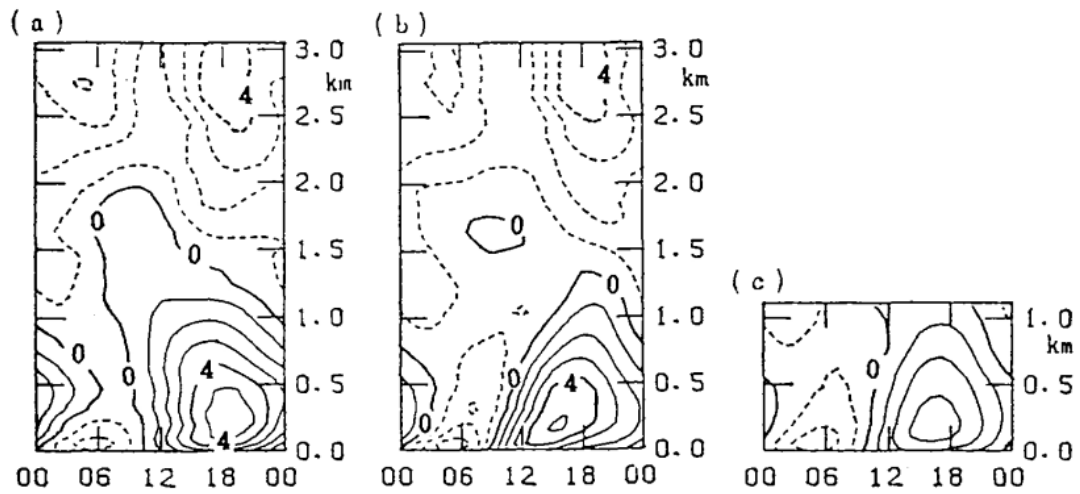


Fig. 1-7 Time-height sections of southerly wind components at (a) Machida (1980) and Sagamihara (1981), (b) Chigasaki and (c) Tansei-maru obtained by the special observation in the Sagami Bay area which was carried out in the periods from 00:00JST 12 August to 00:00JST 14 August in 1980, and from 12:00JST 9 August to 12:00 JST 11 August in 1981. Contour interval is 1 m/s, and the dotted contour lines represent negative values (northerly wind) (Fujibe and Asai, 1984).

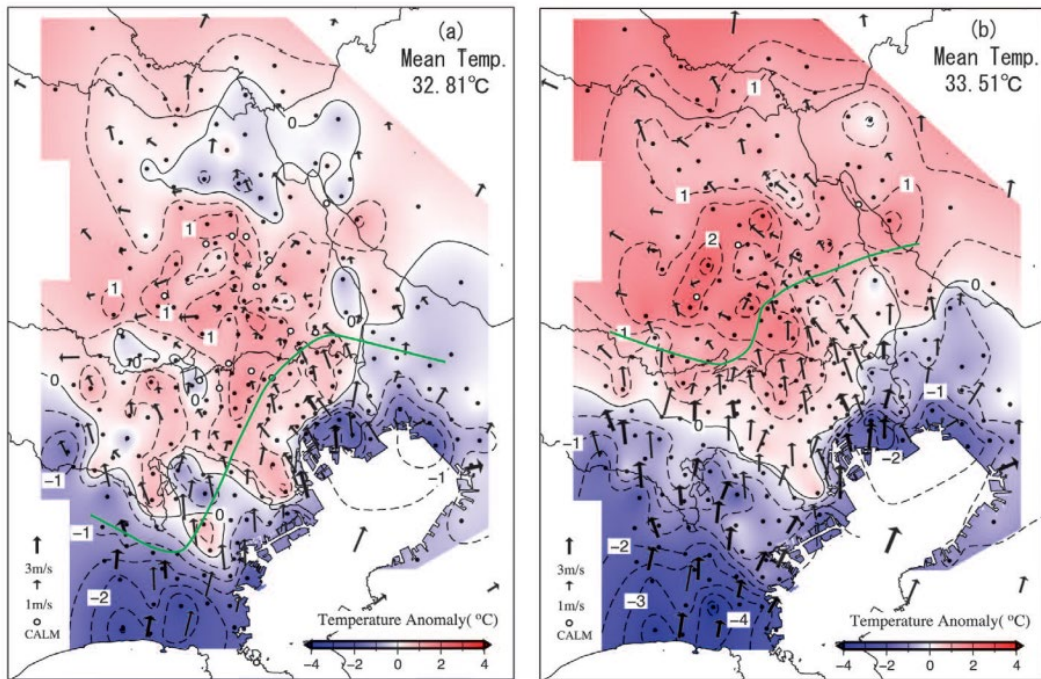


Fig. 1-8 Composite distribution map of temperature anomalies and winds on sea breeze front days (8 days) when sea breeze fronts were observed in the Tokyo metropolitan area in August 2006 and 2007. (a) 12:00 JST (b) 14:00 JST. Sea breeze front days were defined as days when sea breeze fronts were clearly visible among the days selected using the criteria at all AMeDAS stations of mean sunshine duration (7 hours more), precipitation amount (less than 0.5 mm from 6:00 to 18:00 JST), wind direction (average wind direction from 16 to 20 JST is 150 to 225°), and the geostrophic wind speed calculated by data of four stations (less than 6 m/s). Temperature anomalies are obtained by subtracting spatially averaged values (upper right number) from the data at each point. The green curves represent sea breeze front. Wind arrows indicating less than 3 m/s are shown based on the length of the thin arrow, and wind arrows indicating more than 3 m/s are shown based on the length of the thick arrow (Yamato *et al.*, 2011).

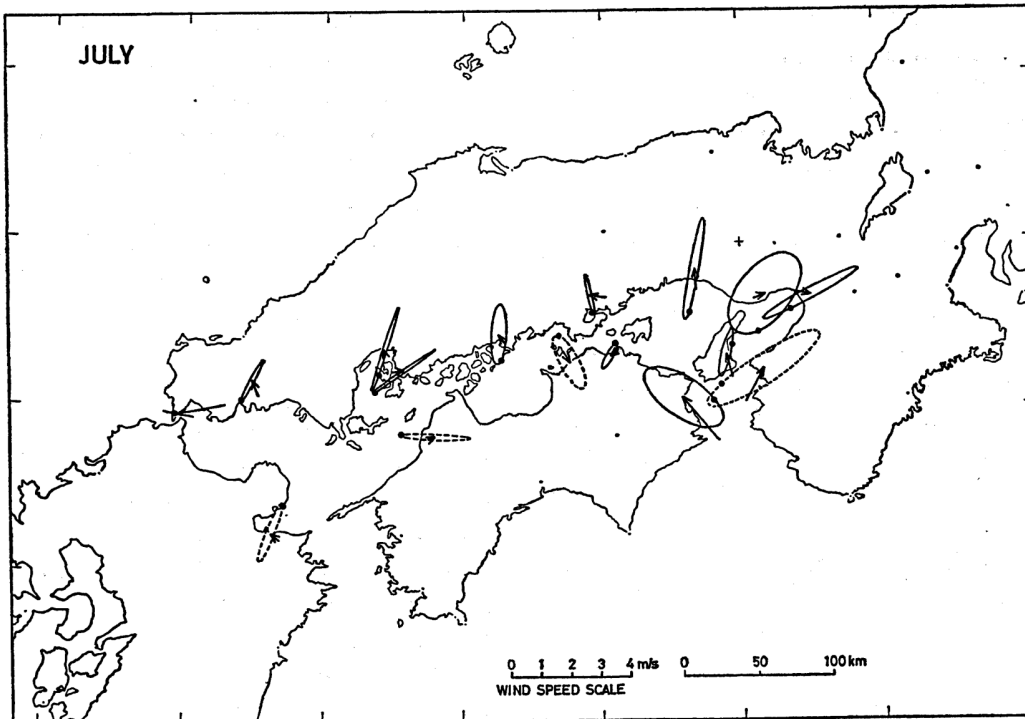


Fig. 1-9 Vector mean wind and daily elliptical distributions in July, 1967-1977. The ellipse indicates the endpoint of the diurnal variation vector, and the black circle on the ellipse indicates the position at 00:00 JST. The solid line indicates clockwise rotation and the dotted line indicates counterclockwise rotation. (Mori, 1983).

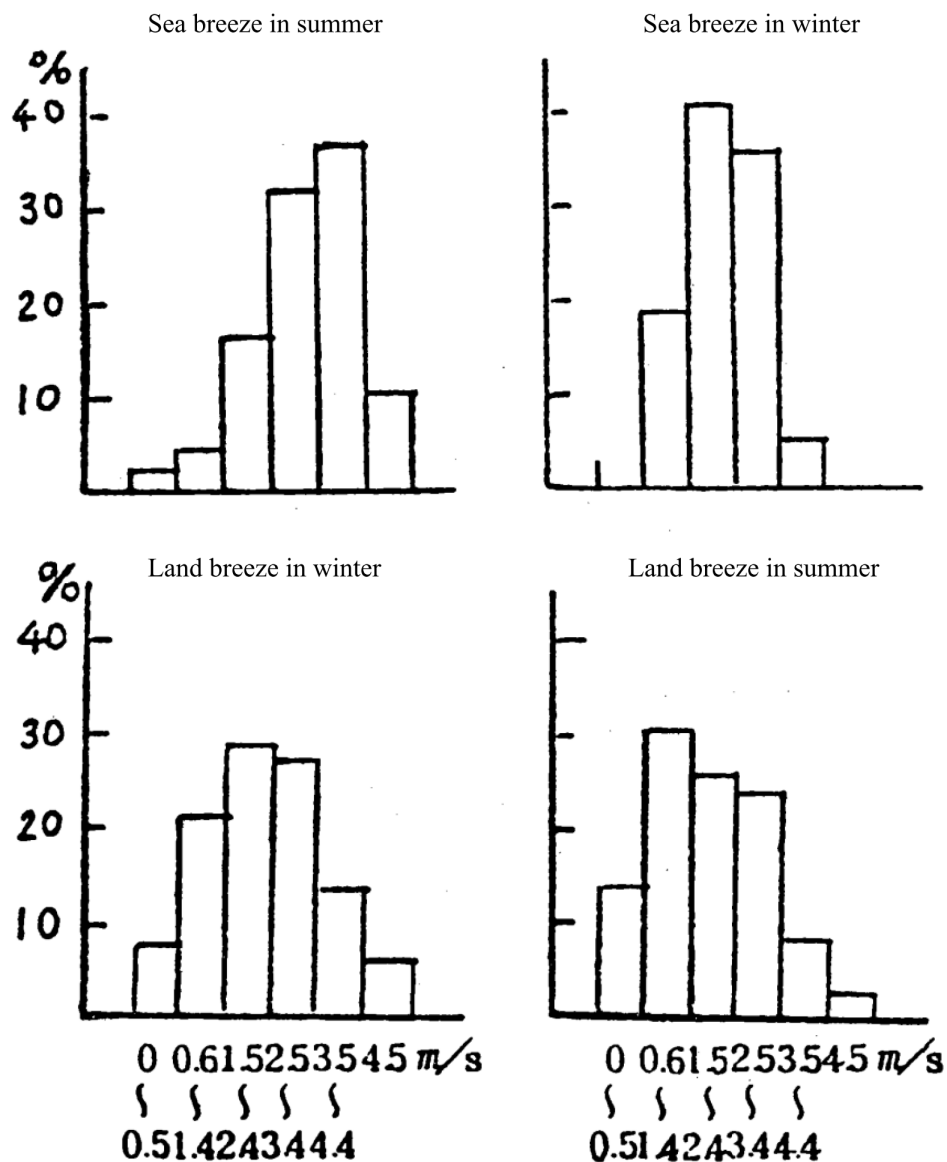


Fig. 1-10 Frequency of occurrence of sea and land breeze by average of the maximum wind speed. The maximum wind speeds were averaged over about 60 observation points along the Seto Inland Sea coastline for sea and land winds in summer and winter, respectively, and then divided into six wind speed classes (Neyama, 1982).

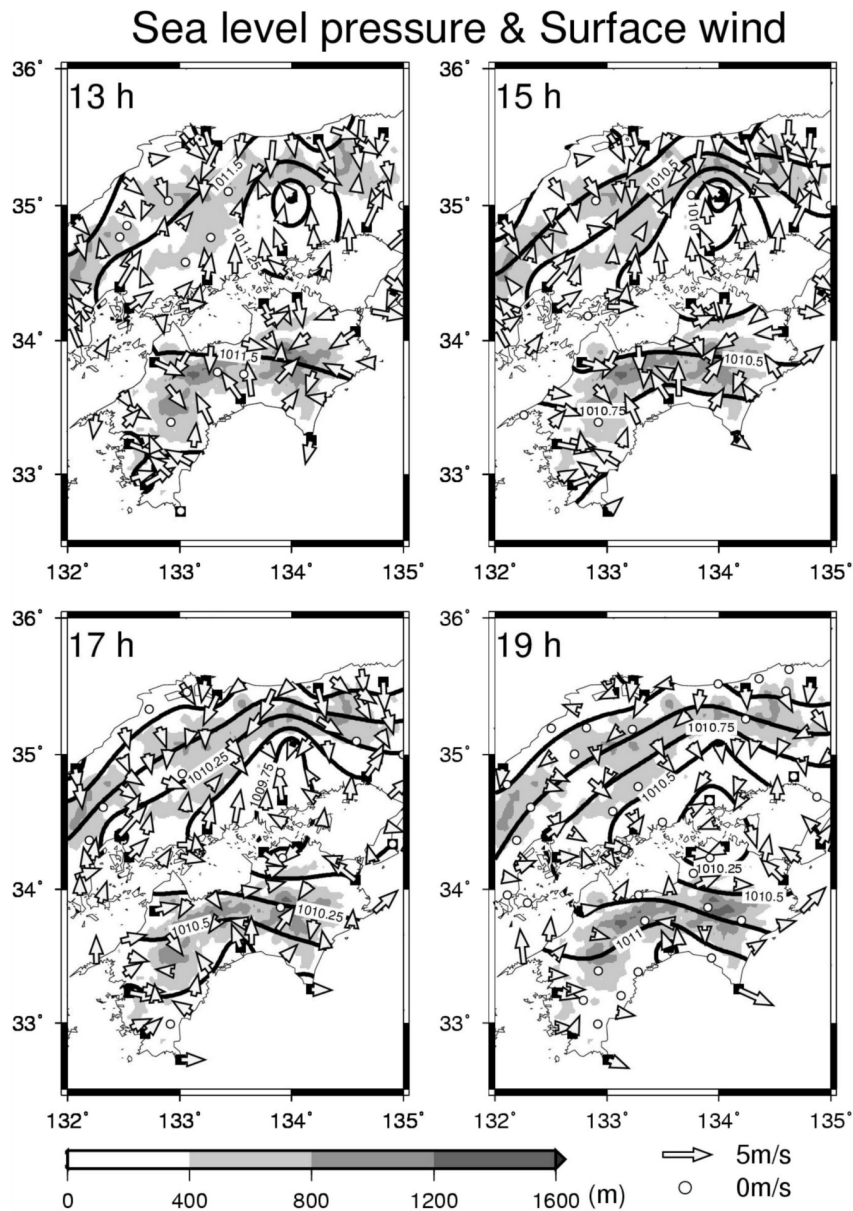


Fig. 1-11 Spatial distribution of sea level pressure, wind direction and speed from 13:00 to 19:00 JST composited of 13 days obtained as summer calm days in July and August from 1996 to 2007. The isopleths indicate sea level pressure at intervals of 0.25 hPa. Vectors indicate wind speed and direction. White circles indicate wind speed of 0 m/s. Black squares indicate meteorological offices. Shading indicates elevation (Kasuya and Kawamura, 2011).

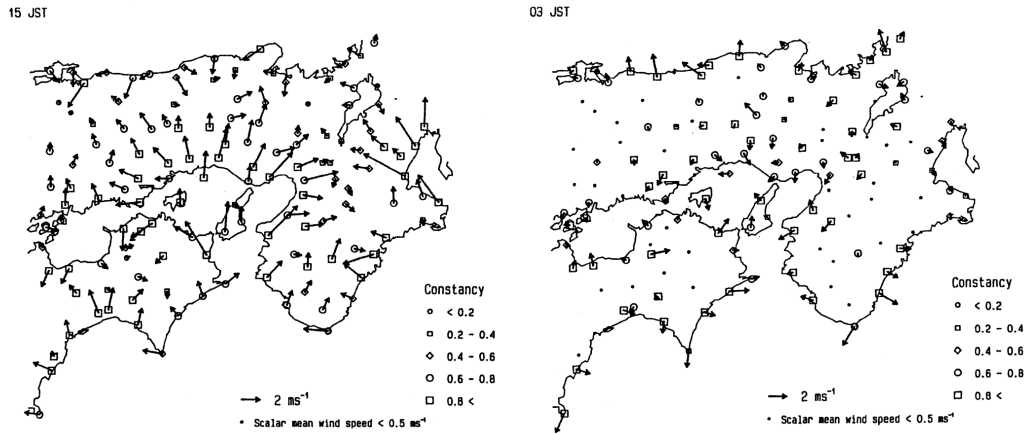


Fig. 1-12 Vector-mean winds at 15:00 and 03:00 JST for Type I-SE. The wind velocity data from the 1st of January, 1989 to the 31st of December, 1990 are utilized. The daily wind maps are drawn for each day of the study period by using seven AMeDAS stations data in Osaka Prefecture. Visual inspection of the daily wind maps leads to the type classification of the diurnal variation of winds. The type I is the observed temporal change in the wind direction of the sea breeze; the northwesterly breeze in the morning gradually backs to a southwesterly breeze in the late afternoon. This southwesterly breeze is considered to be the sea breeze from the Kii Channel. The “SE” in Type I-SE means that the southeasterly sea breeze at Okayama occurs. Type I-SE having the greatest frequency appears during April to September compared to the other four types. Constancy is the vector mean wind speed divided by the scalar mean wind speed. (Mizuma, 1995).

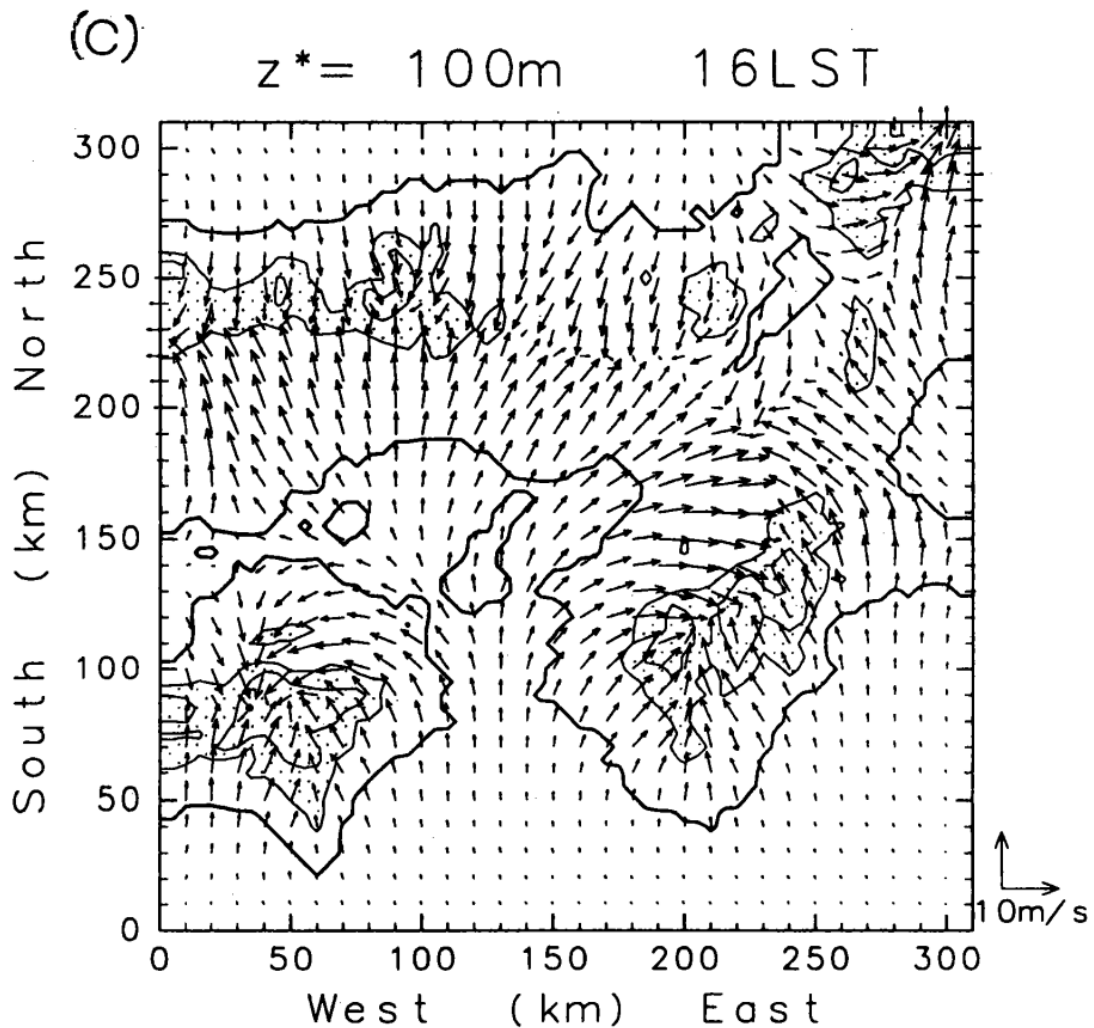


Fig. 1-13 Horizontal structure of the wind at 16:00 JST at $z^* = 100$ m by numerical experiment. Contours are at 500 m and 800 m altitude, and are shaded above 500 m. This numerical experiment was computed using realistic terrain conditions in a basic numerical experiment. The horizontal grid of the model is a staggered grid with a grid spacing of 5 km. The vertical grid consists of 20 layers, starting from the bottom at 0, 10, 50, and 100 m. From there, the grid is spaced at 200 m intervals up to 1700 m, then at 300 m intervals up to 3200 m, and finally at 400 m intervals up to 4400 m. The time step is 20 seconds. Integration began at 6:00 a.m. local time and continued until 24:00 on the second day. Results were stored every 30 minutes (Itoh, 1995).



Fig. 1-14 Windrose at night for weak extended sea and land breeze (July 25-26, 1999 at 18:00 and 16:00 JST) The largest scale on the windrose is the 50% frequency (Takebayashi *et al.*, 2001).

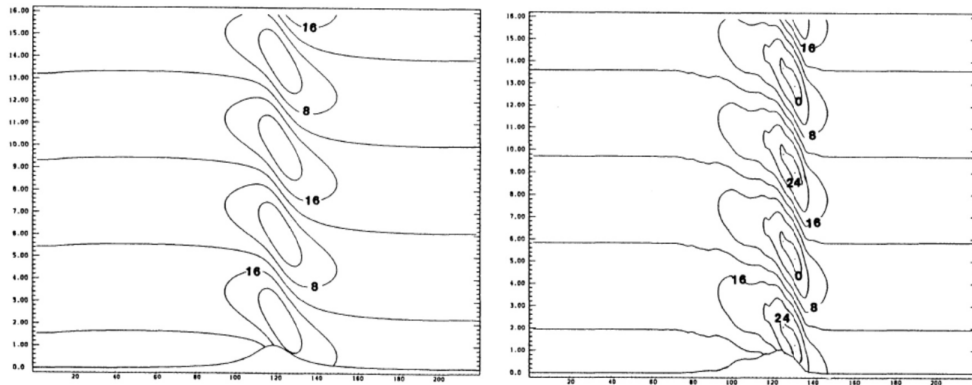


Fig. 1-15 Horizontal wind by statics analysis of 2-dimensional over-mountain airflow. $N \sim 0.01$ /s, $U = 12$ m/s. Left: Solution with nonlinear boundary conditions for bell-shaped mountains. Right: Solution with nonlinear boundary conditions for Shikoku topography. The horizontal axis indicates distance (km), the vertical axis indicates altitude (km), and the numbers in the figure indicate horizontal wind speed (m/s) (Saito and Ikawa, 1991).

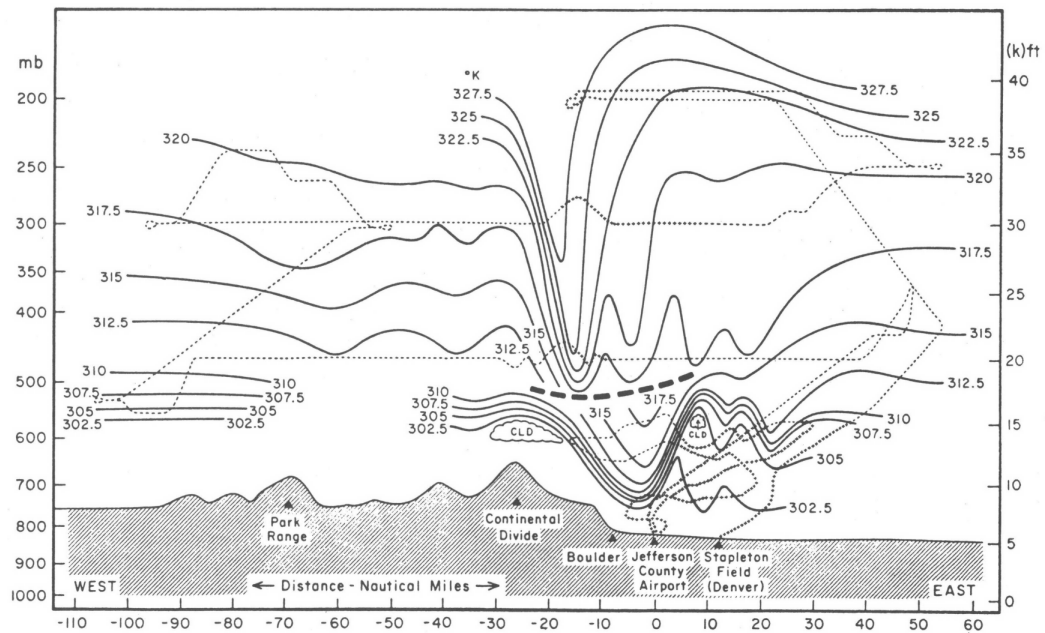


Fig. 1-16 Vertical cross section of potential temperature during downslope wind near Boulder, Colorado in USA obtained by special observation on January 11, 1972. Analysis of the potential temperature field (solid lines) from aircraft flight data and sondes taken on 11 January 1972. The dashed lines show aircraft track. The heavy dashed line separates data taken by the Queen Air at lower levels before 22:00 GMT from that taken by the Sabreliner in the middle and upper troposphere after 00:00 GMT (12 January). The aircraft flight tracks were made along an approximate 130° - 310° azimuth, but the distances shown are along the east-west projection of those tracks. From Lilly and Zipser (1972). (Saito, 1994).

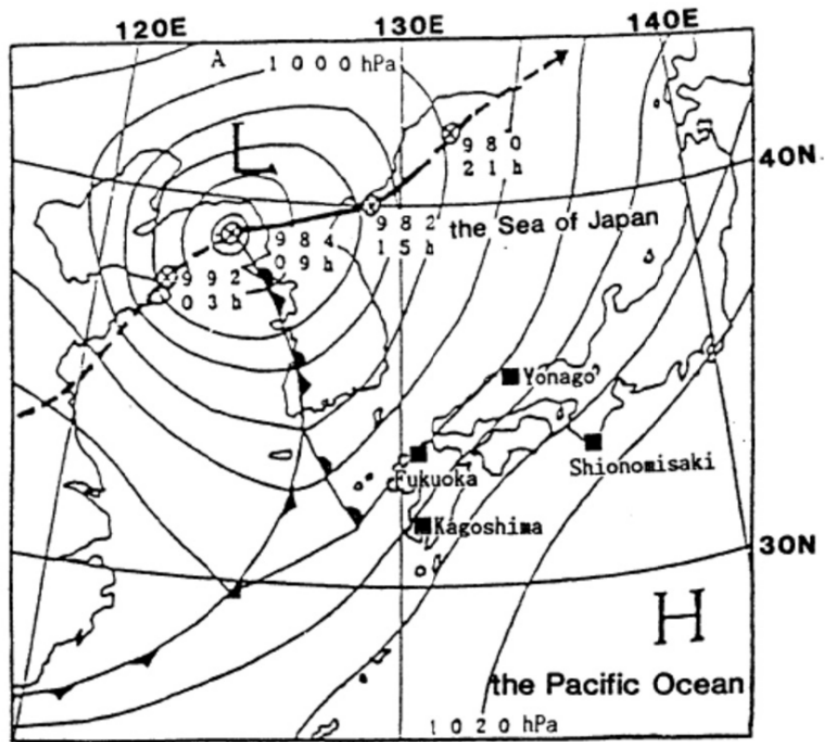


Fig. 1-17 Surface weather chart at the time of *Yamaji-kaze* (09JST, April 21, 1987, arrow indicates depression storm track) (Saito and Ikawa, 1991).

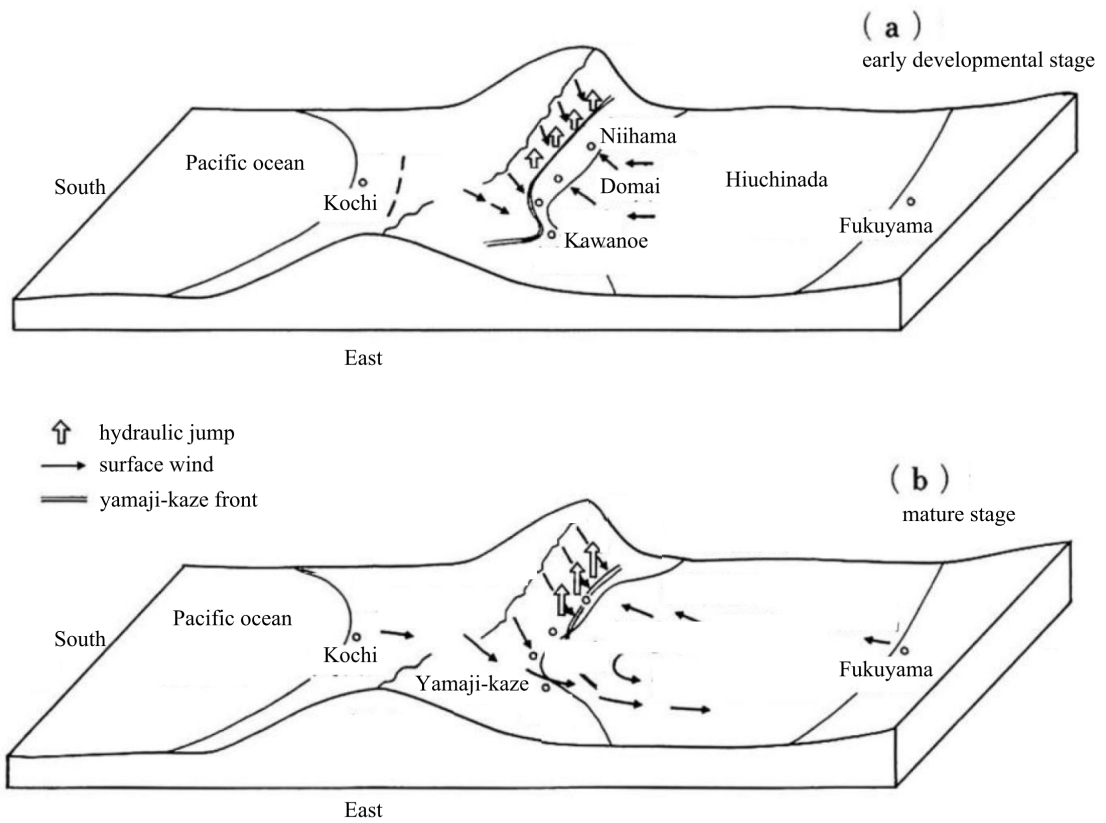


Fig. 1-18 Schematic diagram of *Yamaji-kaze* (Saito, 1994; adapted from Ogura, 1994) (Kii *et al.*, 2019).

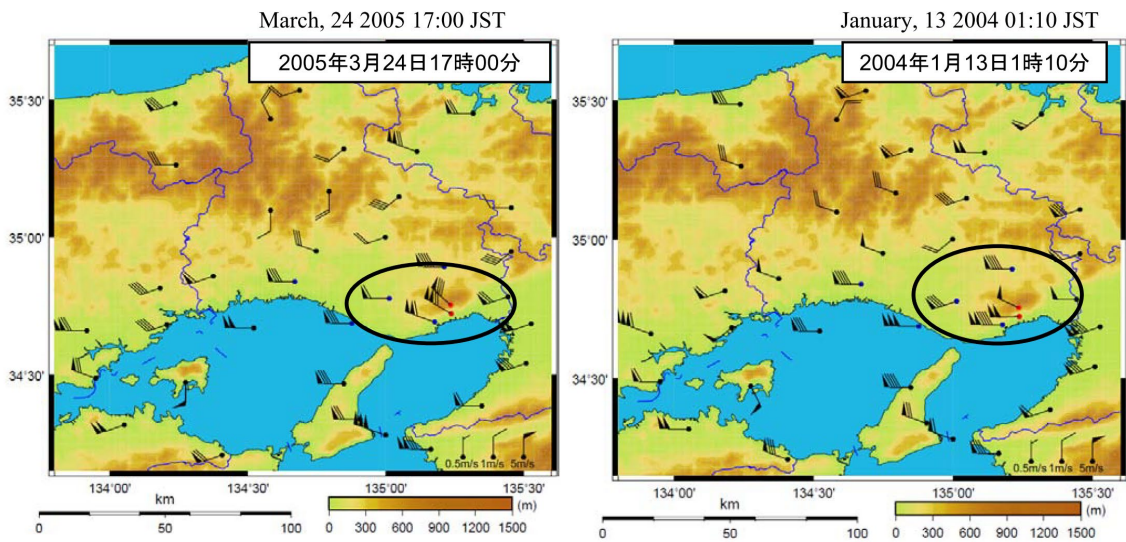


Fig. 1-19 Typical example of surface wind system at the appearance of daily maximum wind speed on the day when the *Rokko-oroshi* occurred. (Left) Case of strong winds blowing from the mountainous direction, (Right) Case of wind direction to the west during strong winds (Ino *et al.*, 2009).

Type B: March 24, 2005, 21:00 JST

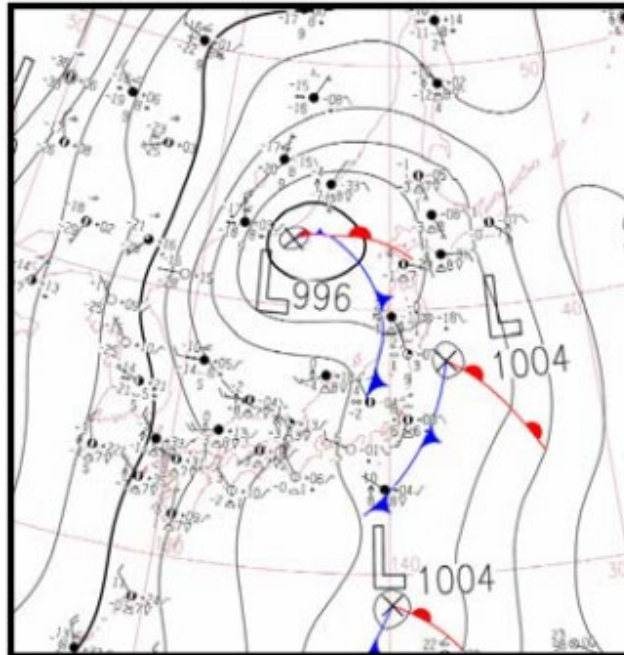


Fig. 1-20 Typical examples of surface weather chart when the *Rokko-oroshi* occurred for type B (Ino *et al.*, 2009). Type B: A case in which an extratropical low cyclone or front passed through the area 6 to 12 hours before the downslope winds blew, followed by an overhang of anticyclone from the Yangtze River area on the continent, resulting in a close to winter pressure pattern or a condition before a winter pressure pattern.

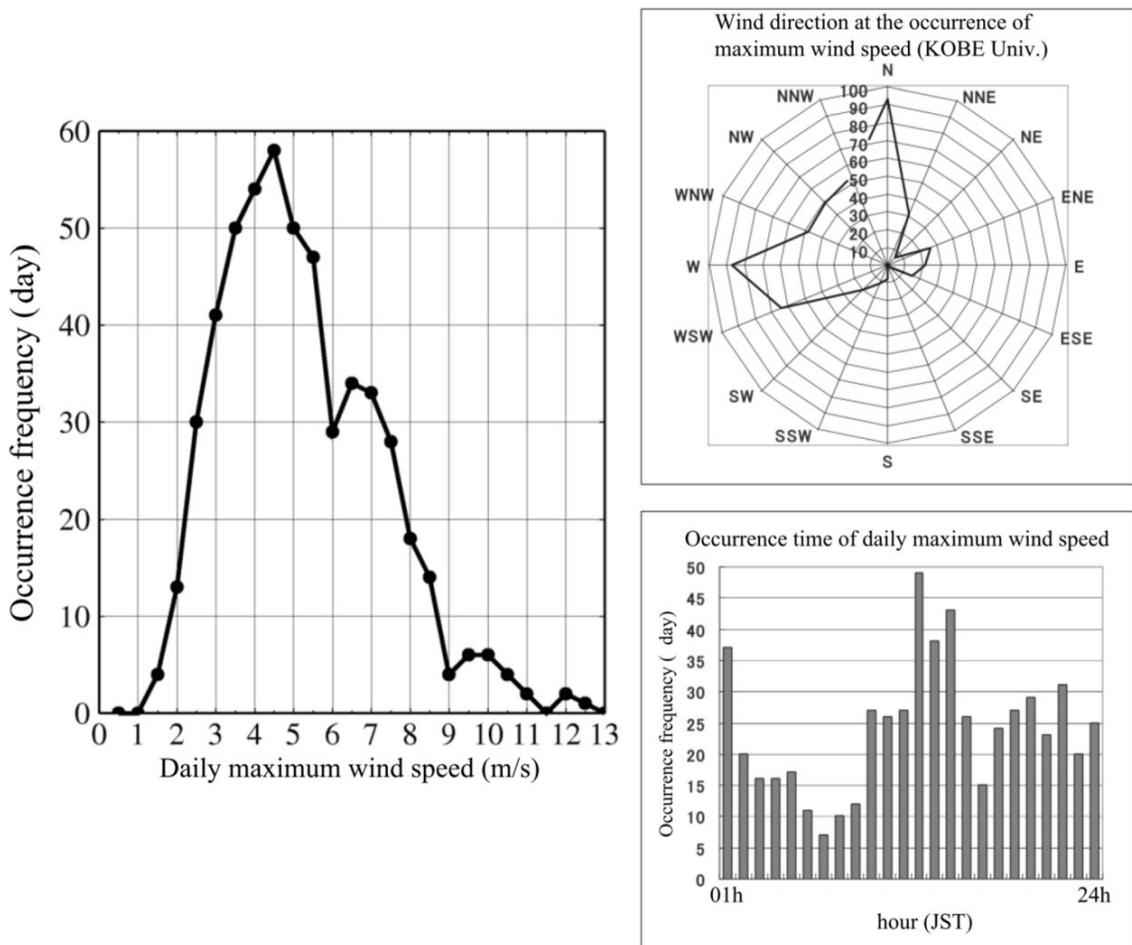


Fig. 1-21 Frequency distribution (based on Kobe University observation data) on 528 days of analysis during the cold season from November to March 2001-2005. Left: daily maximum wind speed. Upper right: wind direction at daily maximum wind speed. Lower right: time of appearance of daily maximum wind speed (Ino *et al.*, 2009).

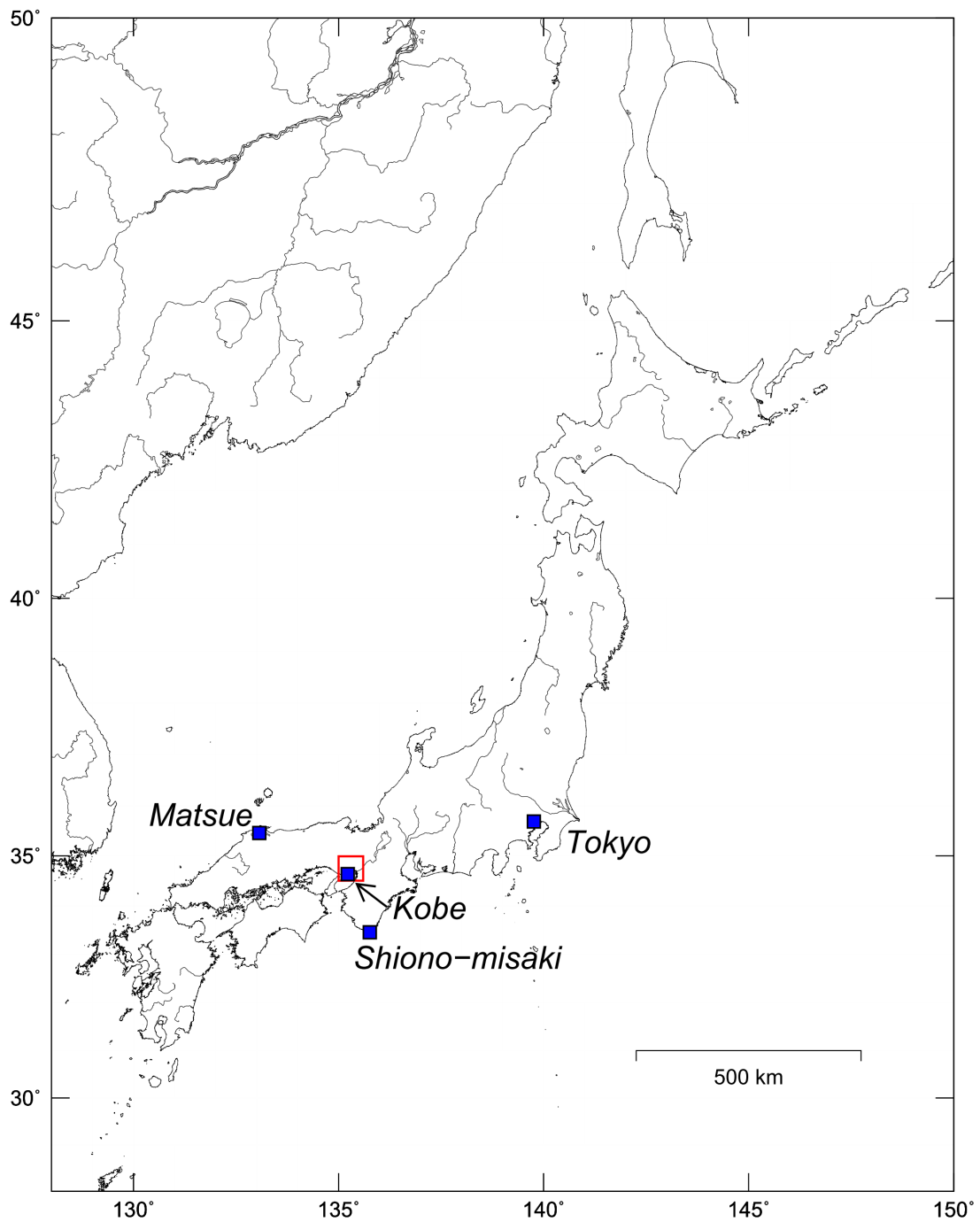


Fig. 2-1 Location of the study area. Red square is the target area. Matsue and Shiono-misaki are the upper-level sonde observatories.

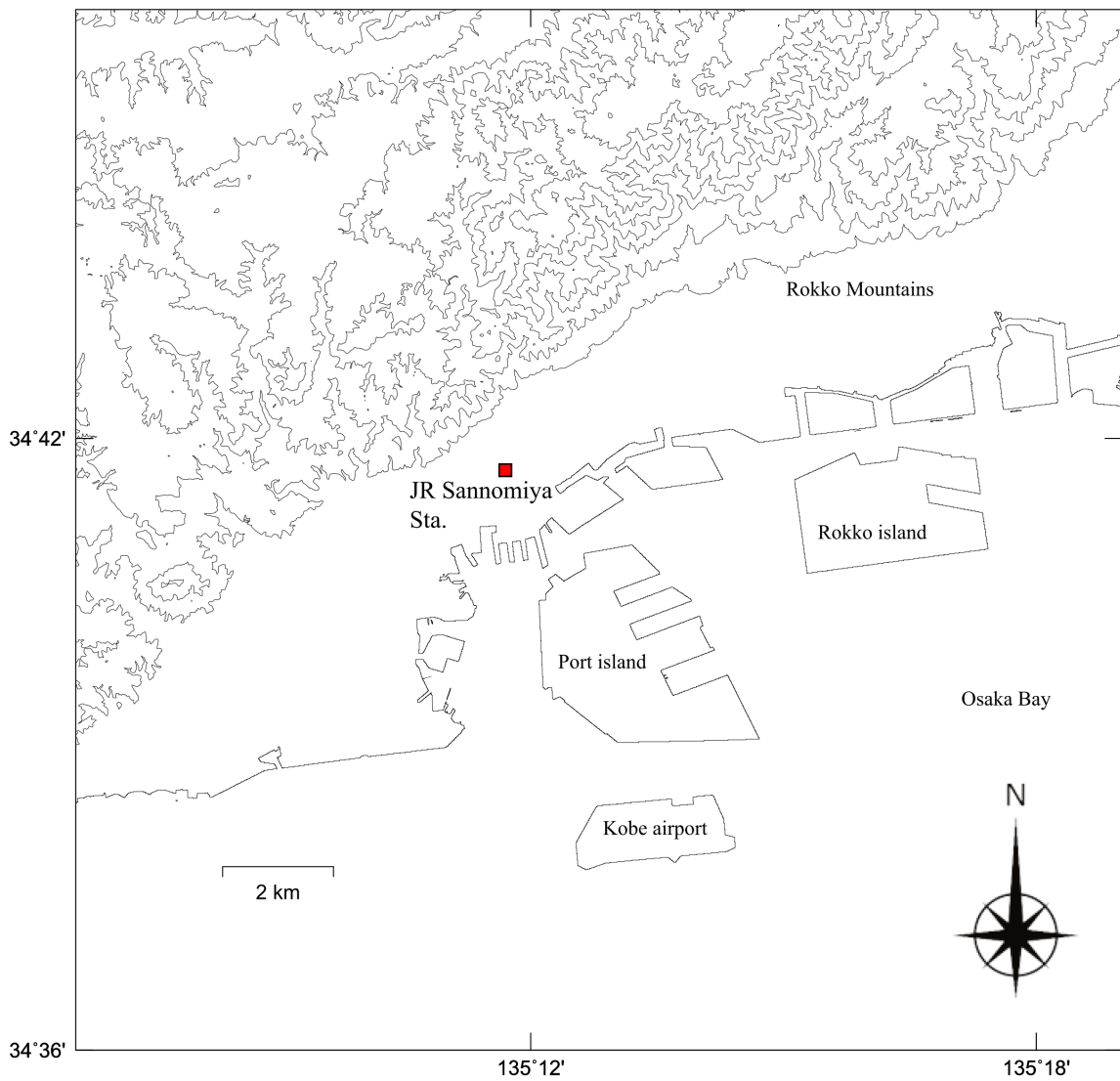


Fig. 2-2 Topography and geographical names of study area. Red square is the JR Sannomiya Station at the center of the Kobe City. Contour lines every 100 m.

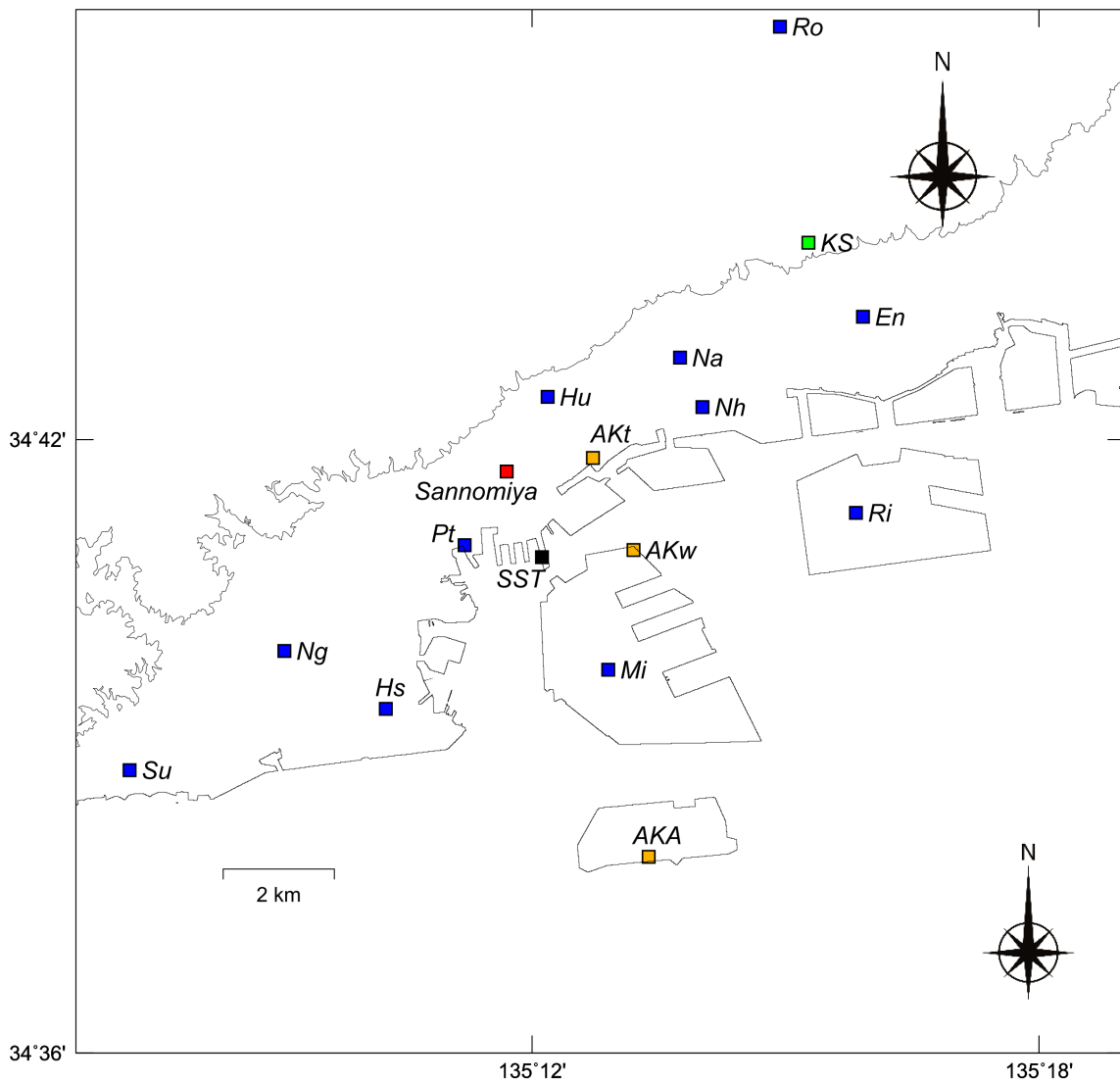


Fig. 2-3 The distribution of the AEROS (blue), AMeDAS (orange) and KS (green). Black square is the SST measurement point. Red square is the JR Sannomiya Station at the center of the Kobe City. Contour lines are shown only at elevation 0 and 100 m.

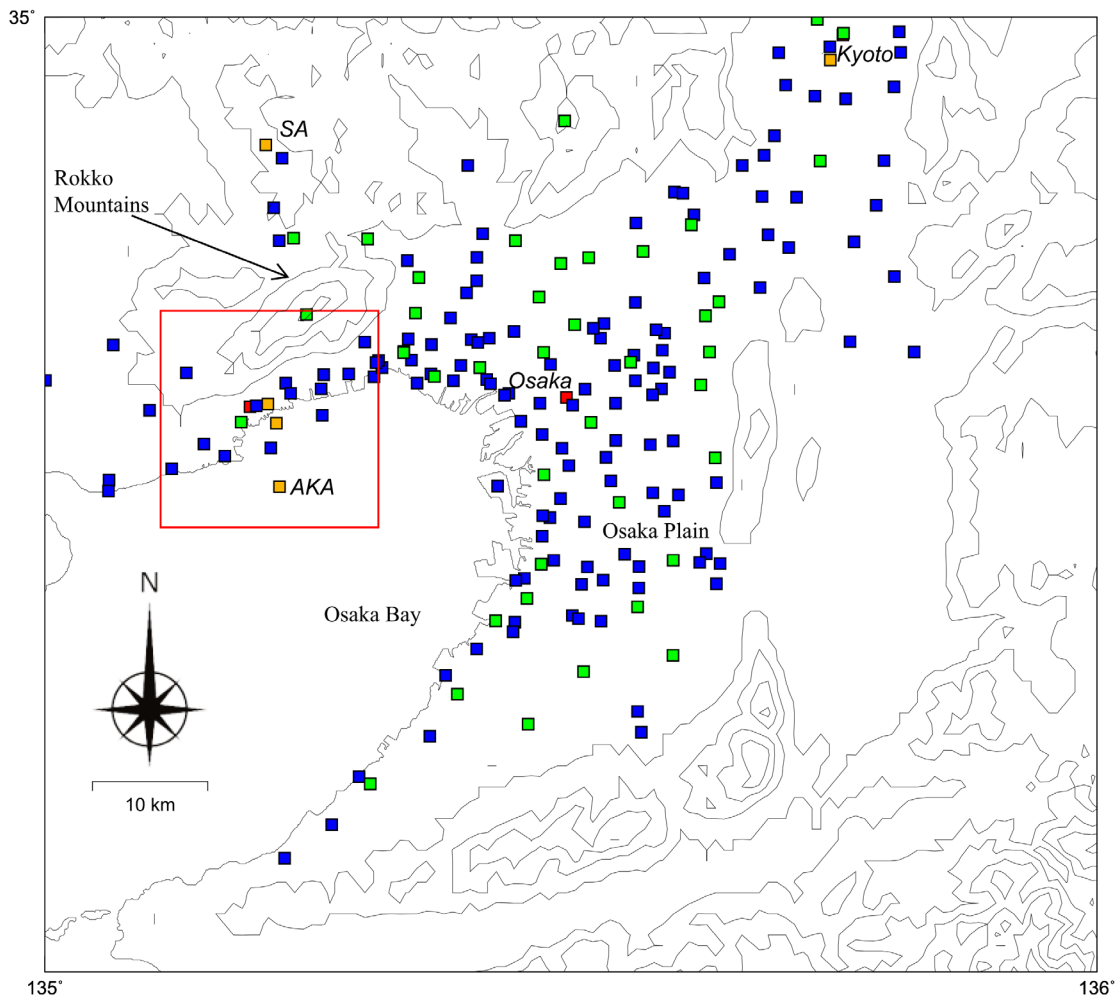


Fig. 2-4 The distribution of the AEROS (blue and green) and AMeDAS (orange) in the Kyoto-Osaka-Kobe area. Blue and green squares indicate wind and temperature observation points, respectively. The red squares indicate the area in Figs. 2-2, 2-3, and 2-6. Contour lines every 200 m.



Fig. 2-5 Details of KS station (158 m above sea level; 15 m above ground level). (a)

Photograph of the temperature and wind measurement instruments. (b) topography around the KS. Red circle is the point where the device is installed. From Google map (<https://www.google.co.jp/maps>).

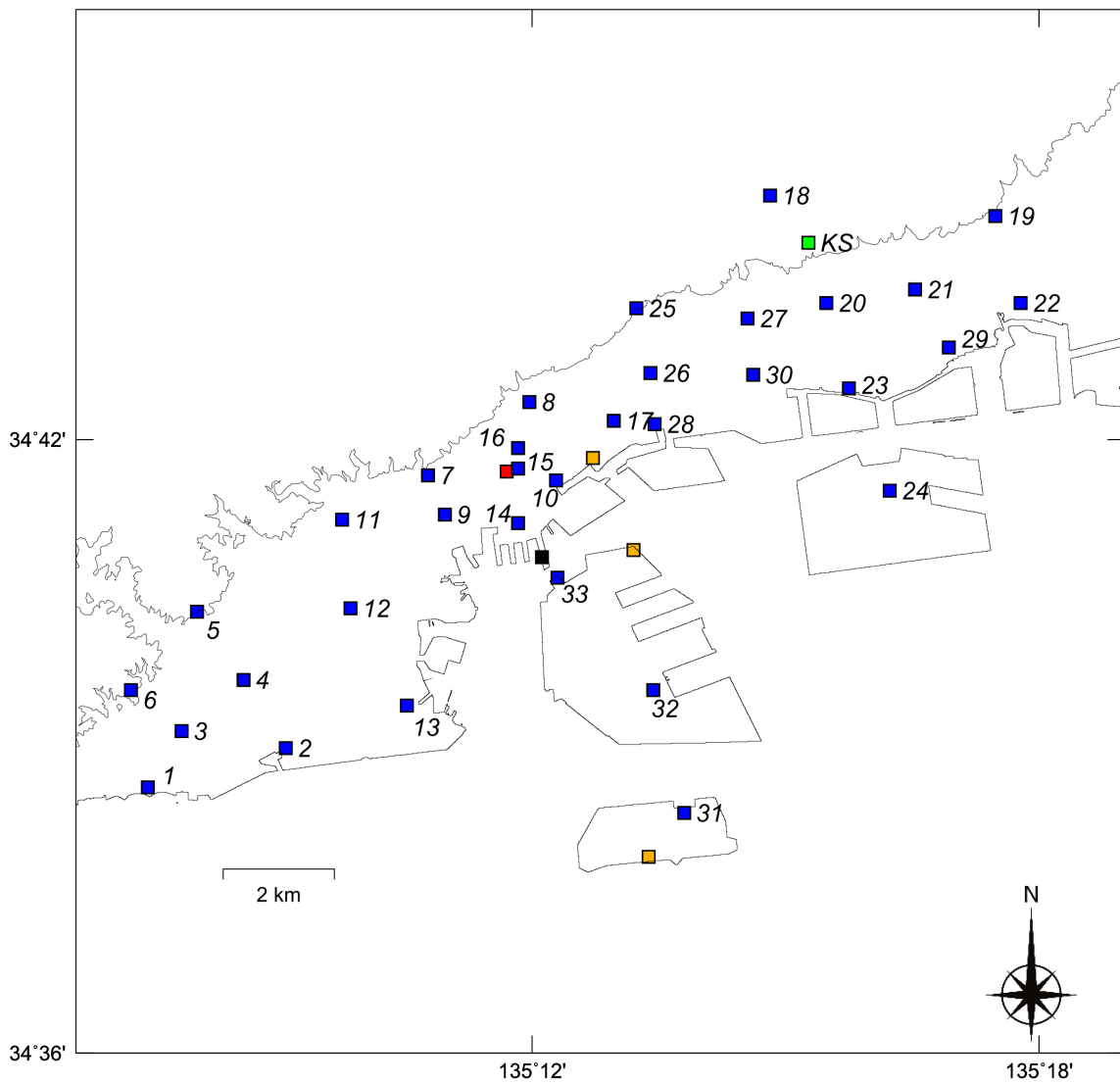


Fig. 2-6 The distribution of the original measurement sites (blue). Red, orange, green and black squares are as described above. Contour lines are shown only at elevation 0 and 100 m.

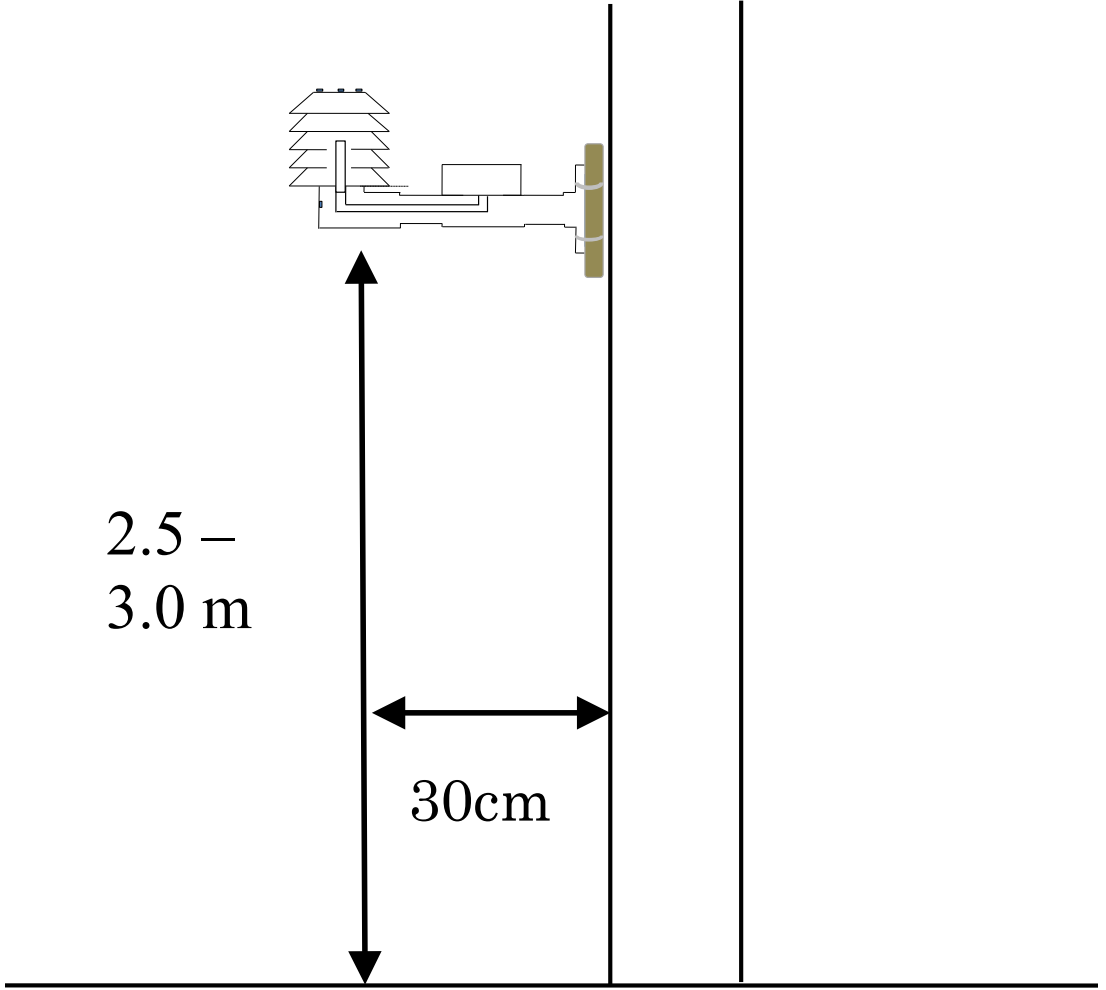


Fig. 2-7 Photographs and schematic diagram of the temperature measurement site.

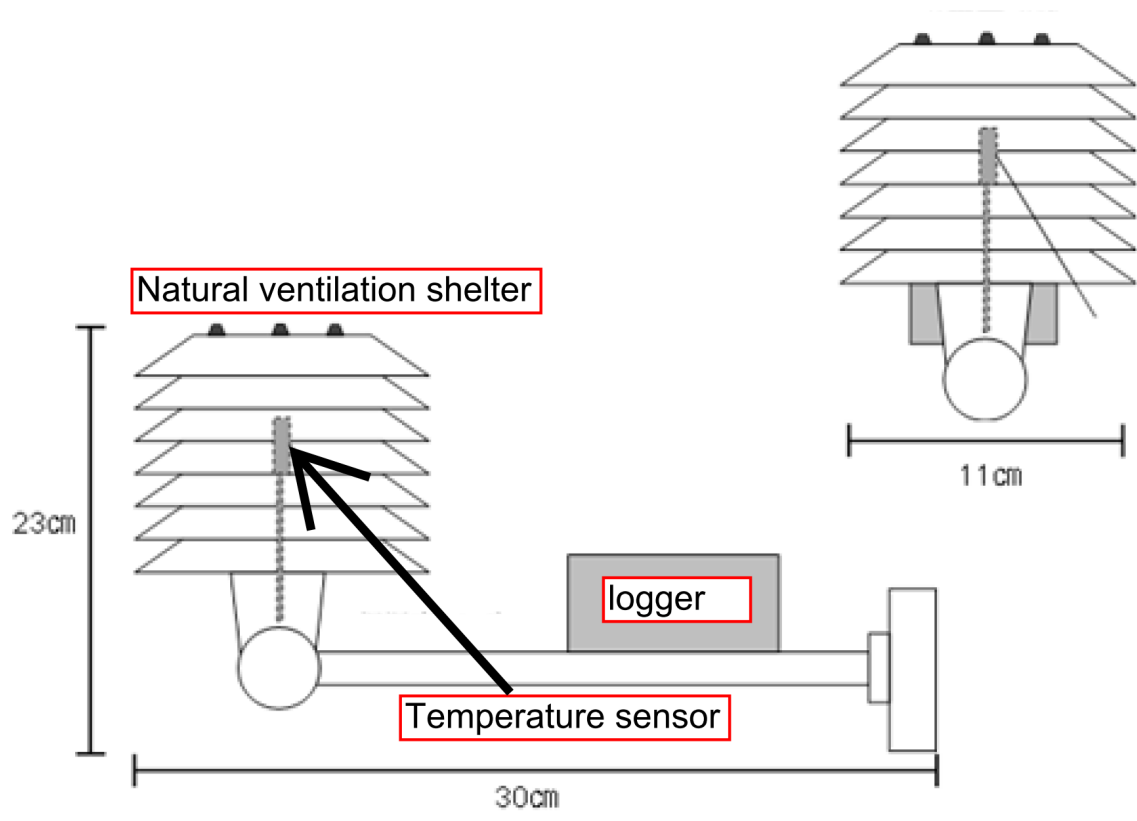


Fig. 2-8 Details of temperature measuring instruments.

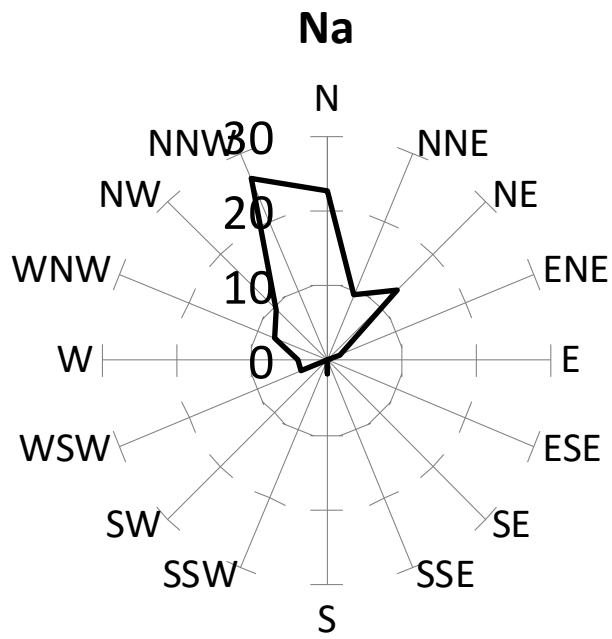
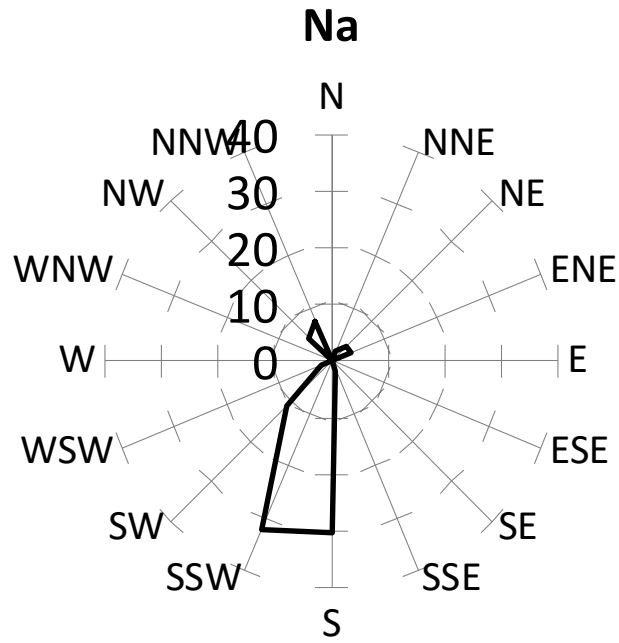


Fig. 3-1 Windrose at Na. (a) 15:00 JST (b) 03:00 JST. Averaged over 53days. Total of all wind directions is 100%.

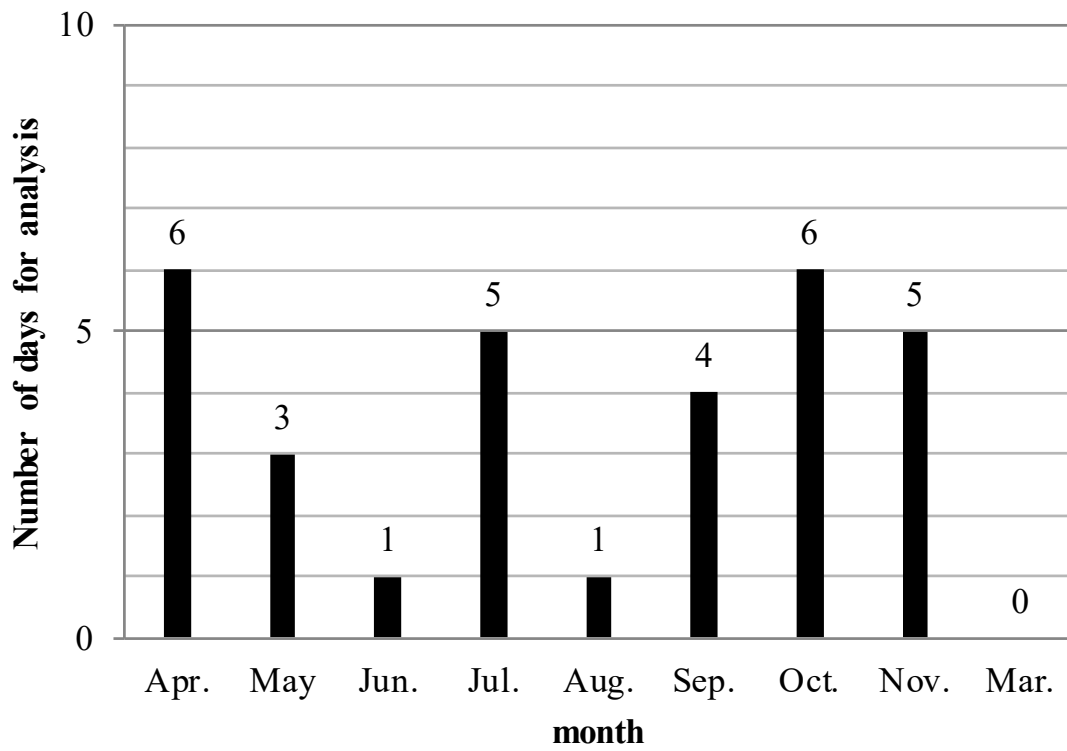


Fig. 3-2 Monthly number of days for analysis on selected 31 days.

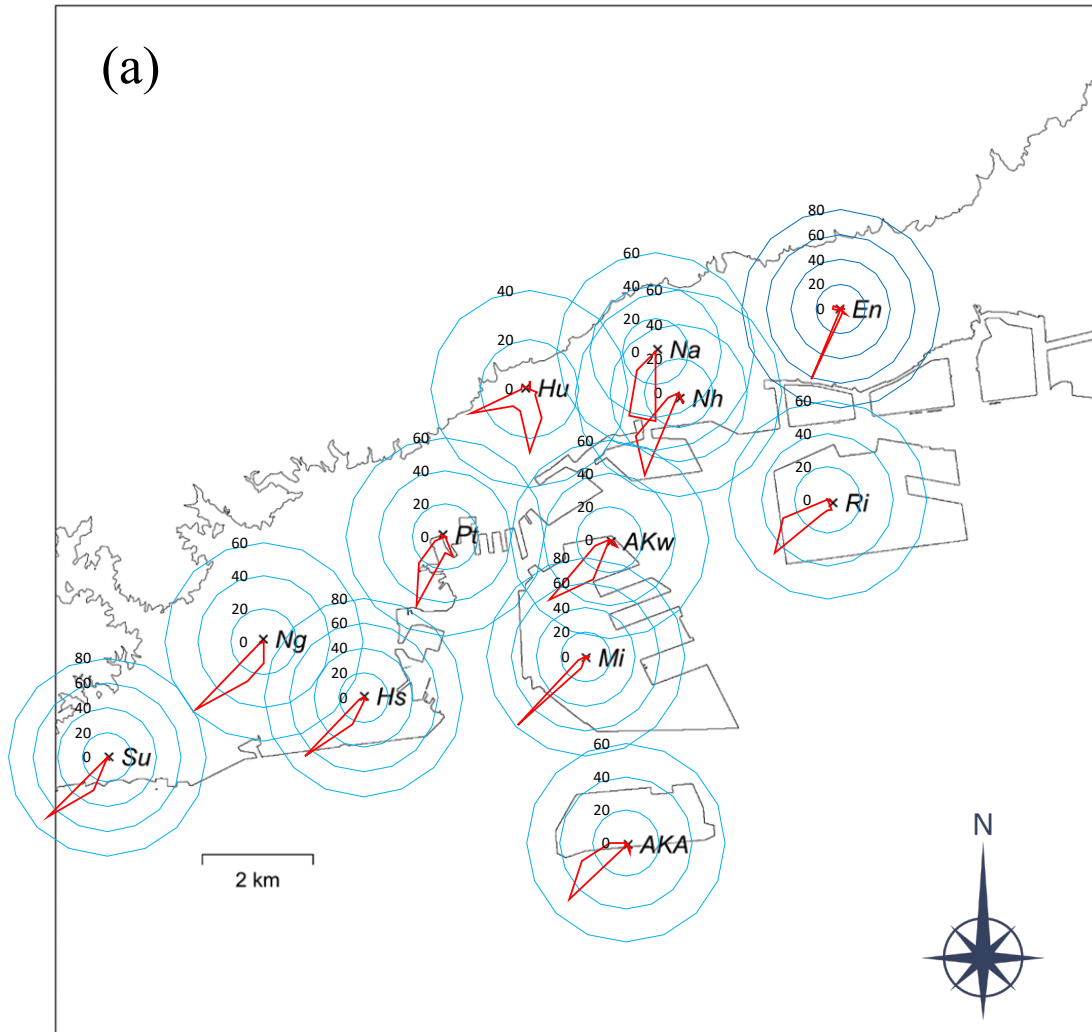


Fig. 3-3 Windrose on selected sunny calm 31 days. (a) 15:00 JST (b) 03:00 JST
 Contour lines are shown only at elevation 0 and 100 m. Total of all wind directions is 100%.

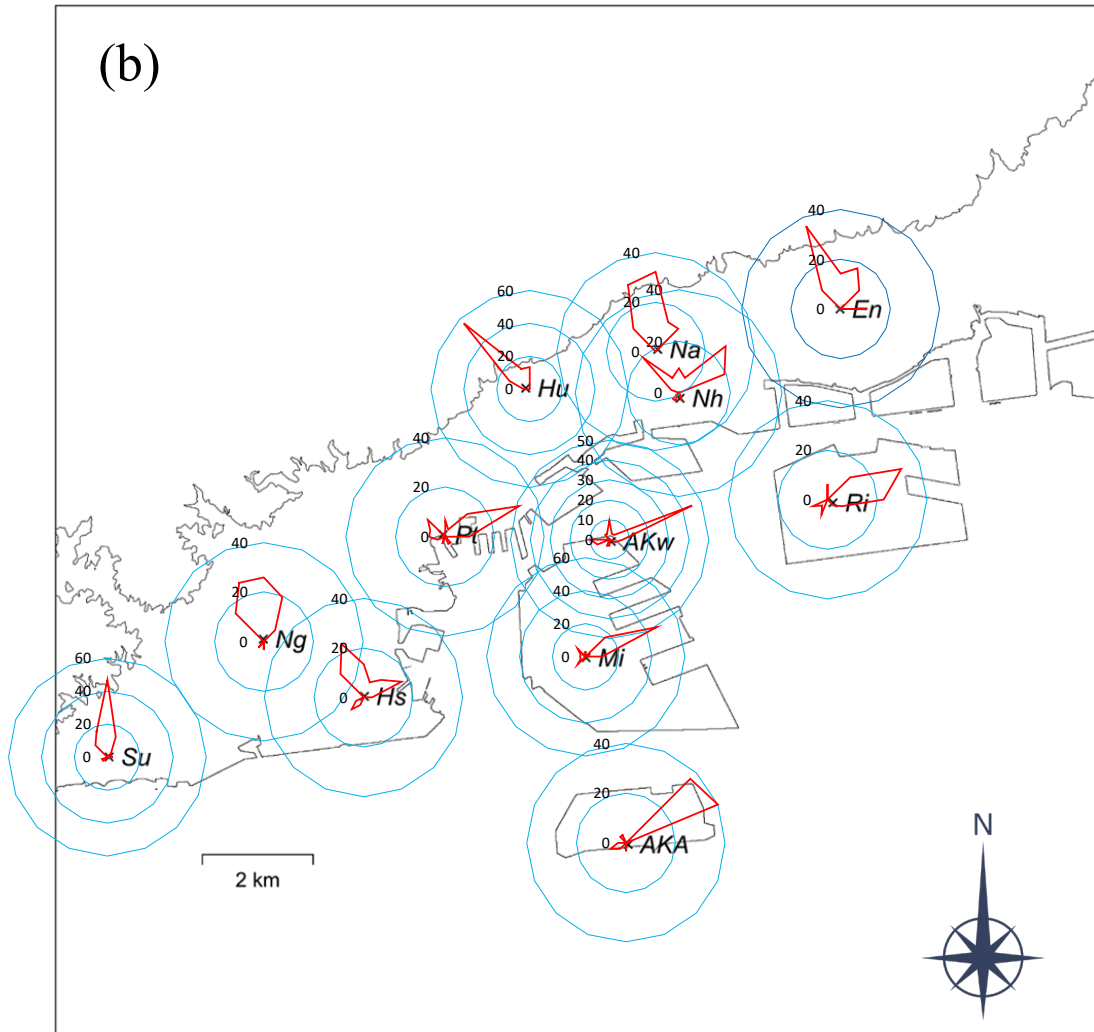


Fig. 3-3 (Continued)

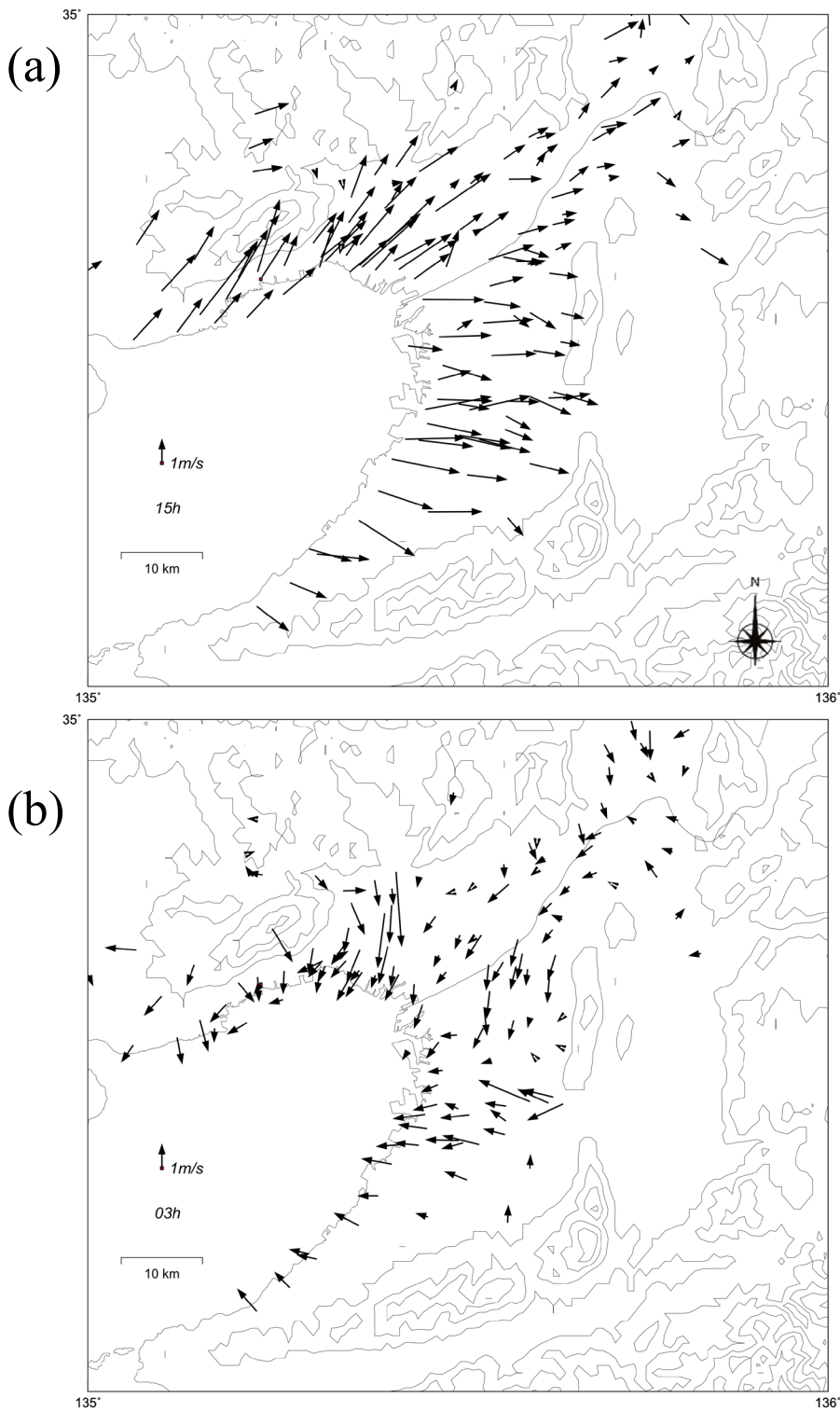


Fig. 3-4 Vector mean wind distributions on selected sunny calm 31 days. (a) 15:00 JST

(b) 03:00 JST Contour lines are shown only at elevation 0, 100, 300 and 500 m.



Fig. 3-5 Hourly vector mean wind distribution on selected 31 days. Contour lines are shown only at elevation 0 and 100 m.



Fig. 3-5 (Continued)

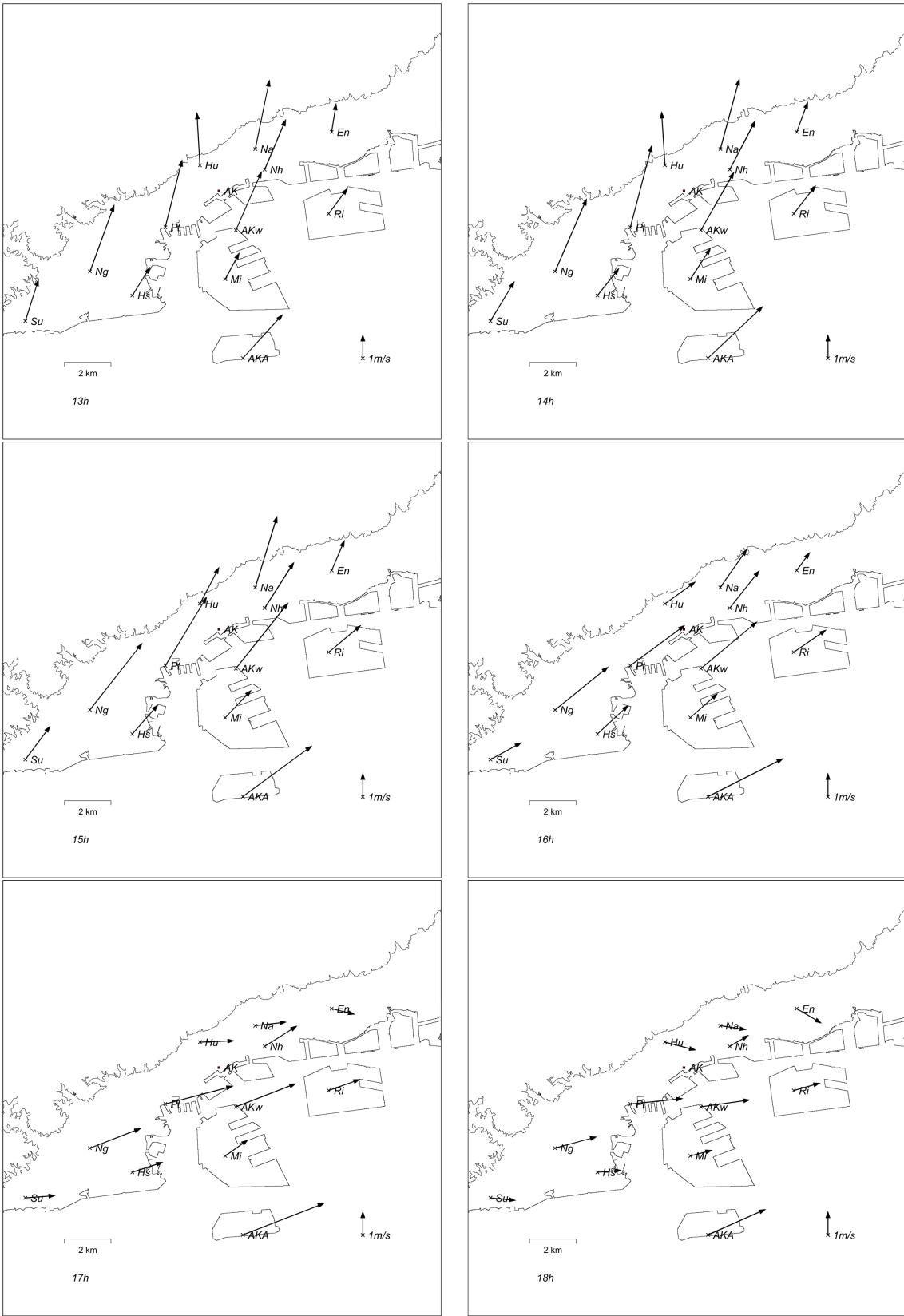


Fig. 3-5 (Continued)



Fig. 3-5 (Continued)

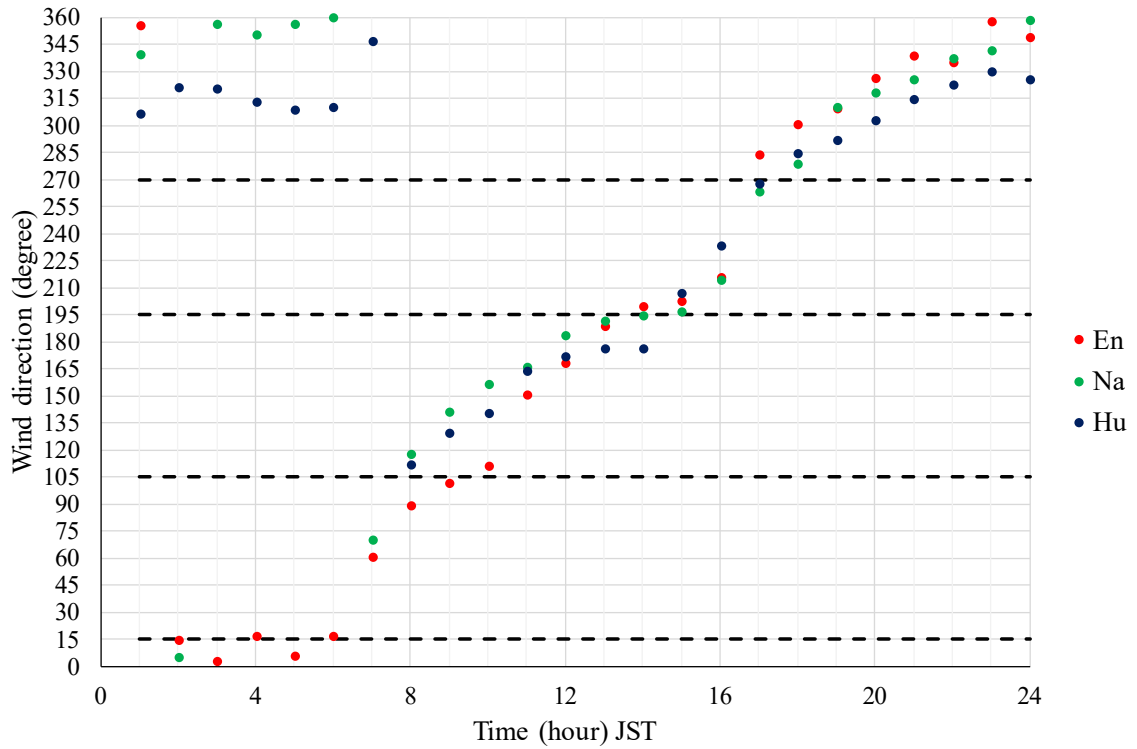
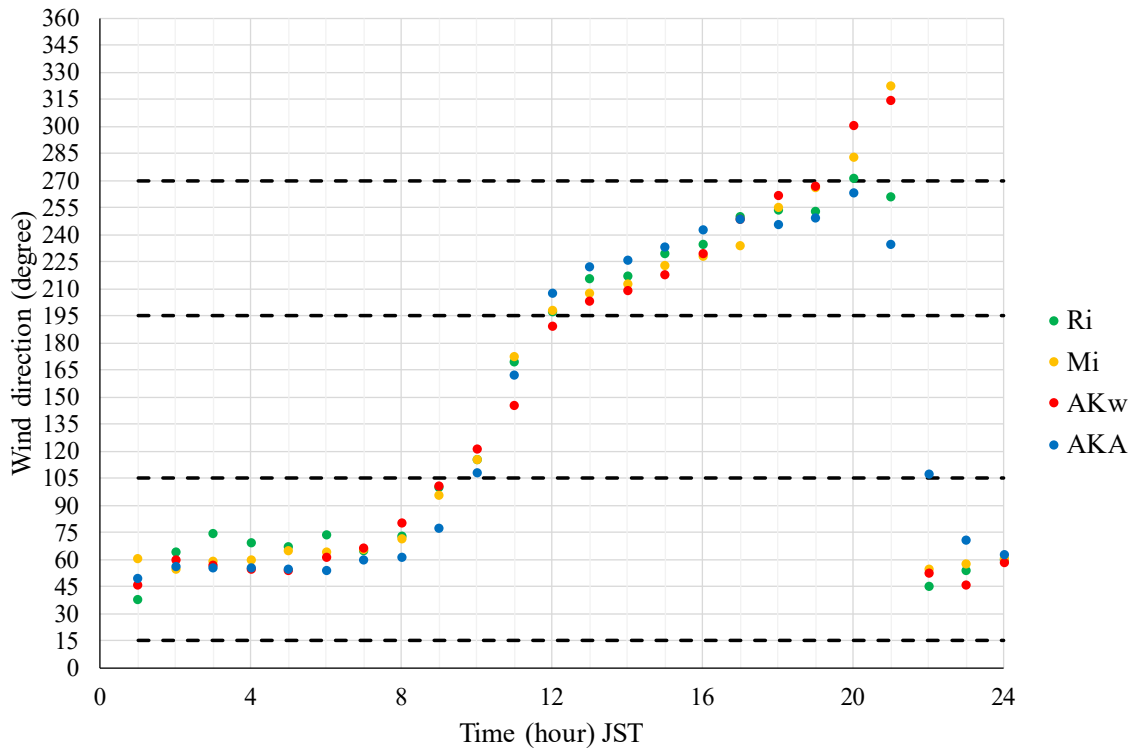


Fig. 3-6 Diurnal change in vector mean wind direction on selected sunny calm 31 days. (a) At artificial island (Ri, Mi, AKw and AKA), (b) at En, Na and Hu. Dashed lines in the figure indicate criterion values for wind system classification (15°, 105°, 195°, 270°)

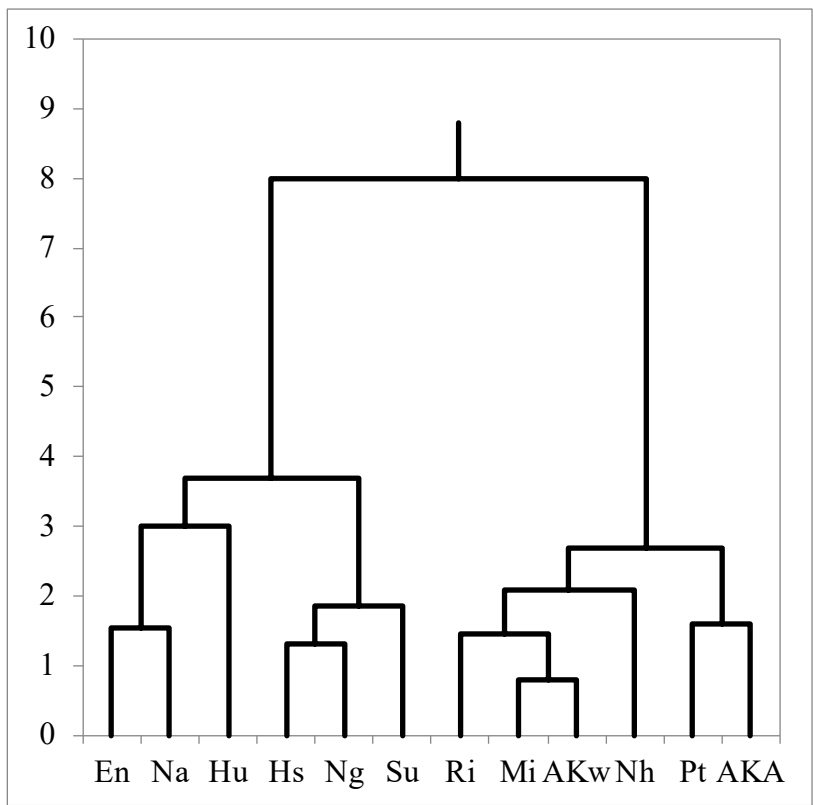


Fig. 3-7 Dendrogram of vector mean wind direction of each station.

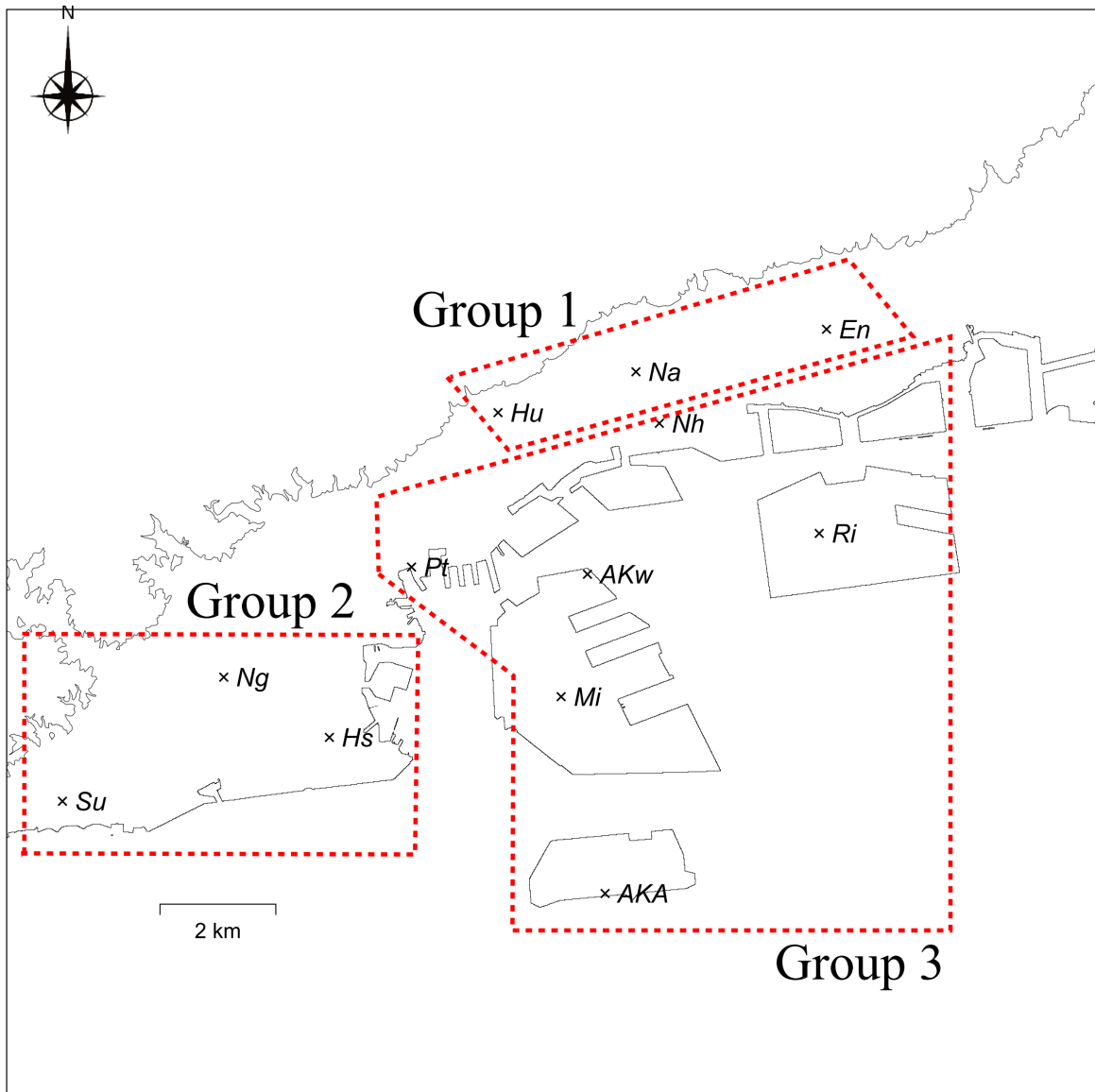


Fig. 3-8 Classification of target area by cluster analysis. Contour lines are shown only at elevation 0 and 100 m.

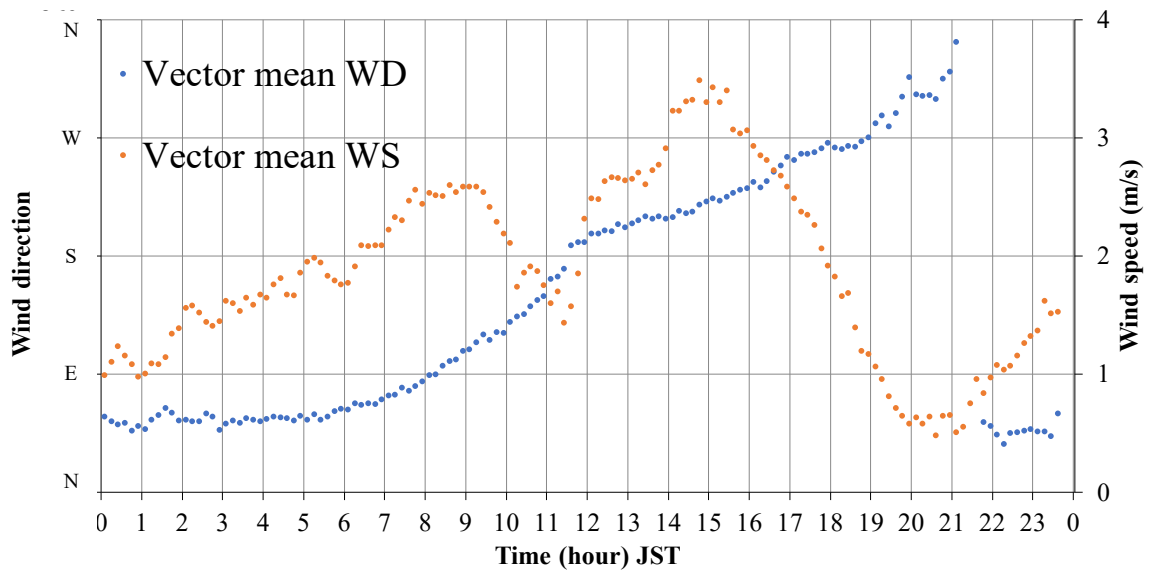


Fig. 3-9 Diurnal changes in vector mean wind direction (WD: blue) and speed (WS: orange) averaged over the target 31 days in AKw.

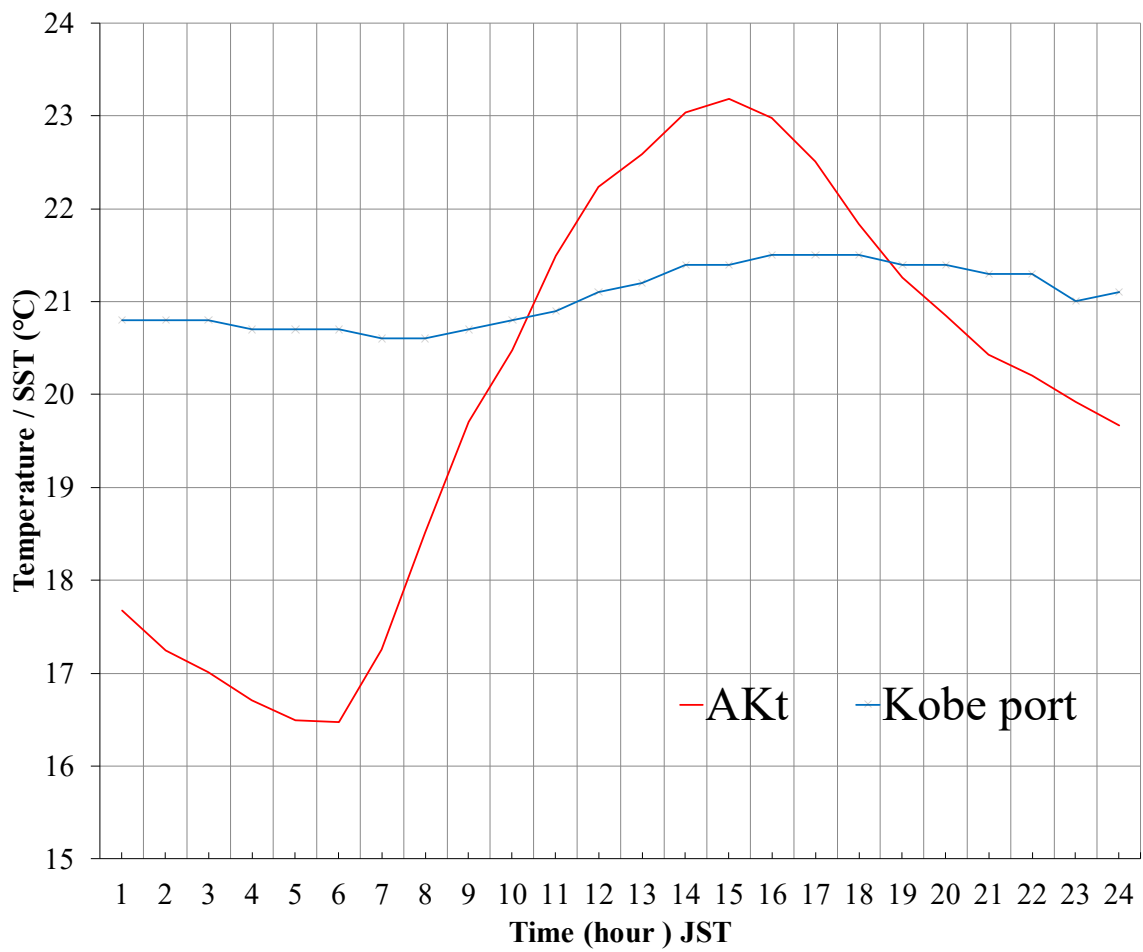


Fig. 3-10 Diurnal changes in temperature and sea surface temperature of AKt (red) and Kobe Port (SST, blue) averaged over the analysis days.

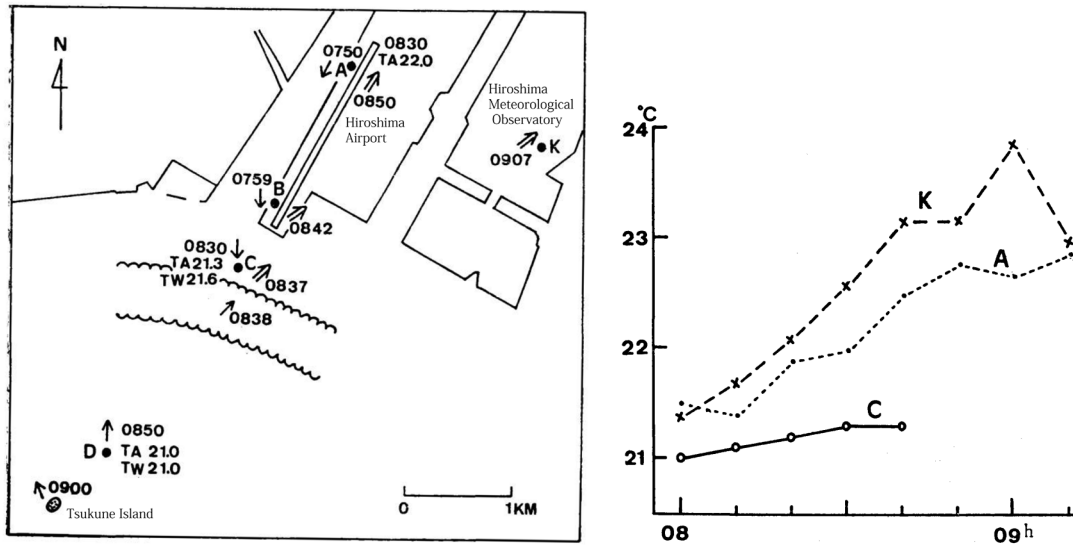
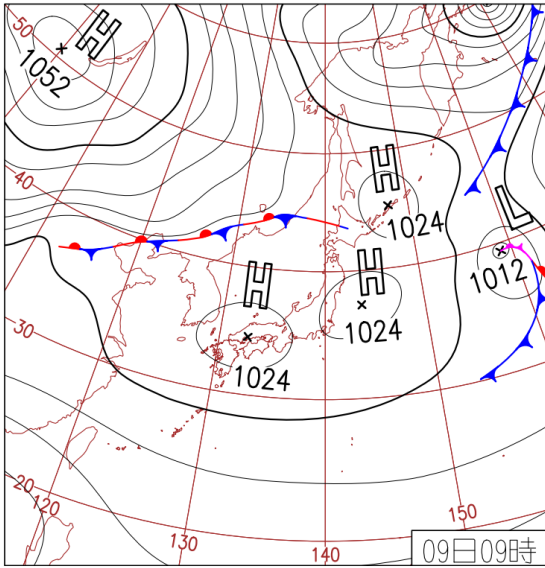


Fig. 3-11 (a) Weather and sea conditions before and after the start of sea breeze on June 12, 1984. The black arrows indicate wind direction, and the white arrows indicate wind direction at the start of sea breeze. Numbers (e.g., 0837) in the figure are observation times. (b) Horizontal temperature gradients over land and sea before and after the onset of sea breeze, June 12, 1984, K: Hiroshima meteorological observatory temperature, A: Hiroshima airport temperature, C: temperature over the sea. (Nakata, 1985)

10/9



10/10

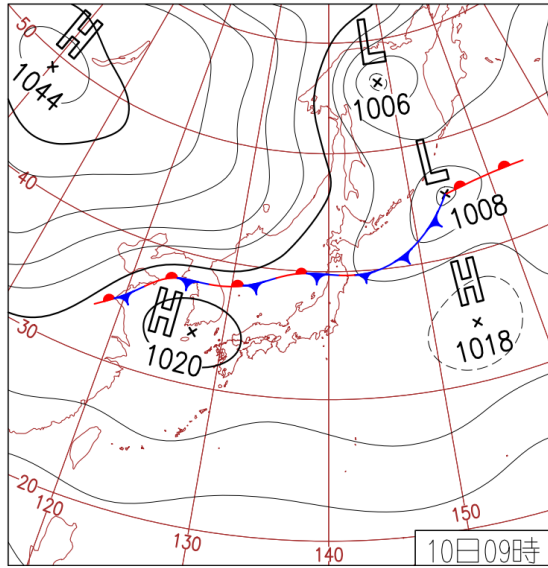


Fig. 3-12 Surface weather chart at 09:00 JST on October 9 and 10, 2017.

From JMA HP <https://www.data.jma.go.jp/fcd/yoho/hibiten/index.html>

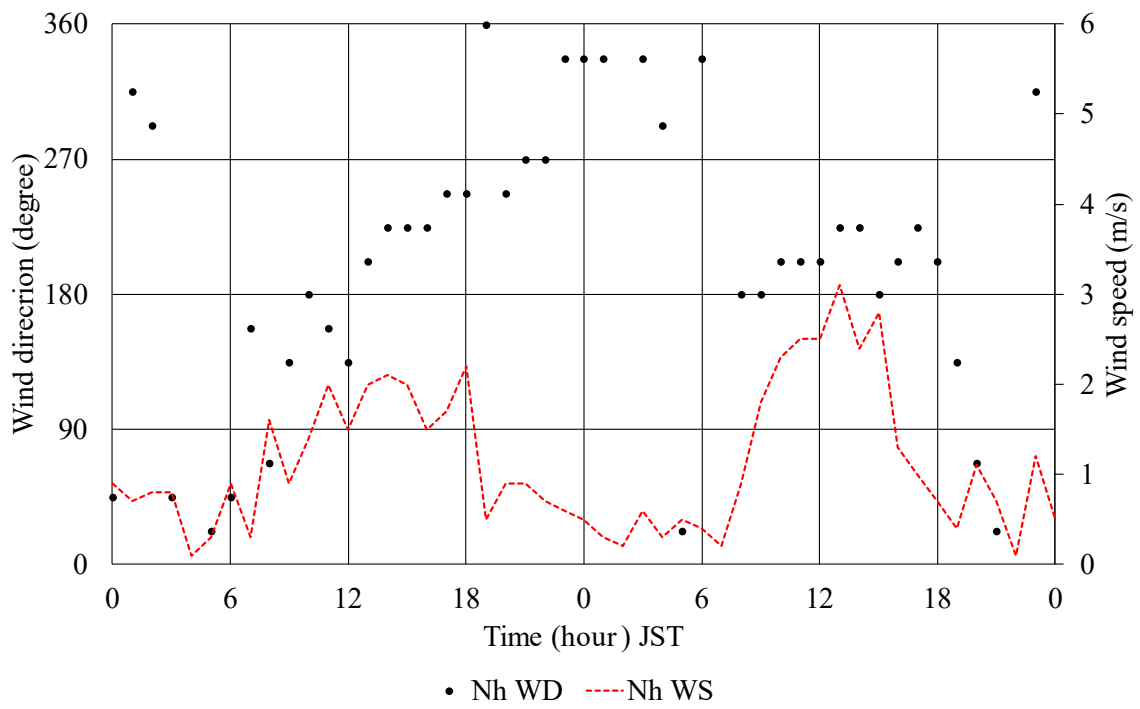


Fig. 3-13 Diurnal change in wind at Nh on October 9-10, 2017.



Fig. 3-14 Surface wind distribution on October 9 and 10, 2017. (a) 03:00, (b) 08:00 and (c) 20:00 JST. Contour lines are shown only at elevation 0, 100, 300 and 500 m.

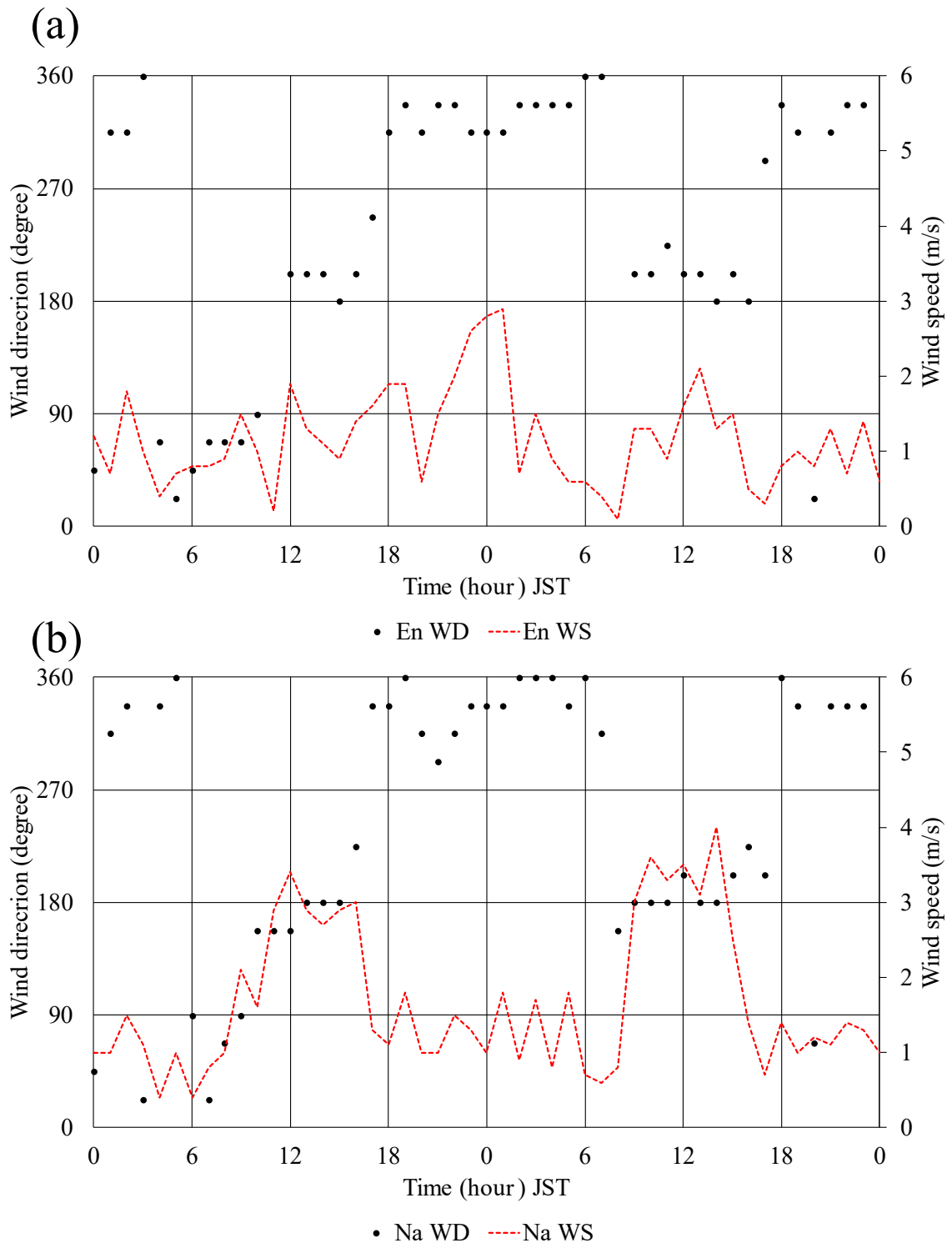


Fig. 3-15 Diurnal change in wind in the plains on October 9-10, 2017. (a) En, (b) Na.

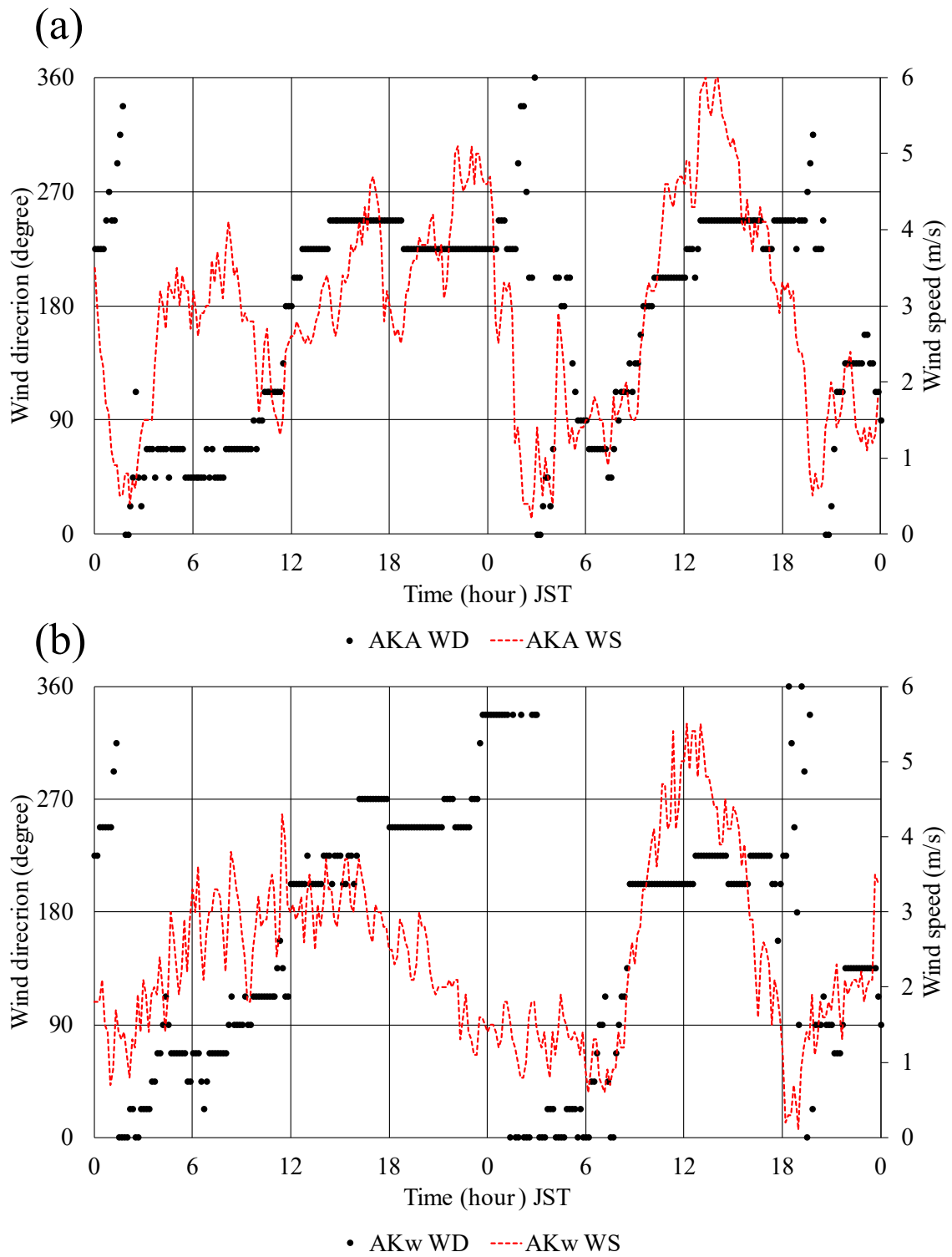


Fig. 3-16 Diurnal change in wind on artificial islands on October 9-10, 2017. (a) AKA, (b) AKw, (c) Ri.

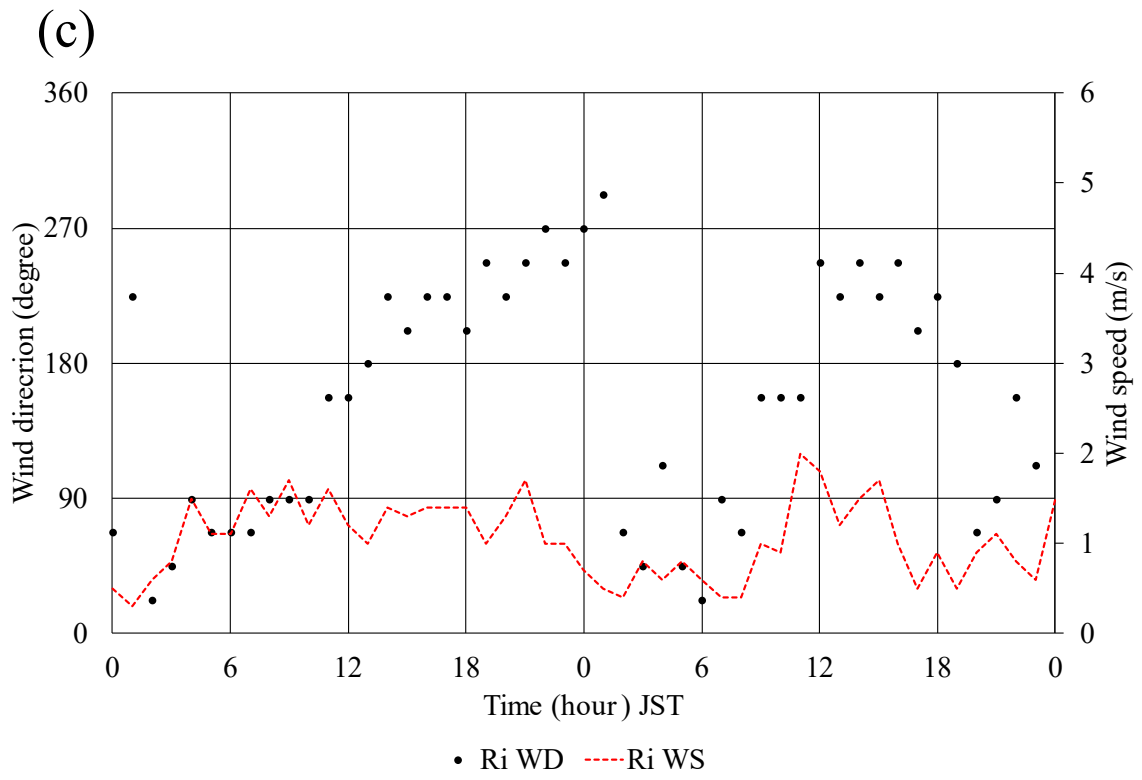


Fig. 3-16 (Continued)

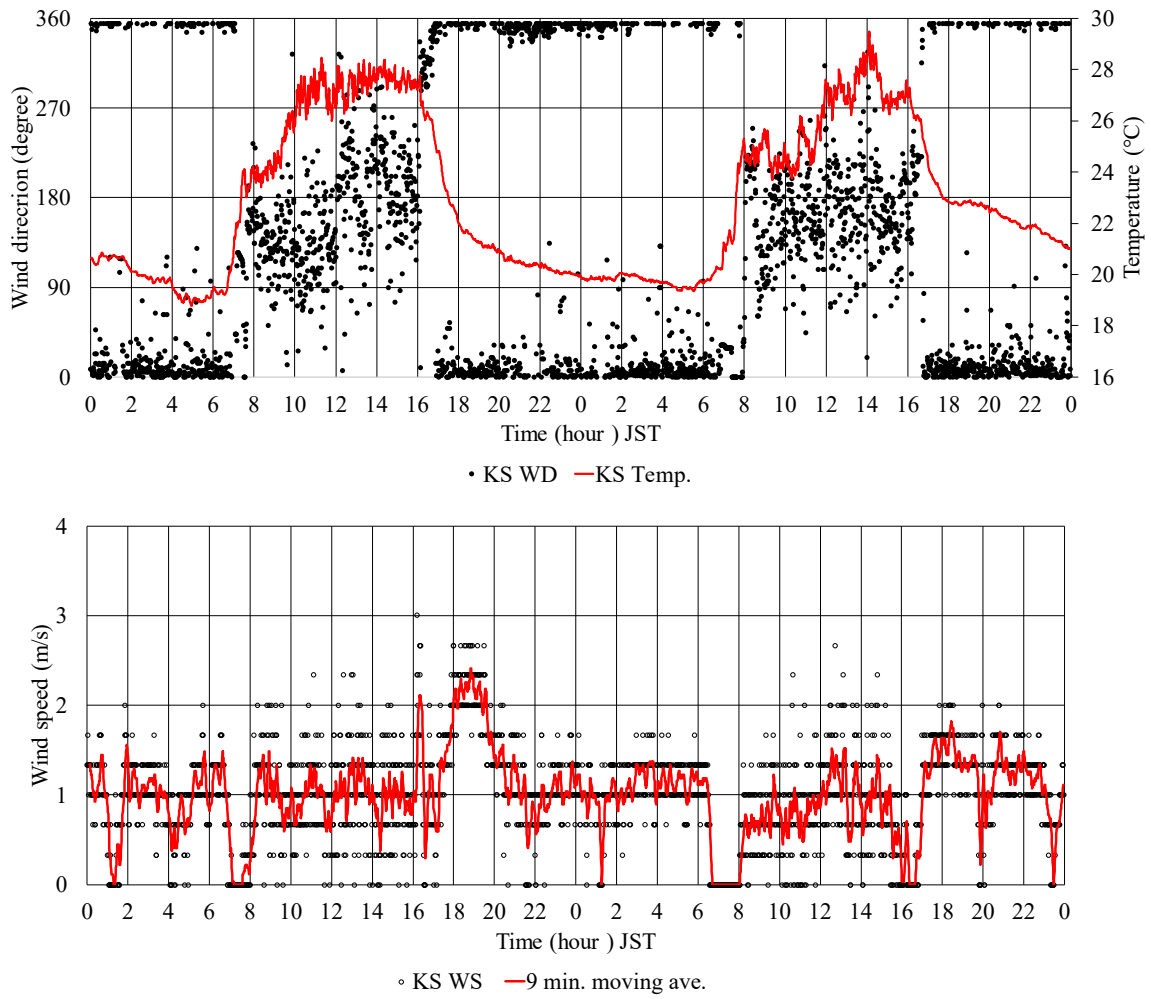


Fig. 3-17 Diurnal change in wind and temperature in the lower-slope of the Rokko Mountains (KS) on October 9-10, 2017.

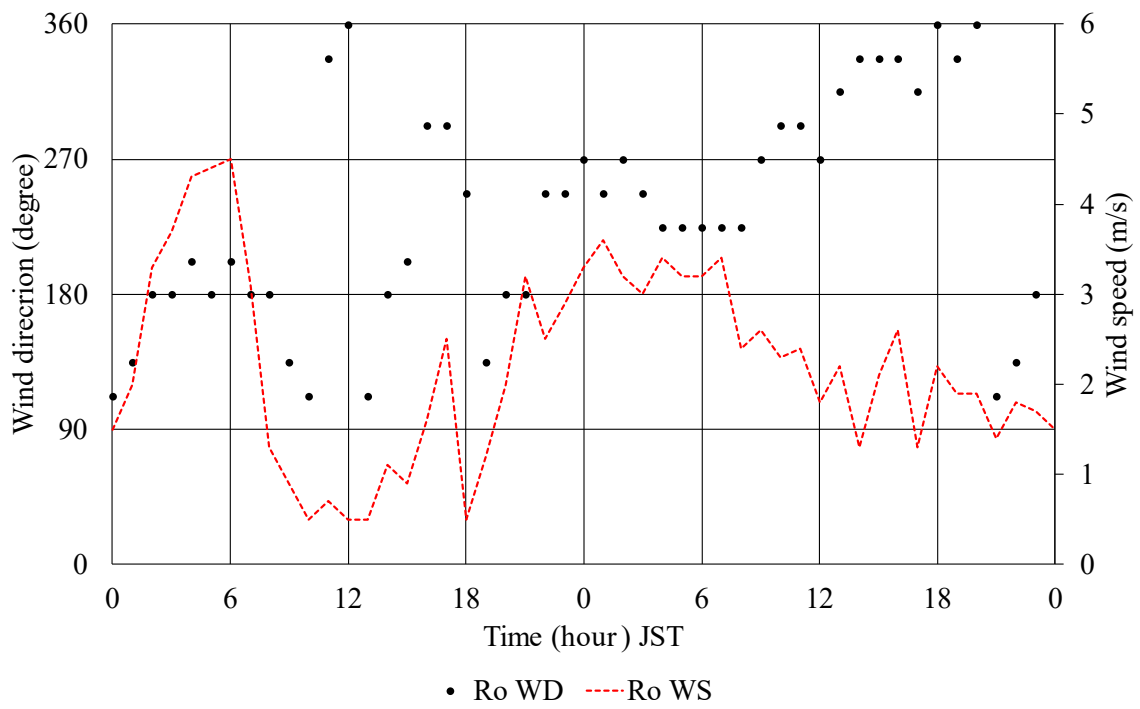


Fig. 3-18 Diurnal change in wind at the top of Mt. Rokko (Ro) on October 9-10, 2017.

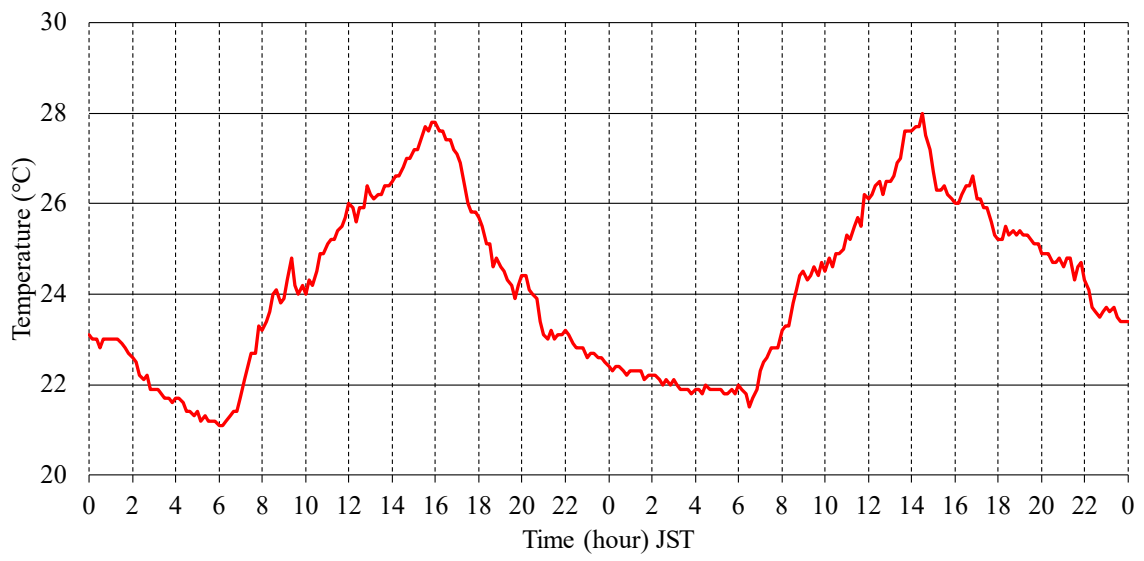


Fig. 3-19 Diurnal change in temperature at AKt on October 9-10, 2017.

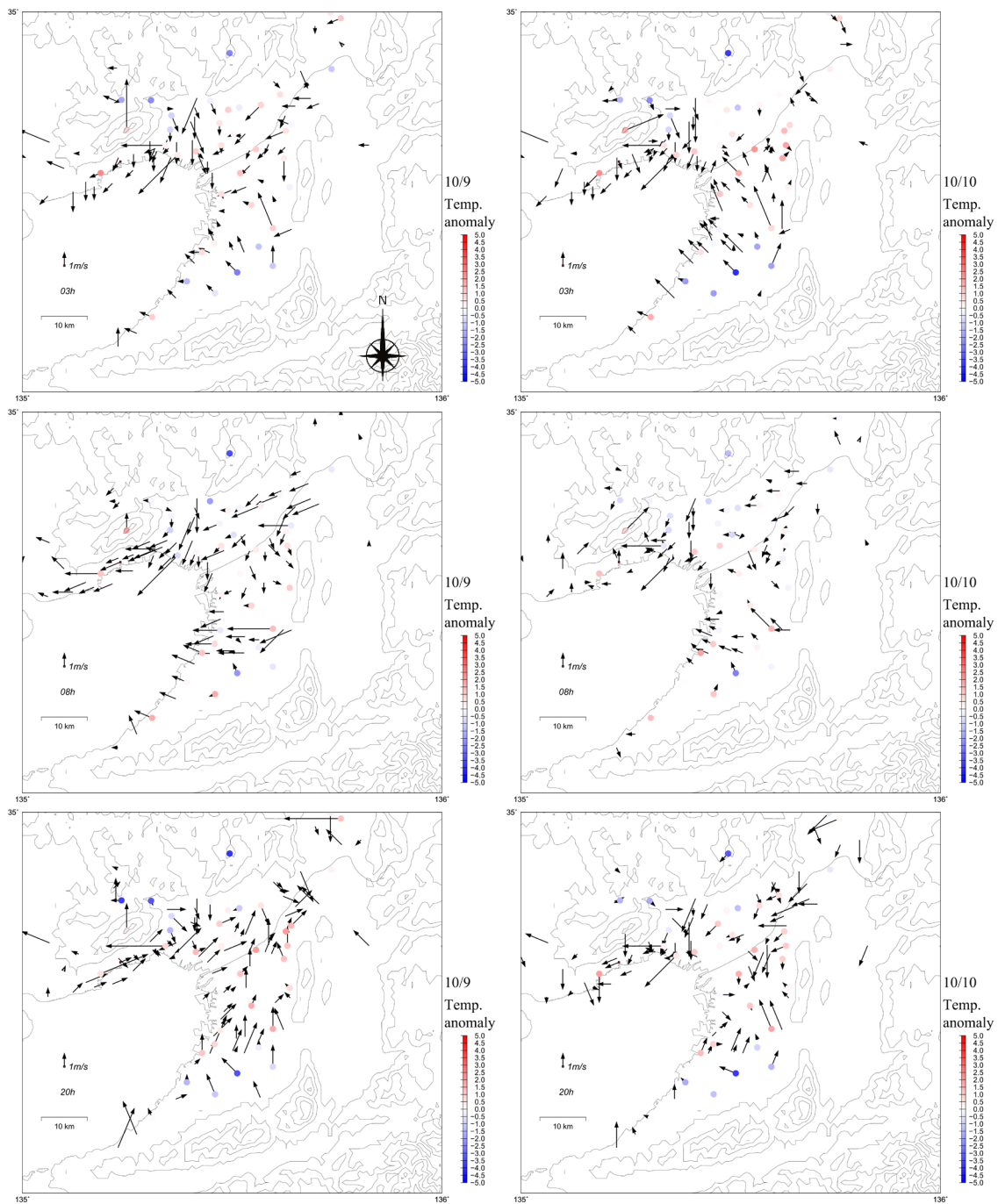


Fig. 3-20 Surface wind and temperature anomaly distributions at 03:00, 08:00 and 20:00 JST, October 9 and 10, 2017. Contour lines are shown only at elevation 0, 100, 300 and 500 m.

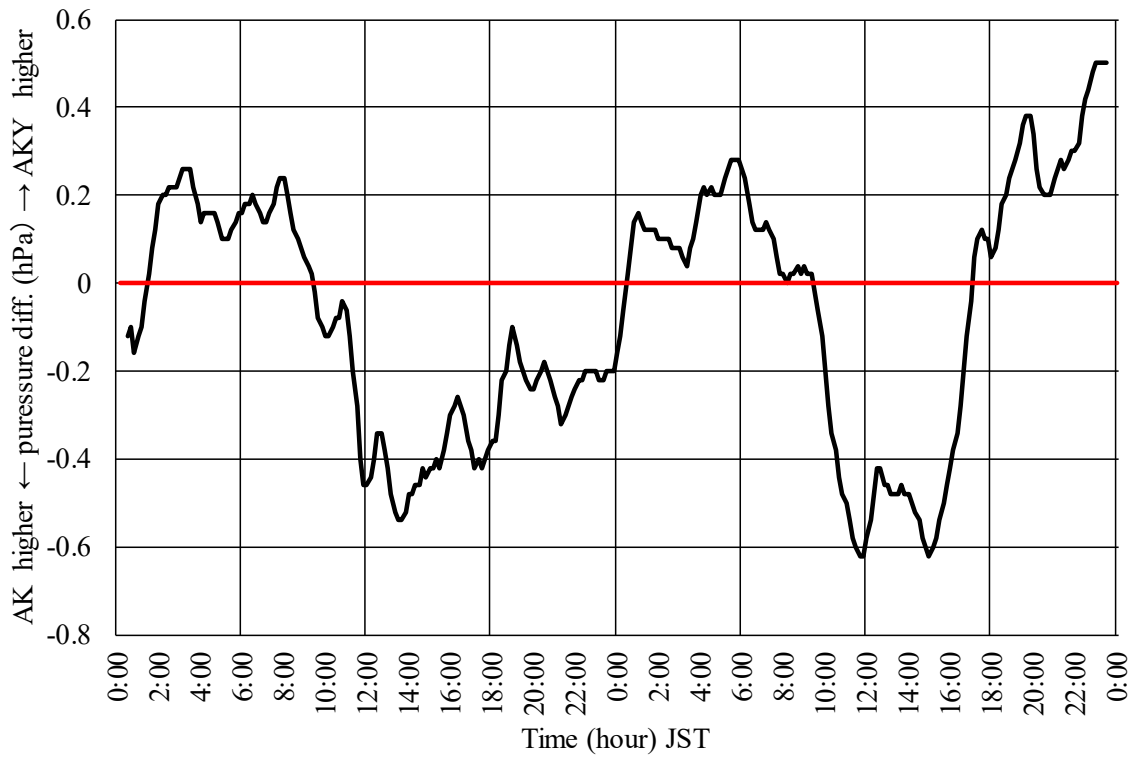


Fig. 3-21 Diurnal change in the pressure difference between AKY and AK on October 9-10, 2017.

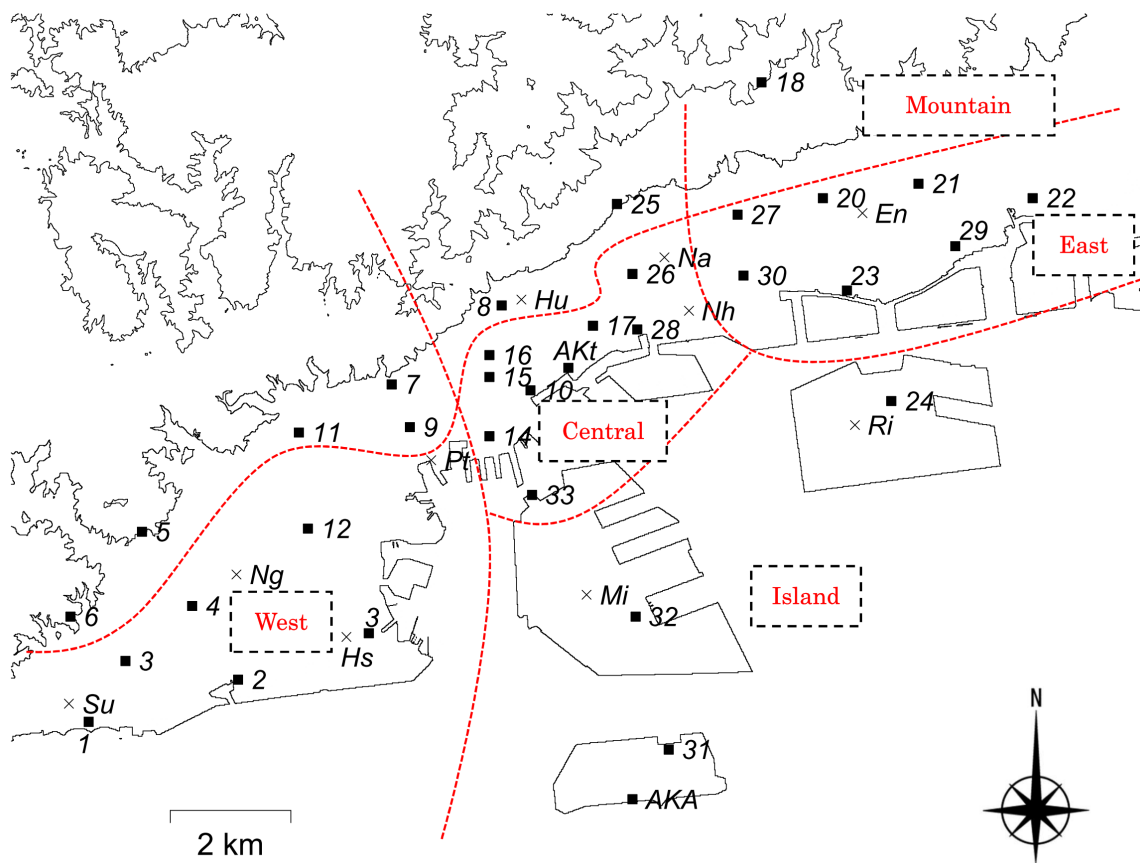


Fig. 3-22 Topography and distribution of air temperature observation points in Kobe City. Contour lines are shown only at elevation 0, 100, 300 and 500 m. The red dotted line in the figure indicates the regional classification based on diurnal changes in air temperature. West, Central, Island, East and Mountain are the names of regional divisions. Numbers indicate surface air temperature stations, and alphabets indicate AEROS and AMeDAS stations.

10/8

10/18

10/24

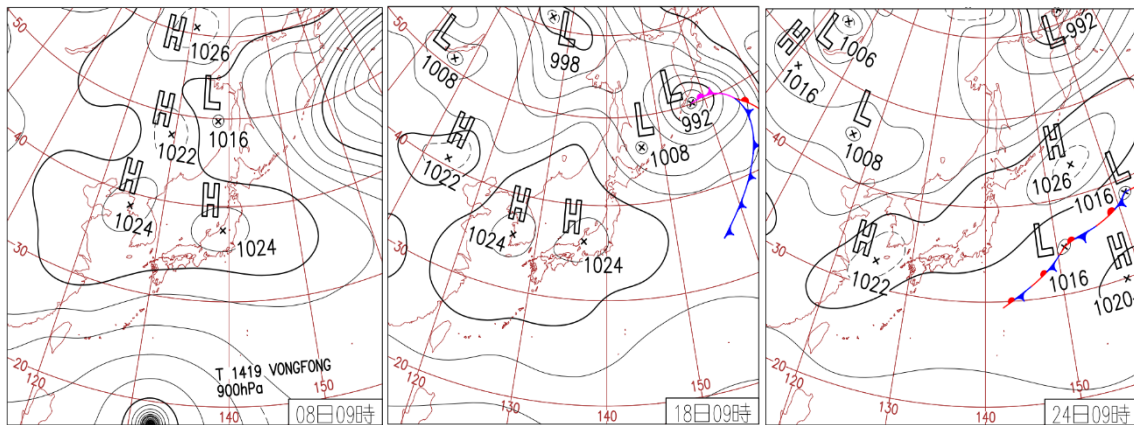


Fig. 3-23 Surface weather chart at 09:00 JST on October 8 (left), 18 (middle), 24 (right), 2014.

From JMA HP <https://www.data.jma.go.jp/fcd/yoho/hibiten/index.html>

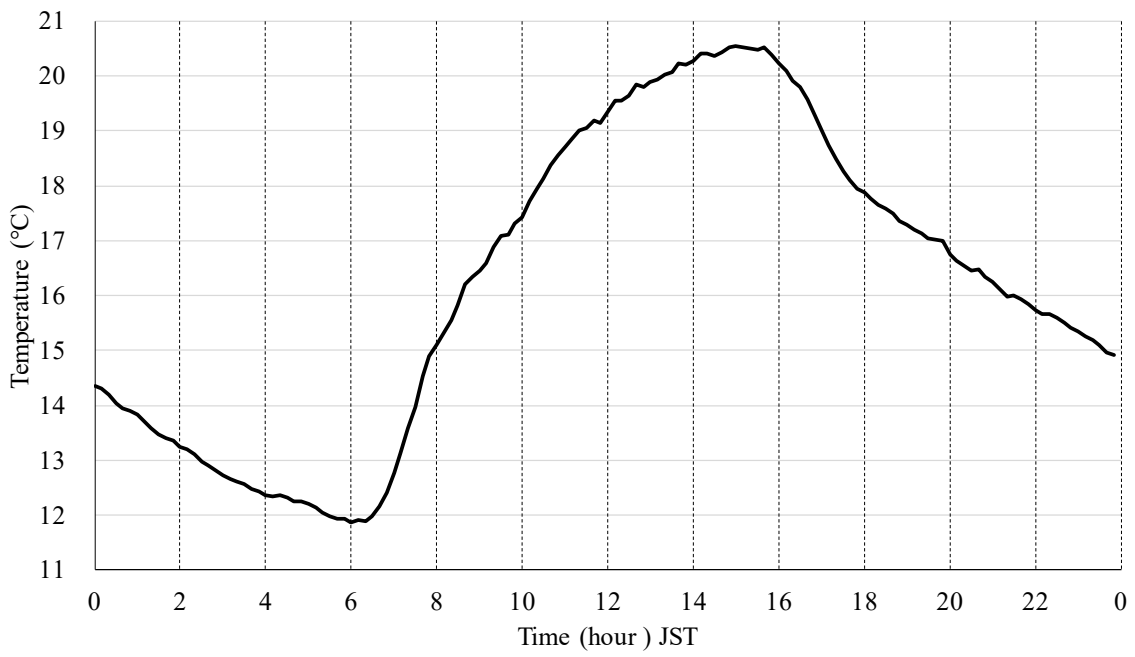


Fig. 3-24 Diurnal change of temperature averaged over all locations (October 18, 2014).

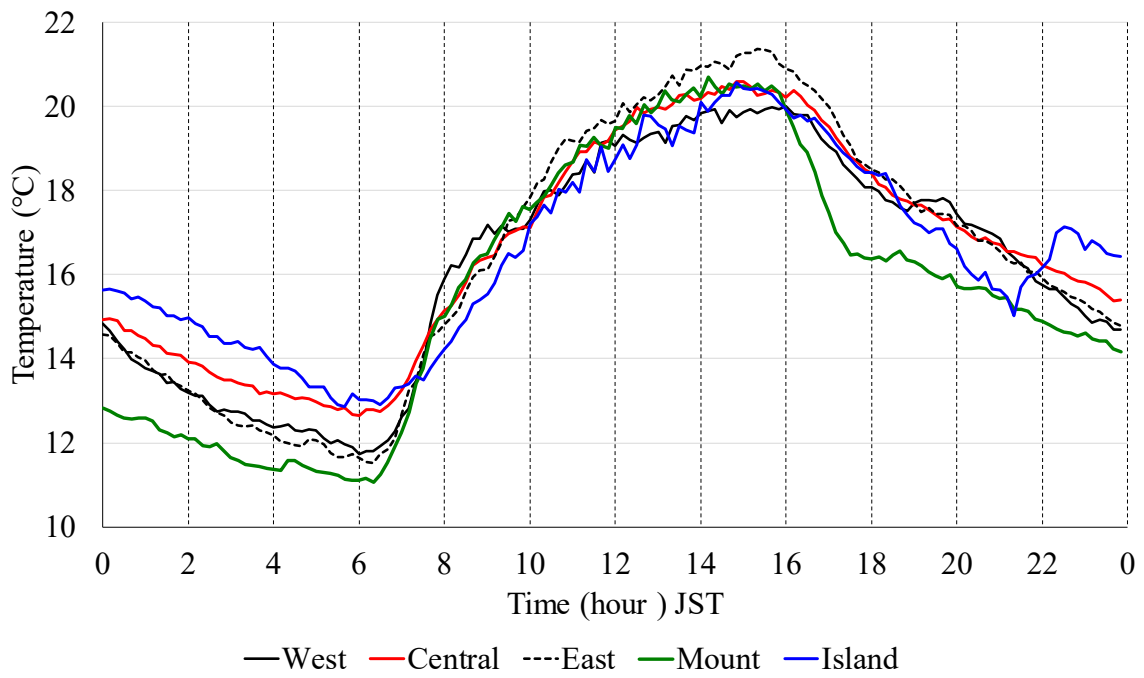


Fig. 3-25 Diurnal change in averaged temperature for five regions (October 18, 2014).

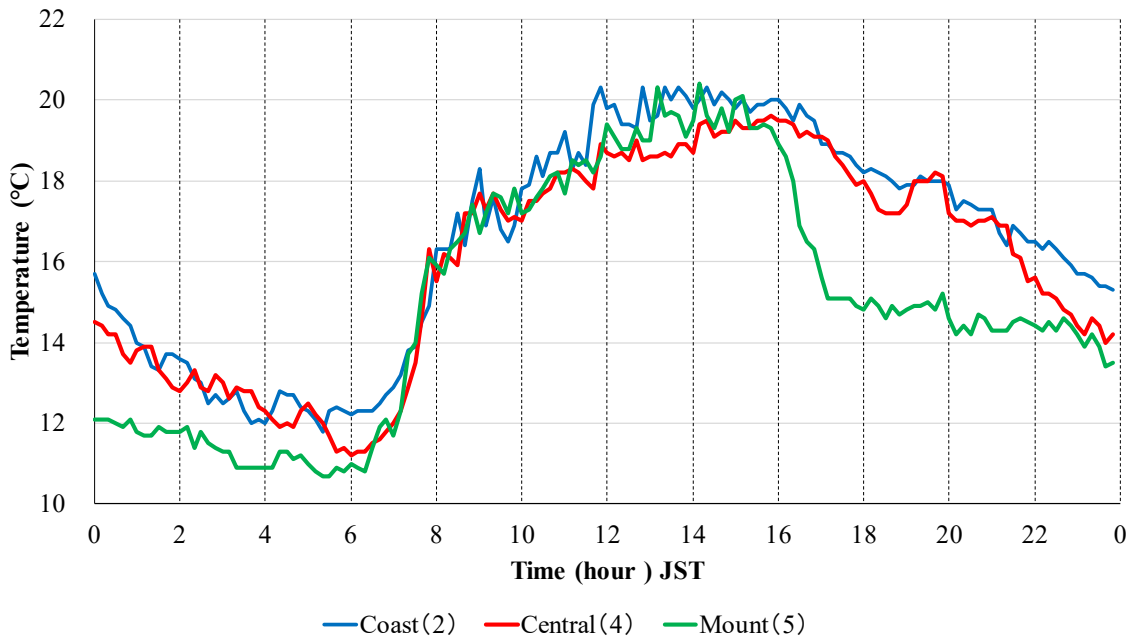


Fig. 3-26 Diurnal change in air temperature at sites 2, 4, and 5 (October 18, 2014).

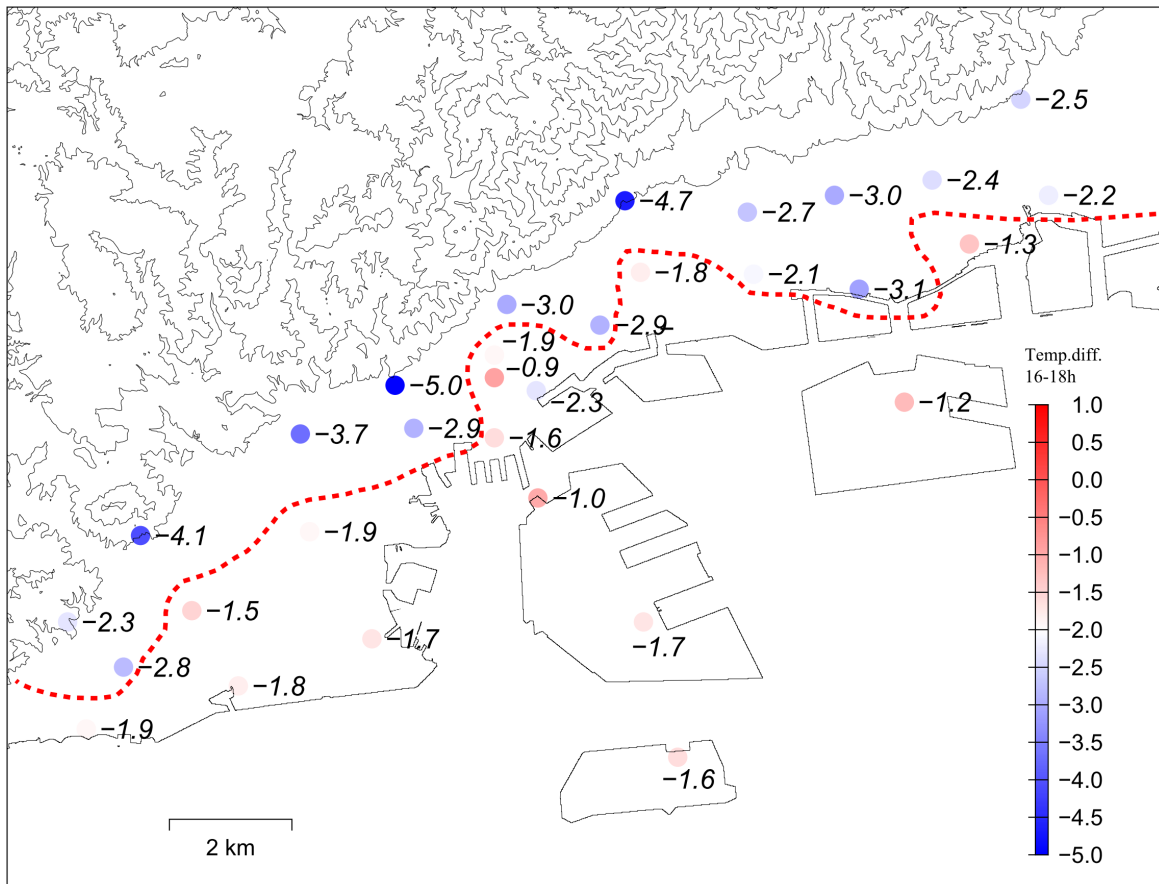


Fig. 3-27 Approximate influence range (red broken line) of cold air drainage on October 18, 2014. The values in the figure indicate the amount of temperature drop from 16:00 to 18:00 JST. Contour lines are shown only at elevation 0, 100, 300 and 500 m.



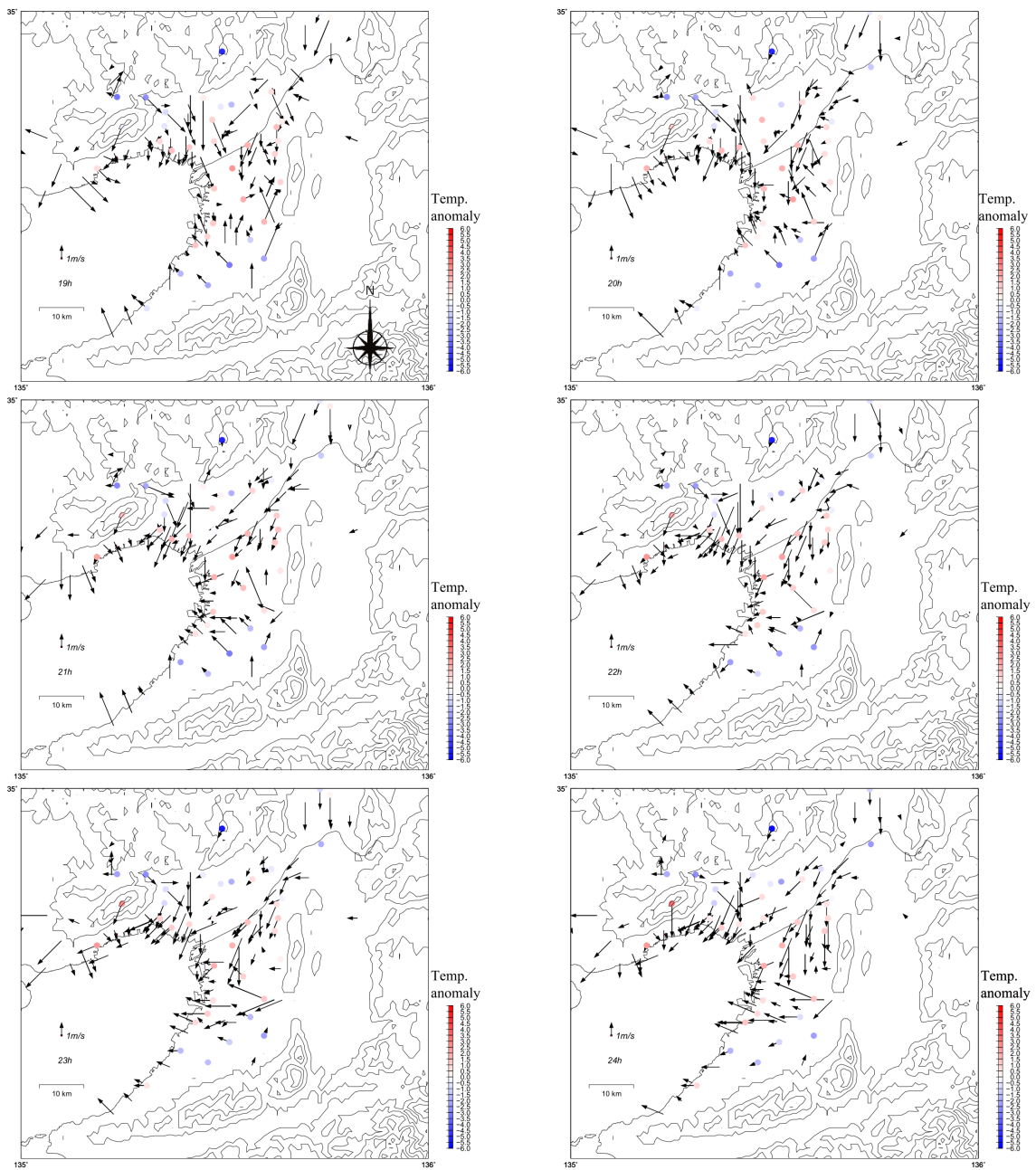


Fig. 3-28 Surface wind and temperature anomaly distribution on October 18, 2014 (19:00-24:00 JST). Contour lines are shown only at elevation 0, 100, 300 and 500 m.

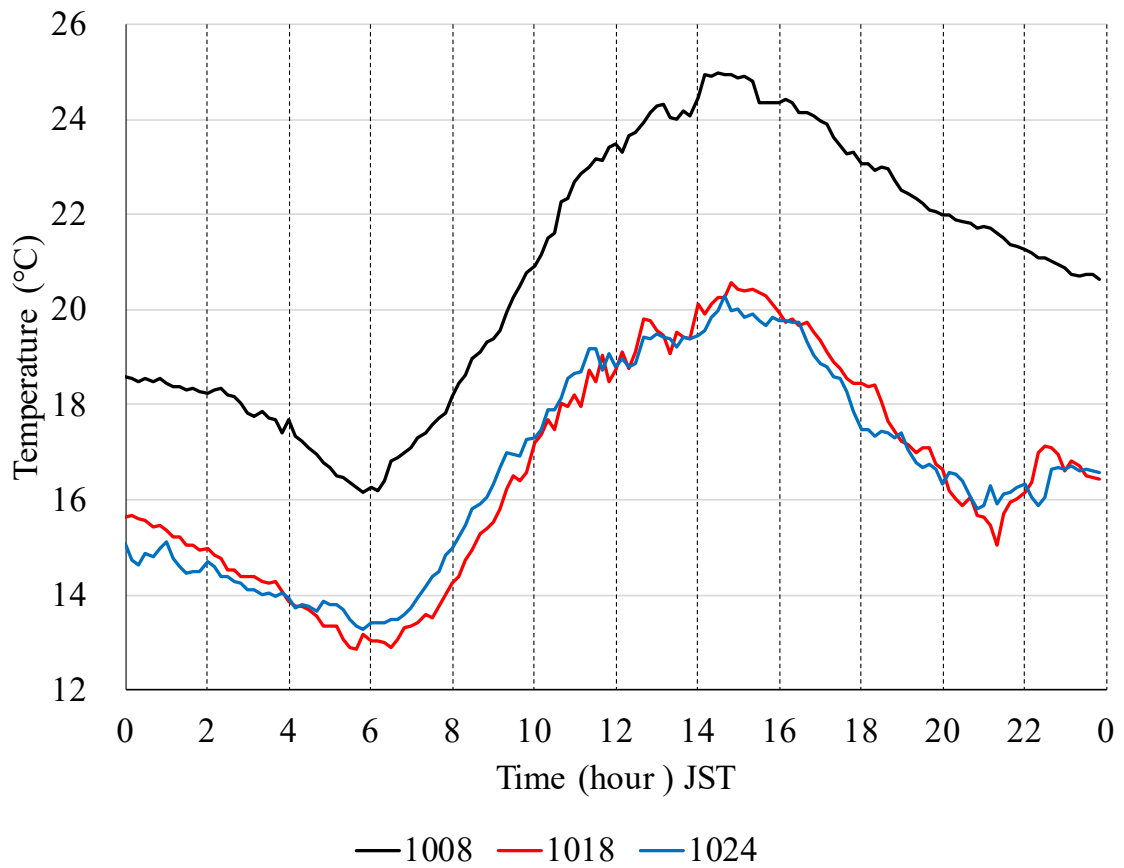


Fig. 3-29 Diurnal change in averaged temperature at the artificial island on October 8 (black), 18 (red) and 24 (blue), 2014.

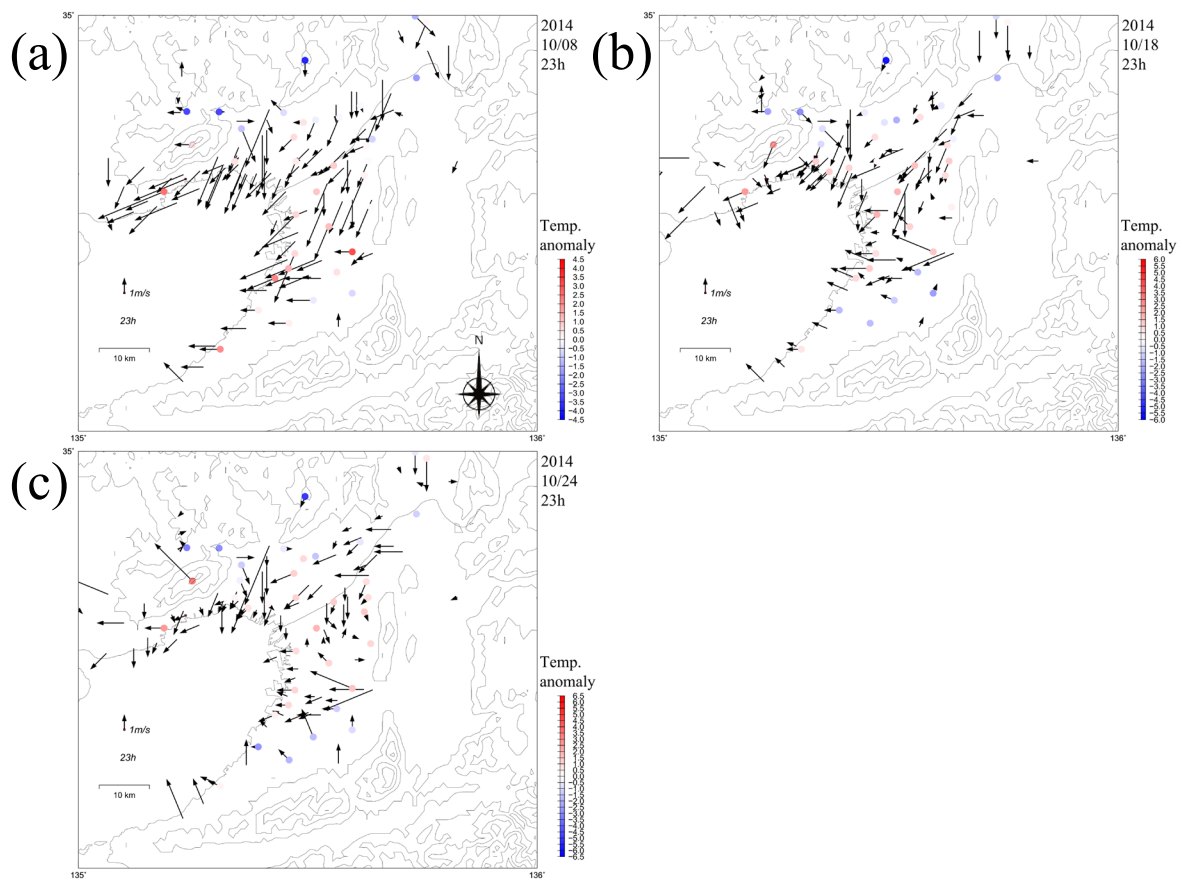


Fig. 3-30 Surface wind and temperature anomaly distribution at 23:00 JST. (a) October 8, 2014, (b) October 18, 2014 and (c) October 24, 2014. Contour lines are shown only at elevation 0, 100, 300 and 500 m.

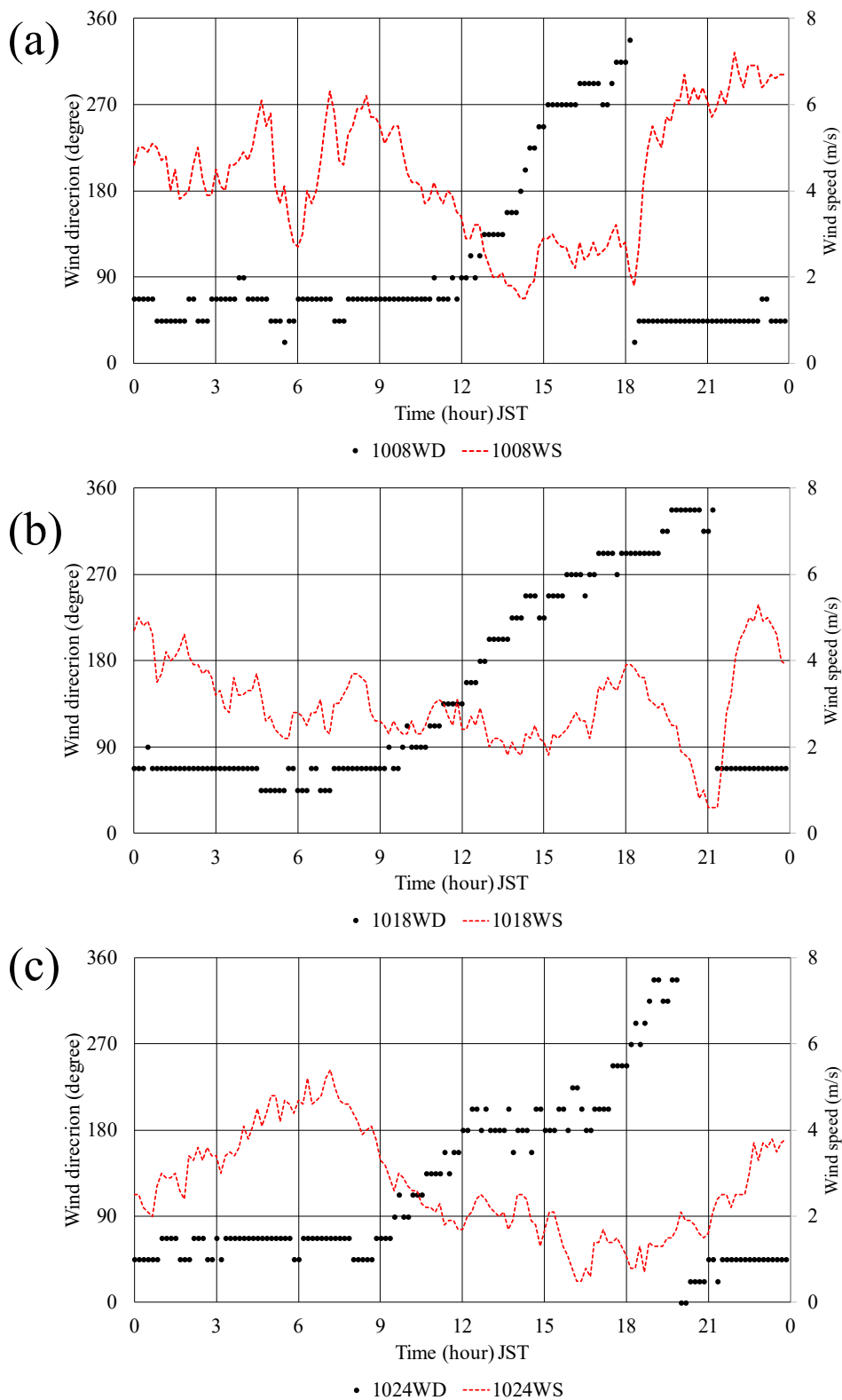


Fig. 3-31 Diurnal change in wind direction and speed at AKA. (a) October 8, 2014, (b) October 18, 2014 and (c) October 24, 2014.

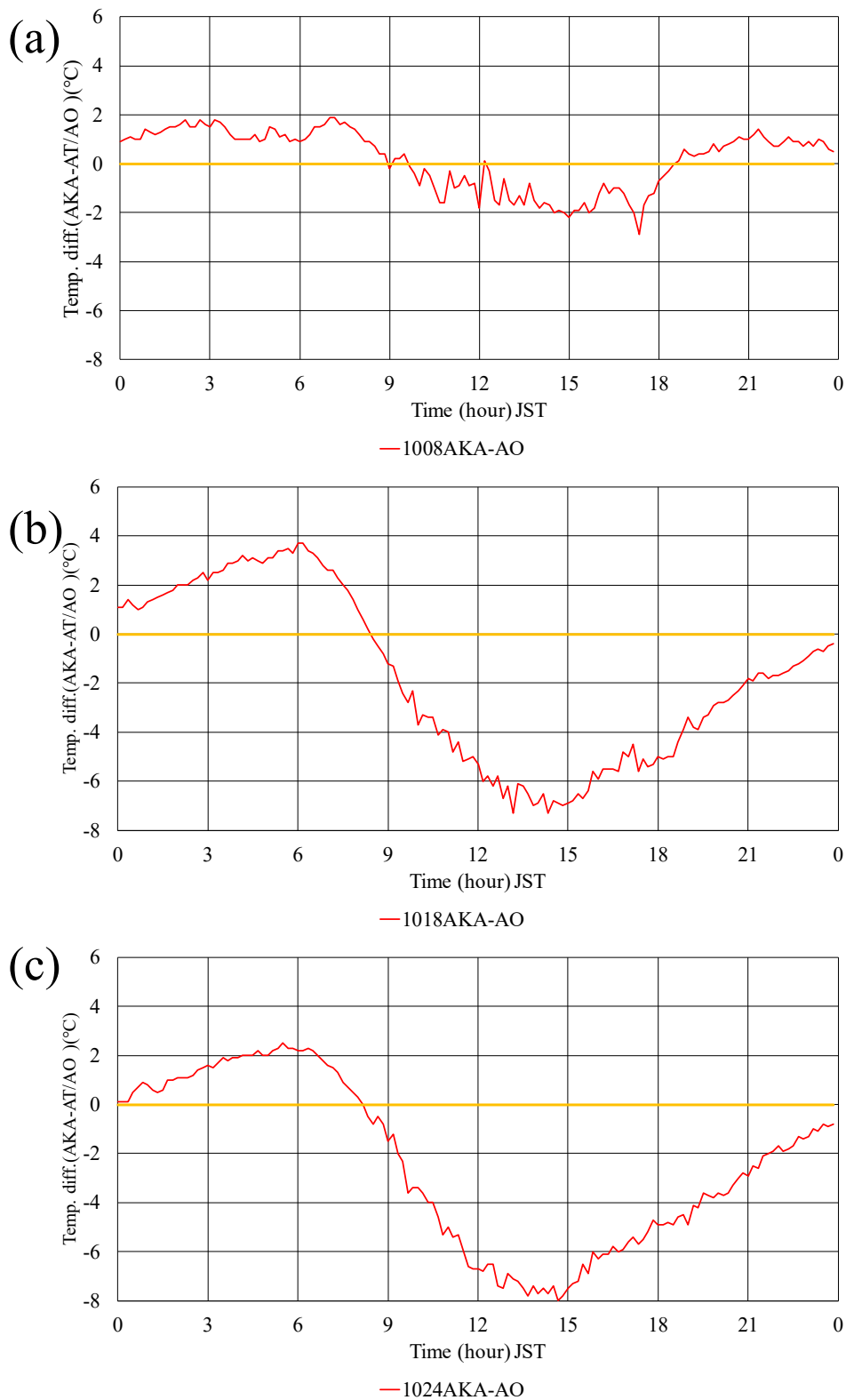


Fig. 3-32 Diurnal change in the temperature difference between AKA and AO. (a) October 8, 2014, (b) October 18, 2014 and (c) October 24, 2014.

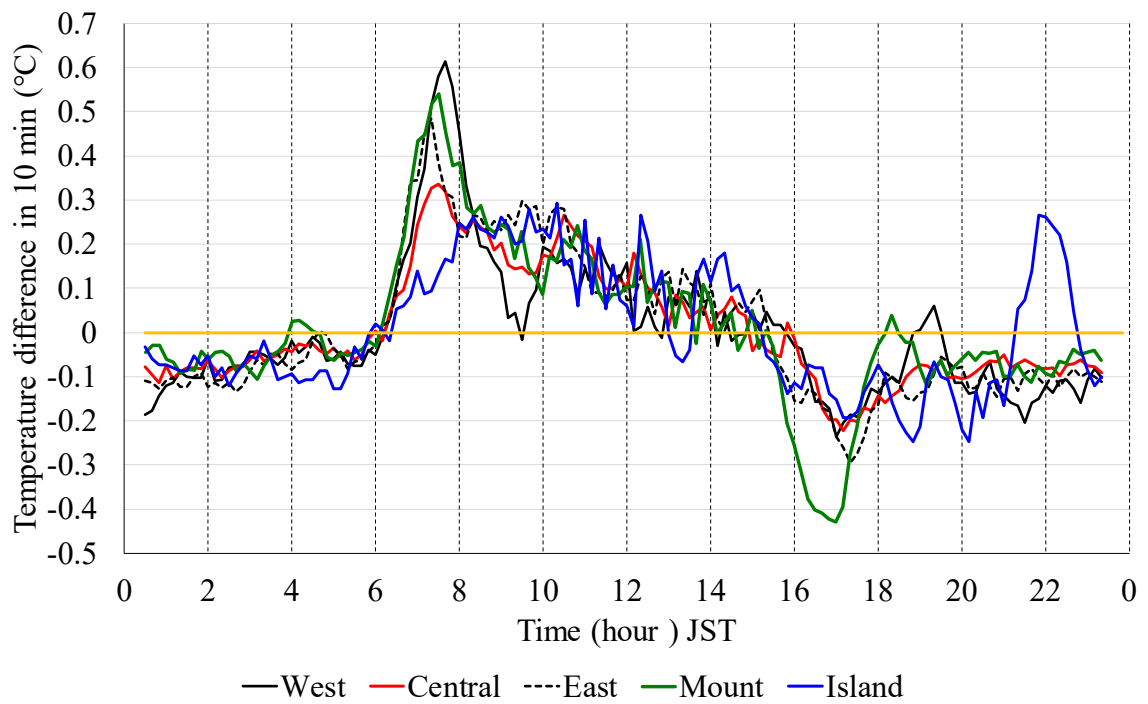


Fig. 3-33 Change in temperature difference in 10 min (5-term moving average) for five regions (October 18, 2014).

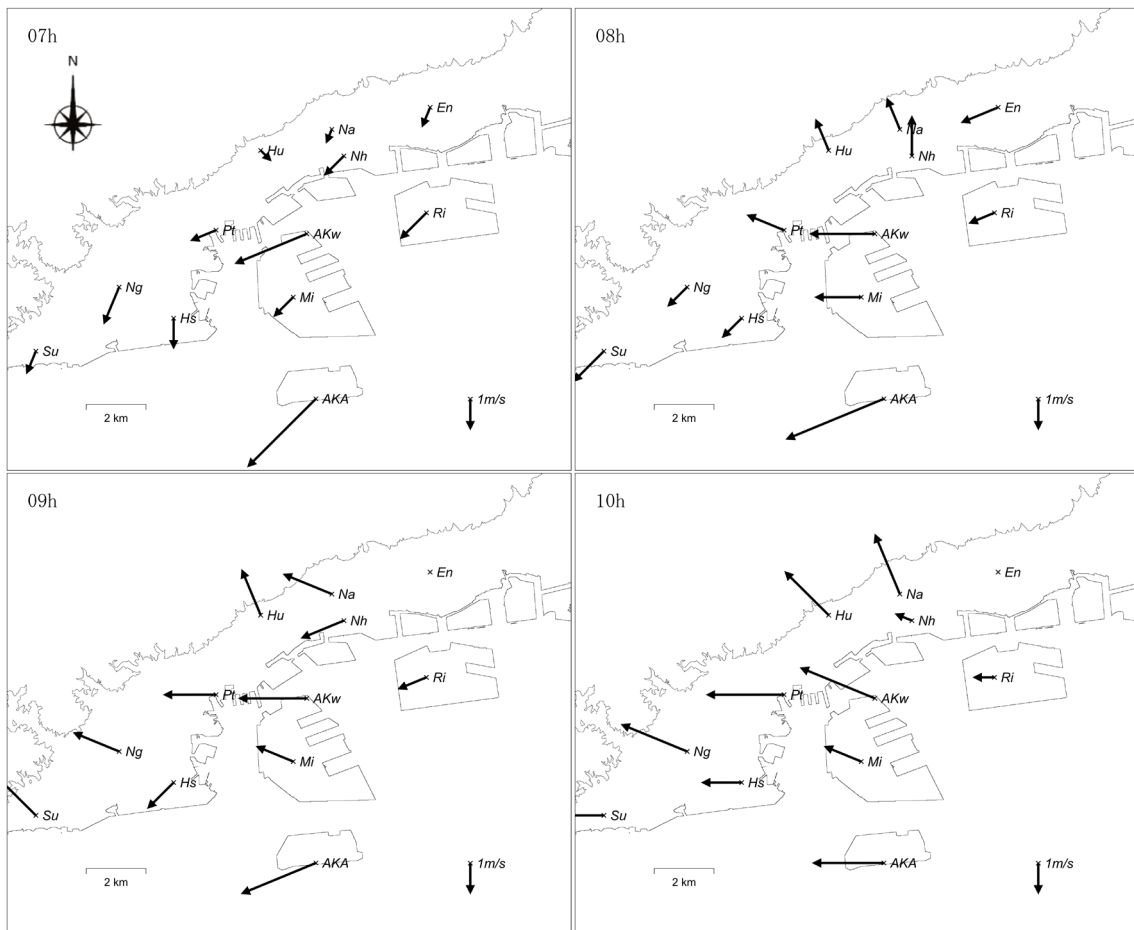


Fig. 3-34 Observed surface wind field at 07:00-10:00 JST (October 18, 2014). Contour lines are shown only at elevation 0 and 100 m.

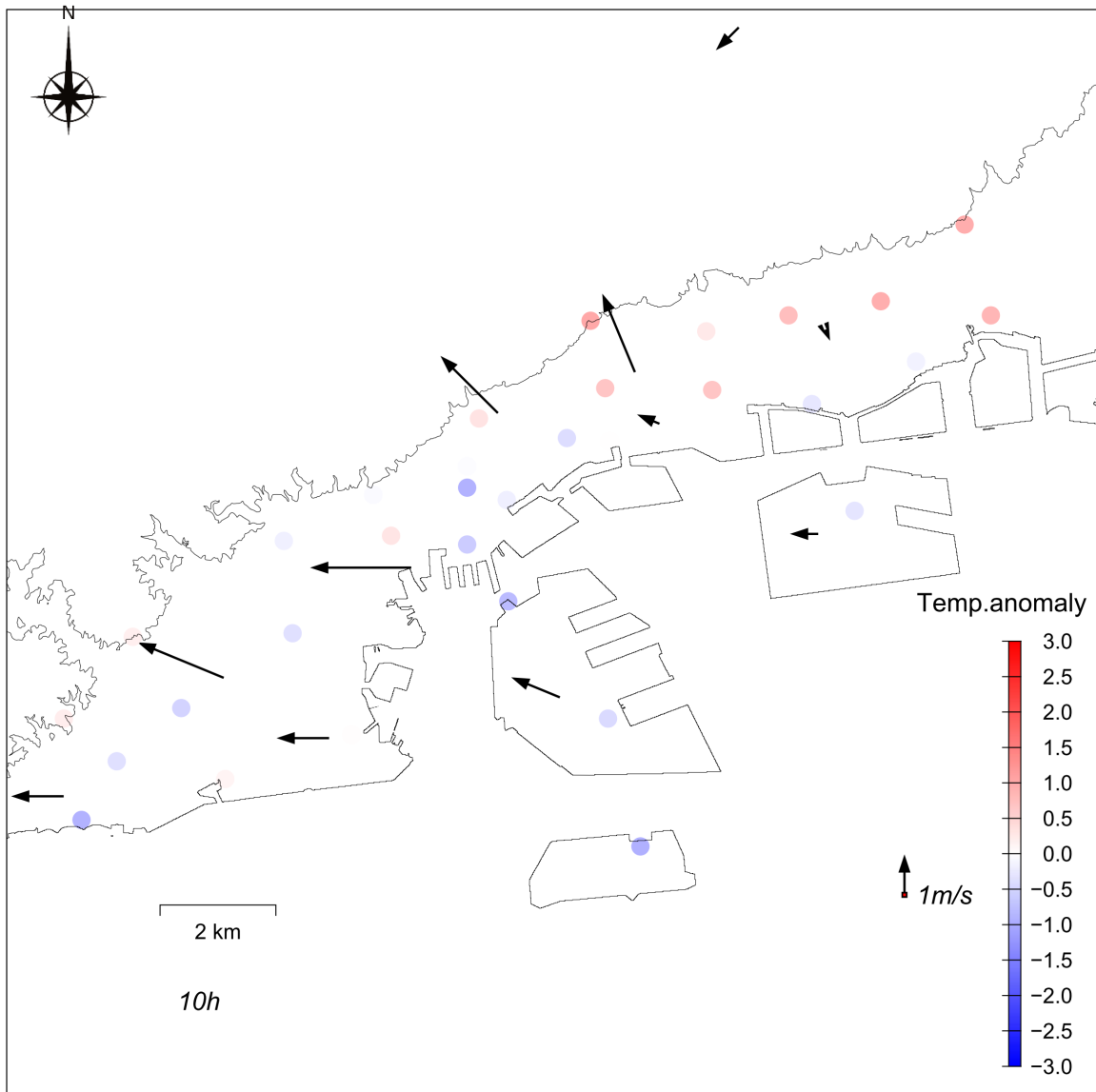


Fig. 3-35 Distribution of wind and air temperature anomaly at 10:00 JST on October 18, 2014. Contour lines are shown only at elevation 0 and 100 meters.

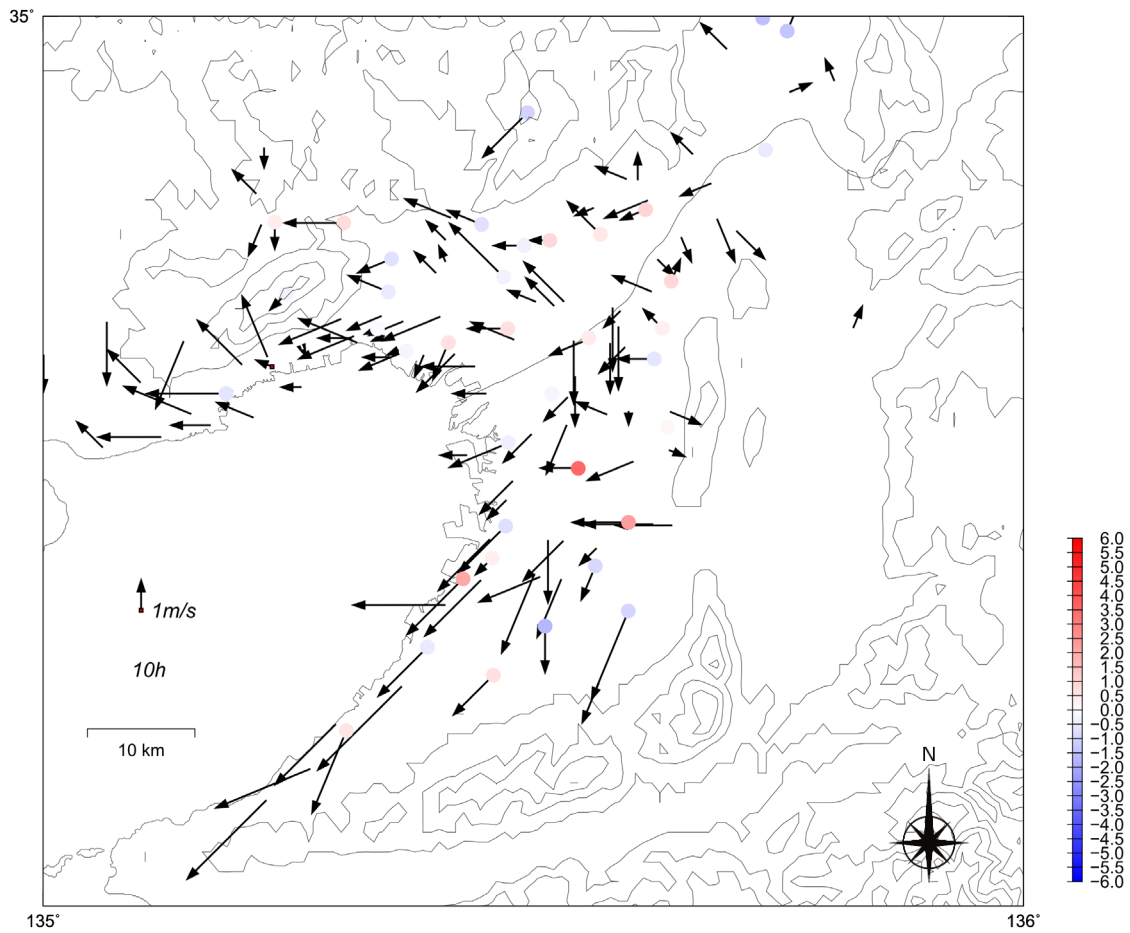


Fig. 3-36 Distribution of wind and air temperature anomaly at 10:00 JST on October 18, 2014. Contour lines are shown only at elevation 0, 100, 300 and 500 m.

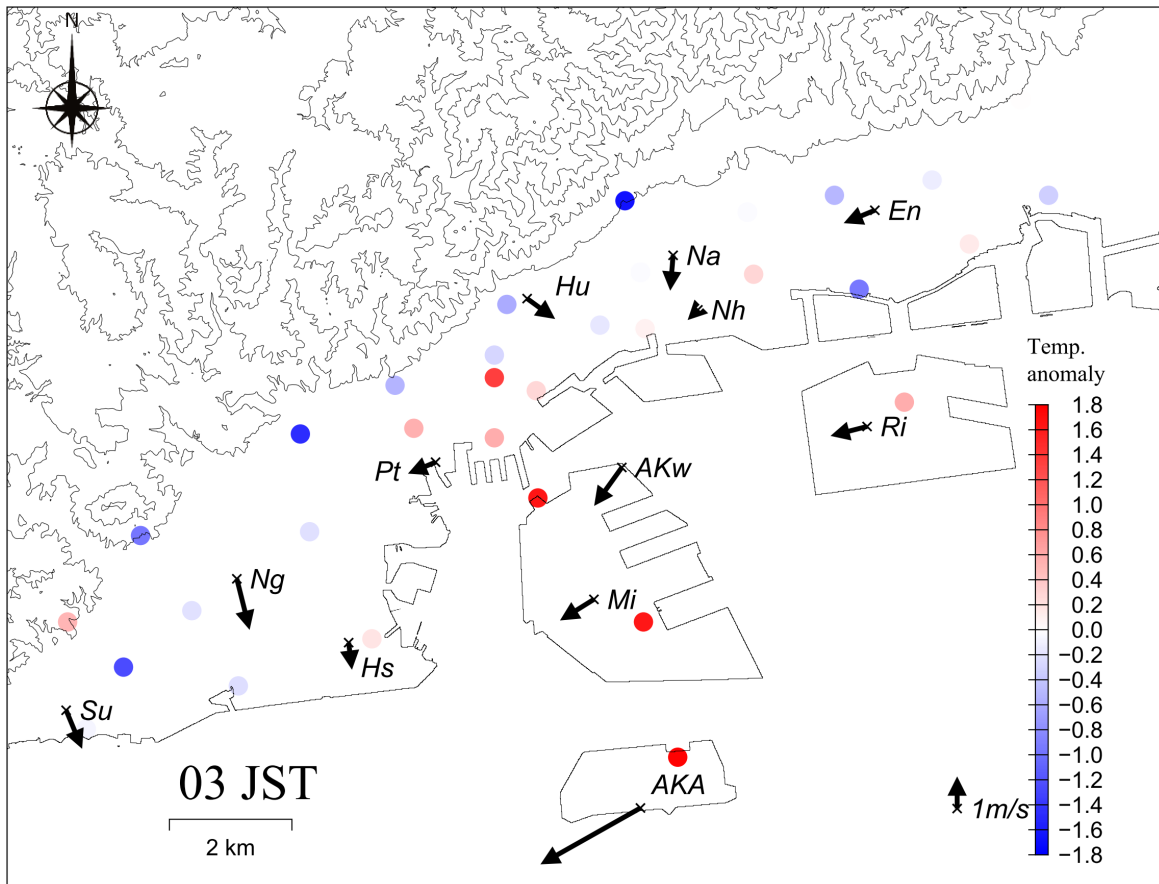


Fig. 3-37 Distribution of wind and air temperature anomaly at 03:00 JST averaged on October 8, 18, 24, 2014. Contour lines are shown only at elevation 0, 100, 300 and 500 m.

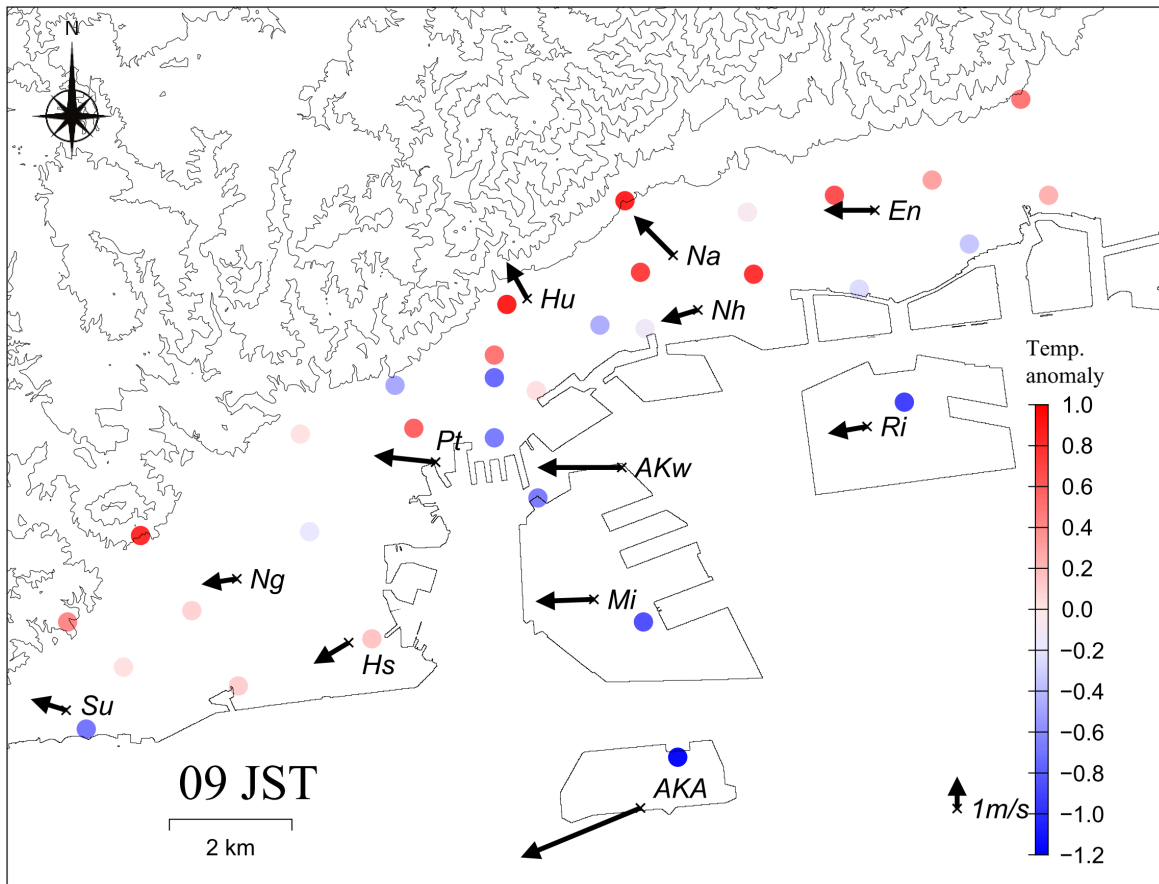


Fig. 3-38 Distribution of wind and air temperature anomaly at 09:00 JST averaged on October 8, 18, 24, 2014. Contour lines are shown only at elevation 0, 100, 300 and 500 m.

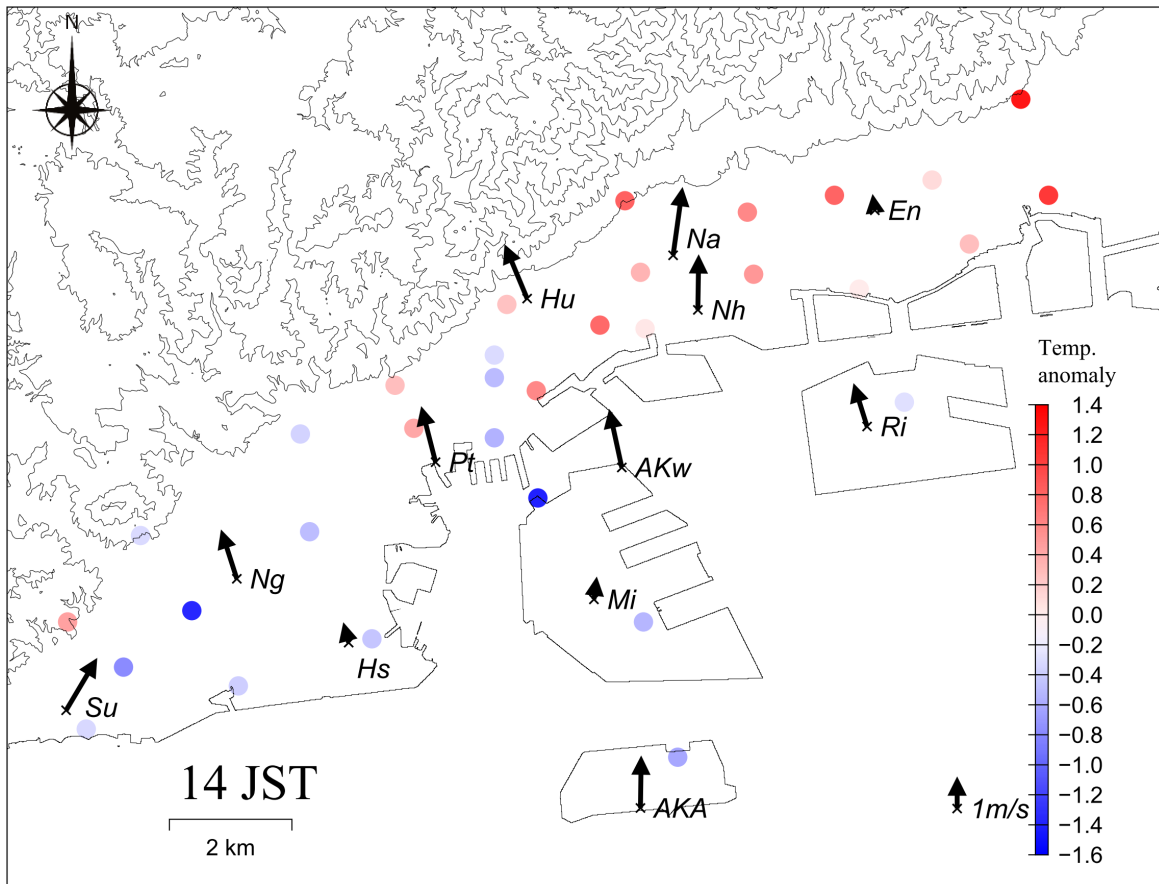


Fig. 3-39 Distribution of wind and air temperature anomaly at 14:00 JST averaged on October 8, 18, 24, 2014. Contour lines are shown only at elevation 0, 100, 300 and 500 m.

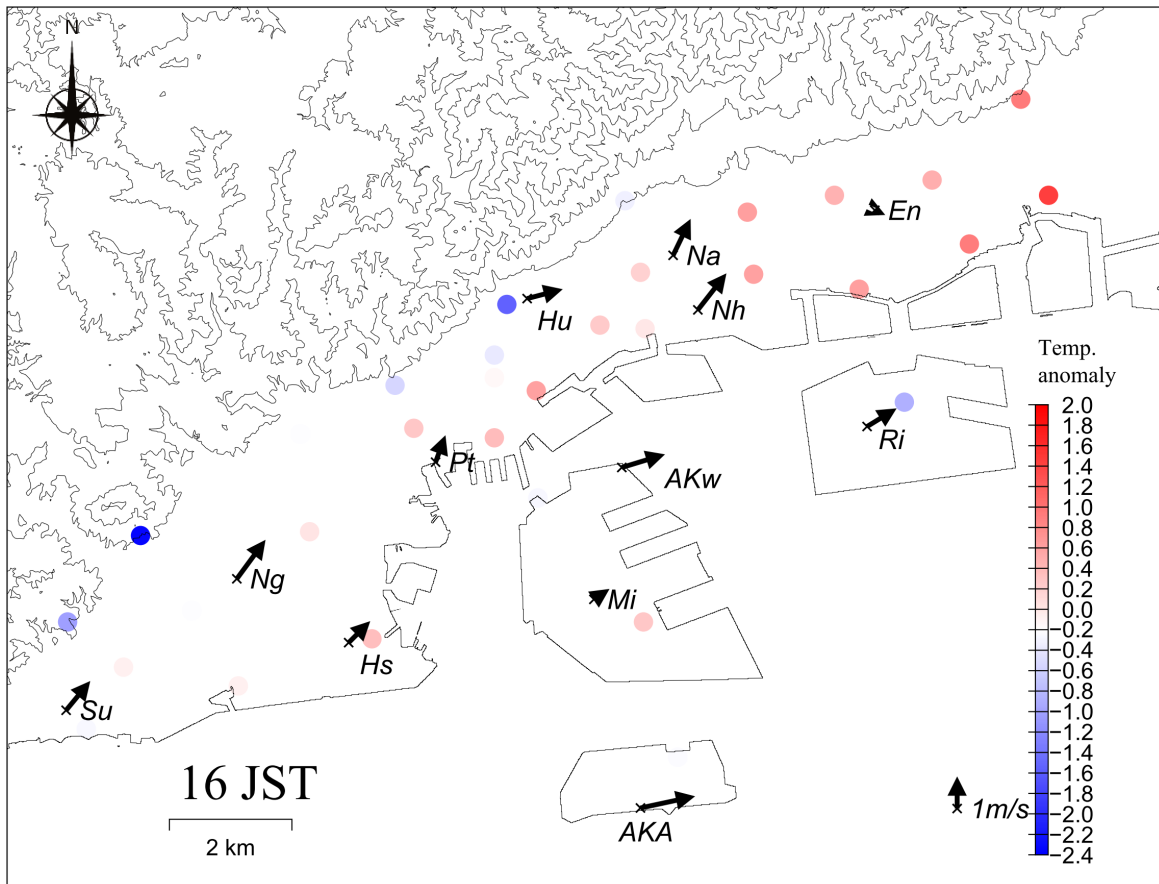


Fig. 3-40 Distribution of wind and air temperature anomaly at 16:00 JST averaged on October 8, 18, 24, 2014. Contour lines are shown only at elevation 0, 100, 300 and 500 m.

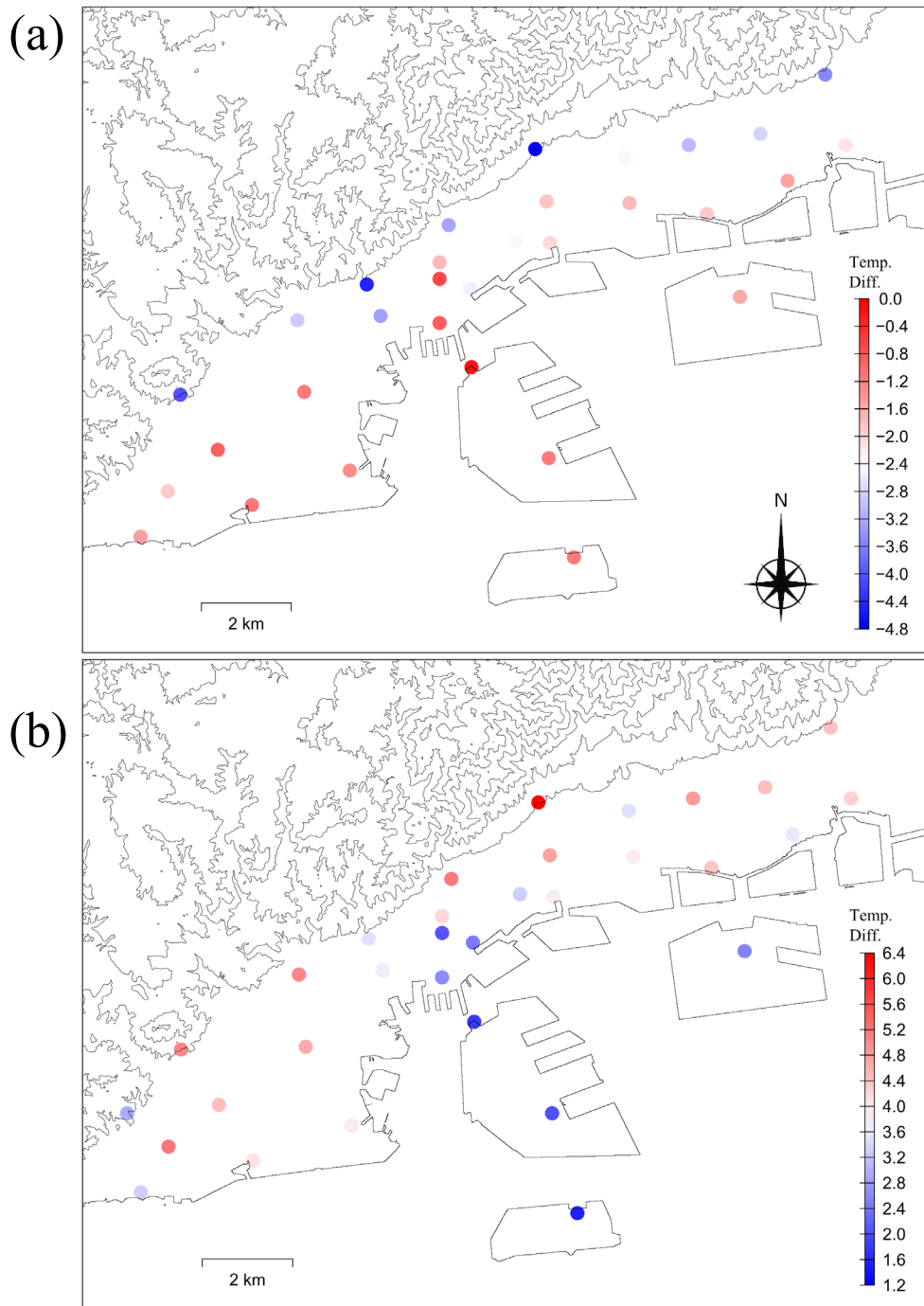


Fig. 3-41 Distribution of 2-hours air temperature change averaged on October 8, 18, 24, 2014. (a) 15:00-17:00 JST, (b) 06:00-08:00 JST. Contour lines are shown only at elevation 0, 100, 300 and 500 m.

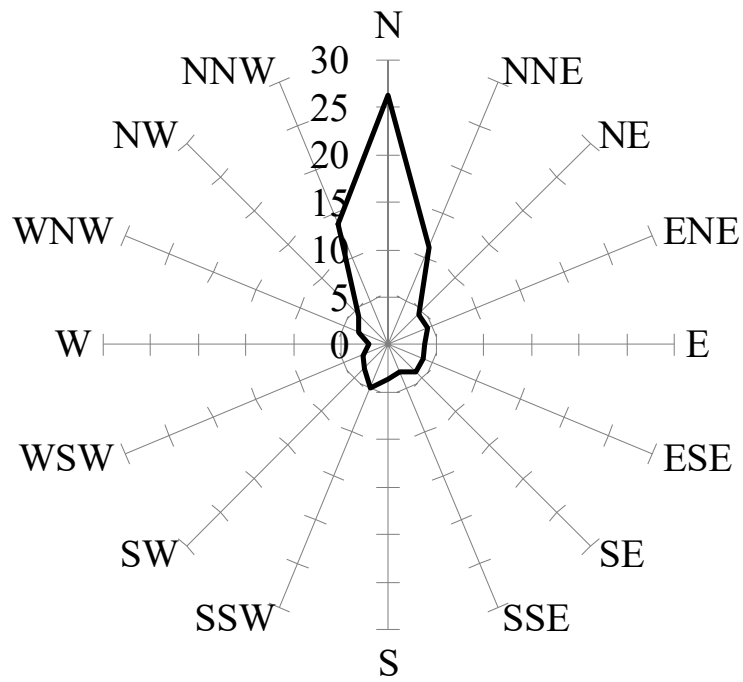


Fig. 3-42 Wind direction frequency for 11 sunny days in KS (Total of all wind directions is 100%).

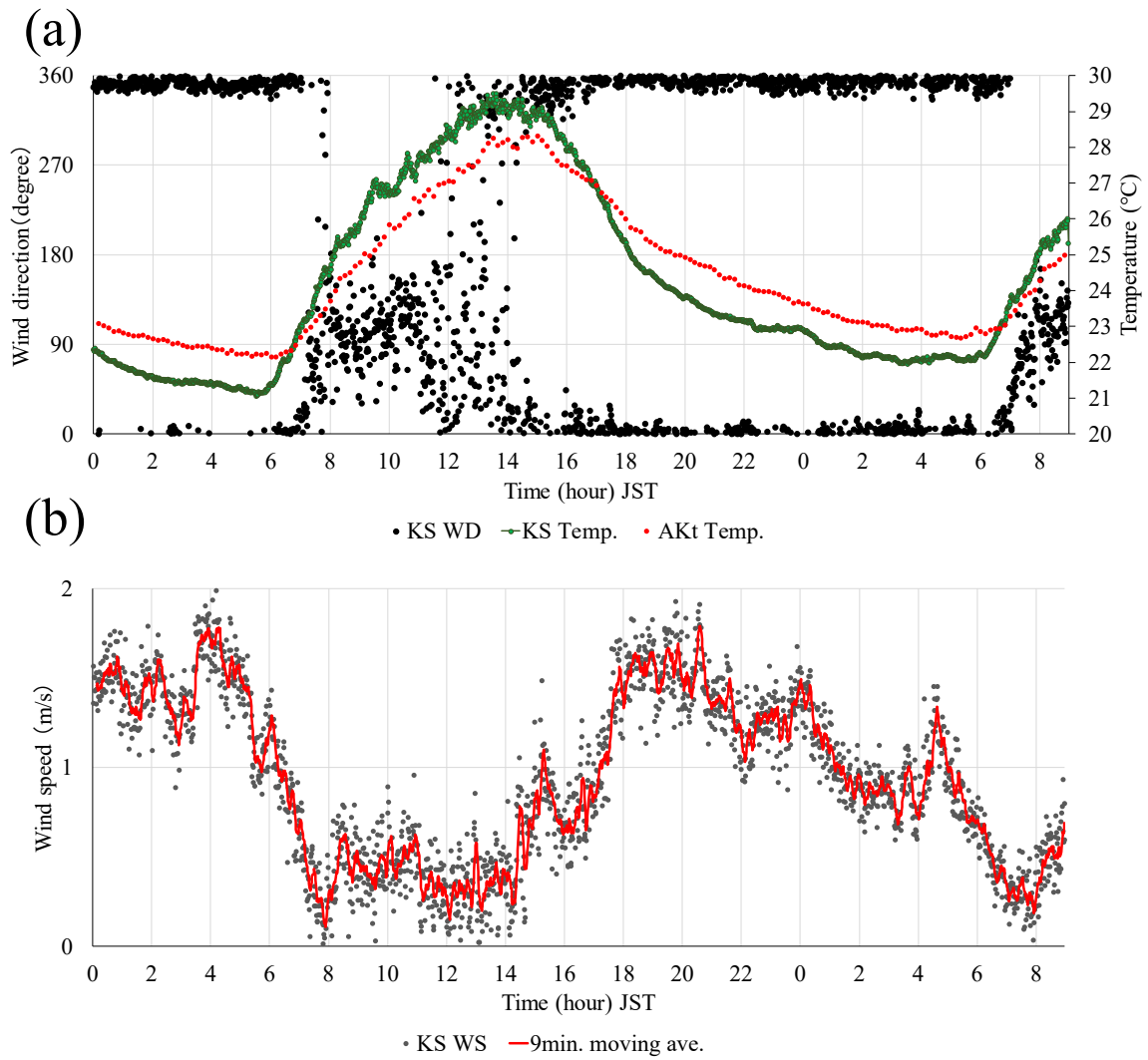


Fig. 3-43 Diurnal change of wind and temperature at KS and AKt averaged on 11 sunny days. (a) Mean wind direction and air temperature, (b) mean wind speed.

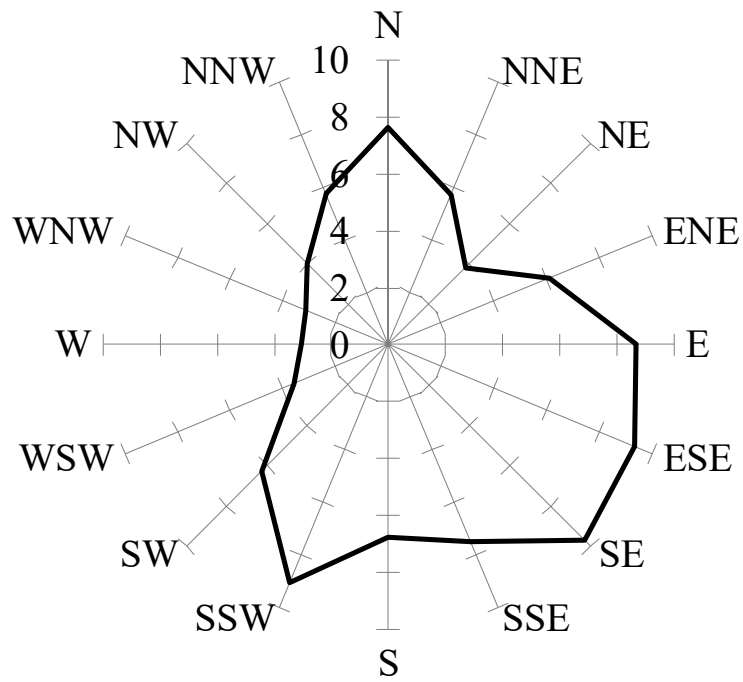


Fig. 3-44 Wind direction frequency from 07:00 to 15:00 JST for 11 sunny days in KS

(Total of all wind directions is 100%).

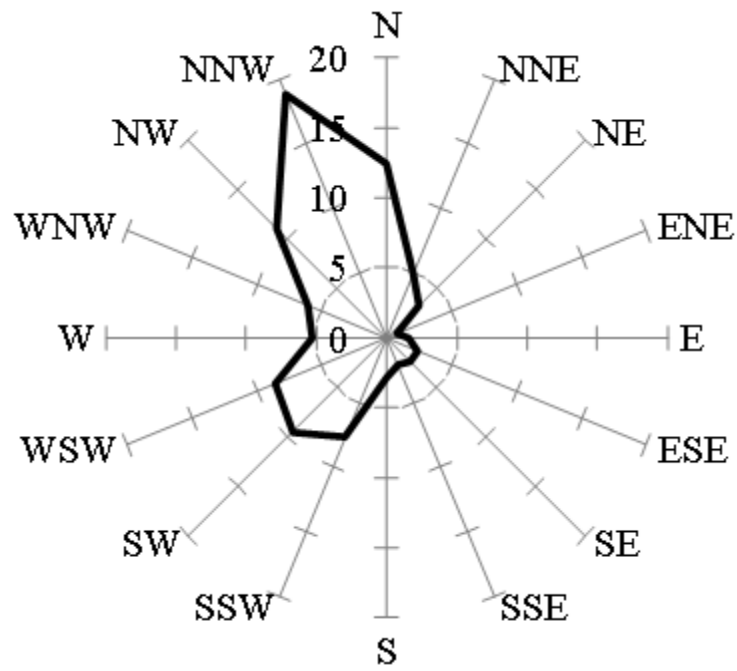


Fig. 3-45 Wind direction frequency for 4 cloudy days in KS (Total of all wind directions is 100%).

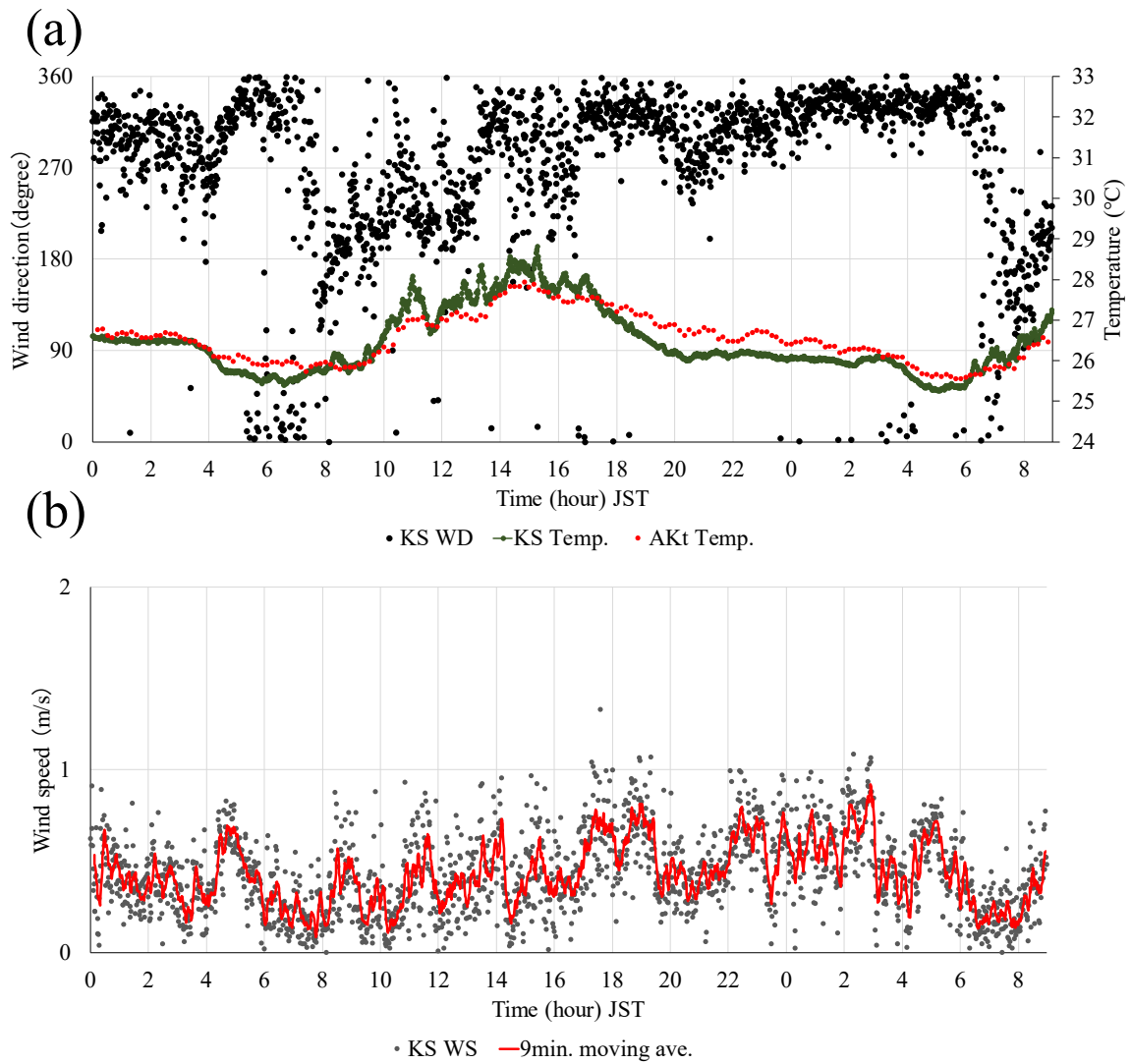


Fig. 3-46 Diurnal change of wind and temperature at KS and AKt on 4 cloudy days. (a) Mean wind direction and air temperature, (b) mean wind speed.

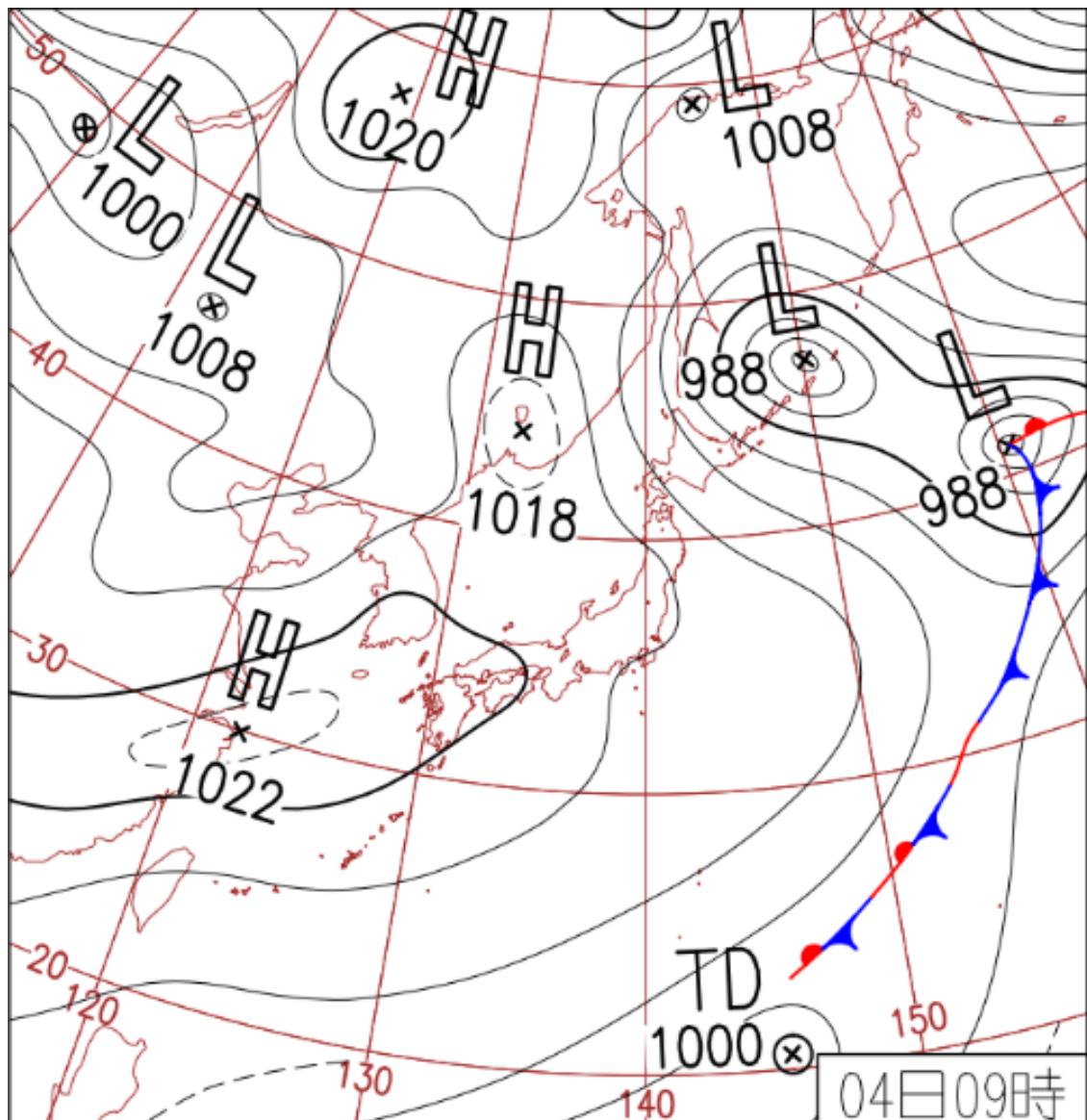


Fig. 3-47 Surface weather chart at 09:00 JST on November 4, 2016.

From JMA HP <https://www.data.jma.go.jp/fcd/yoho/hibiten/index.html>

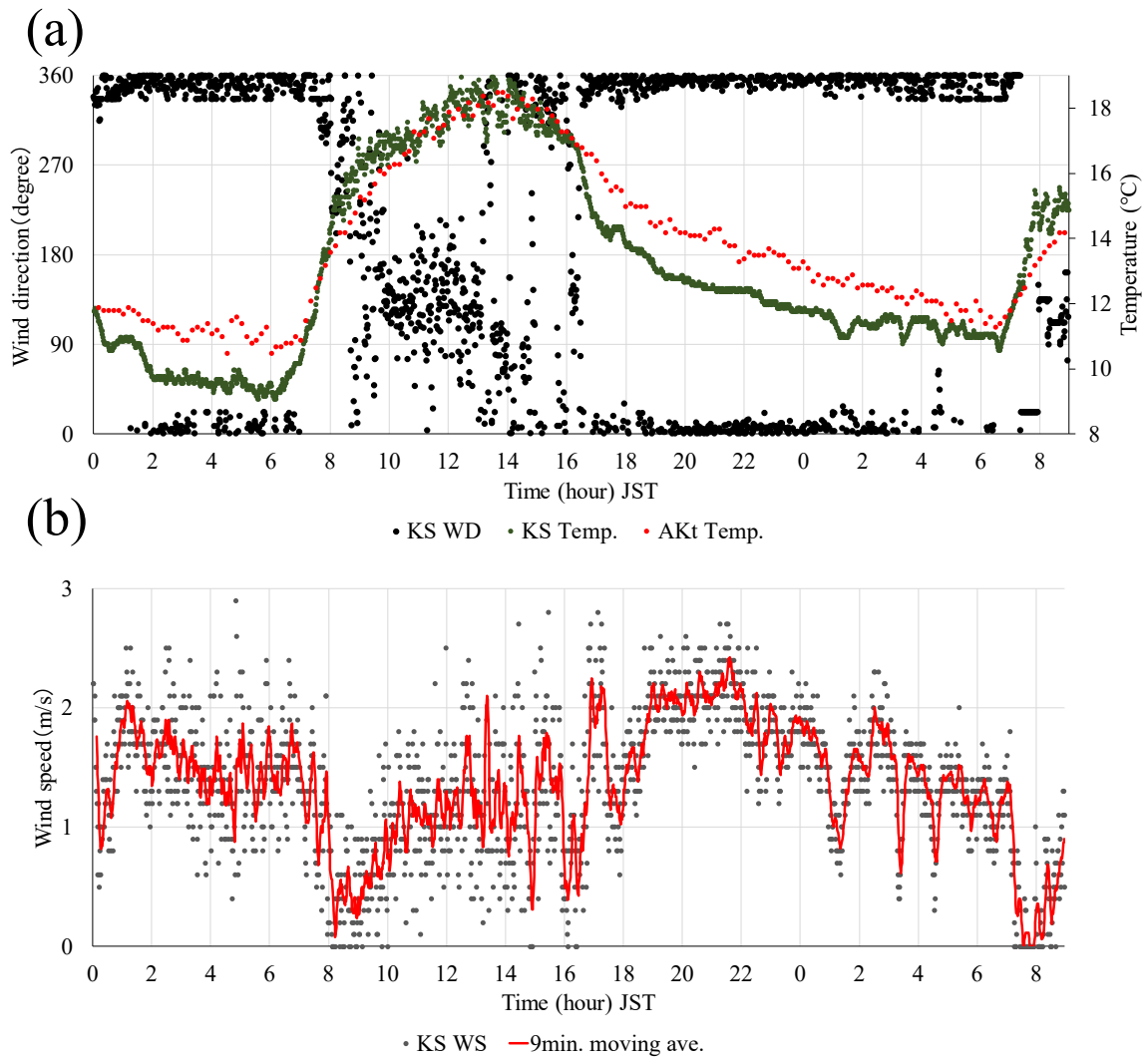


Fig. 3-48 Diurnal change of wind and temperature at KS and AKt on a clear day (November 4, 2016). (a) Mean wind direction and air temperature, (b) mean wind speed.

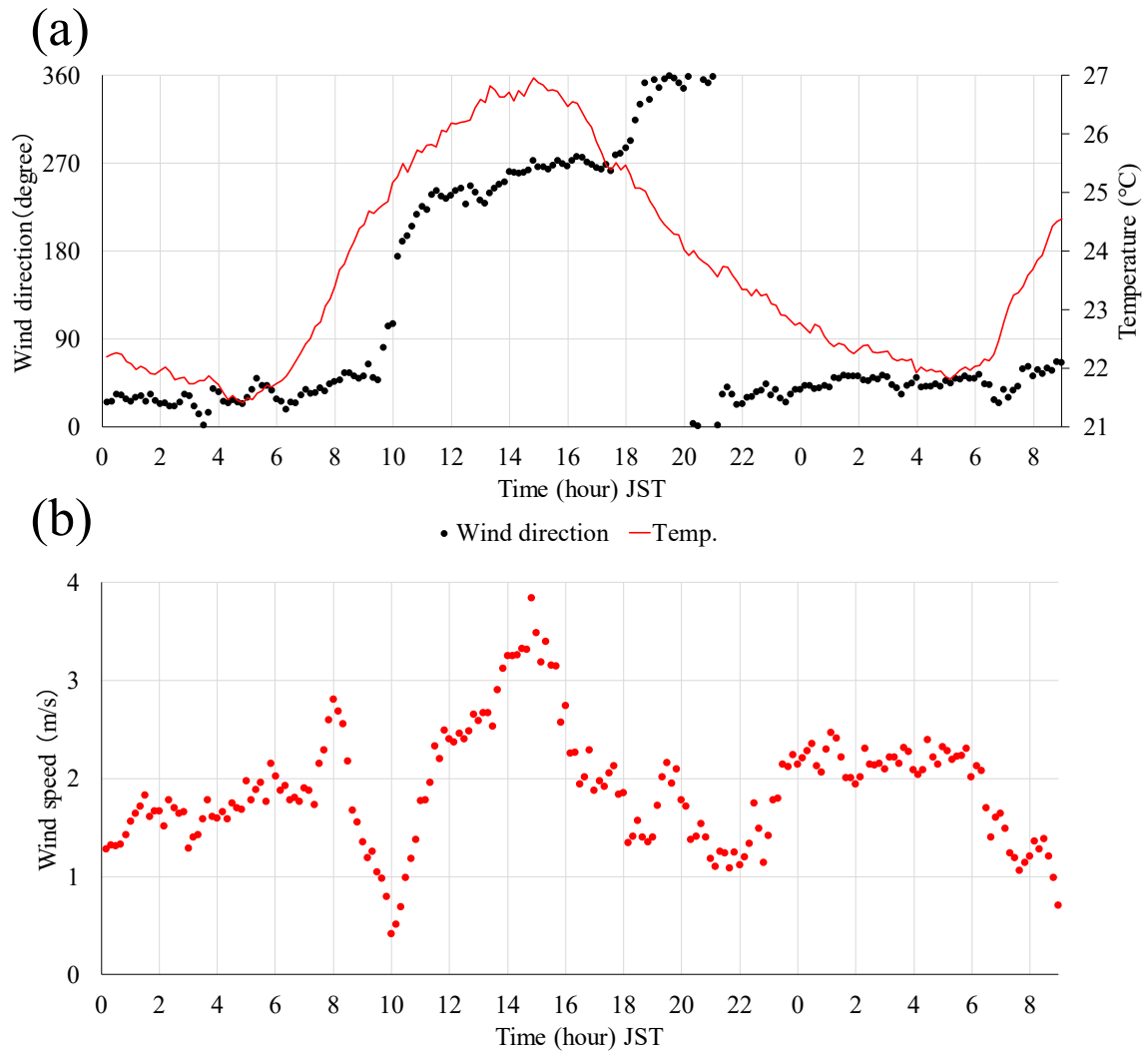


Fig. 3-49 Diurnal change of wind and temperature at AKA averaged on 11 sunny days.

(a) Mean wind direction and air temperature, (b) mean wind speed.

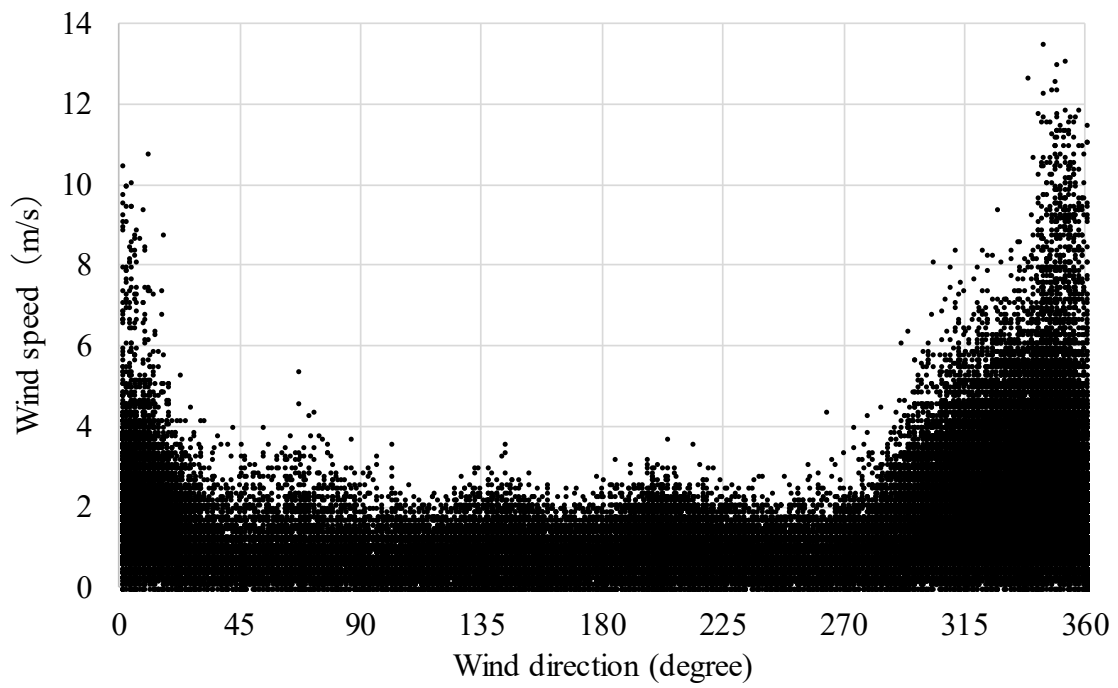


Fig. 4-1 Distribution of wind direction in minute and speed at KS during the research period.

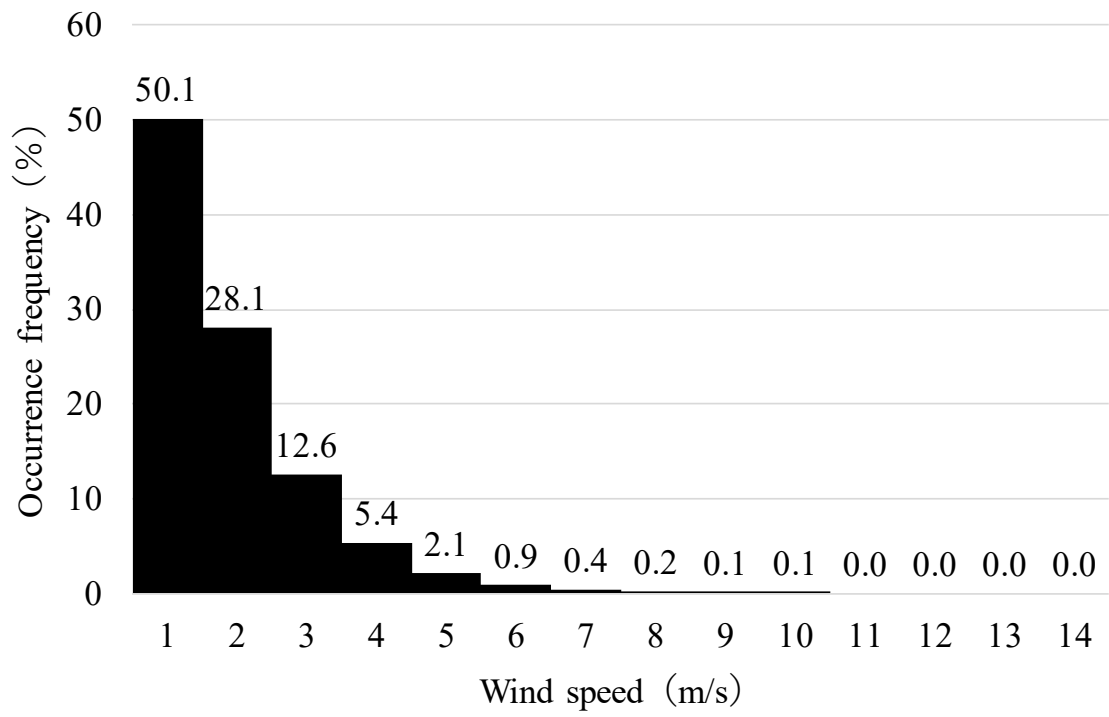


Fig. 4-2 Wind speed frequency distribution at KS during the research period.

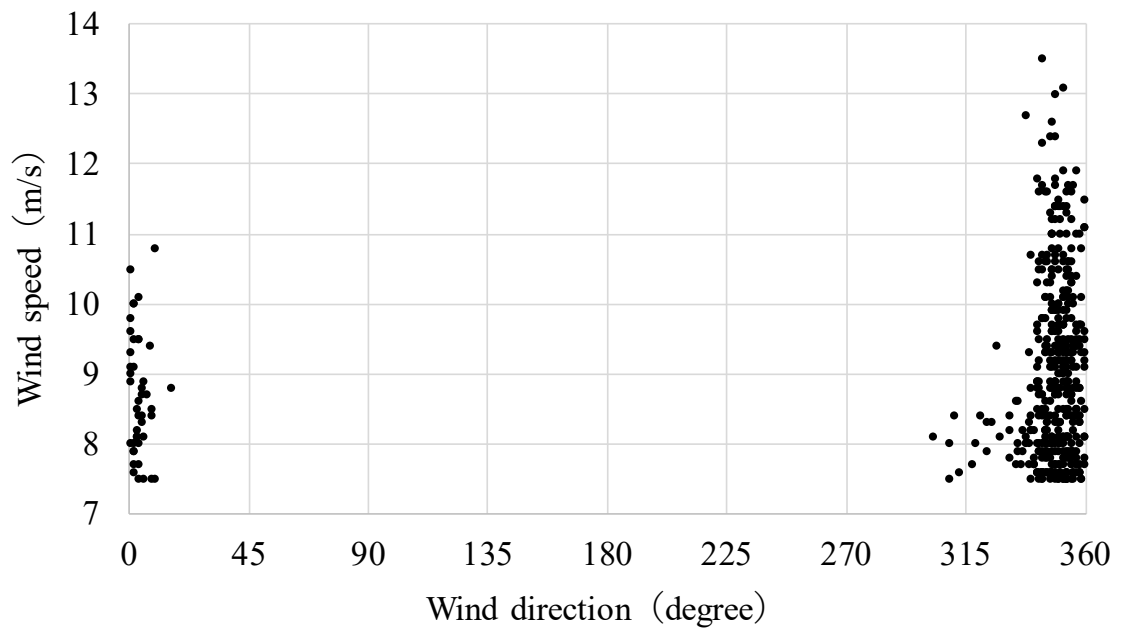


Fig. 4-3 Wind direction and speed frequency distribution during the occurrence of *Rokko-oroshi* at KS during the research period.

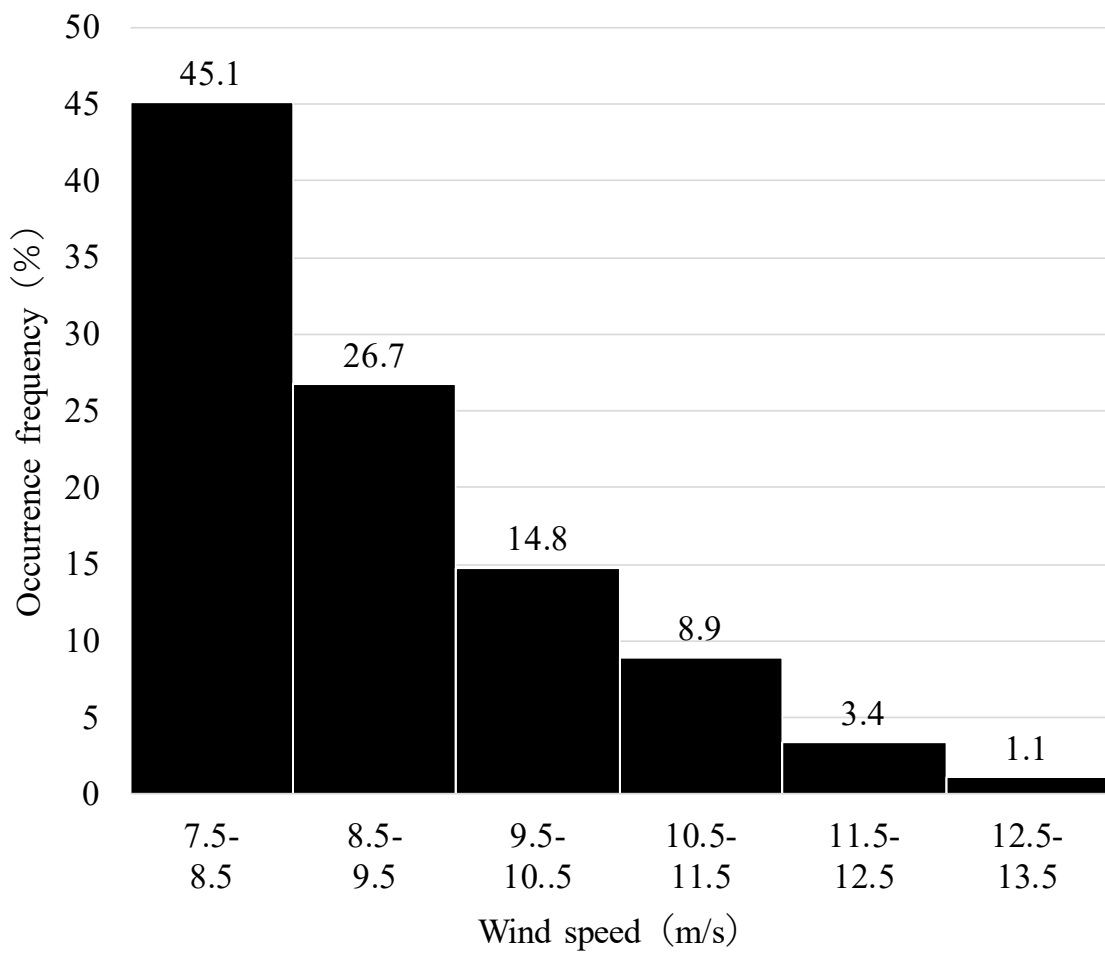


Fig. 4-4 Wind speed frequency distribution during the occurrence of *Rokko-oroshi* at KS during the research period.

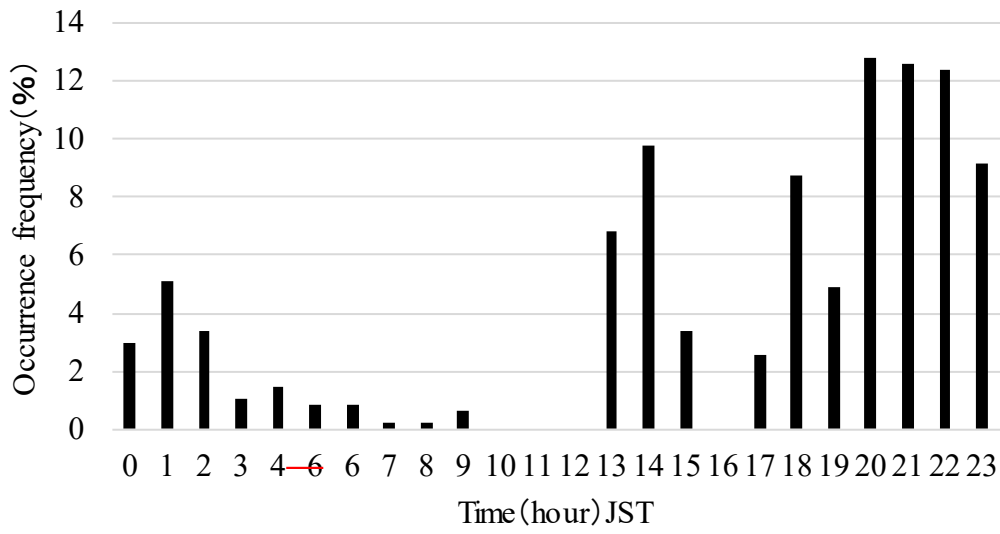


Fig. 4-5 Distribution of *Rokko-oroshi* occurrence time during the research period.

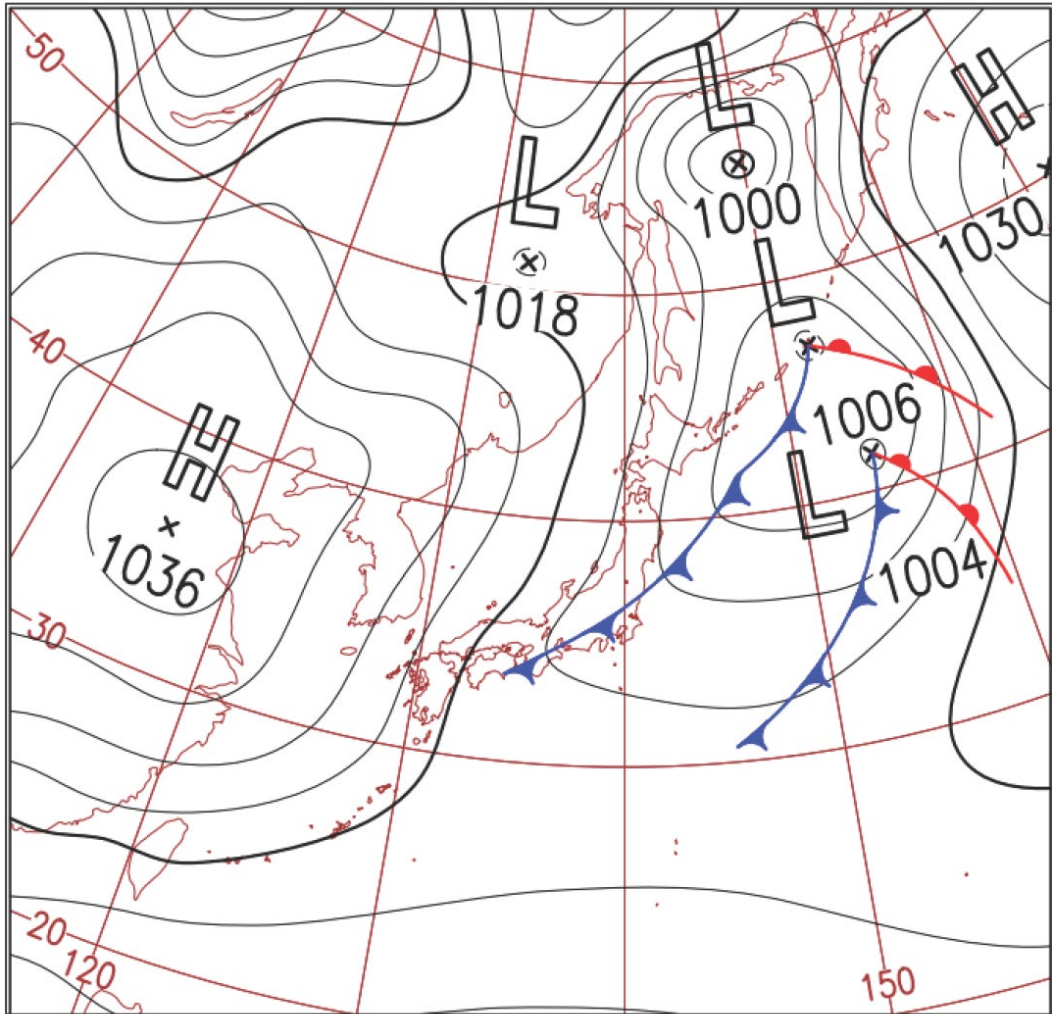


Fig. 4-6 Surface weather chart at 09:00 JST on November 4, 2017.

From JMA HP <https://www.data.jma.go.jp/fcd/yoho/hibiten/index.html>

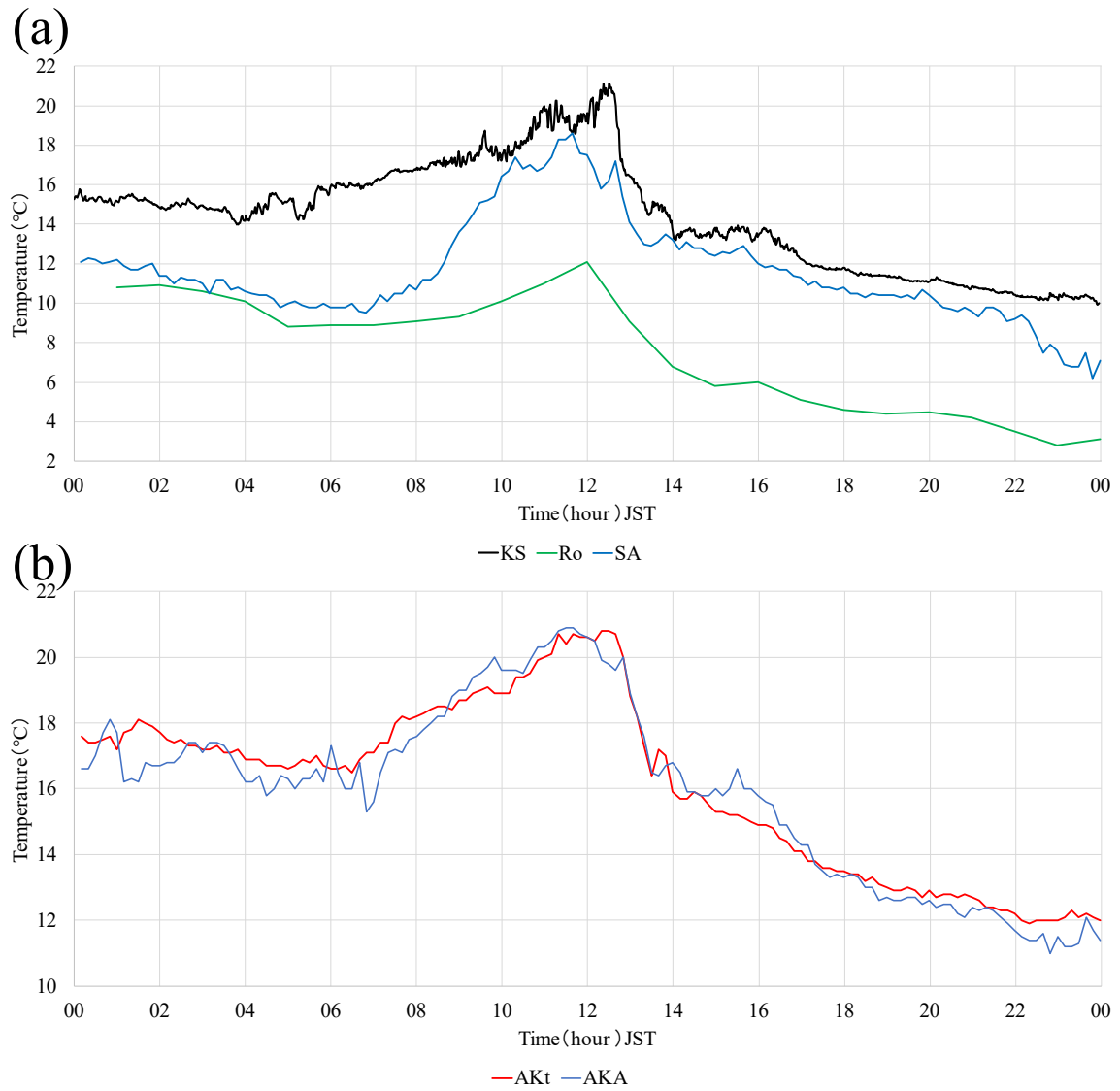


Fig. 4-7 Diurnal change of temperature on November 4, 2017. (a) KS (black), Ro (green) and SA (blue), (b) AKt (red) and AKA (blue)

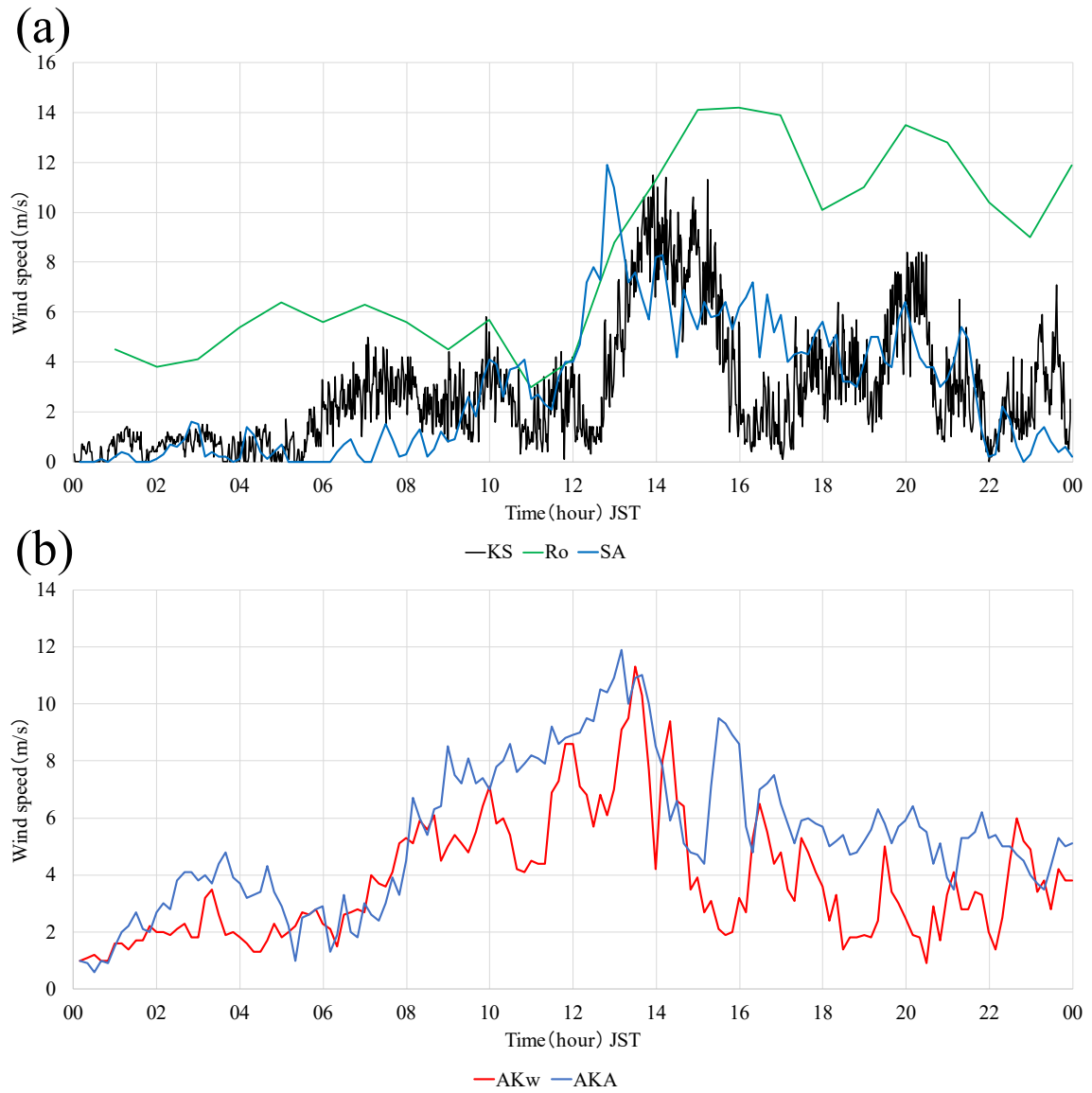


Fig. 4-8 Diurnal change of wind speed on November 4, 2017. (a) KS, Ro and SA, (b) AKw and AKA

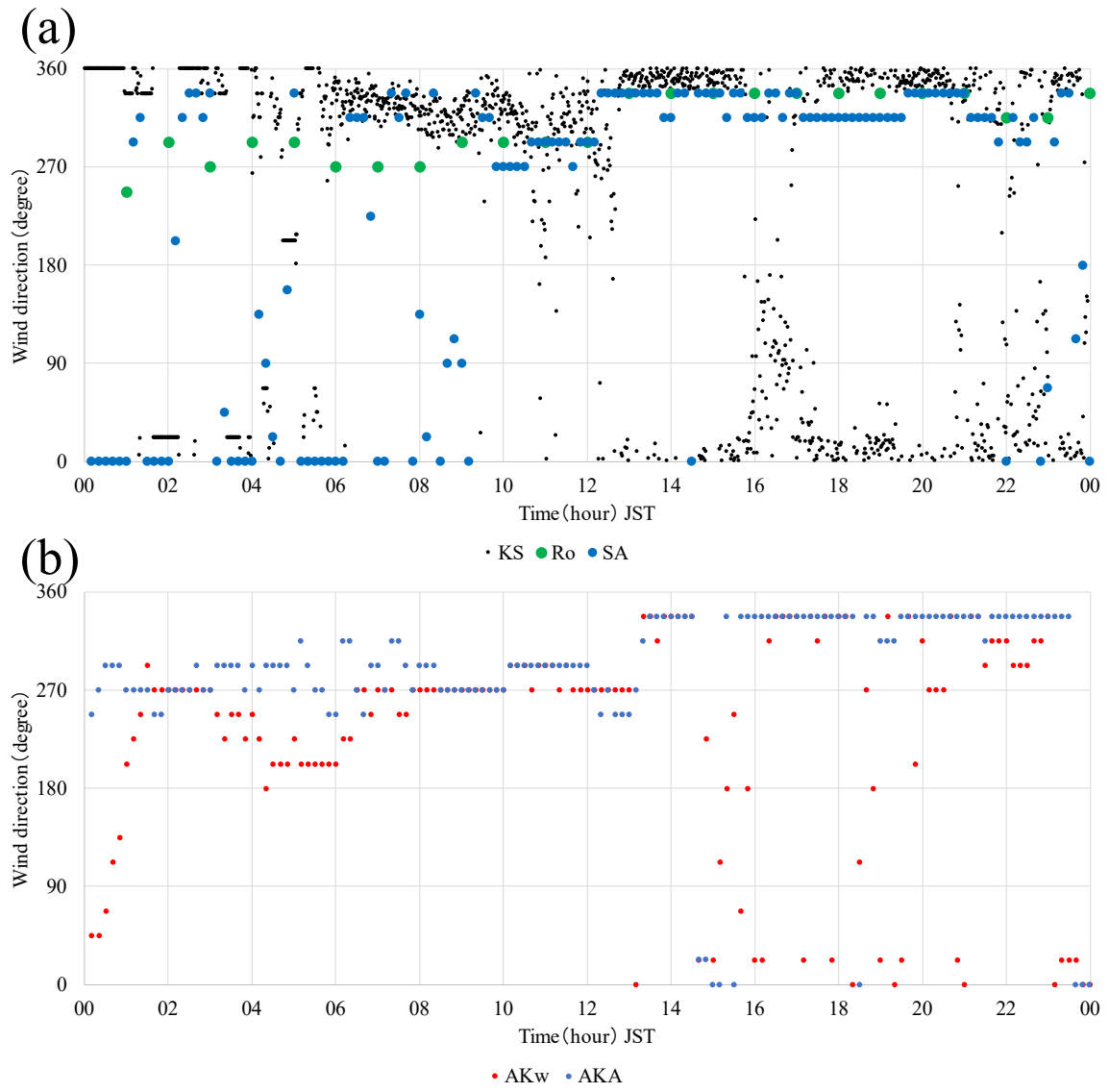


Fig. 4-9 Diurnal change of wind direction on November 4, 2017. (a) KS, Ro and SA, (b) AKw and AKA

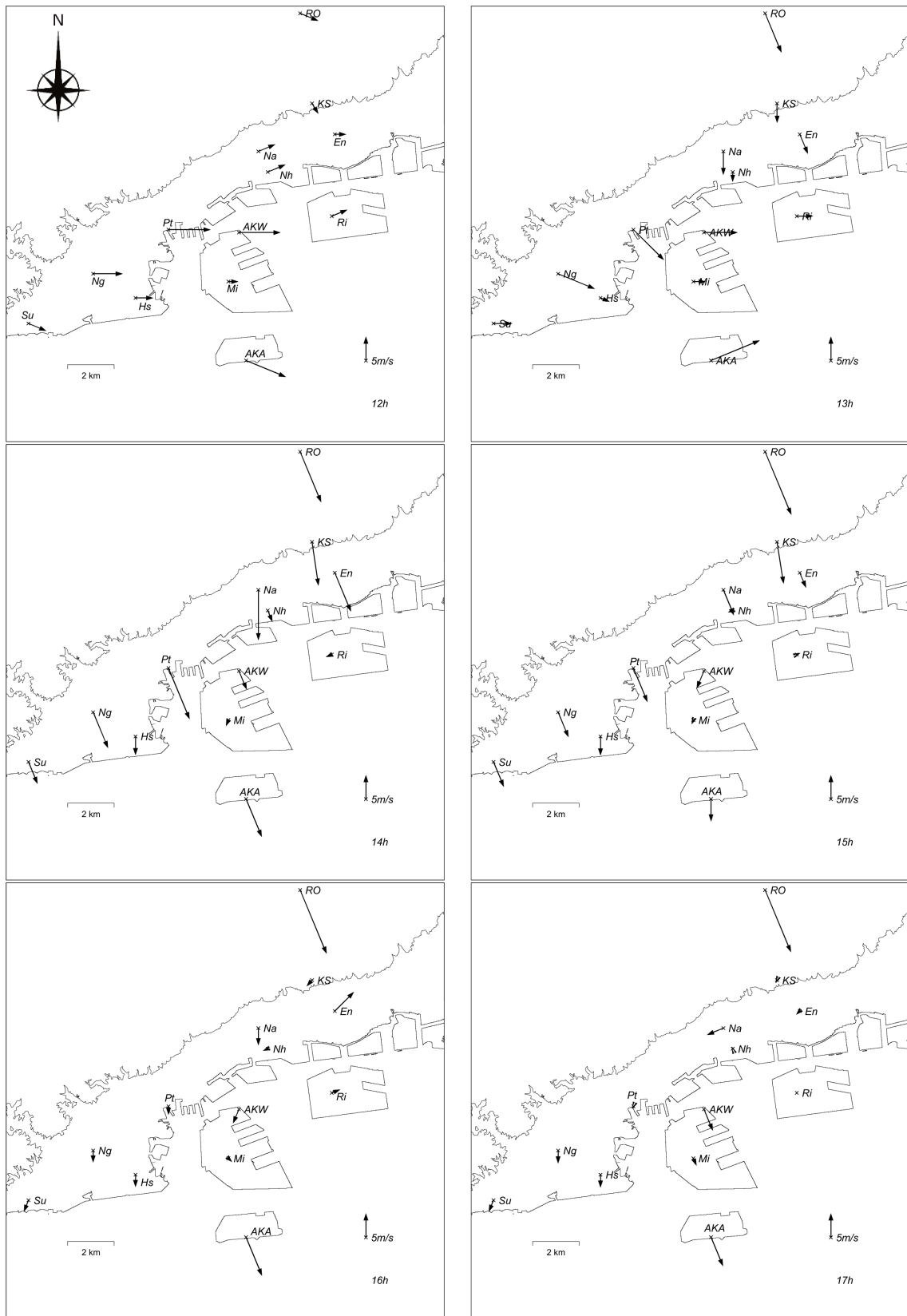


Fig. 4-10 Observed surface wind field at 12:00-17:00 JST on November 4, 2017.

Contour lines are shown only at elevation 0 and 100 m

Table 1-1 Name and synoptic conditions associated with local winds in Japan. The numbers refer to their location on the map in Fig. 1-14 (b) (Kusaka and Fudeyasu, 2017).

| | Name | Weather Chart |
|----|-------------------|----------------------|
| 1 | Hikata-kaze | Cyclone |
| 2 | Tokachi-kaze | Cyclone |
| 3 | Rausu-dashi | Winter monsoon |
| 4 | Suttsu-dashi-kaze | Cyclone |
| 5 | Hidaka-shimo-kaze | Tropical cyclone |
| 6 | Kiyokawa-dashi | Cyclone |
| 7 | Arakawa-dashi | Cyclone |
| 8 | Tainai-dashi | Cyclone |
| 9 | Yasuda-dashi | Cyclone |
| 10 | Nasu-oroshi | Winter monsoon |
| 11 | Akagi-oroshi | Winter monsoon |
| 12 | Haruna-oroshi | Winter monsoon |
| 13 | Tsukuba-oroshi | Winter monsoon |
| 14 | Karak-kaze | Winter monsoon |
| 15 | Dashi-no-kaze | Tropical cyclone |
| 16 | Dashi-no-kaze | Anticyclone |
| 17 | Shougawa-arashi | Anticyclone |
| 18 | Inami-kaze | Cyclone |
| 19 | Mashita-kaze | Winter monsoon |
| 20 | Hira-hakko | Winter monsoon |
| 21 | Suzuka-oroshi | Winter monsoon |
| 22 | Hirano-kaze | Cyclone |
| 23 | Oroshi | Winter monsoon |
| 24 | Rokko-oroshi | Winter monsoon |
| 25 | Hirodo-kaze | Tropical cyclone |
| 26 | Yamaji-kaze | Tropical cyclone |
| 27 | Hijikawa-arashi | Anticyclone |
| 28 | Matsubori-kaze | Cyclone |

Table 2-1 Summary of original meteorological sites.

| No. | Lat. | Lon. | elevation (m;asl) | No. | Lat. | Lon. | elevation (m;asl) |
|-----|--------|---------|-------------------|-----|--------|---------|-------------------|
| 1 | 34.643 | 135.124 | 2 | 17 | 34.703 | 135.216 | 14 |
| 2 | 34.650 | 135.151 | 2 | 18 | 34.740 | 135.247 | 304 |
| 3 | 34.653 | 135.131 | 9 | 19 | 34.736 | 135.291 | 90 |
| 4 | 34.661 | 135.143 | 8 | 20 | 34.722 | 135.258 | 36 |
| 5 | 34.672 | 135.134 | 104 | 21 | 34.724 | 135.276 | 11 |
| 6 | 34.659 | 135.121 | 113 | 22 | 34.722 | 135.296 | 2 |
| 7 | 34.694 | 135.179 | 92 | 23 | 34.708 | 135.263 | 2 |
| 8 | 34.706 | 135.199 | 48 | 24 | 34.692 | 135.271 | 3 |
| 9 | 34.688 | 135.183 | 9 | 25 | 34.721 | 135.221 | 109 |
| 10 | 34.693 | 135.205 | 3 | 26 | 34.711 | 135.223 | 29 |
| 11 | 34.687 | 135.163 | 24 | 27 | 34.720 | 135.243 | 35 |
| 12 | 34.673 | 135.164 | 4 | 28 | 34.703 | 135.224 | 2 |
| 13 | 34.657 | 135.175 | 1 | 29 | 34.715 | 135.282 | 1 |
| 14 | 34.686 | 135.197 | 5 | 30 | 34.711 | 135.244 | 6 |
| 15 | 34.695 | 135.197 | 13 | 31 | 34.639 | 135.230 | 1 |
| 16 | 34.699 | 135.197 | 21 | 32 | 34.659 | 135.224 | 2 |
| | | | | 33 | 34.678 | 135.205 | 0 |

* measurement interval : 10min., measurement height : 2.5-3.0m

| | Lat. | Lon. | elevation (m;asl) |
|----|--------|---------|-------------------|
| KS | 34.732 | 135.255 | 158 |

* measurement interval : 1min., measurement height : 15m

Table 2-2 Summary of AMeDAS and radiosonde sites.

| AMeDAS station | longitude | latitude | elevation (m;a.s.l) | observation height (m;a.g.l) wind | observation height (m;a.g.l) temp. |
|----------------|-----------|----------|---------------------|-----------------------------------|------------------------------------|
| AKw (wind) | 135.22 | 34.68 | 3 | 16 | - |
| AKt (temp.) | 135.21 | 34.70 | 5 | - | - |
| AKA | 135.22 | 34.63 | 5 | 10 | - |
| SA | 135.21 | 34.90 | 150 | 21.6 | 1.5 |
| AKY | 135.73 | 35.02 | 36 | - | - |

* measurement interval : 10min.

| Sonde station | longitude | latitude | elevation (m;a.s.l) |
|---------------|-----------|----------|---------------------|
| Matsue | 133.07 | 35.46 | 17 |
| Shiono-misaki | 135.76 | 33.45 | 68 |

* measurement interval : twice a day (09:00 and 21:00 JST)

Table 2-3 Summary of AEROS sites.

| station | longitude | latitude | elevation (m;a.s.l) | observation height(m;a.g.l) |
|---------|-----------|----------|------------------------|--------------------------------|
| En | 135.265 | 34.720 | 25.8 | 32 |
| Na | 135.229 | 34.713 | 34.5 | 21 |
| Hs | 135.171 | 34.656 | 2.5 | 11 |
| Ng | 135.151 | 34.666 | 9.3 | 46 |
| Su | 135.121 | 34.646 | 11.2 | 15 |
| station | longitude | latitude | elevation (m;asl) | observation height(m;a.g.l) |
| Hu | 135.203 | 34.707 | 52.2 | 20 |
| Ri | 135.264 | 34.688 | 4.6 | 10 |
| Nh | 135.234 | 34.705 | 4.5 | 14 |
| Mi | 135.215 | 34.663 | 8.3 | 13 |
| Pt | 135.187 | 34.683 | 1.8 | 100 |
| Ro | 135.170 | 34.660 | 881 | 9 |

* measurement interval : 60min.

Table 3-1 List of dates for the analysis days (31 days when the sea and land breeze alternation occurred, April to November 2011)

| April | May | June | July | August | September | October | November |
|-------|-----|------|------|--------|-----------|---------|----------|
| 401 | 502 | 606 | 713 | 809 | 908 | 1008 | 1101 |
| 406 | 506 | | 723 | | 914 | 1008 | 1104 |
| 410 | 518 | | 724 | | 927 | 1012 | 1112 |
| 413 | | | 726 | | 928 | 1019 | 1122 |
| 417 | | | 731 | | | 1027 | 1126 |
| 421 | | | | | | 1029 | |

Table 3-2 Direction of prevailing wind at 15:00 and 03:00 JST at each location and wind direction

| station | 15 JST | 03 JST |
|---------|--------|--------|
| En | SSW | NNW |
| Ri | SW | ENE |
| Nh | SSW | NE |
| Na | S, SSW | N |
| Hu | S, WSW | NW |
| Mi | SW | ENE |
| Hs | SW | NNW |
| Ng | SW | N, NNW |
| Su | SW | N |
| Pt | SSW | ENE |
| AKw | SW | ENE |
| AKA | SW | ENE |

Table 3-3 Classification of wind systems and wind direction range in this study.

| Wind direction range (degree) | Wind system |
|----------------------------------|-------------------------|
| 105-195 | Sea breeze |
| 270-360 | Mountain breeze |
| 0-15 | |
| 195-270 | Extended sea breeze |
| 15-105 | Extended land breeze |

Table 3-4 Classification of observation points by cluster analysis.

| group | station |
|-------|--------------------------|
| 1 | En, Na, Hu |
| 2 | Hs, Ng, Su |
| 3 | Ri, Nh, Mi, Pt, AKw, AKA |

Table 3-5 Hourly changes in vector mean wind direction and speed. (a) Wind direction, (b) wind speed

(a)

| Cluster analysis Classification | | Group 1 | | | Group 2 | | | Group 3 | | | | | |
|---|------------|---------|----|----|---------|----|----|---------|----|----|----|-----|-----|
| | Time (JST) | En | Na | Hu | Hs | Ng | Su | Ri | Nh | Mi | Pt | AKw | AKA |
| 22-06 JST Mount.breeze Land breeze | 1 | | | | | | | | | | | | |
| | 2 | | | | | | | | | | | | |
| | 3 | | | | | | | | | | | | |
| | 4 | | | | | | | | | | | | |
| | 5 | | | | | | | | | | | | |
| | 6 | | | | | | | | | | | | |
| 07-09 JST Ext.land breeze | 7 | | | | | | | | | | | | |
| | 8 | | | | | | | | | | | | |
| | 9 | | | | | | | | | | | | |
| 10-12 JST Sea breeze | 10 | | | | | | | | | | | | |
| | 11 | | | | | | | | | | | | |
| | 12 | | | | | | | | | | | | |
| 13-17 JST Ext.sea breeze | 13 | | | | | | | | | | | | |
| | 14 | | | | | | | | | | | | |
| | 15 | | | | | | | | | | | | |
| | 16 | | | | | | | | | | | | |
| | 17 | | | | | | | | | | | | |
| 18-21 JST Mount.Breeze Ext.sea breeze | 18 | | | | | | | | | | | | |
| | 19 | | | | | | | | | | | | |
| | 20 | | | | | | | | | | | | |
| | 21 | | | | | | | | | | | | |
| 22-06 JST Mount.breeze Land breeze | 22 | | | | | | | | | | | | |
| | 23 | | | | | | | | | | | | |
| | 24 | | | | | | | | | | | | |

| | | |
|---------------------|----------------------|---------------|
| 105-195 degree | 0-15, 270-360 degree | 15-105 degree |
| Sea breeze | Mountain breeze | Land breeze |
| 195-270 degree | | |
| Extended sea breeze | | |

Table 3-5 (Continued)

(b)

| Cluster analysis Classification□ | | 1 | | | 2 | | | 3 | | | | | |
|---|------------|-----|-----|-----|-----|-----|-----|-----|-----|-----|-----|-----|-----|
| | Time (JST) | En | Na | Hu | Hs | Ng | Su | Ri | Nh | Mi | Pt | AKw | AKA |
| 22-06 JST Mount.breeze Land breeze | 1 | 0.5 | 0.5 | 0.8 | 0.4 | 0.7 | 0.9 | 0.3 | 0.3 | 0.6 | 0.3 | 1.0 | 1.7 |
| | 2 | 0.7 | 0.7 | 0.8 | 0.5 | 0.8 | 1.0 | 0.5 | 0.5 | 0.6 | 0.4 | 1.2 | 1.7 |
| | 3 | 0.7 | 0.8 | 0.8 | 0.6 | 0.9 | 1.0 | 0.6 | 0.4 | 0.9 | 0.6 | 1.2 | 2.2 |
| | 4 | 0.6 | 0.8 | 0.8 | 0.5 | 0.8 | 0.9 | 0.7 | 0.6 | 0.9 | 0.4 | 1.4 | 2.3 |
| | 5 | 0.7 | 0.7 | 0.8 | 0.6 | 0.9 | 0.9 | 0.8 | 0.5 | 1.0 | 0.5 | 1.5 | 2.7 |
| | 6 | 0.5 | 0.6 | 0.7 | 0.6 | 0.8 | 0.9 | 0.9 | 0.6 | 1.0 | 0.5 | 1.6 | 2.7 |
| 07-09 JST Ext.land breeze | 7 | 0.4 | 0.4 | 0.3 | 0.8 | 0.5 | 0.7 | 1.1 | 0.8 | 1.2 | 0.8 | 1.9 | 3.1 |
| | 8 | 0.9 | 0.6 | 0.5 | 0.7 | 0.3 | 0.6 | 1.2 | 1.1 | 1.3 | 0.9 | 2.3 | 3.2 |
| | 9 | 0.7 | 1.0 | 1.0 | 0.8 | 0.7 | 0.9 | 1.2 | 0.9 | 1.2 | 1.1 | 2.3 | 2.8 |
| 10-12 JST Sea breeze | 10 | 0.4 | 1.5 | 1.2 | 0.6 | 0.8 | 1.3 | 1.0 | 1.0 | 1.0 | 0.9 | 2.0 | 1.8 |
| | 11 | 0.7 | 1.8 | 1.6 | 0.8 | 1.3 | 1.4 | 0.7 | 1.4 | 0.6 | 1.2 | 1.7 | 1.4 |
| | 12 | 0.7 | 2.0 | 1.6 | 1.0 | 1.7 | 1.6 | 1.0 | 1.6 | 1.1 | 1.4 | 1.6 | 1.9 |
| 13-17 JST Ext.sea breeze | 13 | 0.9 | 2.4 | 1.8 | 1.4 | 2.0 | 1.6 | 1.3 | 2.1 | 1.2 | 1.6 | 2.4 | 2.4 |
| | 14 | 1.0 | 2.5 | 1.9 | 1.4 | 2.2 | 1.7 | 1.5 | 2.1 | 1.4 | 2.0 | 2.5 | 3.1 |
| | 15 | 1.0 | 2.6 | 1.4 | 1.6 | 2.4 | 1.6 | 1.7 | 2.1 | 1.5 | 1.9 | 3.1 | 3.5 |
| | 16 | 0.7 | 1.6 | 1.3 | 1.7 | 1.9 | 1.3 | 1.6 | 1.8 | 1.4 | 1.6 | 2.7 | 3.5 |
| | 17 | 0.7 | 1.1 | 1.2 | 1.3 | 1.5 | 1.1 | 1.4 | 1.5 | 1.1 | 1.6 | 2.4 | 3.6 |
| 18-21 JST Mount.Breeze Ext.sea breeze | 18 | 0.9 | 0.9 | 1.1 | 1.0 | 1.2 | 1.0 | 1.1 | 0.9 | 0.9 | 1.2 | 1.8 | 2.6 |
| | 19 | 1.0 | 1.0 | 1.0 | 0.9 | 1.0 | 0.7 | 0.7 | 0.6 | 0.5 | 0.9 | 1.1 | 1.8 |
| | 20 | 0.7 | 0.8 | 0.8 | 0.6 | 0.7 | 0.5 | 0.4 | 0.4 | 0.2 | 0.6 | 0.6 | 1.0 |
| | 21 | 0.7 | 0.7 | 0.7 | 0.4 | 0.3 | 0.3 | 0.3 | 0.3 | 0.1 | 0.4 | 0.6 | 0.3 |
| 22-06 JST Mount.breeze Land breeze | 22 | 0.8 | 0.5 | 0.7 | 0.2 | 0.2 | 0.3 | 0.1 | 0.3 | 0.4 | 0.0 | 0.7 | 0.3 |
| | 23 | 0.7 | 0.6 | 0.7 | 0.2 | 0.1 | 0.4 | 0.2 | 0.3 | 0.6 | 0.3 | 1.1 | 0.8 |
| | 24 | 0.8 | 0.6 | 0.6 | 0.4 | 0.5 | 0.6 | 0.3 | 0.3 | 0.8 | 0.7 | 1.3 | 1.3 |

0-1 m/s
 1-2 m/s
 2-3 m/s
 3-4 m/s

Table 3-6 Hourly wind direction at each station (October 18, 2014).

| Time (JST) | En | Na | Hu | Hs | Ng | Su | Ri | Nh | Mi | Pt | AKw | AKA | Ro |
|------------|-------|-------|-------|-------|-------|-------|-------|-------|-------|-------|-------|-------|-------|
| 1 | 22.5 | 337.5 | 315.0 | 337.5 | 337.5 | 337.5 | 90.0 | 0.0 | 67.5 | 45.0 | 90.0 | 67.5 | 0.0 |
| 2 | 22.5 | 0.0 | 315.0 | 337.5 | 337.5 | 337.5 | 90.0 | 22.5 | 67.5 | 22.5 | 67.5 | 67.5 | 337.5 |
| 3 | 67.5 | 337.5 | 315.0 | 337.5 | 337.5 | 337.5 | 90.0 | NaN | 67.5 | 67.5 | 337.5 | 67.5 | 337.5 |
| 4 | 22.5 | 337.5 | 337.5 | 337.5 | 337.5 | 0.0 | 90.0 | 337.5 | 45.0 | 247.5 | 0.0 | 67.5 | 337.5 |
| 5 | 90.0 | 337.5 | 315.0 | 0.0 | 337.5 | 337.5 | 90.0 | 315.0 | 67.5 | NaN | 337.5 | 45.0 | 337.5 |
| 6 | 22.5 | 67.5 | 315.0 | 0.0 | 337.5 | 337.5 | 67.5 | 67.5 | 45.0 | 67.5 | 45.0 | 67.5 | 337.5 |
| 7 | 22.5 | 22.5 | 315.0 | 0.0 | 22.5 | 22.5 | 45.0 | 45.0 | 45.0 | 67.5 | 67.5 | 45.0 | 337.5 |
| 8 | 67.5 | 157.5 | 157.5 | 45.0 | 45.0 | 45.0 | 67.5 | 180.0 | 90.0 | 112.5 | 90.0 | 67.5 | 0.0 |
| 9 | 90.0 | 112.5 | 157.5 | 45.0 | 112.5 | 135.0 | 67.5 | 67.5 | 112.5 | 90.0 | 90.0 | 67.5 | 22.5 |
| 10 | NaN | 157.5 | 135.0 | 90.0 | 112.5 | 90.0 | 90.0 | 112.5 | 112.5 | 90.0 | 112.5 | 90.0 | 45.0 |
| 11 | 225.0 | 157.5 | 135.0 | 67.5 | 112.5 | 157.5 | 157.5 | 202.5 | 112.5 | 112.5 | 135.0 | 112.5 | 0.0 |
| 12 | 45.0 | 157.5 | 135.0 | 135.0 | 180.0 | 180.0 | 180.0 | 180.0 | 90.0 | 157.5 | 135.0 | 135.0 | 337.5 |
| 13 | 225.0 | 180.0 | 180.0 | 202.5 | 202.5 | 180.0 | 135.0 | 180.0 | 202.5 | 180.0 | 112.5 | 180.0 | 337.5 |
| 14 | 202.5 | 202.5 | 157.5 | 157.5 | 180.0 | 180.0 | 157.5 | 180.0 | 202.5 | 157.5 | 180.0 | 225.0 | 337.5 |
| 15 | 202.5 | 180.0 | 157.5 | 225.0 | 202.5 | 225.0 | 225.0 | 180.0 | 202.5 | 157.5 | 202.5 | 225.0 | 337.5 |
| 16 | 247.5 | 202.5 | 315.0 | 225.0 | 202.5 | 225.0 | 247.5 | 225.0 | 315.0 | 225.0 | 247.5 | 315.0 | 337.5 |
| 17 | 292.5 | 337.5 | 315.0 | 225.0 | 225.0 | 247.5 | 247.5 | 225.0 | 315.0 | 247.5 | 225.0 | 315.0 | 337.5 |
| 18 | 247.5 | 337.5 | 315.0 | 337.5 | 292.5 | 337.5 | 247.5 | 247.5 | 315.0 | 315.0 | 247.5 | 292.5 | 337.5 |
| 19 | 22.5 | 337.5 | 292.5 | 292.5 | 315.0 | 315.0 | NaN | 45.0 | 292.5 | 315.0 | 315.0 | 292.5 | 22.5 |
| 20 | 315.0 | 337.5 | 315.0 | 315.0 | 337.5 | 337.5 | 22.5 | 315.0 | 315.0 | 337.5 | 315.0 | 337.5 | 22.5 |
| 21 | 337.5 | 337.5 | 315.0 | 337.5 | 337.5 | 0.0 | NaN | 315.0 | NaN | 22.5 | 315.0 | 315.0 | 22.5 |
| 22 | 337.5 | 0.0 | 315.0 | 0.0 | 337.5 | 337.5 | 67.5 | 315.0 | 45.0 | 45.0 | 0.0 | 67.5 | 22.5 |
| 23 | 0.0 | 337.5 | 315.0 | 337.5 | 337.5 | 337.5 | 67.5 | 0.0 | 67.5 | 67.5 | 0.0 | 67.5 | 22.5 |
| 24 | 337.5 | 0.0 | 315.0 | 0.0 | 337.5 | 0.0 | 45.0 | 337.5 | 67.5 | 22.5 | 0.0 | 67.5 | 0.0 |

105-195 degree

Sea breeze

195-270 degree

Extended sea breeze

0-15, 270-360degree

Mountain breeze

15-105 degree

Extended land breeze